Application of Divided Exhaust Period and Variable Drive Supercharging Concept for a Downsized Gasoline Engine

Hu, Bo

Award date:
2016

Awarding institution:
University of Bath

Application of Divided Exhaust Period and Variable Drive Supercharging Concept for a Downsized Gasoline Engine

Bo Hu

A thesis submitted for the degree of Doctor of Philosophy

University of Bath

Department of Mechanical Engineering

March 2016

Abstract

Most downsized gasoline engines currently in the market place appear to have a 'downsizing factor' of approximately 30% to 40%. However, as concerns regarding fuel efficiency and emission legislations increase, more aggressive downsizing may have to be introduced. This, although can improve fuel efficiency and enhance power density of a gasoline engine further, has some challenges that must be addressed.

Large backpressure is one of the most important aspects that needs to be improved for a highly downsized gasoline engine, especially if a Regulated 2-stage system is considered. The Divided Exhaust Period (DEP) concept is an alternative gas exchange process, where two exhaust valves from each cylinder separately function, with one valve leading the blow-down pulse into the turbocharger turbine, while the remainder of the exhaust mass flow bypasses the turbine through the other valve. The simulation results suggest that by adopting the DEP concept, the full-load Brake Specific Fuel Consumption (BSFC) and the stability of the engine were all improved due to the fact that the DEP concept features a better gas exchange process and improved combustion phasing. The part-load BSFC could also be reduced by using the scavenging valve to extend the 'duration' of the exhaust valve (thus reducing the re-compression effect) and to achieve internal exhaust gas recirculation (EGR) through reverse flow. However, this depends on the authorities of the scavenging valve timing (and piston clearance) and the combustion stability (EGR tolerance).

Driveability issue and poor fuel efficiency in some engine operating regions of a conventional fixed-ratio positive-displacement supercharging system also need to be mitigated. A continuously variable transmission (CVT) driven supercharging solution, with the capability to decouple the supercharger speed from the engine speed, has the potential to provide the full-load BSFC improvement and to enhance the driveability performance, with a minor penalty in part-load BSFC. Both the simulation and experimental results have demonstrated its advantages over its fixed-ratio positive-displacement counterpart. The high-load fuel consumption can be improved by as much as 17.5%, and the time-to-torque performance can be improved by up to 37%. The low-load BSFC was only degraded by up to 2%, however, given that there was no clutch fitted for the CVT driven supercharging system, a better transient performance is anticipated.

Acknowledgements

I would like to express my great thanks and appreciation to Dr. Sam Akehurst, Professor Chris Brace, Dr. Colin Copeland and Professor James Turner for their long-term supervision, support and guidance. Without their patience, approachability and specialised knowledge, I would have given up and walked away long ago.

This work would not have been possible without the financial support of a Jaguar Land Rover (JLR) Studentship, a Graduate School Scholarship from the University of Bath and the China Scholarship Council (CSC).

I would also like to thank Gavin Fowler and Nick Luard from JLR for providing me with the engine model and teaching me the theoretical and practical aspects of engine simulation. The discussions and assistance from Ford, Torotrak, Honeywell, Imperial College London and Nanyang Technological University have also been greatly appreciated, most notably: Arnd Sommerhoff and Harald Stoffels from Ford; Andrew De Freitas, Dave Burtt and James Shawe from Torotrak; Ludek Pohorelsky from Honeywell; Professor Ricardo Martinez-Botas from Imperial College; and Dr. Alessandro Romagnoli from Nanyang Technological University.

I must also thank Calogero Avola and Dr. Andy Lewis in helping me to operate the test cell, and Dr. Huayin Tang, Dr. Nic Zhang and Dr. Dai Liu for their considerable technical assistance in helping me to understand the engine model validation theory.

I am also grateful to all other colleagues at the PVRC for their emotional support and technical advice throughout this project, Dr. Chris Bannister, Dr. Richard Burke, Dr. Pavlos Dimitriou, Dr. Pin Lu, Pengfei Lu, Dian Liu, Dr. Simon Pickering, Ramkumar Vijayakumar…It has been a great pleasure working with you all.

Finally, I would like to thank my family for their unconditional support and love! Most of all I would like to thank my girlfriend, Hua, who always encouraged me when things felt impossible, and who has shared the happiness when great progress was achieved. I cannot imagine having completed this work without her love and support.

Further Publications

The work that will be presented has led to the publication or a number of articles in peer reviewed journals and at internationally recognised conferences. A list of these publications is provided below and references to these will be provided as necessary within the chapters of this thesis.

Peer reviewed journal articles:

1: Observations on and potential trends for mechanically supercharging a downsized passenger car engine – a review

B. Hu et al., Proceedings of the IMechE, Part D: Journal of Automobile Engineering (2016)

2: Fuel Efficiency Optimization for a Divided Exhaust Period Regulated Two-Stage Downsized SI Engine

B. Hu et al., ASME Journal of Engineering Gas Turbines and Power (2016), Vol. 138, issue 5.

3: Novel approaches to improve the gas exchange process of downsized turbocharged SI engines – A review

B. Hu et al., International Journal of Engine Research (2016)

4: A New De-throttling Concept in a Twin-charged Gasoline Engine System

B. Hu et al., SAE International Journal of Engines. (2015), Vol. 8, issue 4, pp.1553-1561.

5: 1-D Simulation Study of Divided Exhaust Period for a Highly Downsized Turbocharged SI Engine - Scavenge Valve Optimization

B. Hu et al., SAE International Journal of Engines. (2014), Vol. 7, issue 9, pp.1443-1452.

Refereed conference articles

1: Modelling the Performance of the Torotrak V-Charge Variable Drive Supercharger System on a 1.0L GTDI – Preliminary Simulation Results

B. Hu et al., presented at the SAE/JSAE International Powertrain, Fuels & Lubricants Meeting 2015 (Kyoto, Japan, 31 August–4 September 2015), SAE paper number: 2015-01-1971.

2: Fuel Efficiency Optimization for a Divided Exhaust Period Regulated Two-Stage Downsized SI Engine

B. Hu et al., presented at the ASME Turbo Expo 2015 (Montreal, Canada, 15-19 June 2015), ASME paper number: GT2015-43023.

3: A New De-throttling Concept in a Twin-charged Gasoline Engine System

B. Hu et al., presented at the SAE World Congress 2015 (Detroit, US, 21-23 April 2015), SAE paper number: 2015-01-1258.

4: Simulation Study of Divided Exhaust Period for a Regulated Two-stage Downsized SI Engine

B. Hu et al., presented at the SAE International Powertrain, Fuels & Lubricants Meeting 2014 (Birmingham, UK, 20-23 October 2014), SAE paper number: 2014-01-2550.

5: A New Turboexpansion Concept in a Twin-Charged Engine System

B. Hu et al., presented at the SAE International Powertrain, Fuels & Lubricants Meeting 2014 (Birmingham, UK, 20-23 October 2014), SAE paper number: 2014-01-2596.

6: The Effect of Divided Exhaust Period for Improved Performance in a Highly Downsized Turbocharged Engine

B. Hu et al., presented at the IMechE 11th International Conference on Turbochargers and Turbocharging 2014 (London, UK, 13- 14 May 2014).

7: 1-D Simulation Study of Divided Exhaust Period for a Highly Downsized Turbocharged SI Engine - Scavenge Valve Optimization

B. Hu et al., presented at the SAE World Congress 2014 (Detroit, US, 8-10 April 2014), SAE paper number 2014-01-1656.

Non-refereed conference articles

1: Divided Exhaust Period System for a Highly Turbocharged SI Engine – Timing Optimization

B. Hu et al., presented at the SIA International Conference and Exhibition – The Spark Ignition Engine of the Future (Strasbourg, 4-5 December 2013)

Contents

List of Figures

List of Tables

Abbreviations

DEP	Divided Exhaust Period	TVS	Twin Vortices Series
R2S	Regulated 2-Stage	TDC	Top Dead Centre
BSFC	Brake Specific Fuel Consumption	HP	High Pressure
EGR	Exhaust Gas Recirculation	LP	Low Pressure
CVT	Continuously Variable Transmission	D-EGR	Dedicated Exhaust Gas Recirculation
SI	Spark Ignition	VVT	Variable Valve Timing
NA	Naturally Aspirated	EEVO	Early Exhaust Valve Opening
VGT	Variable Geometry Turbine	LEVC	Late Exhaust Valve Closing
1-D	1-Dimensional	EIVC	Early Intake Valve Closing
BMEP	Brake Mean Effective Pressure	LIVC	Late Intake Valve Closing
HCCI	Homogeneous Charge Compression Ignition	VCR	Variable Compression Ratio
FMEP	Friction Mean Effective Pressure	EIVO	Early Intake Valve Opening
IMEP	Indicated Mean Effective Pressure	FGT	Fixed Geometry Turbine
DF	Downsizing Factor	WCEM	Water Cooled Exhaust Manifold
GDI	Gasoline Direct Injection	VEMB	Valve Event Modulated Boost
NVH	Noise Vibration Harshness	DOHC	Double OverHead Camshaft
NEDC	New European Drive Cycle	PWS	Pressure Wave Supercharger
JLR	Jaguar Land Rover	R-Series	Regular Series
TSI	Twincharger Fuel Stratified Injection	V-Series	Volumetric Series
BDC	Bottom Dead Centre	SC	Supercharger
PMEP	Pumping Mean Effective Pressure	SS	Steady State
RGF	Residual Gas Fraction	w/EGR	Without Exhaust Gas Recirculation
RPM	Revolutions Per Minute	CPU	Central Processing Unit
PFI	Port Fuel Injection	MFR	Mass Flow Ratio
CSC	China Scholarship Council	BSR	Blade Speed Ratio

WEDACS	Waste Energy Driven Air Conditioning System	CFD	Computational Fluid Dynamics
TCS	Turbo Cooling System	ECU	Electronic Control Unit
CAC	Charge Air Cooler	PID	Proportional Integration Differentiation
WOT	Wide Open Throttle	PI	Proportional Integration
KLSA	Knock Limited Spark Advance	DoE	Design of Experiment
PR	Pressure Ratio	MOP	Mean Opening Position
GTDI	Gasoline Turbocharged Direct Injection		

Chapter 1 - *Introduction*

Downsizing and down-speeding via turbocharging and supercharging are the primary approaches currently available to improve fuel efficiency and transient performance for a passenger car's internal combustion engine. This thesis will investigate the potential benefits of two innovative concepts for turbocharging and supercharging, in order to satisfy fuel efficiency expectation and emission regulations in the near future.

DEP, which combines the characteristics of a turbocharged engine and the scavenging process of a more normal, naturally aspirated (NA) engine, could enhance the competitive advantages already achieved by turbocharging while simultaneously mitigating the inherent deficiencies. The variable-drive supercharging concept has the potential to enable a further downsizing and down-speeding, thus making a gasoline engine more fuel efficient and more responsive in transient.

This chapter will firstly lay out the background for this project, and will then present the aims and principle objectives. A description of each chapter in this thesis will follow.

1.1. Background

Engine downsizing is the use of a smaller engine with a turbocharger or a supercharger to supply a similar power output as that of a larger one [1]. A boosted downsized spark ignition (SI) engine benefits from reduced pumping losses at part load, improved gas heat transfer, and better friction condition, thereby making it more fuel-efficient than a NA counterpart. The reduced engine package volume, enabled by a smaller engine size and, hence, reduced vehicle mass, also contributes to the improved fuel efficiency in typical driving cycles [2]. Compared to supercharging, turbocharging is more often combined with downsizing, by passenger car manufacturers, to achieve superior thermal efficiency.

Turbocharging - a means of recovering energy from exhaust gases through a turbine, which in turn drives a compressor to increase intake air density - is one of the key technologies to have crucially influenced the development of the internal combustion engine in the last few decades [3]. Initially, turbochargers were mainly utilised in large diesel engines. Gasoline turbocharged engines were developed much later, due to their inherent characteristics (such as knock sensitivity and higher turbine inlet temperature) [4]. However, as concerns regarding fuel efficiency and emission legislations increase, SI turbocharged engines are now expected to play a more important role in reducing the fleet CO_2 emissions [5]. Implementing a range of different turbochargers to the same engine family also allows manufacturers to tune engines in order to achieve different torque and power outputs. An example of this flexibility is Volvo's new modular engine platform, in which four different SI engines with the same geometry are divided into separate power/torque configurations by means of different turbocharger systems [6].

However, even though the turbocharging and downsizing combination has been proven to be a potential trend for SI engines over the next decade, there are still some further challenges that must be addressed. An important aspect of these is the need to optimise the gas exchange process to further improve an SI engine's performance. The need for the refinement of the current gas exchange technologies is clear. But, more importantly, innovative approaches are being required to meet the more stringent emission regulations, and to satisfy the increased fuel efficiency expectation, whilst still maintaining a similar engine performance.

In addition, although turbocharged engines are generally more fuel-efficient, as they utilise a proportion of otherwise-wasted exhaust gas energy, most turbocharged engines are not 'fun' enough due to the perceptible time needed for the turbocharging system to generate the required boost (so-called 'turbo-lag'). Supercharged engines, on the other hand, do not suffer from this problem, because the compressor of a supercharged engine is directly driven by the engine crankshaft; however, they are not as efficient as their turbocharged counterparts, and increase engine friction directly.

Although most of the downsized passenger car gasoline engines in production are turbocharged and the driving performance of turbocharged vehicles is greatly improved by the development of the turbocharger system itself (e.g. reduction of turbocharger inertia) and proper charging system matching, with the requirement of further downsizing to achieve further fuel efficiency [7] to satisfy ever-more strict fuel consumption regulations, supercharging technology may have to be introduced to increase the low-end torque and improve the transient performance when needed.

It might be worth noting that supercharging a gasoline engine can also address some other inherent issues of turbocharged gasoline engines, among which the elimination of pulsation interference and the capability to reduce the high exhaust back pressure are the two major aspects. Improvement of the turbocharging system itself, such as modifying a conventional turbine to a twin-entry one [8-9] to facilitate scavenging and improve the low-end torque particularly in four cylinder groups [10] and/or employing a Variable Geometry Turbocharger (VGT) to achieve optimum efficiency in a wider range of speeds and loads whilst improving the transient performance [11-12] and/or adopting DEP [13-24] or the so-called turbo-discharging concept [25-27] to reduce the backpressure to further improve a turbocharged gasoline engine's performance, can achieve some benefits but not as significantly when compared to a supercharged counterpart.

Mechanically supercharging a gasoline engine was commonplace in aero-engines [28-29], but the development of this technology for a passenger car has only appeared in recent years. This is especially the case for a compound-charging arrangement, in which two or more charging devices are used to provide more system capability [30-33]. Considering the strong possibility that the supercharging technology will be applied to more gasoline engines in the near future, to facilitate further downsizing and more aggressive down-speeding, either in a

Supercharger-Turbocharger or Turbocharger-Supercharger arrangement, a study of the current and concept approaches to achieving supercharging is necessary.

After reviewing the novel turbocharging and supercharging approaches that have the potential to improve fuel efficiency and transient performance of a downsized gasoline engine, it seems that the DEP concept that is able to reduce the backpressure significantly, and the variable-drive supercharging system that targets both fuel economy and transient performance are possible alternative solutions for boosting a downsized gasoline engine that may emerge in the near future.

1.2. Aim and objectives

The principle aim of this project is to demonstrate the potential benefits of the application of the DEP and variable-drive supercharging concept to downsized gasoline engines. A systematic approach will be utilised to compare the performance of a boosted engine system adopting the DEP and the variable-drive supercharging concept with the conventional configuration, both in simulation and experimentally.

In order to understand the process of gas exchange in a downsized turbocharged and supercharged gasoline engine, some advanced simulation techniques and testing experiences will be developed and gained. In addition, a transient control module for a twin-charged gasoline engine system will be built during this project, to assist the engine system to achieve the maximum potential both in steady state and in transient.

Looking at the aim of this project, the following objectives were laid out:

- Review the novel approaches to improve the gas exchange process of downsized turbocharged gasoline engines;
- Review the current methods and potential trends for mechanically supercharging a downsized passenger car engine;
- Develop the simulation techniques, including the build and calibration of a 1-dimensional (1-D) engine model, engine control construction, and in-vehicle simulation analysis;
- Model the conventional DEP concept to understand the benefits of dividing the blow-down and displacement phases in the exhaust process;

- Apply the DEP concept to a two-stage system to try to enhance the advantages which two-stage turbocharged engines have already obtained while offsetting the deficiencies inevitably inherited;
- Model the variable drive positive-displacement supercharging system in a compound charging system;
- Simulate and test the variable-drive centrifugal supercharging system in a compound charging system.

1.3. Scope of thesis

Chapter 2 to Chapter 8 present the work according to each of the project objectives, respectively. The conclusions are summarised in Chapter 9. Here is an overview of the contents of these chapters:

Chapter 2 will first review knowledge on the current state-of-the-art turbocharging technologies that are in production, as opposed to approaches that are currently only being investigated at a research level. More novel methods of the gas exchange process are then introduced, in order to identify the improved synergies between the engine and the boosting machine. Finally, the major findings to improve the gas exchange process that emerge from this review will be presented.

Chapter 3 will first review the fundamentals and types of supercharger that are currently or have previously been used in passenger car engines. Next, the relationships between the downsizing, the driveability and the down-speeding are introduced, in order to identify the improved synergies between the engine and the boosting machine. Then, mass production and prototype downsized supercharged passenger car engines are briefly described, followed by a detailed review of the current state-of-the-art supercharging technologies that are in production as opposed to the approaches that are currently only being investigated at a research level. Finally, the trends for mechanically supercharging a passenger car engine are discussed, with the aim of identifying potential development directions for the future.

Chapter 4 will describe a modelling and calibration theory foundation for the study that will take place over the following chapters. It mainly includes three sub-sections: engine model

introduction and calibration; engine control theory and tuning; and in-vehicle modelling. Each of these has been put into practice by demonstrating a case study.

Chapter 5 will investigate the DEP concept in simulation, using a validated highly downsized 2.0 Litre SI engine model, compared with a conventional single-stage turbocharging system.

Chapter 6 will, for the first time, apply the DEP concept to a two-stage downsized SI engine and study its potential benefits on an engine's full- and part-load fuel consumption.

Chapter 7 will present the simulation results using the turbo-expansion concept at both high and low load. In this chapter, a positive displacement supercharger will act as a turbine in a compound charging system by utilising a variable drive system.

Chapter 8 will simulate and test the variable-drive centrifugal supercharging concept in a compound charging system and compare its performance with a fixed-ratio positive displacement counterpart.

Chapter 2 – *Review of novel approaches to improve the gas exchange process of downsized turbocharged spark-ignition engines*

This chapter will first briefly review knowledge of the current state of the art technologies that are in production as opposed to approaches that are currently only being investigated at a research level. Next, more novel methods of the gas exchange process are introduced to identify the improved synergies between the engine and the boosting machine. The major findings to improve the gas exchange process that emerge from this review comprise four aspects (depending on the location where the novel technologies are implemented) which are as follows: charge air pressurization/de-pressurization improvement, combustion efficiency enhancement within the chamber, valve event–associated development and exhaust system optimization. Although the interaction between these technologies on different aspects of the gas exchange process was found to be highly complex, the optimization or the combination of these technologies is anticipated to further improve a downsized turbocharged spark-ignition engine's performance.

The comparison, discussion and conclusion in this chapter have been published in the form of a review article in the Institute of Mechanical Engineers International Journal of Engine Research.

2.1. Introduction

Engine downsizing, which is the use of a smaller engine that provides the power of a larger engine, is now considered a mega-trend for the internal combustion engine market. It is usually achieved using one or more boosting devices including a supercharger or a turbocharger. Although supercharging is beneficial for engine's transient response, turbocharging technology is more widely adopted considering its advantages in fuel efficiency. Compared to turbocharged compression ignition engines, turbocharged spark-ignition engines tend to be more challenging with respect to the gas exchange process mainly due to their higher pumping loss, the need for throttling and the fact that spark-ignition engines demand more controllability due to the mitigation of knock, particularly with regard to minimizing trapped residuals. These challenges encourage the entire gas exchange process of turbocharged spark-ignition engines to be regarded as a complete air management system instead of just looking at the boosting system in isolation. In addition, more research emphasis should be focused on novel approaches to improve the gas exchange process of downsized turbocharged spark-ignition engines because the refinement of the conventional technologies cannot provide continuous gains indefinitely and only innovative concept may improve the engine performance to meet the fuel efficiency target and the more stringent emission regulation in the future.

In the following, first, some current mass production and highly downsized prototype SI engines will be briefly introduced, followed which, the chapter will describe the gas exchange process and its effect on turbocharged SI engine performance. Some current production technologies will then be categorized for the purpose of understanding the interactions between boosting systems and gas exchange process. Finally, novel approaches that are currently only at a research level are discussed, with the aim of identifying potential developments in the future. Although supercharger technology is also an approach to achieve downsizing, the focus in this work is on turbochargers and turbocharging, due to the higher level of interaction with exhaust back pressure and thus the gas exchange process.

2.2. Mass production and prototype downsized turbocharged SI engines – a brief overview

Most downsized gasoline engines currently offered in the market place appear to have a 'downsizing factor' of approximately 35% to 40% [7]. The downsizing factor (DF) is defined to as

$$DF = \frac{V_{Swept_{N/A}} - V_{Swept_{Downsized}}}{V_{Swept_{N/A}}} \quad \textbf{2.1}$$

N/A: naturally aspirated

* Generally the naturally aspirated and the downsized engines mentioned above have a similar torque and power performance.

However, the DF of some prototype highly downsized gasoline engines can reach to 50% - 60% or even higher with some new technologies currently in development. These new technologies, according to McAllister and Buckley [34] will bring more fuel consumption benefit. **Figure 2.1** shows their investigation of the potential for downsizing based on some validation data from earlier work.

Mass production downsized turbocharged SI engine

In 2005, the Volkswagen 1.4 twincharger fuel Stratified Injection (TSI) was introduced to replace the 1.6 and 2.0 NA engines. The engine is equipped with both a turbocharger and supercharger, the performance of which has been shown to achieve a higher specific power while still benefiting from some fuel economy improvement [35]. More recent examples of production downsized engines include the Ford 1.0 litre Ecoboost engine and PSA 1.2 litre gasoline direct injection (GDI) engine, both equipped with only 3 cylinders [36-37]. These engines are both able to achieve significantly better fuel economy as well as fulfil the most stringent emission regulations. As only three-cylinder are used, the engines need to address some significant noise, vibration and harshness (NVH) challenges. However, the three-cylinder engines can benefit from some other performance attributes such as reduced friction, reduced heat transfer area and less exhaust pulse interference, resulting in improved turbocharger performance, which will be detailed later.

Downsized turbocharged SI engine only at the research stage

Mahle Powertrain developed a technology demonstrator with a 50% DF to showcase some of the technologies they have been developing. The 1.2 litre 3-cylinder two-stage turbocharged SI engine system, compared to its conventional 2.4 litre 4-cylinder NA counterpart, exhibited up to 30% on-road fuel consumption improvement with the Brake Mean Effective Pressure (BMEP) attainable above 30 bar [38]. A more extremely downsized technology demonstrator with a 60% DF termed 'Ultraboost' brought a 2.0 litre four cylinder gasoline downsized engine capable of up to 35 bar BMEP, air pressure charging of up to 3.5 bar absolute and offering over 35% potential for the reduction of fuel consumption and CO_2 emissions over the New European Drive Cycle (NEDC) while still matching JLR's 5.0 Litre V8 NA engine performance figures [7]. Table 1 presents more examples of mass production and prototype downsized turbocharged engines listed by Tang et al. [11]

Table 2.1. Typical downsized and turbocharged gasoline engines [11]

	Ultraboost (target)	MAHLE downsized two-stage (target)	Ricardo HyBoost	Porsche 911 Turbo S engine	Ford 1.0 L EcoBoost	Volkswagen 1.4TSI	Honda Acura RDX 2.3 L engine	MAHLE downsized single-stage
Specific power (kW/L)	142 (6500 r/min)	120 (6500 r/min)	105 (5500 r/min)	103 (6250–6750 r/min)	92	90	78 (6000 r/min)	75 (6000 r/min)
Peak BMEP (bar)	32 (3500 r/min)	30 (2500–3000 r/min)	29 (2500 r/min)	23 (2100–4500 r/min)	21 (1300–4500 r/min)	22 (1750–4500 r/min)	19 (4500 r/min)	22 (2500–3000 r/min)
Displacement (L)	2.0	1.2	1.0	3.8	1.0	1.4	2.3	1.2
Combustion system	DI + PI dual VVT + two-stage variable valve lift	DI dual VVT	DI dual VVT	Multiple DI (up to injections percycle) VVT + two-stage intake valve lift	DI dual VVT	DI dual VVT	PI dual VVT + one intake valve deactivate for improvement	DI dual VVT
Boosting system	Two-stage supercharger + FGT	Two-stage FGT + FGT	Two-stage electric supercharger + FGT	Two VGTs in parallel	Single-stage FGT	Two-stage supercharger + FGT	Single-stage VGT	Single-stage VGT
BMEP at 1000 r/min (bar)	25	16	23 (with electric supercharger assisted)	21 (1950 r/min)	21 (1300 r/min)	16	10	10
Transient response	Better than JLR 3.0 L twin-turbo V6 diesel	At 1250 r/min, 2 bar BMEP to WOT, 2 bar intake pressure achieved within 2.5 s	–	–	–	At 1250 r/min, from 2 bar BMEP to WOT, 2 bar intake pressure achieved within 2.5 s	At 2000 r/min, from low load to WOT, maximum intake manifold pressure achieved within 1.0 s	–
Minimum BSFC (g/kWh)	–	235	–	–			–	235
BSFC at low load (g/kWh)	–	295 (2000 r/min 4 BMEP)	–	–	–	–	–	–
Type	Prototype	Prototype	Prototype	Production	Production	Production	Production	Prototype
Turbine inlet temperature limit (°C)	–	1025	–	1000	1050	980	–	850 (Diesel engine VGT)
Water-cooled exhaust manifold	Yes	No	–	No	Yes	No	Yes	Yes
Fuel enrichment	No	Yes (Lambda 1 up to 5000 r/min)	No	–	Yes (minimum Lambda 0.95)	Yes	–	Yes
External EGR	Yes	Yes (HP)	Yes	No	No	No	No	Yes (HP)

2.3. Gas exchange process metrics and issues on turbocharged SI engines

The gas exchange process in this work refers to the expulsion of exhaust gases and the induction of fresh intake charge during the valve-open period of an engine cycle. An important aspect of the gas exchange process involves pumping work that is calculated by integrating the cylinder pressure with respect to cylinder volume calculated from bottom dead centre (BDC) of the exhaust stroke to BDC of the intake stroke [39]. Pumping work can influence engine performance in several aspects, including the relationship between BMEP, Net/Gross Indicate Mean Effective Pressure (IMEP) and Friction Mean Effective Pressure (FMEP) as shown in **Equation** 2.2 and 2.3.

$$BMEP = Net\ IMEP - FMEP \quad \textbf{2.2}$$

$$Net\ IMEP = Gross\ IMEP - PMEP \quad \textbf{2.3}$$

Since the pumping work required to expel the exhaust gases and draw in the fresh intake charge during the gas exchange process will affect the useful work that can be delivered by the engine, a large pumping loss (therefore more negative Pumping Mean Effective Pressure (PMEP)) can adversely affect the engine's thermal efficiency. In addition, the combustion process is significantly influenced by the gas exchange process via trapping hot residuals. Thus optimizing the gas exchange process is the key to enhancing a downsized turbocharged SI engine's fuel economy performance [24].

For turbocharged SI engines, production of a higher backpressure that leads to large pumping loss can be significant at some operating conditions. This process both subtracts work from the crankshaft and traps hot residual gas in the cylinder, both of which might result in increased fuel consumption, through the direct pumping work and retarded combustion

phasing due to the knock limited spark timing caused by the trapped residuals. In the following section, some important metrics/issues associated with the gas exchange process is analysed together with its effect on the turbocharged SI engine performance.

Scavenging behaviour:

Scavenging is the process of pumping exhaust mass out of the cylinder while drawing in fresh intake charge [40]. This process is essential to smoothly run a NA engine as well as a turbocharged engine because, if the scavenging is not sufficiently complete, a large amount of trapped hot residual gas would remain in the cylinder which would detrimentally affect both the volumetric efficiency and the knock sensitivity. The level of exhaust residuals trapped in the cylinder has also been proved to have a significant effect on the cycle-by-cycle variations in the combustion and the emissions of NO_x [41].

For turbocharged engines, specifically, the higher backpressure developed by the turbocharger turbine hinders the scavenging behaviour and leads to relatively higher trapped residuals [42]. The research by Möller et al. [21] found that a larger residual gas fraction occurred during the operation at low engine speed full load for a turbocharged SI engine. More specifically, the residual gas fraction (RGF) increased from approximately 4% at 4000 revolutions per minute (RPM) to approximately 8.3% at 1000RPM. Meanwhile, knock is often observed at low engine speed (spark timing usually needs to be retarded as a counter measure). For example, Chadwell et al. [43] stated that at low engine speeds, spark timing can often be retarded by as much as 30 degrees or more from the optimum condition for a modern boosted engine. This retarded timing is partly due to the low burning speed resulting in the propensity to pre-ignite and is partly attributed to the fact that a larger RGF at this region increases the knock propensity.

Note that the terms for scavenging in different literatures are not always fixed. For clarity, in this work, the blow-through effect is included in the scavenging behaviour. The blow-through

effect may be differentiated from the normal scavenging behaviour by allowing fresh charge to directly flow from the intake valve to the exhaust valve during a valve overlap period. The scavenging ratio, which is the percentage of intake air flowing into the exhaust port directly, is often a measure to indicate the blow-through effect. It has been proved that with a higher rate of scavenging, less residual gases will be remained in the cylinder [41]. However, port fuel injected (PFI) engines require very careful consideration in designing the valve overlap because the blow-through effect would flush the fuel/air mixture directly into the exhaust without a proper combustion. This blow-through, on one hand affects fuel economy and, on the other hand, increases the hydrocarbon compounds emission level. For a direct injection engine, however, the blow-through can help increase the low-end torque by shifting the turbine operating points into a more efficient area, thereby increasing the boost pressure [10]. This method is often referred to as a scavenging strategy which is widely adopted for turbocharged engines.

Back-flow:

The flow direction that is opposite to scavenging is usually referred to as back-flow. This reversed flow often occurs when the exhaust pressure exceeds the in-cylinder pressure or the intake pressure during the valve overlap period resulting in hotter trapped residuals and poorer volumetric efficiency. It is suggested that the overlap between the intake and the exhaust valve should be reduced to avoid such phenomena at some engine operating points [44]. For example, a valve overlap in SI engines is usually reduced during the part throttle and idling operation to avoid large back-flow [2].

The effect of each gas exchange process mentioned above for a standard turbocharged engine is illustrated in **Figure 2.2**. The upper two curves from the first pane indicate the scavenging mass flow rate with the second maximum curve strongly influenced by the blow-through effect and the lower curve from the same pane is significantly affected by back-flow. It is known that by varying the duration and the timing of the exhaust camshaft, the ratio of

both effects can be altered and optimised. For example, if the low-end torque and transient response is to be optimized, a short exhaust camshaft duration and relatively late exhaust valve opening must to be adopted. These conditions will guarantee the blowdown pulse from the next cylinder in the firing order to arrive late and reduce the pulse interference period while still maintaining large blow-though. Large blow-through then would be beneficial for the efficiency & mass flow of the turbine which leads to higher boost pressure and improved transient performance.

The scavenging and backflow effects covered above not only apply to turbocharged SI engines but also apply to NA gasoline engines. In the following, a unique gas exchange issue termed pulse interference is demonstrated.

Pulse interference is an issue for turbocharged engines with more than three cylinders without the use of the twin-scroll turbocharger layout. Some authors state that the event duration of a camshaft is usually approximately 210 degrees which is a common compromise between the maximum utilization of the power stroke and a minimal charge-cycle work [3]. Considering the inter-cylinder firing interval for 3 and 4 cylinder engine is 240 and 180 crank angle degree respectively, a 4-cylinder engine will suffer pulse interference, whereas a 3-cylinder engine will have sufficient pulse separation. For example, **Figure 2.3** shows that the blowdown pulse of cylinder 3 causes an increase of the pressure in cylinder 1 during the open period of the exhaust valve. This increase in pressure results in unnecessary pumping losses and a reduction of the breathing performance of the turbocharged engine. The pulse interference is often avoided by connecting several cylinders of an engine through a single branch to a single turbine inlet.

Note that although the definition described above could be used as a measure to indicate the gas exchange performance of a turbocharged engine, it is not appropriate to regard the gas exchange process as occurring within a closed system. In the following, an example is

made to explain the synergistic effect of the gas exchange process and combustion phasing on the overall engine's thermal efficiency.

For turbocharged SI engines, the intake charge is pressurized above the ambient to boost the engine performance, which inevitably introduces a higher intake charge temperature. This higher temperature affects both the volumetric efficiency and the knock resistance. The engine performance at high load would be improved with a higher pressure and a lower temperature of the charge (higher air density). An inter-cooler is a common means to achieve these conditions; however, the temperature cannot be reduced to ambient or sub-ambient levels as intercoolers do not have 100% effectiveness. In this case, the performance of the gas exchange may be compromised for the purpose of enhancing the combustion phasing to achieve total efficiency improvement. The turbo-expansion concept detailed later is such an example, which utilizes the exhaust energy to cool the intake charge while compromising some of the pumping work to achieve a better net efficiency improvement.

Table 2.2. Technology categories for the improvement of gas exchange process

Charge air pressurization/de-pressurization improvement	**Combustion efficiency enhancement within the chamber**	**Valve event associated development**	**Exhaust system optimization**
Inlet Manifold Design	Stratified Charge	VVT	Twin-scroll turbine
WEDACS	EGR		VGT
Turbo-expansion	Cylinder deactivation		WCEM
	HCCI		DEP
			Turbo-discharging
			Mirror Gas turbines

2.4. Strategies for optimizing the gas exchange process

In the following section, a number of technologies will be reviewed with focus on the gas exchange process. In **Table 2.2**, four categories are identified including charge air pressurization/de-pressurization improvement, combustion efficiency enhancement within the chamber, valve event associated development and exhaust system optimization. This category system is based on the location at which the technology is implemented. However, note that some of the technologies are optimized for several locations of the turbocharged engine and in this case the technology is categorized into the most relevant classification. In the same category, the knowledge of the current state-of-the-art technologies in production is discussed first, and then the relatively novel approaches of the gas exchange process that may be currently at a research level are demonstrated. The major findings that emerge from reviewing the literature and future potential directions are then finally discussed.

2.4.1 Charge air pressurization/de-pressurization improvement

Intake Manifold Design:

Intake manifold design is crucial for optimizing engine performance. A typical intake manifold, in its most simplistic form, consists of two main parts: the plenum and the intake runner. The plenum acts like a resonating chamber which allows the pressure wave to bounce back and forth in the manifold. If the valve opens at the exact time when the wave of the air arrives, the added pressure will boost the air into the cylinder producing higher volumetric efficiency, vice versa [47]. The Chrysler 300SL is one of the first cars to have intake manifold design in mind. By optimizing the intake geometry, the vehicle managed to produce higher power at high RPMs instead of higher torque at low RPMs, due to its racing heritage [48]. It is known that for a fixed-geometry intake manifold, the desired engine performance can only be achieved at very narrow engine operating range. In this context, variable intake manifold is introduced for automotive applications. Compared to the similar technology – variable valve timing, the variable intake manifold concept can provide similar output with a cheaper cost and less complications. Of course, it is evident that these two technologies can be combined to enhance both strengths. Honda's variable valve timing and lift electronic control system engine is such an example, which is demonstrated to improve the engine thermal efficiency by 13% equipped with these two technologies [49]. It is suggested, as

turbocharging is a very prominent trend amongst all manufacturers & can achieve better performance, VIM will probably be seen less in new cars.

Waste Energy Driven Air Conditioning system (WEDACS)

WEDACS is an engine load control system that provides electrical energy and cooling power by the energy that is otherwise lost in throttling [50-51]. This technology patented by the Eindhoven University of Technology replaces the conventional throttle valve with a turbine-generator combination. Throttling losses are reclaimed by expanding the intake charge through a turbine coupling with a generator, which lightens the load of the alternator. In addition, the intake temperature is reduced due to the expansion effect of the turbine, which can be used to cool the air conditioning fluid. This system was demonstrated to improve the fuel efficiency by up to 19% in the MVEG-A drive cycle. However, in this layout, even though the de-throttling concept is achieved, a throttle valve might still be needed because the air mass flow might be out of range for the turbine at idle. Meanwhile, a bypass throttle is also a necessary component to enable the engine to operate under high load, without which the turbine would act like a restricted nozzle to constrain the intake mass flow at high load.

The small operating range of the system was then improved by the same group of authors attempting to use a variable nozzle turbine to expand the control range of the engine. Two variable nozzle mechanisms were adopted to adjust the high engine power and the low engine power. Through the optimization of the VGT mechanism, the system exhibited up to 8% fuel efficiency improvement for typical turbine operating conditions.

Turbo-expansion:

Turbo-expansion, a termed first introduced in the study by Turner et al. [52] is basically achieved by deliberately over compressing the charge air, intercooling it at the resulting elevated pressure, and then expanding it via an expander to the desired plenum boost pressure, thereby ensuring a plenum temperature that can potentially become sub-ambient at full-load. Several means could be used to achieve similar outcome i.e., reducing the start of the compression temperature including water injection and introduction of the fuel before the pressure charging device [53-54]. However, neither of them has the same potential to be utilized for automotive applications. [52]

There are two configurations investigated in turbocharged SI engines to achieve turbo-expansion. One is from the research by Turner et al., the schematic of which is shown in **Figure 2.4**. The other is from the study by Whelan et al., the schematic of which is shown in **Figure 2.5**. The latter one, which is also termed the turbo-cooling system (TCS), is slightly different from the former concept. In the TCS, both an additional compressor and a turbine are utilized to pressurize and expand the intake charge. By removing the heat with an intercooler and making the expansion ratio greater than the compression ratio, a sub-ambient temperature could be achieved [55-56]. However, unlike the traditional turbo-expansion concept, the turbo-cooling system does not reclaim energy to the crankshaft but lead to lower pumping loss. In the following, the traditional turbo-expansion concept will be reviewed, followed by a brief discussion of the turbo-cooling system.

There are two potential types of expander that may be used in the traditional turbo-expansion concept: aerodynamic-expansion and positive-displacement device. For optimum efficiency, a high-speed aerodynamic-expansion turbine is beneficial. However, the following obstacles prevent such technology from being implemented into practice: the necessity of coupling such a turbine to an electric motor and the difficulty to absorb the reclaimed power. A low-speed positive-displacement device (due to its similar air consumption characteristics to those of an internal combustion engine, thereby removing the need for some of the potential control strategies) may be appropriate for use in the turbo-expansion concept. Two types of positive-displacement expanders were simulated and experimentally studied in the literature: Lysholm twin-screw and twin vortices series (TVS) R-Series Eaton.

The turbo-expansion concept using an Opcon twin-screw expander at the high-pressure stage of a twin-charged SI engine was demonstrated to reduce the likelihood of knock at high engine loads in simulations due to the intake temperature reduction. However, the engine test results were not realistic due to the low isentropic efficiencies of the components used on the investigated engine [52, 57]. More specifically, in the simulation work, the concept was proven to be able to configure a heavily pressure-charged engine with a high, fixed compression ratio. The authors stated that, with such a configuration (see **Figure 2.4**), 150 PS/litre and 200 Nm/litre specific value could be achieved with a compression ratio as high as 10.5:1. Full-load BSFC was demonstrated to attain just over 240 g/kW, but this result did not consider the requirement of the turbine inlet temperature, and the combustion model used was not able to predict knock onset. The fuel consumption benefit came only from the

recovery power by the expander in their modelling work and was in the range of 5.1 kW out of the total of 187.6 kW. In the later engine test investigation by Turner et al., the results were unfortunately unrealistic. Taitt et al. [58] proved that, for the isentropic efficiencies of the components used on the engine investigated, the system was not capable of delivering significant reductions in the inlet charge air temperature. They also indicated that system effectiveness is the least sensitive to compressor isentropic efficiency and the most sensitive to intercooler effectiveness, with the sensitivity of the expander isentropic efficiency being in between.

Romagnoli et al. [59] conducted experimental research on an Eaton-type supercharger (R410 TVS) as an expander. The results of this research were considered to be the first available performance test data of an Eaton supercharger acting as an expander. From the research results, to deliver a similar mass flow range to the engine when it is operated as an expander, the supercharger must spin at a slower rotational speed. Thus, a different supercharger drive ratio (CVT preferred) must to be used to accommodate various engine operating points. Hu et al. [60] continued the research on use of the Eaton-type supercharger as an expander by implementing the obtained experimental data into a calibrated downsized SI engine system model in GT-Power. Although the expansion cooling effect could be achieved, the BSFC improvement was found to be limited due to the associated larger pumping loss and the corresponding larger residual gas fraction resulting in degraded combustion phasing. However, as there is no proper positive-displacement expander template in GT-Power, the results might not be sufficiently accurate. Note that the limited BSFC improvement might be 'good' enough, as the supercharger was initially not intended to be used as an expander. If the supercharger was optimized for the purpose of expansion, more energy could be reclaimed and some of pumping loss could be saved which might result in better BSFC performance.

Although the Eaton-type supercharger as an expander concept showed limited fuel efficiency improvement at full load, it might be beneficial to use the same configuration to achieve the de-throttling purpose at part load. This proposed configuration is basically a combination of the traditional turbo-expansion concept and the WEDACS concept, and it has been studied by Hu et al. [61] In their study, a CVT-drive Eaton-type supercharger (R410 TVS) was utilized as an expander to control the engine load and reclaim some of the throttling loss at part load without the use of a conventional throttle plate. By altering the CVT ratio the engine's BMEP

was demonstrated to be controllable, with the fuel efficiency able to be improved by up to 3%, depending on the engine operating points. In addition, the supercharger outlet temperature could reach sub-ambient or sub-zero temperature due to the expansion effect of the supercharger functioning as an expander, which could cool the after-cooler's liquid, resulting in improved knock resistance and improved engine volumetric efficiency in the following possible high load drive cycle.

By the adoption of a CVT drive to the supercharger mechanism for a twin-charged engine system, the Eaton-type supercharger's operating range could be significantly extended. At high load/low-engine-speed when the extra boost is needed, the supercharger could be utilized as a boosting device with the appropriate CVT ratio. The characteristics of a CVT drive can enable the supercharger to deliver the exact boost without any recirculation of the intake mass flow, resulting in reduced mechanical loss and the flow loss. Such a scheme might also benefit from improved knock resistance as the intake charge temperature is reduced. At high-speed/high-load, when the exhaust energy is sufficient for the turbocharger to provide the required boost, the supercharger could function as an expander, presenting an indirect means to recover some of the exhaust energy. At low load, the CVT drive could cause the supercharger to act as a de-throttling mechanism to deliver the required vacuum whilst reclaiming some of the throttling loss and reducing the supercharger outlet temperature. The CVT drive supercharger may also have some benefits for the engine's transient performance, as the CVT drive mechanism (at high drive ratio) can offer some potential to over-shoot. In addition, compared to the fixed-ratio supercharger system (with the necessarily to de-clutch at part load), the CVT drive supercharger could function as an expander at part load, thus constantly connecting to the crankshaft. This function, on one hand, indicates the eliminated time for the conventional clutch to phase in, and, on the other hand, it provides the benefits from improved NVH performance during the transient.

There are some issues that must be addressed, including the achievable CVT ratio in reality and the condensation effect. The current maximum belt drive CVT can only achieve a value of approximately 10, which indicates that the very low supercharger speed might not be attainable to reach the low BMEP target if the rated torque at the corresponding engine speed is maintained. In this case, a throttle might be needed to provide an additional vacuum. The condensation effect must also be considered, as this might affect the performance of the

expander/combustion. In addition, the associated temperature rise due to the condensation effect would not have as much cooling effect as that predicted in the numerical simulation.

A turbo-cooling system is beneficial for lowering the intake pressure and temperature of a turbocharged SI engine. This system also provides a lower turbine inlet temperature (exhaust temperature). However, such a concept suffers from a larger backpressure due to the additional power required to drive turbocharger 2 (shown in **Figure 2.5**). This situation will result in a larger pumping loss and an increased pressure ratio for turbocharger 1. As a consequence, from the perspective of gas exchange, the turbo-cooling system is apparently not a good solution to improve the fuel economy of a turbocharged engine. Nevertheless, the advantages of the turbo-cooling concept could be realized by exploiting a reduced intake pressure and temperature. This approach could have some benefits, such as an improved combustion phasing at fixed knock index, and a reduced requirement of fuel-enrichment. [55-56]

Major findings: The novel inlet gas exchange processes of turbocharged engines focus on two parts: pressurized intake charge cooling at high load and throttling loss reduction at low load. Some technologies utilize the otherwise wasted exhaust energy after the turbine to cool the intake charge, such as the traditional turbo-expansion concept, which will inevitably induce higher backpressure, thus resulting in a larger pumping loss and a poorer combustion phasing. The net BSFC improvement by adopting such a concept should depend on the balance of the pumping loss, the combustion phasing and the energy recovered.

For the purpose of reducing the throttling loss at part load on the intake, the currently possible method is via the adoption of a turbine-like expander to reclaim some of the throttling loss. Considering the fact that most of the current two-stage SI engines have a positive-displacement supercharger on the intake, implementing a CVT drive for the positive-displacement supercharger might be a good direction to reduce the throttling loss in the near future.

2.4.2 Combustion efficiency enhancement within the chamber

Stratified charge:

The development of gasoline direct injection technology not only mitigates the requirement to reduce the compression ratio for downsized gasoline engines, but also facilitates the progress of stratified charge SI engines. Under normal stratified operating conditions, fuel injection is often delayed until the piston approaches top dead centre (TDC) [62-64]. By enriching the mixture near the spark plug with the remaining cylinder well above the stoichiometric condition, it is expected to achieve a very high overall air/fuel ratio with good stability and fuel consumption [65]. Chadwell et al. [43] stated that the stratified charge, which is one of the lean concepts, can benefit from better pumping work under the lean limit due to de-throttling. Sauer et al. [39] demonstrated that the stratified charge had a better cycle efficiency due to the lower mean temperature because of dilution.

The stratified charge mode is more EGR-tolerant in a turbocharged engine, in addition, based on simulations, the operating regimes of a NA stratified engine can be significantly extended by turbocharging the engine. Moreover, the stratified charge mode might be beneficial to reduce the likelihood of knock for a turbocharged engine due to the reduced combustion temperatures [66].

However, the issue of compressor surge for the stratified charge turbocharged engine might exist because excess air, and thus a higher pressure ratio, is required at some engine operating points. In addition, stratified charge prevents a three-way catalyst to completely convert the emissions, which is expected to require a lean NOx trap, resulting in additional cost and packaging challenges [67].

EGR:

The conventional method to avoid or mitigate knock for a downsized turbocharged engine consists of retarding the spark timing and/or fuel enrichment, with the drawbacks of higher exhaust temperature, inefficient catalytic conversion and poor fuel efficiency. For highly downsized SI engines, the compression ratio must still be reduced, which inevitably results in degraded fuel efficiency at part load. A cooled external EGR is widely accepted to be a suppressant of knock without compromising performance in turbocharged SI engines [68]. Moreover, it is demonstrated that the tolerance to EGR is improved for downsized turbocharged engines than for NA engines, and the NOx level could be further reduced

through increased EGR ratios [57]. Brustle and Hemmerlein [69]. investigated the effects of a cooled external EGR on the performance of a turbocharged SI engine under stoichiometric conditions with a pre-turbine temperature limit of 1000 degC. An increase of up to 1 bar BMEP was demonstrated to be attained when the EGR rate was controlled to be 12%. They also suggested that a small increase of the compression ratio could be implemented to improve the fuel economy across the entire engine operating map. Alger et al. [70]. also suggested that engines with an EGR loop had the ability to operate at high compression ratio above 12:1. The knock intensity is limited due to the reduced rate of mass burning with the reduced rate of temperature rise during the combustion. In the following, different EGR concepts from different angles of view will be reviewed.

External EGR vs. Excess air:

A number of researchers compared the utilization of the excess air with the external EGR in a given engine operating point (5000RPM and 16.5 bar BMEP). Although the combustion stability for both cases were deteriorated, the EGR was demonstrated to facilitate a more stable burn and showed substantial advantage in terms of reducing the level of NOx [71]. In a similar study by Duchaussoy et al [72]., the external EGR was proved to provide benefits over excess air dilution in terms of performance, heat exchange and specific fuel consumption.

Note that EGR coolers can further reduce NOx emissions by lowering the combustion temperatures even further. There are many considerations when sizing and matching an appropriate EGR cooler for a turbocharged SI engine application. For the low-pressure EGR configuration specifically, the EGR cooler must have a high efficiency to maintain the compressor isentropic efficiency and avoid excessive outlet temperature [73]. Implementing an EGR cooler might have some other issues such as EGR cooler fouling and added backpressure which has a negative effect on fuel efficiency.

External EGR vs. Internal EGR:

When internal and external EGR were compared, Alger et al. [74] demonstrated that the former benefited at low and part loads due to reduced pumping loss and re-heat of the intake charge, while a cooled external EGR at high load can significantly improve fuel consumption by mitigating the requirement of over-fuelling and reducing the knock tendency. An internal

EGR will be discussed in the following, and the external EGR will be reviewed in the next section.

Unlike the external EGR, which is fulfilled by a separate air path, the internal EGR is usually achieved by controlling the valve timings. Recompression and rebreathing are the most commonly used valve strategies to achieve the internal EGR. Other strategies may be used, but the above-described strategies are representative.

Recompression, also termed as negative valve overlap, refers to the strategy with exhaust valve closes before TDC and the intake valve opens after TDC. The crank angle duration between the exhaust valve closing and the intake valve opening is known as the negative valve overlap. This method traps some exhaust gas, but might cause a cylinder pressure rise during the end of the exhaust stroke, resulting in some negative pumping work. The rebreathing approach uses a delayed exhaust valve closing or a second separate exhaust valve event which results in an increased overlap between the exhaust valve and intake valve. During this overlap, depending on the pressure difference between the intake port and exhaust port, some of the exhaust gases will flow back into the cylinder. Some issues may arise by adopting such an approach, including the requirement for a complicated valve control system under different engine operating points and the intervention between the exhaust valve and piston around TDC [75].

High pressure EGR vs. Low Pressure EGR:

From the literature [76] the high-pressure (HP) EGR system had the advantage of a minimum volume between the EGR control valve and the intake valves, which is beneficial for controlling the EGR rate during engine load transitions. In contrast the low-pressure (LP) EGR prevailed over the high-pressure EGR on the exhaust gas temperature controllability, and LP EGR is more perfectly cylinder-to-cylinder distributed. Takaki et al. [77] stated that LP EGR was possible to supply sufficient EGR under the high-load low-speed engine operating region, where the boost pressure is larger than the exhaust (see the black outlined region in **Figure 2.6 and Figure 2.7**). In addition, LP EGR could be beneficial for knock suppression due to the removal of the NOx if the EGR path is placed downstream of the catalyst.

For a high-pressure EGR system, the Dedicated EGR concept, which is shown in **Figure 2.8**, is a new approach proposed by Christopher et al. [43, 78]. In the system, only one cylinder was

used to produce the entire EGR mass flow, and the dedicated cylinder was run rich of the stoichiometric condition, with an equivalence ratio between 1.3 and 1.4 to produce the reformate, such as CO and H_2. By using the EGR and reformate (CO and H_2), such a layout was demonstrated to have a positive compounding influence on the knock mitigation, resulting in an increase in the compression ratio from 9,3:1 to 11.7:1. Note that the engine featured a constant 25% EGR rate, which made the control less complex.

Pre-catalyst EGR vs. post-catalyst EGR:

Because almost every modern emission-controlled gasoline engine has a close-coupled catalyst, it is possible to utilize the additional pressure drop across the catalyst to help drive the LP EGR, which is especially valuable at low engine speed/load [79]. In the same literature, the authors stated that the pre-catalyst source EGR could also facilitate the engine breathing (less pumping loss) as a result of the improvement of the pressure drop across the turbine, which is beneficial for the reduction of the size of the EGR valve. In addition, the pre-catalyst EGR has some other advantages over the post-catalyst EGR including enhanced peak engine output, improved EGR cooling effect and the ability to re-burn the hydrocarbons and H_2. From the perspective of the pre-catalyst source EGR on the combustion efficiency and burn rate, it was demonstrated that as little as 0.2% H_2 yielded significant increases in the combustion speed, improvement in the combustion stability and reduction in the HC emissions in a stoichiometric SI engine running external EGR. [72] Kwon and Min. [80] also showed that the CO content in EGR can enhance the combustion rate, but it is strongly dependent on the CO to H_2 ratio and the combustion temperature. BorgWarner. [79] summarized that the pre-catalyst LP EGR has 1.5 to 3.5% BSFC benefit over the post-catalyst EGR due to the improved combustion efficiency, improved PMEP and the ability to re-burn the exhaust. In addition, the turbine inlet temperature was reduced compared to the post-catalyst configuration. Negative effects of pre-catalyst EGR generally include the oxidization for the compressor and a lower knock resistance attributed to the NOx content in the EGR [81].

<u>Cylinder deactivation (variable displacement):</u>

Cylinder deactivation, usually referred to as a method to achieve variable displacement, is not a novel concept, but rather has existed for decades. Cylinder deactivation allows the engine to be further ‘downsized’ at the light-load operation and offers maximum performance under the full-load condition.

In typical light-load circumstances, only a small proportion of the available torque at the corresponding engine speed is utilized. In this context, a throttle valve must be partially closed, which prevents the engine from breathing freely. Some of the power is therefore not used to propel the vehicle forward, but to overcome the drag to draw air through the small opening and the accompanying vacuum resistance at the throttle valve. In addition, the combustion efficiency at part-load operation is not as efficient, considering the fact that the combustion chamber pressure is relatively low when the spark plug is about to fire, resulting in a low IMEP.

The cylinder deactivation concept generally keeps the intake and exhaust valve closed through all cycles for a particular set of cylinders in an engine. The fuel delivery for each deactivated cylinder is also cut-off by electronically disabling the appropriate fuel injection nozzles. By doing so, the throttle valve is forced to be opened more fully resulting in better pumping work, accompanied with an improved combustion chamber pressure, thus resulting in a higher combustion efficiency. The reduced power train friction through the absence of the actuating forces on the deactivated valves was also demonstrated to contribute to improvement of the fuel consumption [82].

This concept has only been applied to relatively large displacement engines, but recent research shows that it can also be applied to small displacement turbocharged SI engines. For example, Volkswagen implemented the cylinder deactivation concept on its four-cylinder 1.2 Litre engines. Its system, named Active Cylinder Technology, was demonstrated to reduce the fuel consumption in the EU driving cycle by approximately 0.4 Litre per 60 miles [83]. The two issues of unbalanced cooling and vibration must be overcome for production cylinder deactivation concept engines.

Homogeneous Charge Compression Ignition:

Rather than using an electric discharge to ignite the charge for SI engines, homogeneous charge compression ignition (HCCI) increases the charge's density and temperature via compression until the entire mixture reacts spontaneously. The approach is best regarded as a combustion mode of internal combustion engines distinct from the conventional spark ignition and compression ignition operating modes and it potentially offers the advantages of the two conventional combustion modes with high-efficiency and ultra-low NOx (due to lower temperature) and soot emissions (attributed to pre-mixed charge) 84]. By use of a very

dilute mixture, the HCCI engine could operate un-throttled at part load, thus reducing pumping loss. In addition, the HCCI cycle is more approximate to the ideal Otto cycle (shorter combustion duration), resulting in better thermodynamic efficiency at fixed geometric compression ratio. Furthermore, the lean mixtures can contribute to the higher ratio of specific heats, thus improving the thermal efficiency of the engine. Although stable HCCI operation and its substantial benefits have been demonstrated, several technical barriers must be overcome before HCCI can be widely applied to production SI engines.

However, due to the nature of the HCCI combustion, robust HCCI operation can only be realized in a limited operating range, with the lowest bound restricted by misfiring at low load and the highest bound by a high rate of pressure rise at high load. Thus, most SI engines using HCCI have dual-mode combustion systems in which the SI combustion is used for the operating conditions where HCCI operation is not possible, which includes low-loads, high-loads and cold start. To operate such an engine, a transition between SI and HCCI and SI modes in different engine operating points should be seamless in operation, whilst keeping all associated engine, combustion and emission parameters in an acceptable range. Milovanovic et al. [85] performed an experimental investigation using trapped exhaust gas for the transition from SI to HCCI to SI combustion mode on a single cylinder research engine equipped with a fully variable valve train system. The experimental results suggested that a SI to HCCI mode transition could be performed in one engine cycle without affecting driveability, combustion and emissions. However, a considerable change in engine torque and emissions were observed during the HCCI to SI mode transition due to the weak combustion or misfire resulting from unsynchronised valve profile change, throttle response and unadjusted fuelling rate. This observation is consistent with the research by Wu et al. [86]. However, Zhang et al. [87] suggested that the transition from HCCI to SI was easier than the reverse transition via a quick and dynamic control of the residual gas fraction.

Turbocharging is demonstrated to have the ability to extend the high-load and high-speed operating limit by raising the air mass flow through the engine to dilute the mixture, resulting in better knock resistance [88-89]. However, due to the limit of the gas exchange process (compressor surge), the higher load and speed region might still be unattainable. In this case, a twin-charged configuration might be needed to provide enough fresh air for the HCCI SI engine. Moreover, the low exhaust gas enthalpy available to the turbine results in a high exhaust backpressure, leading to increased negative pumping work that affects the fuel

economy [88]. Another problem with HCCI is that turbocharging can increase the rate of the peak pressure rise to unacceptable levels sometimes, so high EGR fractions or reduced compression ratio may be required to keep the rate of peak pressure rise low [89-90].

Major findings: For turbocharged SI engines in the combustion chamber, the corresponding gas exchange process is mainly for the purpose of the combustion efficiency (or combustion phasing) improvement and the reduction of the pumping loss. In thermodynamics, any approaches, such as EGR and stratified charge, which facilitate a larger geometric compression ratio are beneficial for the combustion efficiency. In addition, if the requirement of three-way-catalyst is not considered (air/fuel ratio is not fixed) and different combustion operation mode can be switched seamlessly by a proper control, lean combustion approaches, including HCCI and the stratified charge concept, might be a good direction. Such concepts not only increase the combustion efficiency but also benefit from the reduction of the pumping loss, resulting in improved thermal efficiency. At low load, the associated pumping loss must be a high priority. In this case, the cylinder deactivation concept can be adopted to further 'downsize' the engine.

2.4.3 Valve event associated development

Variable Valve Timing (VVT):

There are a number of studies in the literature on VVT to improve the gas exchange process on turbocharged gasoline engines. It is widely accepted and examined that the inlet valve timing is the most important parameter to optimize volumetric efficiency, whereas the exhaust valve timing determines the RGF and NOx [91]. The reviews below will be organized by the most common VVT operation strategies, with a focus on the gas exchange.

Basic rules of exhaust valve timing variation with engine speed:

As the engine speed increases, both valve durations and valve overlaps should be increased to offset the decreasing amount of time taken by the intake and exhaust strokes, thereby minimizing pumping losses and maximizing volumetric efficiency [92]. For a fixed duration VVT mechanism, the normal approaches to alter the overlaps could be by the adoption of early exhaust valve opening (EEVO) and late exhaust valve closing (LEVC) if the intake valve timing is fixed.

Asmus et al. [93] noted that early opening of the exhaust valve leads to reduction in the effective expansion ratio and expansion work, but this reduction is compensated by the reduced exhaust stroke pumping work and better scavenging. Part of the expansion work was also recovered from the turbine in a turbocharged engine. However, according to Siewert. [94] EEVO resulted in an increase of un-burned or incomplete hydrocarbon due to the interruption of the completion of the cylinder hydrocarbon reaction. Nevertheless, the NOx level could be reduced due to the reduction of the combustion temperature.

Based on the literature. [91], the LEVC (or the overlap between the intake and the exhaust valve) should be kept small at low engine speed to prevent back-flow, whereas it should be enlarged at high engine speed to take more advantage of flow inertia. Asmus et al. [93] demonstrated that with the higher boost pressure or higher speed for which the engine performance is optimized, a later LEVC time should be implemented to avoid any compression of the cylinder contents. He also stated that the level of the residual gas was not sensitive to the exhaust valve closing time, but the LEVC should be limited for PFI engines due to larger blow-through.

Miller Cycle

Application of the Miller cycle, which could be realized by either early or late intake valve closing (EIVC or LIVC), has the potential to reduce the effective compression ratio, thus mitigating knock at high load. In addition, it has been suggested in literature. [95] that the application of LIVC and EIVC could modulate the engine load without throttling on SI engines, and such an effect is expected to be more advantageous for NA engines than for downsized engines.

Miller. [96] proposed the use of EIVC to reduce the effective compression ratio to decrease the gas temperature and enhance the knock resistance of a supercharged gas engine. Other authors also stated that the lowered gas temperatures using the Miller cycle also resulted in reduced NOx emission [97-98]. Bozza et al. [99] tested the EIVC concept in a small-sized turbocharged SI engine at 3000 RPM and 3 bar BMEP, which is of interest of the European homologation urban driving cycle. The test results showed that significant BSFC reduction could be achieved with the pre-lift configuration allowing for the increase in the effective compression ratio and multi-lift, enhancing the combustion speed due to the higher turbulence intensity promoted by the second lift.

Asmus et al. [93] examined the idea of the LIVC and stated that there was a strong connection between the LIVC and the volumetric efficiency, depending on the mean piston speed. Taylor et al. [95] tested the LIVC concept on a Mahle 1.4 litre downsized engine (only turbocharged with the supercharger removed) and concluded that with their CamInCam system, at part load, the LIVC could achieve better pumping work due to de-throttling, thus resulting in better fuel economy; however, the use of a variable compression ratio (VCR) device was preferred to attain more benefits. The study by Martins et al. [100] provided additional proof of the advantage of combining the Miller cycle and the VCR by demonstrating that engines equipped with the Miller cycle had better fuel efficiency over the conventional Otto cycle, while significant efficiency improvements were found with the assistance of VCR devices. At high load, LIVC was also beneficial due to the enhanced knock resistance, but the improvement was limited by the heat transfer when the charge went back to the intake system. Akihisa and Sawada. [101] also proved that the decoupling of the compression and expansion stroke yielded up to 20% fuel efficiency improvement by exceeding the expansion ratio to be 20:1.

Li et al. [102] compared the performance of EIVC and LIVC operation for a highly boosted, high compression ratio, direct-injection gasoline engine. An improved anti-knock performance was found to be achieved when implementing either EIVC or LIVC strategies at high load (1000 RPM, 13.2 bar BMEP). LIVC seems to be advantageous over EIVC in high-load BSFC due to the better knock resistance and greater pumping work. However, at low load (2000 RPM, 4 bar BMEP), the fuel economy was better for EIVC, primarily owing to the reduced pumping loss. The improved fuel-air mixing and enhanced in-cylinder turbulence strength were also noted in EIVC operation, which was consistent with the earlier studies of Bozza et al. [99]

For a downsized engine, KJ-ZEM introduced by Mazda Motors Corporation is a good example. This engine was shown to be able to achieve 10-15% fuel efficiency improvement while still attaining a very high geometric compression ratio (10:1) [103-104]. For the mass production engine, the valvetronic concept first introduced by BMW on the 316ti compact in 2001 is a variable valve lift system, which, in combination with variable valve timing, allows for infinite adjustment of the intake timing and duration [105]. This system claimed to negate the need for a throttle body in regular use and utilized the valve lift and timing to control the engine load. Such system, via de-throttling, was demonstrated to be able to save at least 10 percent

fuel throughout the entire engine operating range, with a corresponding reduction in exhaust emissions.

Residual fraction control (usually achieved by EIVO):

The replacement of combustible gases with inert residual gases reduces the throttling requirements, but increases the indicated specific fuel consumption. The reduced throttling loss effect usually dominates, thereby enabling fuel consumption improvement. Hara et al. [106] stated that the back-flow caused by early intake valve opening (EIVO) could be used for internal EGR and might be helpful in reducing NOx. The literature review by Hong et al. [91] also reported a similar phenomenon, in which the EIVO allows the exhaust gas to be in contact with the low-temperature intake system, thus reducing NOx. EIVO could also be beneficial for pumping work as some of the exhaust mass reverses into the intake which indicates less burnt gas is expelled during the exhaust stroke. However, Asmus et al. [93] showed that EIVO was only beneficial at full engine load to purge the hot residual gas, with a large back-flow detected at part load, which led to poor behaviour for combustion.

Note that only controlling the valve timing may not always achieve the required engine performance across the entire engine speed range. As a result two or more sets of cam profiles are often adopted to switch between different engine speeds for automotive applications.

Major findings: For a turbocharged SI engine, the gas exchange process is strongly related to the valve event. A considerable effort of calibration must be conducted to optimize the engine performance under different engine operating points. In particular, at high load, where engine knock is an issue, the Miller cycle could be utilized to reduce the effective compression ratio, resulting in decreased gas temperature, thus mitigating the knock. At low load, the intake valve throttling (Also achieved by EIVC and LIVC, but not usually referred to as Miller cycle) might be able to achieve de-throttling purpose to minimize throttling losses.

2.4.4 Exhaust system optimization

Twin-Scroll Turbine:

Twin-scroll or twin-entry is achieved by dividing the entry of the exhaust mass flow into two scrolls [44]. This technique can use scavenging techniques, which is beneficial for decreasing

the exhaust gas temperature and the NOx emissions. It is also anticipated that such a layout could achieve better turbine efficiency and reduce the turbo lag at low engine speeds due to the elimination of pulse interference.

VGT:

Conventional downsized engines with a waste-gated turbocharger can only achieve high specific torque during medium to high engine speed owing to the fact that the turbine design is not optimized for the low engine speed [107]. In addition, waste-gated turbocharged engines also characteristics apparent turbo-lag compared with their NA counterparts. This is attributed to the period of time required for the turbocharger to reach high speed whilst providing enough boost pressure [108-109].

Compared to the fixed geometry turbine (FGT) which acts as a fixed restriction in the exhaust system, the VGT can vary the effective area in the turbine housing according to the engine operating condition. The VGT can thus achieve optimum efficiency in a wider range of speeds and loads [110]. In addition, because of the flexibility of controlling the engine load by controlling the throttle and the vanes in the VGT, a better strategy can be defined to improve both the steady state and transient performance [66,111].

However, VGT mechanisms have a tendency to stick resulting in possible failure [112]. Apart from that, cold start performance of VGT is generally deemed to be worse than that of NA engines considering the higher overall efficiency thus lower exhaust temperature after the turbine [113].

Water Cooled Exhaust Manifold (WCEM)

As the degree of downsizing is increased the component protection over-fuelling region becomes more significant, which limits the fuel consumption benefits. **Figure 2.9** shows the typical downsized gasoline engine component protection over-fuelling region [114]. The over-fuelling region is found to often occur at high loads, which is due to the higher peak cylinder temperature and is also attributed to the fact that at high loads the spark timing usually must be retarded, resulting in increased exhaust gas temperature. WCEM technology functions by cooling the exhaust gas temperature between the exhaust port and the turbine, thereby allowing a leaner air/fuel ratio to be achieved. This technology provides the benefits of controlling the air/fuel ratio to be stoichiometric, resulting in improved three-way-catalyst

efficiency and allowing for the use of low-cost materials for the turbine (VGT could also be used in gasoline engines). However, the cost of implementing such a technology into production gasoline engines and the requirement of increased boost pressure must be addressed.

DEP:

In the following, a review on a novel gas exchange process named DEP is presented. The process utilizes two exhaust valves in a turbocharged engine separately. The blow-down valve is connected to the turbine inlet to provide the target boost pressure whilst the scavenging valve bypasses the turbine mainly for the scavenging behaviour. By combining the exhaust system of a turbocharged engine and a NA engine, the strength of both could be enhanced while the limitations for each could be offset [15]. The engine with the DEP concept could benefit from a reduced 'averaged' backpressure (improved PMEP), reduced RGF, better combustion phasing, improved transient performance and enhanced cold start behaviour. The findings and results in the associated literature are detailed below.

The DEP concept was first mentioned in a British patent. [115] in 1924 and further patent claims have been made since then by several companies, including Deutz AG. [116], Fleming Thermodynamics Ltd. [117], Saab Automobile AB. [118], Borgwarner. [119] and TU Dresden. [120]

The first paper. [21] that can be traced on this concept involved both experimental and simulation work on a passenger car SI engine. The results showed that a positive pressure difference over the engine at the gas exchange TDC could be realized over the entire speed range. This observation, on one hand, significantly reduced the pumping loss and, on the other hand, reduced residual gas fraction compared to the baseline engine. This study also showed that the time to catalyst light off could be reduced because the exhaust mass flow can bypass the turbine by deactivating the blow-down valve. The author suggested that engines equipped with port fuel injection would not benefit as much from the DEP concept than that with direct fuel injection due to the possible blow-through. However, as most of the air/fuel ratio sensors are mounted on the exhaust side, DI engines require more calibration efforts for a DEP turbocharged SI engine. Pulse interference was also briefly investigated, and the author noted that the 200 CAD duration of the exhaust blowdown valve has already showed the ability to limit the pulse interaction, which is quite difficult to achieve

in other turbocharged engines. It should be noted that the exhaust valve diameter was designed to increase by 4 mm, but the author did not mention the benefits that the engine could gain without the DEP concept. Some other limitations, such as the requirement of utilizing a trapping valve at low engine speed, higher turbine inlet temperature and more severe choked flow in the exhaust valves were noted, and the author mentioned that adopting a fully variable valve mechanism, enhancing the material and cooling system in the exhaust blow-down system and the variation of the exhaust valve sizes might prove valuable to address the problems above. Last, a new turbocharger matching using a smaller turbocharger might need to be adopted because some of the exhaust mass flow bypassed the turbine which made it difficult to attain the target boost level.

BorgWarner. [18-19] has explored the DEP concept further using both simulation and engine tests for a turbocharged SI engine. Their concept, which is named the Valve-Event Modulated Boost (VEMB) system, applied a cam-phaser controlled concentric camshaft system to the exhaust side of a divided exhaust port 4-valve per cylinder double overhead camshaft (DOHC) GDI engine. The turbocharger boost was demonstrated to be controllable without the need of a conventional wastegate. In addition, a unique external EGR system from the scavenging path was used to effectively control the turbine inlet temperature. Their model and engine test results indicated the ability for the turbocharged engine using the VEMB concept to operate at a higher BMEP across the engine speed and load with some fuel efficiency improvement (up to 12.24%) due to increased PMEP and better combustion phasing (up to a 17 degree crank-angle). As in the literature described above, the exhaust valve area in the VEMB system was also increased, and the port flow characteristics were redesigned, resulting in an improvement of 13-15%. The possibility of increasing the compression ratio was briefly mentioned in the paper, but more investigation is required to validate the statement. Hu et al. [17] performed some simulations on the possibility to increase the compression ratio for a DEP based engine. In their model, the compression ratio was found to be increased by at least 0.5.

A more recent research paper by BorgWarner and PSA. [20] provided a summary for the DEP research. They noted that, based on the improvements the VEMB system has already shown on the 4-cylinder turbocharged engine, the potential of utilizing such a system on extremely downsized engine applications could also be high. A PFI turbocharged 2-cylinder engine was selected to validate the assumption. By using proper valve events, the VEMB was found to

also be very promising for PFI engines with high specific output. The authors also suggested that engine efficiency at partial load might not be as beneficial as that at the mid to high load operating points.

The DEP concept was also investigated on heavy-duty diesel engines [22-24]. (although this chapter concentrates on the SI engine, some conclusions or summaries from the described literatures are still useful for the design of a DEP concept SI engine). The author concluded that the optimum valve timing was determined by the trade-off between the produced turbine power and the increased PMEP that gives the lowest BSFC. The possibility to control the mass flow and therefore the pressure ratio over the turbine was also noted. By optimizing the timing event, the turbine could be operating in a higher efficient area. However, this higher efficiency might only be true for 6-cylinder turbocharged engines because this effect was not evident in the model Hu et al. [13] were studying. The valve size was considered to have a large impact on the engine efficiency, and the author made the point that different optimal relationships between the intake, blow-down and scavenging valve area strongly depend on the current EGR system and EGR rate. Last, it was stated that at low engine speed, where the valves are less choked, it is possible to increase the full load curve because the DEP concept uses a smaller turbine than the standard.

A novel simulation study of the DEP was conducted at TU Dresden [3]. The difference in this study is that the two manifolds were connected to different turbocharger turbines to provide the possibility of a sequential or two-stage-regulated system. At the first operating range, which began at the lowest engine speed, a maximal portion of the available exhaust mass flow was directed either to the primary turbocharger (sequential) or the high-pressure turbocharger (two-stage) until the rated mean pressure was achieved through minimizing the scavenging valve duration. After the rated mean pressure was attained, a larger portion of the exhaust mass flow was then fed into the second turbine (sequential) or the low-pressure turbine (two-stage) to limit the torque increase whilst reducing the pumping loss. With the transition of the staged turbocharging system into the second operating mode, the sequential system would have the mode of parallel operation of both turbochargers; while for the two-stage-regulated system, the high-pressure stage would be phased out. The results showed a clear improvement in the scavenging behaviour in the lowest speed range, a reduction in the BSFC in the rated output range, as well as substantially more spontaneous torque build-up. The author also noted that the sequential turbocharged model showed

advantages in dynamic operation, while the two-stage system exhibits more continuous system behaviour overall.

Hu et al. [16] conducted a similar simulation study on a two-stage heavily downsized SI engine from the perspective of gas exchange (not considering combustion phasing). The schematic layout of the system is shown in **Figure 2.10**. By adjusting the three bypass valves, the two-stage system was demonstrated to behave similar to a standard DEP system, with one valve feeding the turbine and one valve evacuating the remaining mass flow directly into the exhaust. In addition, such system could also achieve the regulated-two-stage DEP concept with one valve feeding the high-pressure turbine and the other valve feeding the low-pressure turbine. At high and medium speeds, such a layout could achieve low backpressure during the end and the beginning of the exhaust stroke respectively, and at low engine speed, low backpressure was fulfilled across the entire exhaust stroke range. Reduced pulse interferences were observed for the entire range of engine speeds, which, together with the reduced 'averaged' backpressure, resulted in an improved pumping situation. Although, in their system, the combustion phasing was not considered, it was anticipated that the two-stage DEP system can also benefit from better combustion phasing due to the reduced intake boost and temperature together with decreased RGF. The geometric compression ratio could also be increased to further improve the fuel efficiency at part load, but more investigation must be conducted.

Turbo-discharging

At Loughborough University, a novel DEP called turbo-discharging was first investigated by means of both simulations and engine tests [25-27]. This concept can be applied to both NA and turbocharged engines. For NA engines (see **Figure 2.11**), the blow-down pulse is fed into the turbine while the scavenging mass flow is directed to the post-turbine or the pre-compressor. Different from the conventional turbocharger system, the compressor in the TD system is used to depressurize the scavenging manifold rather than compressing the inlet charge. This process, on one hand, leads to sub-atmospheric pressure (< 0.5 bar) in the scavenging manifold, which is beneficial for the pumping work as well as the reduction of trapped residual gas fraction; on the other hand, the depressurization of the post turbine side leads to an increased pressure ratio across the turbine for the same blow-down pulsation. The TD concept, when implemented on a turbocharged engine, will have a similar layout, which shown in **Figure 2.12**. Note that both the scavenging manifold and the primary

turbine outlet is connected to a secondary turbine before the primary compressor. This configuration has proved to have a similar effect of improving the pumping work and increasing the pressure ratio across the turbines for the same blow-down energy. Simulation results showed that up to 5% fuel consumption could be reduced and the torque performance could be improved by 7% due to reduced pumping loss and better combustion phasing.

For clarity, **Figure 2.13** presents the idealised part load in-cylinder pressure-volume diagram, showing the primary and secondary gains of a Turbo-Discharging system compared to a conventional engine configuration (NA or turbocharged). The lower exhaust pressure is observed to be developed by the depressurization of the exhaust contributes to significant reductions in the pumping work. Although the improvement of the engine's breathing characteristics is counteracted partially by the increased engine throttling to maintain a given engine load, which has been shown to be a small effect in comparison to the pumping work benefit gained by the lower exhaust pressure. Such a concept also has some secondary gains which include a reduced trapped hot residual resulting in additional spark advance in SI engines and a potential to increase the compression ratio.

Although the TD system has shown fuel economy benefits for the NA and turbocharged configuration in simulation, the integration of after-treatment systems was not considered. The authors suggested that a wastegate feature could allow control of TD system to balance the thermal and breathing requirements of the engines at high loads, and there is no apparent difference between the TD concept engine and the NA or turbocharged engine at part load for thermal management, as there is no blowdown event to activate the TD system. In addition, some issues might exist for the matching of the EGR system to the TD concept engine as the peak exhaust pulsing pressure is comparable to the conventional engine solution, but the average pressure is lower.

Mirror gas turbine:

The mirror gas turbine is a novel concept focusing on how to improve the gas turbine's thermal efficiency by the regeneration of the otherwise wasted energy after the turbine. The basic schematic is shown in **Figure 2.14**. The ambient air is drawn into the first compressor, where it is pressurized. The compressed air runs through a combustion chamber where fuel is burned heating the air. The heated, pressurized mass flow then gives up its energy

expanding through the first turbine to produce the work output (if the gas flows into the ambient, then the cycle is called the Brayton cycle). The hot gas after the gas turbine expands through a second turbine rather than flowing into the ambient and cools down by a heat exchanger. A second compressor that is coaxial with the second turbine compresses the mass flow to the ambient to complete a circulation. This process can be imaged as a reflection by a mirror virtually placed between normal Brayton cycle and inverted Brayton cycle, thus termed a mirror gas turbine [121]. Note that one or more compressors could be linked to the second turbocharger to achieve more exhaust energy recovery, and it can be said that with infinite compressors, the recovered exhaust energy can be maximized.

Although this concept has been, to the author's knowledge, only proposed for gas turbine plants, a similar configuration could also be applied to turbocharged SI internal combustion engines. For turbocharged SI engines, the exhaust energy after the turbocharger turbine is still high, which can then be fed into the inverted Brayton cycle to reclaim some of the otherwise wasted exhaust energy (see **Figure 2.15**).

Figure 2.16 shows a temperature and entropy diagram of a turbocharged SI engine with three stages of inverted Brayton cycle compression. The intake charge enters the cycle at state 1 through the turbocharger compressor where it is pressurized and then leaves at state 2. The air then goes through the compression process to state 3, the heat addition process to state 4 and an expansion process to state 5. The air subsequently expands through a turbocharger turbine before leaving at state 6. As the exhaust gas still carries a large amount of thermal energy, the gas can be further expanded within the next turbine to state 7, where the pressure of the gas could be below atmosphere. The depressurized gas then passes through an intercooler to remove the remainder of the heat to state 8 before the gas is compressed back up to atmospheric pressure by one or more compressors. As suggested by the TS diagram, adding additional compressors will improve the exhaust energy recovery, thus increasing the thermal efficiency. Chen and Copeland. [122] recently suggested that up to 6% fuel efficiency improvement could be achieved depending on the engine operating points, by the adoption of Mirror gas turbine concept.

Major finds: The gas exchange process focused on the exhaust is mainly for the purpose of reclaiming the maximally possible exhaust energy whilst attempting to improve the corresponding backpressure. Twin-scroll turbine, VGT and WCEM are the approaches in the

production to improve the engine's breathing characteristics. For approaches only at the research stage, both the mirror gas turbine concept that could further recover the blow-down energy and the DEP/turbo-discharging layout focusing on the reduction of the engine backpressure have some potential to improve the engine's thermal efficiency, but with the penalty of additional cost, package and control complexity.

In the following table, the improvements of some important parameters in a turbocharged engine system have been summarized for each technology reviewed above. It can be seen that almost all the technologies have a positive effect on the enhancement of compression ratio. However, there is no technology which can simultaneously improve all the important parameters of a turbocharged engine. It is therefore anticipated that by combining different technologies reviewed above, higher fuel efficiency could be achieved through a better gas exchange process.

Table 2.3. Improvement of some important parameters for each technology

	De-throttling	Intake temperature at high load	Back-pressure	Turbine inlet temperature	Turbocharger performance	Compression Ratio
Inlet Manifold Design	√	√				√
WEDACS	√	√				√
Turbo-expansion	√	√				√
Stratified Charge	√			√		√
EGR	√		√	√		√
Cylinder deactivation	√					√
HCCI	√			√		
VVT	√		√		√	√
Twin-scroll Turbine			√		√	√
VGT			√		√	√
WCEM				√	√	√
DEP			√		√	√
Turbo-discharging			√			√
Mirror Gas Turbine		√				√

2.5. Chapter summary and conclusions

The gas exchange process (breathing characteristics) is crucial for the optimization of turbocharged SI engines, the behaviour of which is strongly related to the pumping work and also has a significant effect on the corresponding combustion efficiency. A number of novel technologies have been utilized to further improve the performance of turbocharged engines from the primary gain of the improved gas exchange process and/or the secondary gain, which includes enhanced combustion efficiency, increased compression ratio and reduced RGF. They have been categorized into four sub-sections including charge air pressurization/de-pressurization improvement, combustion efficiency enhancement within the chamber, valve event associated development and exhaust system optimization.

1: Novel charge air pressurization/de-pressurization improvement of turbocharged engines focus on two directions: pressurized intake charge cooling at high engine load and throttling loss reduction at low load. The intake charge cooling could be realized by the utilization of the otherwise wasted exhaust energy at high load, while the de-throttling purpose could be achieved by allowing the intake charge to expand through a turbine-like expander to reclaim some of the throttling loss.

2: The combustion efficiency improvement concentrates on the pumping loss reduction and the improvement of the combustion efficiency. If lean combustion is allowed, then the HCCI and stratified charge concept might be a good solution to improve the pumping work and the corresponding combustion efficiency. However, the limited operating width and the requirement of the seamless operation switch should be considered in advance. At stoichiometric condition, cylinder deactivation to further ‘downsize’ the SI engine or EGR to recirculate a portion of the exhaust gas back to the engine cylinders could have some benefits on turbocharged engine performance at low load and high load respectively.

3: Valve event associated development emphasize the mitigation of knock at high load and the realisation of de-throttling at part load. VVT is a proven technology currently applied to turbocharged gasoline engines, featuring improved breathing characteristics across all the engine operating points.

4: Technologies optimized for the exhaust system are mainly for the purpose of reducing the exhaust backpressure/temperature and utilizing the maximum possible exhaust energy. A twin-scroll turbine could lighten or even eliminate the negative effect of pulse interference. WCEM is the technology to reduce the pre-turbine temperature, with which VGT could be implemented in production gasoline engines. For approaches only at the research stage, both the mirror gas turbine concept, which further recovers the blow-down energy, and the DEP/turbo-discharging layout focusing on the reduction of the engine backpressure have potential to improve the engine's thermal efficiency with the penalties of additional cost, package and control complexity.

Figures in Chapter 2

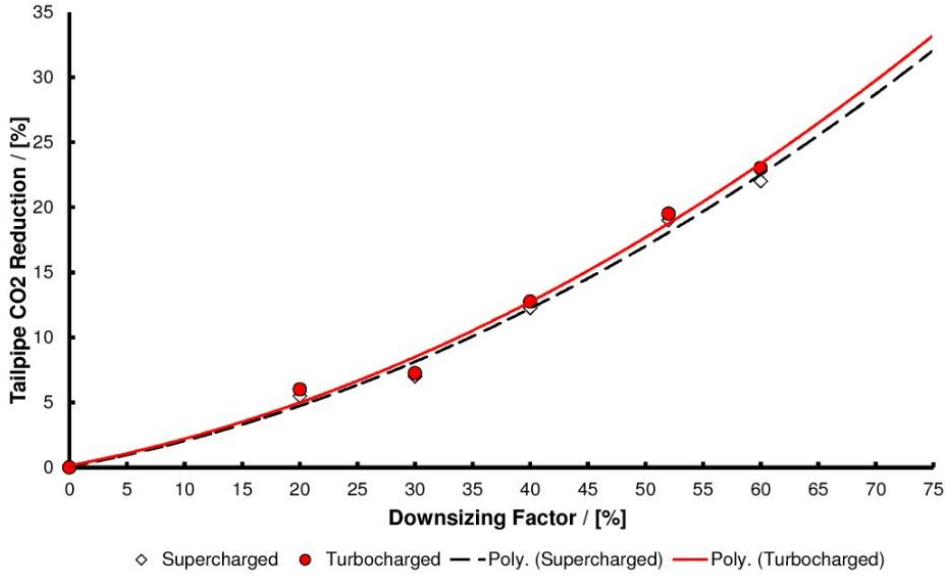

Figure 2.1. The potential for downsizing based on validation data from earlier work. [1]

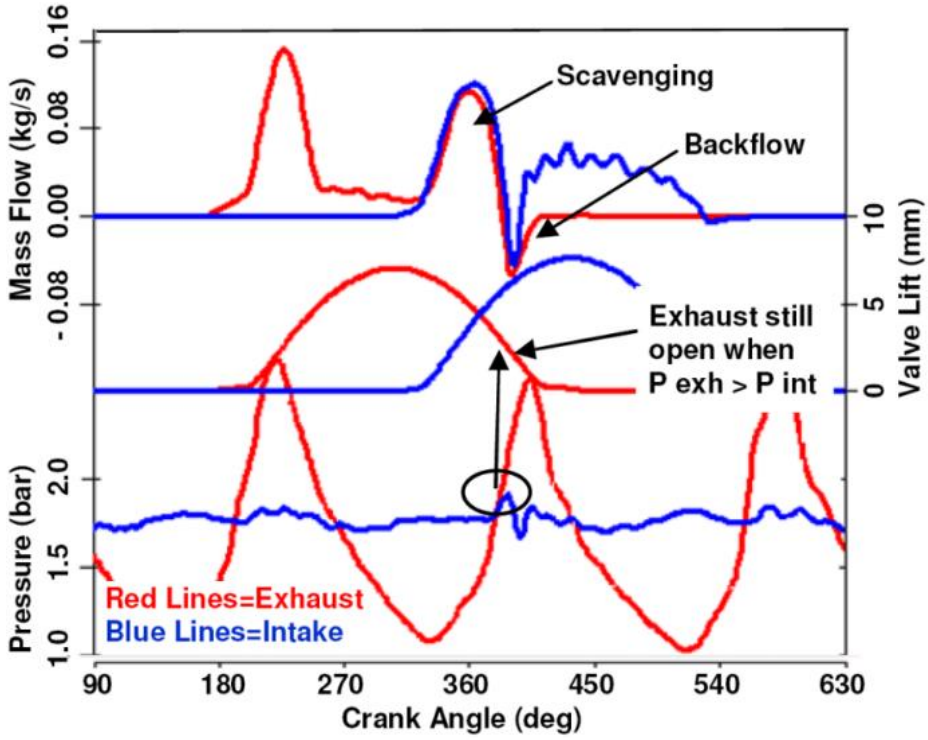

Figure 2.2. Blowdown interference on the Inline four cylinder engine with standard exhaust duration. [45]

P exh: exhaust pressure; P int: intake pressure

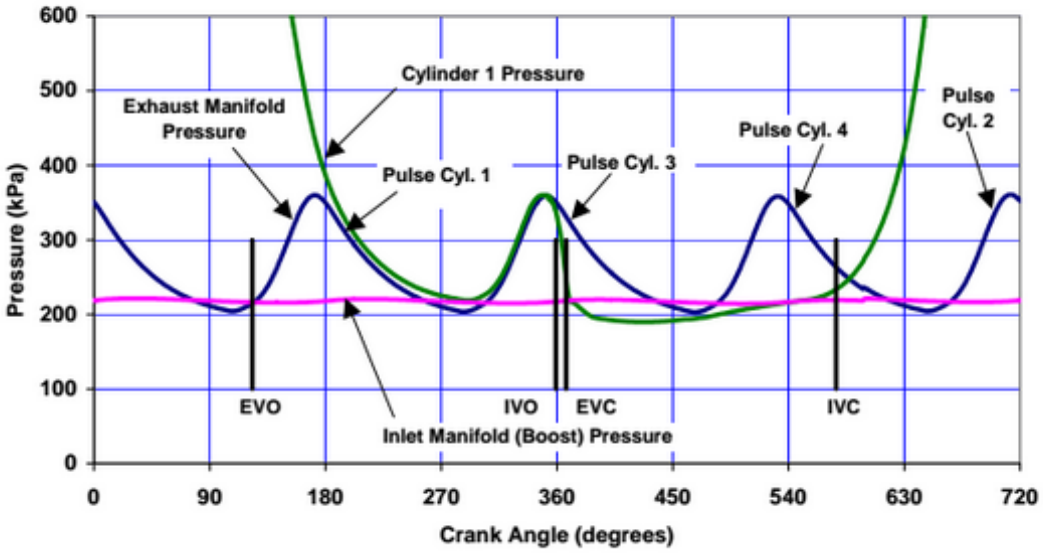

Figure 2.3. Four cylinder engine gas exchange diagram – cylinder 1. [46]

Cyl. 1: cylinder 1; Cyl. 2: cylinder 2; Cyl. 3: cylinder 3; Cyl.4: cylinder 4.

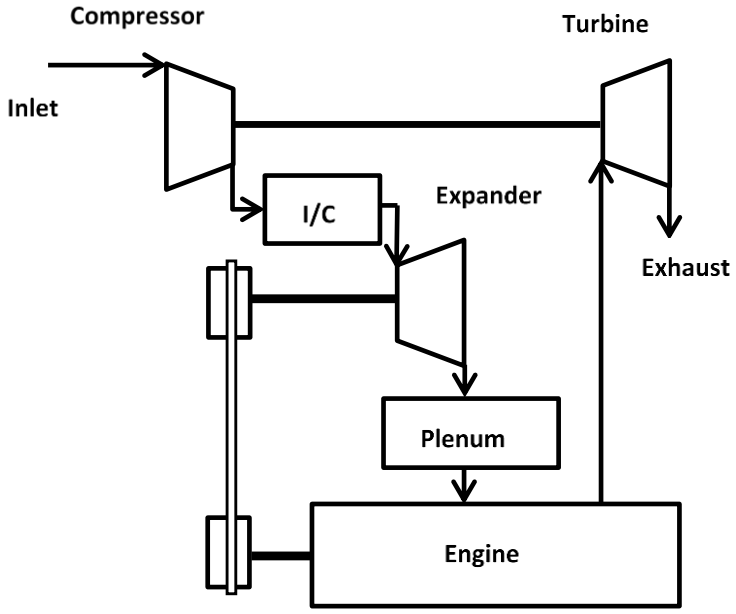

Figure 2.4. Proposed test engine system using an Opcon twin-screw expander.

I/C: inter-cooler

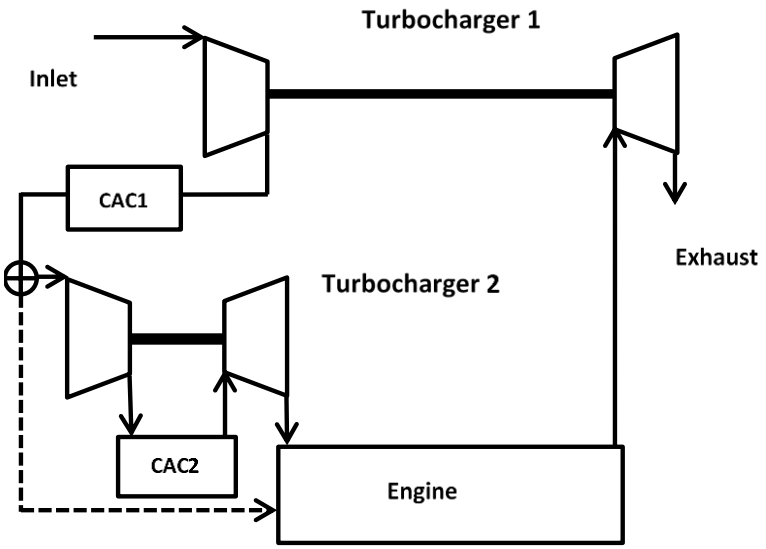

Figure 2.5. A turbo-cooling system.

CAC1: charge air cooler 1; CAC2: charge air cooler 2.

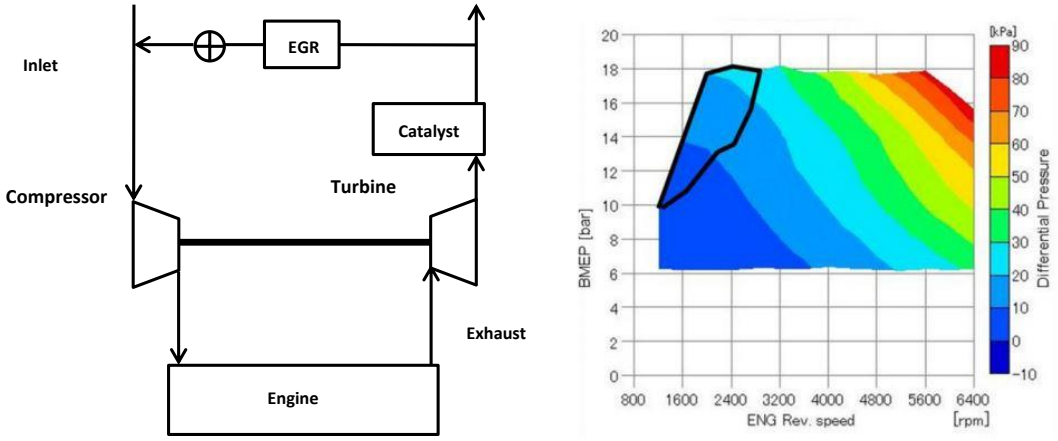

Figure 2.6. Low pressure loop EGR and a comparison of the differential pressures between the EGR gas extraction and the supply ports (EGR valve closed). [77]

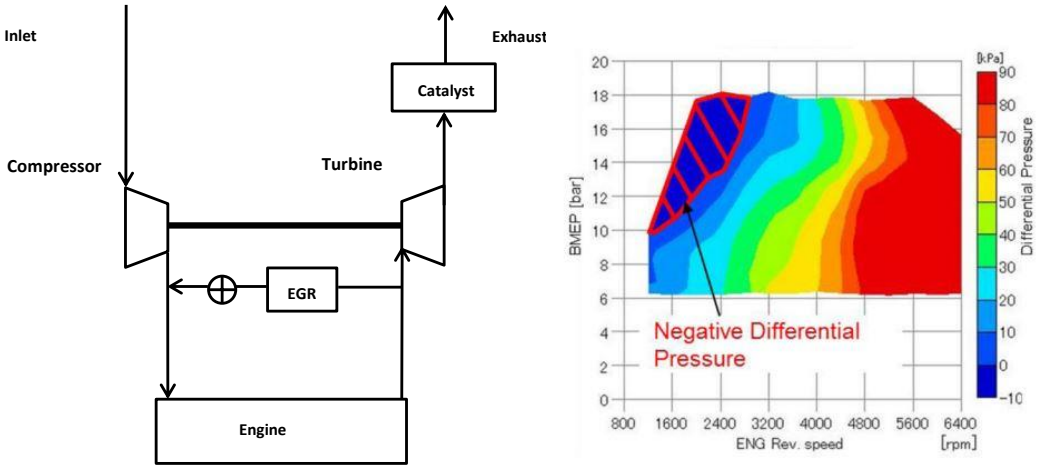

Figure 2.7. High pressure loop EGR and a comparison of differential pressures between the EGR gas extraction and the supply ports (EGR valve closed). [77]

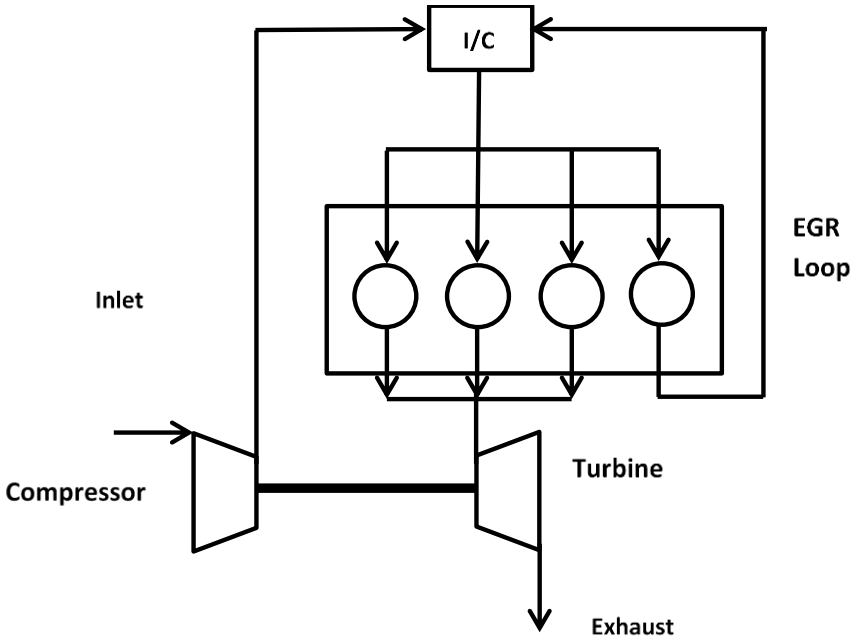

Figure 2.8. Schematic of a turbocharged 4-cylinder engine in a D-EGR configuration.

D-EGR: Dedicated Exhaust Gas Recirculation I/C: inter-cooler.

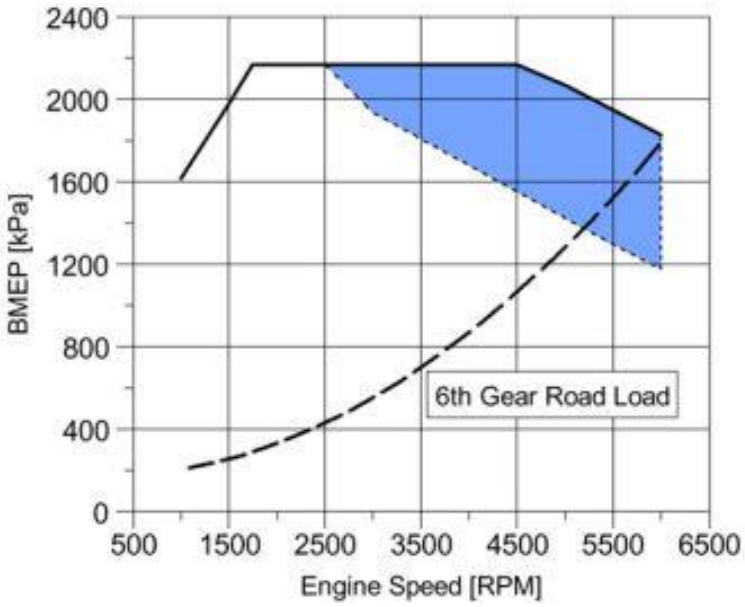

Figure 2.9. Typical downsized gasoline engine component protection over-fuelling region. [114]

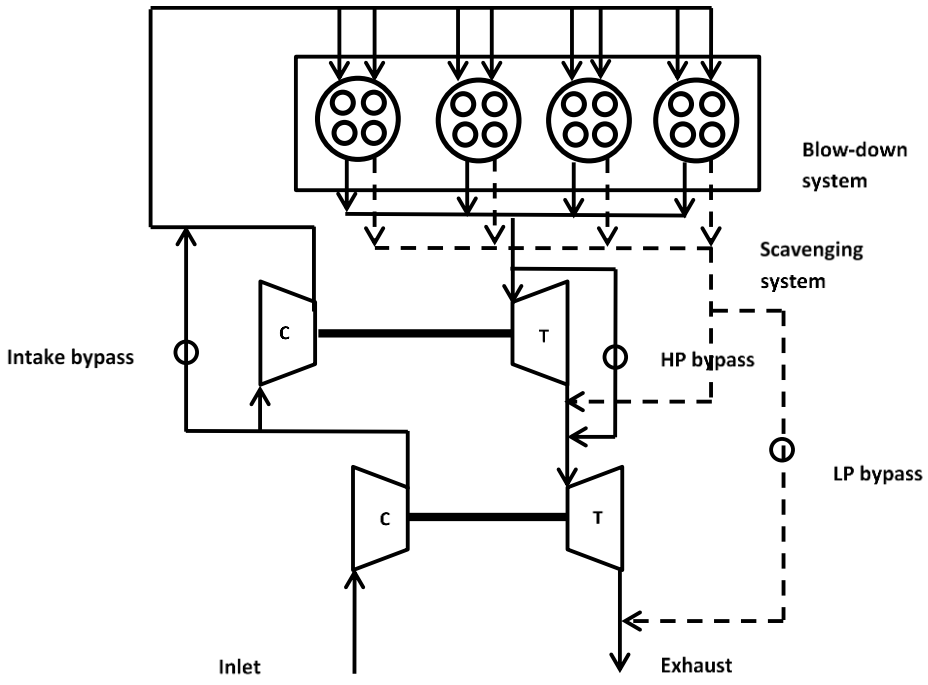

Figure 2.10. Regulated-two-stage DEP system

C: compressor; T: turbine; HP: high pressure; LP: low pressure.

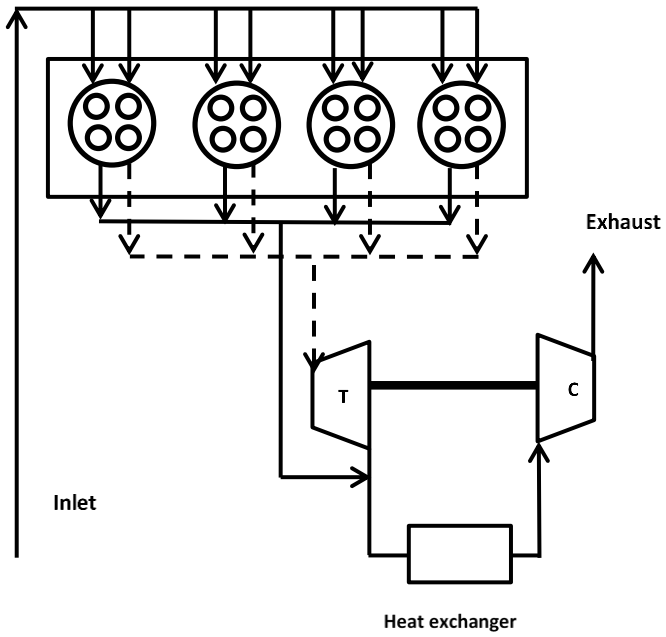

Figure 2.11. Schematic of an example exhaust arrangement of a turbo-discharged NA engine

T: turbine; C: compressor.

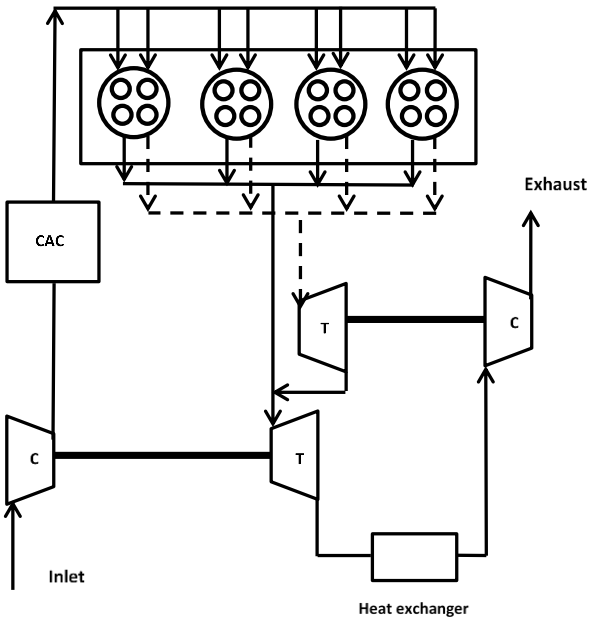

Figure 2.12. Schematic of an example exhaust arrangement of a turbo-discharged turbocharger engine.

CAC: charge air cooler; T: turbine; C: compressor

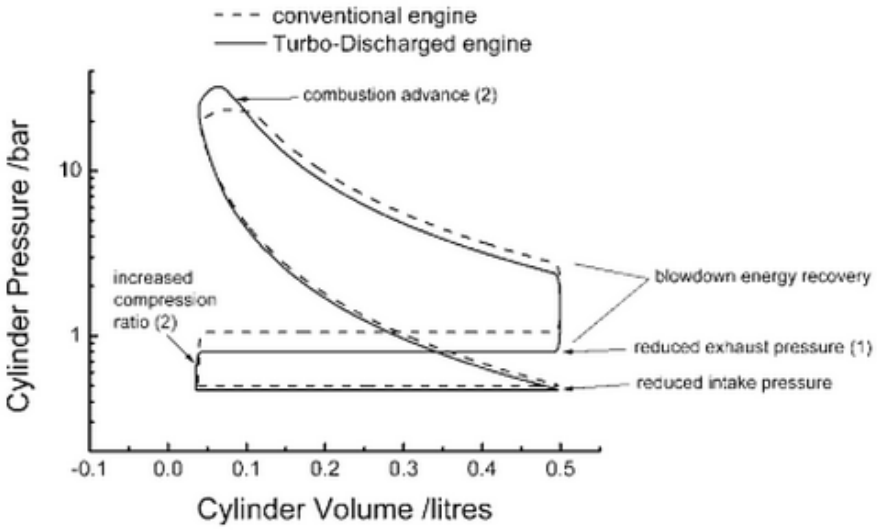

Figure 2.13. Idealised part load in-cylinder pressure-volume diagram showing the primary and secondary gains ((1) and (2) respectively) of a Turbo-Discharging system. [26]

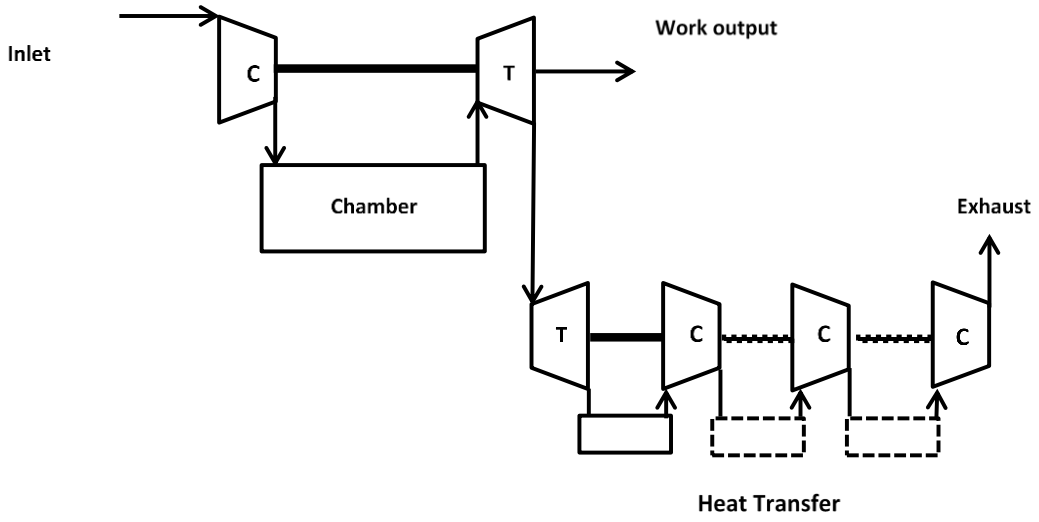

Figure 2.14. Mirror gas turbine

C: compressor; T: Turbine.

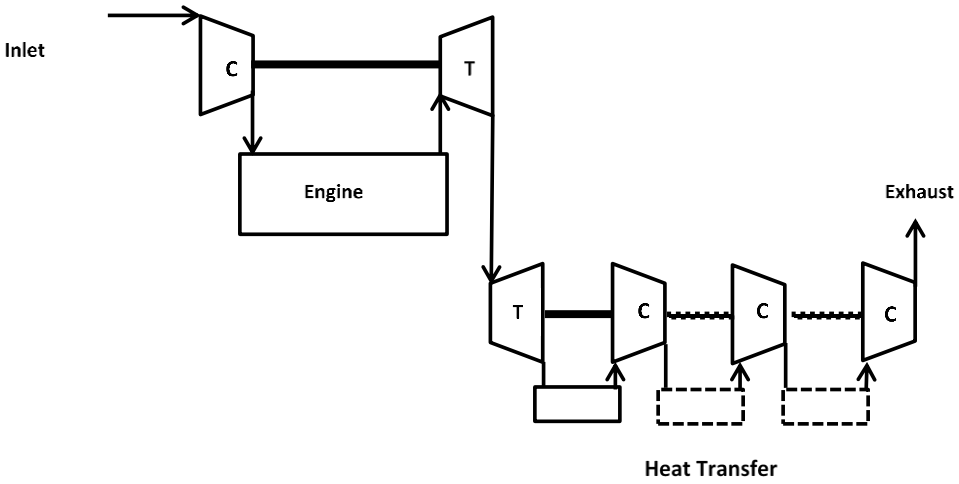

Figure 2.15. Proposed turbocharged SI engine adopting mirror gas turbine concept

C: compressor; T: Turbine

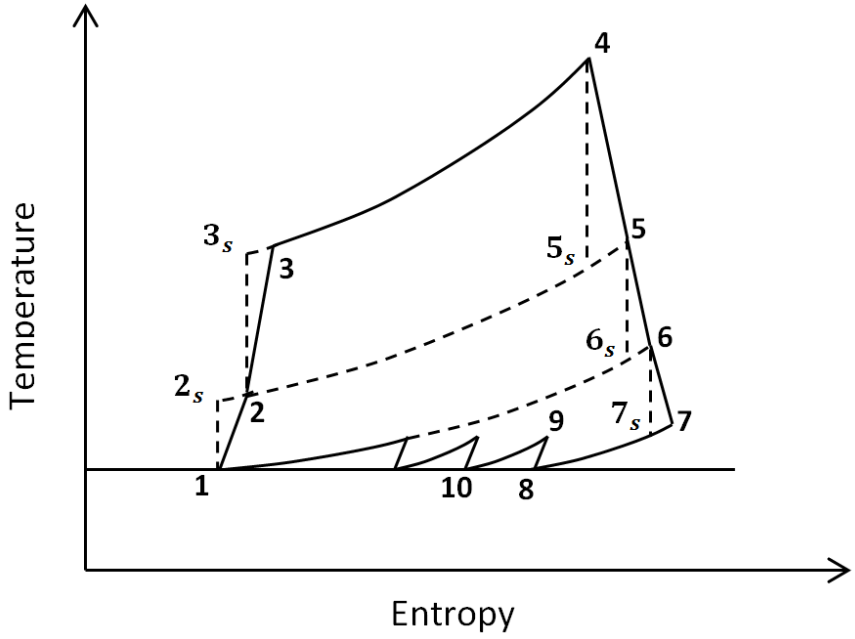

Figure 2.16. Temperature and Entropy diagram of a turbocharged SI engine with three stages of inverted Brayton cycle compression

Chapter 3 - *Review of the observations and potential trends for mechanically supercharging a downsized passenger gasoline car engine*

This chapter will present the observations on and potential trends for mechanically supercharging a downsized passenger car gasoline engine. It will first review the fundamentals and the types of supercharger that are currently or have been used, in passenger car gasoline engines. Next, the relationships between the downsizing, the driveability and the down-speeding are introduced to identify the improved synergies between the engine and the boosting machine. Then, mass production and prototype downsized supercharged gasoline engines are briefly described, followed by a detailed review of the current state-of-the-art supercharging technologies that are in production as opposed to the approaches that are currently only being investigated at a research level. Finally, the trends for mechanically supercharging a gasoline engine are discussed, with the aim of identifying potential development directions for the future.

The comparison, discussion and conclusion in this chapter have been published in the form of a review article in the Proceedings of Institution of Mechanical Engineer, Part D: Journal of Automobile Engineering.

3.1. Introduction

Engine downsizing is a proven approach to achieve superior fuel efficiency. It is conventionally achieved by reducing the swept volume of the engine and by employing some means of increasing the specific output to achieve the desired installed engine power, usually in the form of an exhaust-driven turbocharger. However because of the perceptible time needed for the turbocharger system to generate the required boost pressure, turbocharged engines characteristic degraded driveability when compared to their naturally-aspirated counterparts. Mechanical supercharging refers to the technology that compresses the intake air using the energy taken directly from the engine crankshaft. It is anticipated that engine downsizing that is realized either solely by a supercharger or by a combination of a supercharger and a turbocharger will enhance a vehicle's driveability without significantly compromising the fuel consumption at an engine level compared with the downsizing by turbocharging. The capability of the supercharger system to eliminate the high exhaust back pressure, to reduce the pulsation interference and to mitigate the surge issue of a turbocharged engine in a compound charging system offsets some of the fuel consumption penalty incurred in driving the supercharger. This, combined with an optimized down-speeding strategy, can further improve the fuel efficiency performance of a downsized engine while still enhancing its driveability and performance at a vehicle level.

In this chapter, the fundamentals and the types of supercharger are first briefly introduced, following which a description of the relationship between the downsizing, the driveability and the down-speeding is given for the purpose of understanding the interactions between the fuel economy and the vehicle performance. Some current mass production and highly downsized prototype passenger car engine will then be discussed. Finally, conventional and novel approaches to supercharging are compared, with the aim of identifying potential developments in the future.

3.2. Fundamentals and types of supercharger

The term 'supercharger' in this work refers to an air pump that increases the pressure and thus density of the charge air supplied to an internal combustion engine by directly connecting to an engine's crankshaft (and thus taking power from it) by means of a belt, gear or chain [37].

In general, there are two main types of superchargers defined according to the method of gas transfer: positive-displacement compressors and centrifugal compressors [2].

Positive-displacement units offer a relatively constant boost characteristic since they pump air at a fixed rate relative to the engine speed and the supercharger size. In many respects, a positive-displacement supercharger may be a more easily integrated device than an aerodynamic supercharger is. It is a lower speed machine and can therefore have a simple drive system to the crankshaft; it also has air consumption characteristics similar to those of a typical internal combustion engine [123].

For passenger car engines, the most frequently used positive-displacement superchargers are the Roots[1] type and the twin-screw type (the latter incorporates internal compression and therefore is correctly termed a compressor; the former achieves all compression externally and therefore is properly called a 'blower') [124-125]. Both Volkswagen and Volvo used Eaton (Roots-type) superchargers in their production compound-charged gasoline engines [31-32,126], and Lotus, Audi and Jaguar have used them as single-stage boosting devices in recent production engines [127-129].

Figures 3.1 and 3.2 show an Eaton TVS Roots-type supercharger [130] and the lobes from a Lysholm screw-type supercharger [131] respectively.

Centrifugal compressors are generally more efficient, smaller and lighter than their positive-displacement counterparts. Their drawback lies in the fact that the supplied boost increases with the square of the rotational speed, resulting in a low boost at low engine speeds [123]. This is ideal in aircraft and marine engines, which are commonly matched to a propeller [29], but not for an automotive engine which uses far more of its operating map. Furthermore, the pressurization requires high tip speeds and therefore, in order to provide sufficient boost, centrifugal superchargers usually need to be driven by some form of step-up gearing which inevitably incurs some additional mechanical losses [132].
Until now, centrifugal superchargers have generally been aftermarket parts for passenger car engines, and one application, the BRM V16 racing engine, famously demonstrated the

[1] Philander and Frances Roots patented what is now referred to as the Roots blower in 1860 as a machine to force air into blast furnaces and mine workings. It thus predates the Otto cycle engine.

challenge of mitigating the speed-squared relationship between the engine speed and the boost pressure [133]. One means of alleviating the undesirable boost build-up characteristic is to employ a drive-ratio-change mechanism. Such systems became commonplace on aero engines in order to match the performance to altitude better [29-30, 134], and one engine, namely the Daimler-Benz DB601, used a continuously variable speed-change mechanism, albeit with relatively high losses [28]. Recently two devices SuperGen and V-Charge have been produced which achieve continuous variation in the drive ratio, and this capability has shown a significant performance potential over a Roots-type device as the high-pressure stage in a compound charging system [132, 135]. **Figure 3.3** shows the Torotrak V-Charge device [132].

Apart from external positive-displacement devices that provide boost for a passenger car engine, the engine cylinder itself can also be treated as a positive-displacement unit. The Scuderi engine shown in **Figure 3.4** is an example of this approach which divides the four strokes of a conventional combustion cycle over two paired cylinders (one intake/compression cylinder and one power/exhaust cylinder), connected by a crossover port [136-137]. By dividing the function of compression and power into two paired cylinders in a 'split cycle', in theory the thermal efficiency is improved owing to the increased flexibility in optimizing the combustion and the pumping work. In addition, the possibility for pneumatic hybridization [138-139] and the Miller cycle [140] can also provide additional fuel consumption benefits. However, pumping losses past the crossover valves and through the crossover ports, energy losses during the heat transfer from the compressed air to the compressed cylinder and crossover port walls and thermal loading are challenges for this type of devices. Nevertheless, recent advances show promise, albeit with greater levels of complication [141].

The pressure wave supercharger (PWS) (sometimes termed a Comprex), which is illustrated in **Figure 3.5**, is an unconventional device that, unlike any other supercharging system described above, pressurizes the intake air directly by the compression wave generated by the pressure difference between the exhaust mass flow and the intake mass flow [142-146]. The transient response of a PWS-based gasoline engine is superior because the pressure wave propagates at the speed of sound. In addition, for some engine operating points the isentropic efficiency of the PWS system is much better than that of a turbocharged counterpart. For example, the maximum efficiency of a PWS was 75% at 3000 r/min

according to the research conducted by Oguri Y et al [146]. It should be noted that, unlike any other conventional mechanical supercharging system with the power directly provided by the engine crankshaft, the PWS system scarcely consumes the useful engine power (more like a turbocharger), even though the rotor is usually driven by the engine. There are several challenges for the PWS system when it is adapted to a passenger car engine. For example, the length of the rotor channel cells, the port timing and the rotor speed all have to be matched to the engine size and can be adjusted for different engine operating points. In addition, the relatively lower isentropic efficiency of this device at higher exhaust pressure also needs to be overcome before applying it to a production passenger car engine [146].

3.3. Novel compressor designs

In this section, three compressor types which are new to the market are discussed: the TurboClaw, the Eaton TVS Volumetric Series (V-Series), and a novel compressor from Honeywell. These compressors are able to enhance the low-end torque and to improve the transient performance of a boosted downsized engine, thus providing the potential to downsize and down-speed it further. In the following, first the characteristics of the Turboclaw are presented, followed by a critical discussion of the Eaton TVS V-Series and the novel Honeywell compressor.

The TurboClaw compressor is able to provide a higher boost at a lower speed range, by radically changing the geometry of the compressor to a geometry with highly forward swept blades (see **Figure 3.6**) [147]. A Turboclaw compressor map can be seen in **Figure 3.7** [147]. It is similar to that of a conventional turbocharger compressor but it operates at a significantly lower speed. Pullen et al. [148] demonstrated that, by electrically supercharging a gasoline engine using the TurboClaw compressor, which is not possible for a conventional radial compressor, the low-end torque and the transient performance of the engine are greatly improved.

In conventional Roots-type positive displacement blowers, due to manufacturing tolerances, smaller clearances at multiple locations between two opposing supercharger rotors, between the rotor and housing (see **Figure 3.8**) and between the end plates and the rotor ends (see **Figure 3.9**), cause leakage from the outlet of the conventional series-production Eton TVS R-Series to the transfer volume and from the transfer volume to the inlet, resulting

in a reduced volumetric efficiency. In particular, the smaller TVS R-Series devices, which typically match a three-cylinder or four-cylinder engine with a displacement from 0.5 L to 2.0 L, have substantially reduced low-speed volumetric efficiency owing to the increased ratio of the leakage area to the displacement. In order to improve the low speed volumetric efficiency, Eaton has optimized multiple parameters including the ratio of the rotor length to the rotor diameter, the number of lobes, the rotor twist and the inlet and outlet port geometries. The output of several optimization iterations is a new TVS V-Series. Compared with the R-Series, the V-Series features approximately 32% less leakage cross-sectional area per unit displacement. In addition, V-Series devices have better isentropic efficiency at lower supercharger speed owing to its physical characteristics. The combination of a higher volumetric efficiency and a higher isentropic efficiency in the low supercharger speed range allows the minimum engine peak torque speed to be reduced or the low-end torque target to be met with a lower drive ratio than that required by the R-Series, in turn reducing the intake mass flow recirculation at higher engine speeds, which results in better pumping work. It should be noted that the V-Series can also increase the low-end torque to downsize a passenger car engine further if the boost capability rather than the engine knock was the constraint [130].

The novel compressor supplied by Honeywell is also a device that can provide the same pressure ratio at lower rotational speeds [132]. It is not clear from the literature at the moment which technology has been implemented to achieve this. The deficiencies of this type of compressor are a lower maximum pressure ratio and a narrower speed range. The merits of this device when fitted on a passenger car engine are similar to those of the TVS V-Series, i.e. it reduces the minimum engine peak torque speed if the same drive ratio is applied or it reduces the drive ratio if the same peak torque speed is desired, which in turn minimizes the pumping losses at higher engine speeds. Both scenarios can help to downsize or down-speed a gasoline engine further [132].

3.4. The relationship between downsizing, driveability and down-speeding

The engine downsizing refers to the use of a smaller-displacement engine to replace a larger-displacement engine, usually employing turbocharging or supercharging in order to maintain

in-vehicle installed power [40, 149]. Most downsized passenger car engines currently offered in the marketplace appear to have a DF of approximately 35% to 40% [7].

It is anticipated that the DF of future highly downsized engines may reach levels at or above 60% as some current prototype engines can now achieve approximately a DF of 50%-60% using some new technologies currently in development. This is mainly due to the demand to reduce the carbon dioxide (CO_2) emissions of the vehicle further in the near future. Practically, this can only be achieved by a two-stage boosting system together with at least one turbocharger to make use of the waste exhaust gas energy [150]. These two-stage configurations can also realize a higher overall isentropic efficiency as both the high-pressure boosting devices and the low-pressure boosting devices are able to operate in their higher-isentropic efficiency area in two different flow regimes.

The motivation for further downsizing a passenger car engine can also be seen in **Figure 2.1** from the last chapter, which shows the potential for downsizing based on some validated data [7, 34]. The increase in the improvement is mainly due to the reduced pumping losses at part load, the reduced heat losses and the lower friction, which result in a higher mechanical efficiency for smaller displacement engines.

However, appropriate engine downsizing is also important when the driving cycle fuel consumption and the driveability are considered. The so-called 'correct sizing' of the engine should be able to handle the power requirement of the frequent operating points without the assistance of boosting devices. This is especially true for a fixed-drive-ratio supercharger system equipped with a clutch, because a large amount of parasitic losses occurs when only little boost is required and the driveability quality is greatly impaired when a clutch is transiently engaged [151].

The driveability, which in this chapter is defined as the degree of smoothness and steadiness of acceleration of an automotive vehicle, describes the driver's expectation of a vehicle. It is, by its nature, a subjective rating, and hence is difficult to quantify. However, there seems to be some correlation between subjective assessments and objective measurement (characteristic values are given in **Figure 3.10**) of a vehicle's behaviour. More specifically, we find the following [152]:

a) There is a strong correlation between the delay time or the initial acceleration and the launch feel, while there is no clear correlation between the jerk and the launch feel.
b) There is a clear correlation between the delay time or the initial acceleration or the jerk and the performance feel.
c) There is a degree of coupling between the delay and the initial acceleration in the subjective assessment of the launch and the performance feel.

Boosted engines and, in particular, turbocharged engines are considered to have poorer driveability than do their naturally-aspirated counterparts because of the perceptible time needed for the boosting system to generate sufficient intake mass flow. With the requirement of further downsizing, the driveability issues become more severe. In this context, supercharging might have to be introduced either in a single-stage configuration or in a compound charging arrangement in order to overcome turbo-lag at low engine speeds.

Since downsizing is arguably already reaching a limit [7], down-speeding may become much more important for increasing fuel efficiency in the near future [153]. Down-speeding refers to lowering the engine speeds by means of using longer gear ratios or by optimization of the transmission gear shift strategy to improve the vehicle fuel economy of a downsized engine further. In many respects, down-speeding functions similarly to downsizing, i.e. it moves the engine operating points to a higher-efficiency region on the engine characteristic map. However, down-speeding can be expected to affect a vehicle's transient performance negatively; thus, for a particular application, the driveability needs to be considered before optimizing the transmission gear ratio or the strategy.

It should be noted that it may not be fair to compare the fuel economies of different boosting systems using only the same engine operating points of an engine, as in a real driving cycle the different transient characteristics of different boosting configurations coupled with different transmission shift strategies result in different operating points of the engine. For instance, **Figure 3.11** shows the engine torque and speed trajectory after full–load acceleration for 5s from near idle speed in each gear for a turbocharged engine [154]. Thus, a relative accurate fuel economy calculation should be based on the transient performance of the engine and transmission events. In addition, fuel economy comparisons are better conducted for similar vehicle performance metrics, such as a similar time interval from 0

km/h to 100 km/h. In the following, first the effects of down-speeding are studied by using longer gear ratios, followed by some down-speeding control that is achieved by optimization of the transmission gear shift strategy. In both situations, the vehicle was operated in a dynamic environment, and the vehicle performance metrics were maintained.

Birckett et al. [155] simulated and tested a mechanically supercharged 2.4 litre in-line 4-cylinder gasoline direct injection engine employing the Miller cycle and a high compression ratio. It was proved that down-speeding, which was obtained by altering the transmission ratios (compared with downsizing the engine, in combination with supercharger de-clutching, compression ratio augmentation and a Miller cycle, and cooled EGR), contributed most to the improvement in the fuel economy over the 2.4 Litre NA baseline. However, it is worth noting that the low speed torque capacity was increased by approximately 100Nm and that, without the enhancement of the low speed torque and the corresponding increase in transient capabilities, the vehicle performance would have been greatly affected [153].

Wetzel [153] compared three different two-stage boosting systems, namely a twin-sequential-turbocharger, a supercharger turbocharger configuration and a turbocharger supercharger configuration, while maintaining the transmission and final gear ratio in simulation. It was shown that, at an engine level, the twin-sequential-turbocharged configuration had a slightly lower full-load BSFC while, at the vehicle level, the supercharging boosting systems benefitted from a BSFC approximately 8%-10% lower over the NEDC and 12%-14% lower over the Assessment and Reliability of Transport Emission Models and Inventory Systems urban driving cycle when compared with the twin-sequential-turbocharged configuration, because of its capability to allow down-speeding.

Ostrowski et al. [156] studied the effects of down-speeding and supercharging a passenger car diesel engine in test and simulation. Their results suggested that optimisation of the transmission shift schedule can produce greater fuel consumption benefits than does down-speeding by changing the drive ratios. In addition, after optimization of the transmission, their in-vehicle simulation results on the supercharged configuration showed an improvement in the fuel economy of up to 12% over that of the turbocharged counterpart, together with a corresponding reduction in the transmission shift frequency of up to 55% while maintaining the same first-gear acceleration, top-gear passing and acceleration performance of 0-60 mph.

From the analysis above, it is clear that there is a strong relationship between the downsizing, the driveability and the down-speeding. For boosted engines specifically, further downsizing can be enabled by the assistance of supercharging in a compound charging system; The driveability issue of a downsized engine can be mitigated by proper matching of a supercharger; and from the perspective of the real driving fuel economy, downsized passenger car engines could employ supercharging technology to move the operating points of an engine further into a more efficient area while maintaining a similar vehicle driveability.

3.5. Mass production and prototype downsized supercharged gasoline engines – an overview

A number of mass production and prototype downsized supercharged passenger car engines are listed in **Table 3.1**, which satisfy various customer requirements currently. They all have enhanced specific power and low-end torque together with an improved transient performance compared with that of a similar-size turbocharged counterpart. It should be noted that, among the list, the supercharger type is almost positive displacement, and most are Roots-type; and an active valve is usually employed to bypass or 'recirculate' the flowing through the supercharger when boost is not required. In addition, approximately half of the listed supercharged systems are equipped with a clutch, and clutched configurations have larger drive ratios than systems without a clutch.

Table 3.1. Typical downsized and supercharged gasoline engines

	Ultraboost (target) [7]	Ricardo HyBoost [157]	Ford 1.0L ECOBOOST – V-Charge [132]	Volkswagen 1.4TSI [35]	Volvo T6 [3, 158]	Jaguar Land Rover AJ126 [159]	Audi V6 TFSI [128]	Mercedes-Benz C32 AMG [160]	Mazda KJ-ZEM [104, 161]	Nissan HR12DDT [162]
Specific power (kW/l)	142 (6500 RPM)	105 (5500 RPM)	-	90	113	92	71	81	70.5	60
Peak BMEP (bar)	32 (3500 RPM)	29 (2500 RPM)	-	22 (1750-4500 RPM)	25 (2000-45000 RPM)	19 (5000 RPM)	17.5 (2500-4850 RPM)	17.7 (3000-4600 RPM)	16 (3500 RPM)	15
Displacement (l)	2.0	1.0	1.0	1.4	2.0	3.0	3.0	3.2	2.3	1.2
Compression ratio	9.0	9.0	9.0			10.5	10.5	-	10.0	13.0
Boosting configuration	Two stage supercharger + FGT	Two stage electric supercharger + FGT	Two stage supercharger + FGT	Two stage supercharger + FGT	Two stage Supercharger + FGT	Single stage supercharger	Single stage supercharger	Single stage supercharger	Single stage supercharger	Single stage supercharger
BMEP at 1000 RPM (bar)	25	23 (with electric supercharger assisted)	-	16	15.7	12	-	-	-	-
Transient response	Better than JLR 3.0L Twin Turbo V6 Diesel	-	At 1100 RPM, from 2 bar BMEP to full load, engine torque rising to 90% of the target full load within 0.73s.	At 1250 RPM, from 2 bar BMEP to WOT, 2 bar intake manifold pressure achieved	-	At 1000 RPM, from 1 bar BMEP to full load, engine torque rising to 90% pedal position within 2.3s	-	-	-	-
Drive ratio	5.9	-	Step-up: 3 CVT:0.281-2.82			2.483	2.5	-	-	2.4
Clutch	Yes	-	No	Yes	Yes	No	No	-	No	Yes
Engine Type	Prototype	Prototype	Simulation-phase	Production	Production	Production	production	Production	Production	Production
Supercharger Type	Eaton R-series R410	Centrifugal	Honeywell Compressor	Eaton	Eaton	Eaton R-series R1320	Eaton R-series R1320	Teflon-coated rotors Twin-screw	Lysholm compressor	Eaton Roots
Bypass Type	Active		Passive	Active	Active	Active	Active	Active	Active	Active

TSI: twin-charged stratified injection; BMEP: brake mean effective pressure; JLR: Jaguar Land Rover; BSFC: brake specific fuel consumption; CVT: continuously variable transmission; FGT: fixed geometry turbine; TVS: Twin Vortices Series; TFSI: turbocharged fuel stratified injection; RPM: revolutions per minute.

3.6. Challenges of conventional supercharged gasoline engines

Clutch control:

In a compound-charging system, at high engine speeds, for a supercharger with a fixed-ratio-drive configuration, both positive-displacement devices and centrifugal devices may violate their maximum speed limits because of their corresponding physical characteristics. In addition, for a low load within the naturally-aspirated region, constantly connecting a supercharger to the crankshaft increases the engine's parasitic losses which inevitably results in a degraded fuel efficiency. In this context, a clutch may be a necessary component for a supercharged engine in order for it to be disengaged in the high-engine-speed and steady-state low-load operating regions and to be engaged at low-speed high-load operating points and when a transient signal is triggered [132].

It should be noted that in **Table 3.1** the JLR AJ126 3.0 L V6 does not use a clutch as standard and, according to Meghani et al. [159], de-clutching delivered a peak improvement of only 2.6%. This may be because the clutch was mounted on the supercharger nose, i.e. after the drive pulley and the belt system, and thus a large amount of associated parasitic losses still existed. In the non-clutched configuration, the control strategy is much easier to implement as only a throttle or a combination of a throttle and an active bypass valve needs to be controlled. This also has some other benefits such as improved NVH and more compact packaging. However, the effect of the increased temperature after the supercharger due to the recirculation of the intake mass flow needs to be taken into account, especially when a turbocharger is installed after the supercharger to provide an enhanced boost capability and possibly better fuel efficiency. Another factor worthy of note is that the non-clutch configuration may only be feasible for positive displacement configurations since, because of the characteristics of a fixed-drive-ratio centrifugal counterpart (i.e. its boost increases with the square of the rotational speed), possibly higher parasitic losses are incurred.

Fully developed boost control (with or without clutch control) is a key technology when implementing a supercharger in a passenger car engine or a vehicle as part of a compound charging system when the supercharger has a high drive ratio to generate a high boost at low engine speed. To the present authors' knowledge, there does not seem to be any literature

covering this topic. However, from some simulation and test projects conducted at the University of Bath [7, 123, 132, 135, 152, 163], it is still possible to summarize some key challenges for developing a viable control strategy for the supercharger system (it should be noted that these follow only some suggestions arising from the engine simulation and test results from the University of Bath and these should not be interpreted to represent or be calibrated for any specific application).

First, if a clutch is mounted, having the clutch always closed (termed Sport Mode below) provides the best scenario for the transient performance owing to elimination of the transient delay of this element, but the fuel efficiency is also largely compromised. The economy mode refers to when the clutch is disengaged during the steady-state low load operation and is engaged when a boost is demanded. Economy mode requires selection of a proper clutch engagement time, as a shorter time will either break the clutch because of the unavoidable torque (given in **Equation 3.1**) or generate a torque dip (due to the referred inertia of the supercharger rotors) during a transient event affecting driveability. For example, in the simulation study by Rose et al. [163], the clutch acceleration torque can be seen in **Figure 3.12**. The engine torque dip phenomenon can also be seen in **Figure 3.13**, in which it can be observed that the economy mode (labelled SC disengaged) has a significantly lower engine torque during the first part of a transient event in comparison with the sport mode (labelled SC engaged). A longer engagement time is also undesirable since this negatively influences the engine's time-to-torque performance, also resulting in a degraded driveability. For the active-bypass-valve configuration, the timing to close the valve is also important during a transient; too fast a response will impede the gas transfer when the supercharger is still rotating slowly after the closing of the bypass valve. Thus a considerable time is needed to calibrate the system before a good transient response and an acceptable driveability is achieved.

$$T = I \times \dot{\omega} \qquad \textbf{3.1}$$

T: torque; I: inertia; $\dot{\omega}$: angular acceleration

Second, given the context that some automotive manufacturers partially close the wastegate of their turbocharger at part load to trade some fuel-efficiency for an enhanced transient performance, the supercharger could also be boosting within what is normally the naturally aspirated region or, if a compound charging system is considered, the turbocharger is boosted at the steady-state low-load operating point in order to consider the trade-off

between part-load fuel efficiency and transient performance. For a positive-displacement supercharger fitted with a clutch, the supercharger pre-spin strategy can also be utilized. It is when the bypass is closed with the clutch still disengaged, engine pumping speeds up the rotors to approximately 1/3 of the engagement speed, minimizing engagement time [164].

Finally, the ability to hand over the boost generation from a supercharger to a turbocharger is also challenging for a twin-charged passenger car engine. Also note that at high engine speeds when the fixed-ratio supercharger is not operational, a longer transient response is anticipated which delivers an inconsistent driveability characteristic [135].

Selection of the bypass valve type:

For a positive-displacement fixed-drive-ratio supercharger system, an active supercharger bypass may be a necessary component to fulfil the function of bypassing the supercharger when it is not needed if a clutch is fitted and controlling the boost. This is illustrated in **Figure 3.14**; although throttle control is able to alter the engine torque this incurs generating a larger amount of driving torque for the supercharger. In addition, an active bypass system allows linear air control, as seen in **Figure 3.15**, which is considered to be beneficial for noise suppression [162]. However, as discussed, adopting an active bypass valve creates extra complexity for the control system and may require a considerable time for calibration before the supercharger system can function for all the possible operating regions of the engine.

Although some passive bypass valves can function similarly like active bypass valves by tuning the action of the valve (Lotus used a passive, boost-capsule-operated bypass, see for example, the paper by Turner et al. [127]) i.e. the valves open on throttle lifts and idle, progressively close as the throttle is opened and open partially at peak boost to control the level reached, they may suffer some fuel consumption penalty at part load. In addition, the passive bypass valve may not be able to effectively use the supercharger pre-spin strategy, the operation of which is to close the active bypass valve with the clutch still disengaged to allow the engine to pump the supercharger rotor speed to approximately 1/3 of the engagement speed, thereby minimizing engagement time [164].

When boost control is specifically considered, a large amount of intake mass flow recirculates around the supercharger via the bypass valve at high engine speeds and part load, resulting in a reduced fuel efficiency; this also affects the intake manifold temperature which may

trigger knock. Although the reduction of drive ratio mitigates the recirculation phenomenon at high engine speeds, the low-end torque may suffer.

3.7. Potential trends for mechanically supercharging a gasoline engine

In order to overcome the deficiencies in the performance and driveability of production supercharged engines, its development has been continuous. Enhancement of low-end torque, improvement of transient driveability and reduction of low-load parasitic loss are three of the major development directions, and there is a degree of coupling between them. For example, an improved low-end torque also helps the time-to-torque transient performance.

Low-end torque enhancement:

As mentioned earlier, selecting some 'low speed compressor' increases the low-end torque, because of their capacity to provide a higher pressure ratio (PR) at low engine speeds. For instance, Meghani et al. [159] replaced the Eaton R-Series R1320 with a new Eaton V-Series V1270C in their JLR AJ126 3.0L V6 engine. Their test results indicated that even when equipped with a reduced drive ratio (from 2.483 to 2.472) and with a lower swept volume the device can deliver a noticeable torque gain at low engine speed. This is mainly due to the increased volumetric efficiency of the Eaton V-Series device and possibly also enhanced isentropic efficiency. However, they also pointed out that, with the clutch engaged, because of the more severe recirculation of the intake mass flow, the fuel consumption increases rather than decreases at low loads, where an improvement is expected to arise from the reduction in the drive ratio. Hu et al. [132] studied a similar configuration using a novel compressor supplied by Honeywell. This compressor was also claimed to have a higher boost capability at low engine speeds and its peak isentropic efficiency occurred in the low-speed and low-pressure-ratio area. Their simulation results indicated that by using the same drive ratio, this novel compressor configuration can increase the low-end torque performance. In addition, if the same BMEP is maintained, the novel compressor still benefitted from an enhanced isentropic efficiency which is important in designing a supercharger-turbocharger system. They also showed that in the Torotrak V-Charge variable drive supercharger system, this compressor had a better transient response than did a conventional centrifugal

compressor when the other control parameters were fixed. As such, their findings were in line with those of Turner et al., who investigated the SuperGen electromechanical supercharger in a highly downsized compound-charged engine application [135].

Increasing the drive ratio is another option to increase the low-end torque. However, a fixed-drive-ratio unit may not be suitable in this case, as a higher drive ratio will cause more intake mass flow recirculation at high engine speeds resulting in higher parasitic losses [165]. The high drive ratio may also mean that the supercharger reaches the over-speed region at a lower engine speed, therefore, the clutch has to be let out earlier in a compound-charging systems, which in turn results in less boost assistance at higher engine speeds. Thus, a CVT might be preferable to adjust the drive ratio for different engine operating points.

Several CVT-driven supercharger applications have been studied and reported in the literature. They have all been demonstrated to markedly enhance the low-end torque of a supercharged engine. However, there are also some other trade-offs to be considered. For example, the research by Rose et al. [163] focused on the relationship between part-load efficiency and transient response in a highly boosted downsized gasoline engine. Hu et al. [60] and Turner et al. [52, 57], on the other hand, studied the Turbo-expansion concept (as can be seen in **Figure 2.4**) by treating the positive-displacement device as an expander. It was shown that if a positive-displacement supercharger's speed can be reduced sufficiently (CVT preferred), the supercharger moves to an 'expansion mode' from its conventional compression mode, as seen in **Figure 3.16**. However, the isentropic efficiency of a compressor in its 'expansion-mode' drops significantly to approximately 45%, as seen in **Figure 3.17** [59]. Turner et al. [52] claimed that in simulation (although the later test results were not realistic [57]), by placing the supercharger at the high-stage of a compound charging system and over-compressing the turbocharger system by further closing the wastegate whilst using the supercharger as an expander to reduce the boost pressure after the supercharger to that required, some BSFC benefits are obtained as some of the otherwise wasted exhaust energy can be reclaimed directly from the supercharger to the engine. The combustion efficiency can also be increased as the intake manifold temperature was reduced by the 'expansion effect'; this may enable advancement of the spark timing depending on the increase in the RGF which results from the higher exhaust back pressure. The undesirable test results finally achieved by Turner et al. [57] were studied by Taitt et al. [58]. They proved

that for the components used on the investigated engine, it was the low isentropic efficiencies that prevented the necessary temperature reduction of the inlet charge air.

Improvement in the transient driveability:

First, since a transient clutch engagement event causes some NVH issues, a non-clutch configuration seems to be an ideal option. However this results in a reduced fuel efficiency at part load when boost is not needed, because of increased pumping work through the bypass valve (or the throttle if it is the only control parameter) and larger mechanical losses via constantly connecting a supercharger with the engine. More importantly, supercharging a passenger car engine without a clutch can cause the supercharger to over-speed or can affect its reliability and durability. In this context, a CVT-driven supercharger demonstrates its advantage as, by altering the CVT ratio, the supercharger rotor speed can be kept within its prescribed limits, also resulting in fewer parasitic losses at part load. The research by Hu et al. [132] has proved this. Their simulation results suggested that a clutch may not necessarily be needed for a CVT-driven centrifugal compressor as, at low load, by reducing the CVT ratio there was a fuel consumption penalty of only approximately 2% and, at higher engine speeds, the supercharger was well within the speed limit together with a fuel consumption of only approximately 0.5% to drive the supercharger constantly.

It should be noted that the CVT-driven supercharger (both positive-displacement and centrifugal) can also help the boost handover (from supercharger to turbocharger) during the end of a transient for a twin-charged passenger car engine and mitigate the inconsistent driveability characteristic at high engine speed when the fixed-ratio supercharger is not operational [135].

Second, a compressor suitable for generating increased boost at low engine speeds can also help improve the transient driveability owing to its quicker boost generation ability. A CVT inherently provides this capability, given that its ratio range is wide enough. For the detailed analysis of this effect on an engine, it is suggested that the previous section is referred to.

Finally, in this section, some novel mechanisms to provide supercharging are discussed. The followings are organised by the categories from purely mechanical supercharging to purely electric supercharging. As this work is focused on mechanical supercharging, electric supercharging is only briefly introduced to discuss the advantages and deficiencies of a

mechanical supercharger system compared with its electric counterpart. It should be noted that, as there is a degree of coupling between the torque capability and the transient response, the mechanisms discussed below are all beneficial for the low-end torque of the engine.

The Lontra Blade Supercharger is a variable flow compressor with the ability to meet the boosting requirements of a heavily downsized engine. **Figure 3.18** shows this positive displacement rotary device with a simple variable inlet port that provides dynamic control of the air mass flow rate and the internal compression ratio without changing its rotational speed [167].

The VanDyne SuperTurbo is also an enabling technology for heavily downsizing an engine without loss of the vehicle transient response and the peak power [149]. This technology, with its schematic shown in **Figure 3.19**, can achieve the benefits of turbocharging (via 1-2-3-4 in the figure) and supercharging (via 6-5-3-4) and turbocompounding (via 1-2-3-5-6) by uniquely controlling the CVT ratio.

Turner et al. [135] described the performance of the SuperGen device on an extremely downsized gasoline engine (Ultraboost in **Table 3.1**, DF = 60%) compared with a fixed-ratio positive-displacement counterpart (the Eaton TVS R410 used in original development of this engine [7]). The basis of the SuperGen supercharger is a power-split electromechanical transmission technology with an epicyclic traction-drive and two small permanent-magnet motors that provide a fully variable transmission between the engine front-end accessory drive (FEAD) belt and the high-speed radial flow supercharger impeller (see **Figure 3.20**). It should be noted that in the work of Turner et al. the system voltage was 12 V; this is possible since the energy path into the device is mostly mechanical (some power can be taken from a battery for transients, but this is only a small proportion of the whole) [135]. It was concluded in their work that, in steady-state 1000 RPM condition, SuperGen can allow a torque which is significantly higher by approximately 26.5% than that of its fixed-ratio positive-displacement counterpart. The transient performance also proved to be superior with an improvement of approximately 68%. Finally, since it is, in essence, a variable-ratio-drive device, a better match for the compressor speed was achievable which can provide an improvement in the fuel efficiency of 1.3% to 4.3% in part-load conditions, owing to elimination of the recirculation and the wind age losses associated with the Roots blower.

Some of this improvement was also attributed to the use of a centrifugal compressor, which the drive mechanism permitted.

Electrical boosting (e-boosting), which is realized by electrically driving a compressor (usually centrifugal), is able to decouple the boost process from the operating point of the engine. It is usually used in series with a turbocharger to increase the low-end torque and to reduce the turbo-lag. Typically an e-booster runs to approximately 1.4 bar-1.6 bar absolute on a standard 12 V setup within 200 ms–500 ms [169]. For example, the Ricardo's HyBoost project (the schematic can be seen in **Figure 3.21**) showed that by using a 12 V unit, the electric supercharger could provide boost generation twice as fast as without an electric supercharger [157]. This is mainly because the higher engine exhaust mass flow, achieved by the electric supercharger assistance, releases more power to the exhaust, thus accelerating the turbocharger's run-up.

It is worth noting that some, if not all, of the energy used to drive the supercharger is essentially free (on the assumption that it is gathered from regenerative braking by the alternator and stored in the battery), and this device is able to eliminate completely the torque dip issue challenging the control strategy. There are also other benefits from employing such a micro hybrid-type configuration (a total improvement in the fuel consumption of 12.5% was simulated during the HyBoost programme), including smart charging, improved stop-start and enhanced torque assistance. However, a potential drawback is that it is challenging to produce an e-booster that can run continuously owing to design considerations regarding overheating the motor (if it is high powered) and the subject of battery depletion in-vehicle during extended periods of operation. If it can run continuously and the alternator can supply sufficient power, the round-trip power transmission losses can then be significant. In this area the SuperGen approach shows merits since, during steady state operation, all power to the compressor comes into the machine from the FEAD, and the mechanical energy path through the device (which can transmit a significant proportion of the power – see **Figure 3.20** [135]) should be more efficient, while the electrical path does not go through the battery.

As voltages are set to increase to 48 V, so the efficacy of such an integrated approach improves on two levels: greater amounts of regenerative energy can be gathered by the higher-powered alternator; and the e-booster can generate more air flow and boost for

longer (due to the greater amount of energy gathered, and assuming the battery has the capacity to support this). At this point the technology becomes viable in larger and heavier vehicles.

Employing an e-booster at higher system voltages does assume that original equipment manufacturers (OEMs) are able to manage the transition from 12 V to 48 V across multiple engine and vehicle platforms simultaneously. However, in 'old' 12 V vehicle platforms attempting to deploy a 48 V engine platform is not be without its difficulties; extra work on the electrical system, employing a 48 V sub-net in the engine bay for example, may be necessary. Again, as an alternative to this a SuperGen-type device, which is voltage agnostic (because the drive energy is supplied via the FEAD with only limited and occasional draw from the battery), appears to be an ideal bridging technology to e-boosting as well as a complete solution to the problem, which is capable of delivering higher boost pressures because of its mechanical drive path.

As a final point when considering e-booster systems as part of a mild hybrid configuration with an increased voltage, Aymanns et al. [170] investigated the merit of using the energy stored in a battery to drive a supercharger versus applying it directly to the wheels via an electric motor. They reported that, because of the addition of fuel energy to the air supplied by the e-booster and the subsequent combustion providing increased work to the crankshaft, e-supercharging could provide approximately 10 times the torque to the wheels that just using the electrical energy in a motor can. Depending on driving situation, there is thus a trade-off to be investigated between the two means of utilization of regenerated energy in a driving cycle or real-world operation of a vehicle.

Reduction in Low-load parasitic losses:

As mentioned above, a supercharger system without a clutch suffers some reduction in fuel economy in the low-load region. It seems that parasitic losses always exist even though the drive ratio and the transmission efficiency could be further improved. However, Hu et al. [61] first proposed a novel concept to eliminate the parasitic losses completely at part load without the use of a clutch. They extrapolated the test data seen in **Figure 3.16** and **Figure 3.17** and imported the data into their twin-charged gasoline model. By controlling a CVT-driven unit, it is demonstrated that the conventional throttle control could be replaced by the CVT ratio control of the supercharger (the supercharger is now in its 'expansion mode')

while still reclaiming some of the throttling losses that are otherwise wasted during the throttle control. Since no clutch is needed, the NVH issues of supercharging a gasoline engine are also greatly improved. Other benefits such as the simplified control and the reduction of the intake manifold temperature can also show their potential. Nevertheless, some major deficiencies have to be overcome before applying this concept to a production engine. They include the requirement of a large CVT ratio range (as wide as 30) and consideration of the condensation effect, which may have some effect on the combustion behaviour. Meghani et al. [159] tested this concept by adopting a fixed-overall-ratio of 0.74. Four engine operating points (including 1000 RPM 2.5 bar BMEP, 1500 RPM 8.3 bar BMEP, 1750 RPM 8.3 bar BMEP and 2000 RPM 5 bar BMEP) were compared. The trends in the results are consistent with the simulation study by Hu et al, although they used a different Eaton supercharger on their test engine (Eaton V1270C V-Series). However, they also pointed out that the effect of supercharger leakage needs to be borne in mind, particularly at low supercharger rotational speed.

Re-matching a turbocharger to a twin-charged system can also be beneficial for the low-load parasitic losses. Here the parasitic losses refer to the pumping work incurred by the slightly higher backpressure in a turbocharged system. Since a supercharger can be used to provide boost at low engine speed, a larger size of a turbocharger can be selected in a compound charging system. This not only improves the isentropic efficiency of the turbochargers in the high-speed and high-load region, but also more importantly reduces the fuel consumption at part load owing to a reduction in the pumping losses. For example, King et al. [157] stated that by deploying a larger turbocharger in HyBoost system, an average improvement in the BSFC of 2% occurs at the key driving-cycle engine speeds and loads.

The Miller cycle, which can be realized by either early (EIVC) or late intake valve closing (LIVC), is also a viable approach to reduce the low-load parasitic losses (the parasitic losses here refer to the throttling losses) and the nitrogen oxide (NO_X) output in a supercharged gasoline engine [95-98, 102, 171]. Li et al. [102] tested the performance of EIVC and LIVC operation for a twin-charged, high-compression-ratio, direct-injection gasoline engine. It was demonstrated that at a low load (2000 RPM, 4 bar BMEP), the fuel efficiency was better for EIVC than for LIVC, primarily owing to the reduced throttling losses. Improved fuel-air mixing and enhanced in-cylinder turbulence strength were also noted in an EIVC operation, which was consistent with the research by Bozza et al. [99]

The ‘five-stroke’ internal combustion engine [173-179], which was proposed and patented by Schmitz, is also a concept to increase the expansion ratio without shortening the compression ratio. The five-stroke engine consists of two outer high-pressure cylinders working in conventional four stroke cycle and one inner low-pressure cylinder working in only expansion and exhaust stroke (see **Figure 3.22**). By optimizing the geometric compression ratio of the outer cylinders and the displacement of the inner cylinder, the research by Li T et al. [173] showed that this concept not only improve the fuel conversion efficiency at the middle loads and high loads, because of the increased combustion efficiency, the reduced exhaust energy and the extra expansion work in the inner cylinder, but also can facilitate a reduced fuel consumption at low loads, where the reductions in the pumping loss and the exhaust energy are the primary contributions. The fuel consumption of the most frequently operated conditions were improved by 9-26% in comparison with that of the baseline engine. However a much higher intake boost was anticipated because of the further downsizing. In this context, a two-stage system is currently considered as a potential solution, and the novel supercharging technology discussed in this chapter may be needed in a compound charging system to provide the additional boost requirement.

3.8. Future development for a mechanically supercharged passenger car engine

Table 2 shows the summary of each assessed technologies from the literature concerning the development of a mechanically supercharged passenger car engine. It can be seen that separation of the supercharger speed from the engine speed, improvement of the compressor isentropic and volumetric efficiency and innovation of the supercharger mechanism seem to be the potential trends for mechanically supercharging a passenger car engine and there is a degree of coupling between them.

Table 3.2. Summary of each technology from the literature concerning the development of a mechanically supercharged passenger car engine

Future direction / Potential Trends	Low-end torque enhancement	Transient driveability improvement	Low-load parasitic loss reduction
Separation of the engine and the supercharger speed	CVT mechanism, Pressure wave supercharger, clutch, SuperGen, Lontra and HyBoost	CVT mechanism, SuperGen and HyBoost	CVT mechanism and clutch
Improvement in the Isentropic efficiency	Pressure wave supercharger, TurboClaw, Eaton TVS V-Series, Honeywell novel compressor, SuperGen	TurboClaw, Honeywell novel compressor and Eaton TVS V-Series	
Improvement in the volumetric efficiency	Eaton TVS V-Series	Eaton TVS V-Series	
Innovation of the Supercharger mechanism	Split cycle engine, Pressure wave supercharger, SuperGen, Lontra and VanDyne SuperTurbo	Pressure wave supercharger, SuperGen and VanDyne SuperTurbo	Positive displacement in low speed and Five stroke engine
Others	Combustion optimization, material innovation	Advanced control, combustion optimization and material innovation	Active bypass, turbocharger/supercharger matching, advanced control and Miller cycle

From the findings in the literature, it seems that neither purely mechanical nor purely electric supercharger system is able to provide an ideal performance at high loads in the near future; this is because of the nature of the direct connection for a mechanical supercharger to the crankshaft, thus constraining its freedom, and because the e-boosting system currently is not reliable and durable. A hybrid approach such as SuperGen that features both a mechanical

and electric path may be a potential trend that bridges the gap between mechanically supercharging an engine and electrically supercharging an engine. In addition, although the ratio range of a mechanical variable-drive-ratio supercharger system is not as wide as those of an electric supercharger system or a hybrid supercharger system, a mechanical variable-drive-ratio supercharger system can also be adopted as a low-cost alternative that enhances the performance of an engine in the area of both low-end torque and transient behaviour.

The engine displacement of a supercharged engine should be further optimized in order to satisfy the power requirement of the frequent operating points without the assistance of boosting devices, in particular when a clutch is fitted. In addition, the low-load parasitic losses incurred by constantly driving a supercharger system (if a clutch is not installed) is suggested to be either mitigated by adopting a variable-drive system or offset via the energy that is reclaimed by the expansion work of a 'supercharger' depending on the ratio range. This approach can also benefit the transient behaviour as the clutch engagement is not required, thus NVH issues can be largely addressed. Future trends could also include boosting system matching optimization and a Miller cycle that is able to offset some (if not all) of fuel efficiency penalty incurred by driving the supercharger from other related technologies. If an automatic transmission gearbox is considered, a systematic approach that considers the trade-off between the part-load fuel efficiency and the transient behaviour is another important area that needs to be noted and optimized.

The development of the isentropic and volumetric efficiencies of the supercharger compressor itself should be ongoing. In addition, the matching of a supercharger with an engine, especially when a two-stage compound charging system is considered, should be evaluated extensively, which must take both devices into account.

In order to achieve the competitive functionality, a suitable control strategy is always a driving factor. During a transient event, the boost should be triggered from the supercharger seamlessly that behaves like a NA engine and if a two-stage compound charging system is considered, the boost should be seamlessly handed over from the supercharger to the turbocharger after the target is reached. This requires a sophisticated and robust control module and needs an extensive calibration in order for the system to operate well for the whole engine operating range. Although a traditional proportional and integral (PI) control

could be adopted here but a more sophisticated control algorithm such as the neural network is preferred in the future development [180].

3.9. Chapter summary and conclusions

Mechanically supercharging a passenger car engine is considered to be an alternative or complementary approach to enable heavy downsizing to be carried out. Since it is directly driven by the engine crankshaft, the transient performance of an engine boosting system realized either solely by a supercharger or by a combination of supercharger and turbocharger is significantly better than that of its turbocharged counterpart. The following conclusion are drawn from a review of the literature.

1: There are two main types of compressor that are currently adopted in passenger car engines namely positive-displacement compressors and centrifugal compressors.

2: Some of the current state-of-the-art technologies for mass production downsized supercharged engines indicate some synergies between the engine and the boosting machine, i.e. a strong relationship between the downsizing, the driveability and the down-speeding.

3: Enhancement of the low-end torque, improvement in the transient driveability and reduction in low load parasitic losses are the three development directions for a supercharger system, among which the adoption of a CVT to decouple the supercharger speed from the engine speed, improvement of compressor isentropic and volumetric efficiency and innovation of the supercharger mechanism seem to be the potential trends for mechanically supercharging a passenger car engine.

Figures in Chapter 3

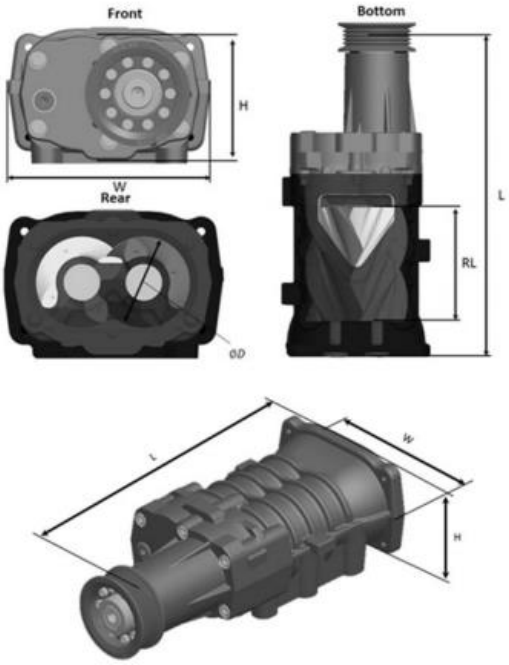

Figure 3.1. Eaton TVS R-Series supercharger view. [130]

Figure 3.2. Lysholm screw supercharger. [131]

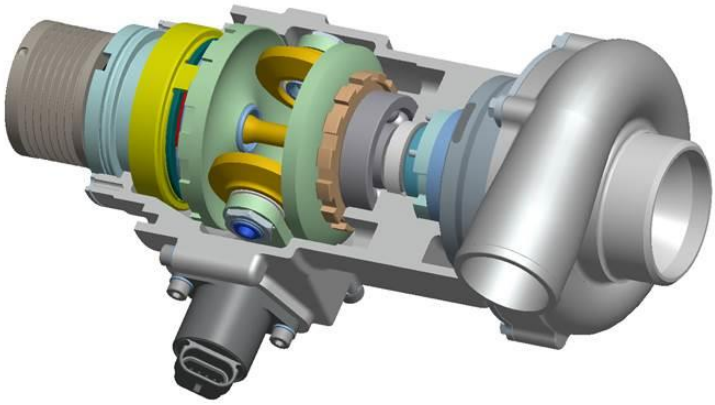

Figure 3.3. Torotrak V-Charge mechanism. [132]

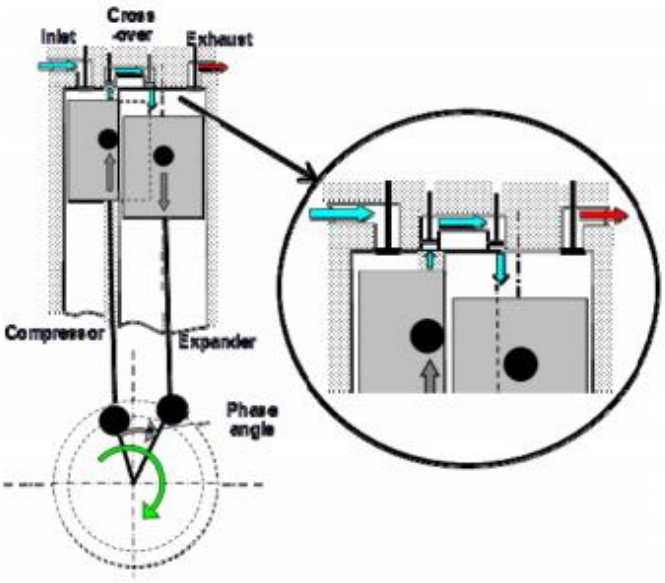

Figure 3.4. Principal elements of split cycle engine. [50]

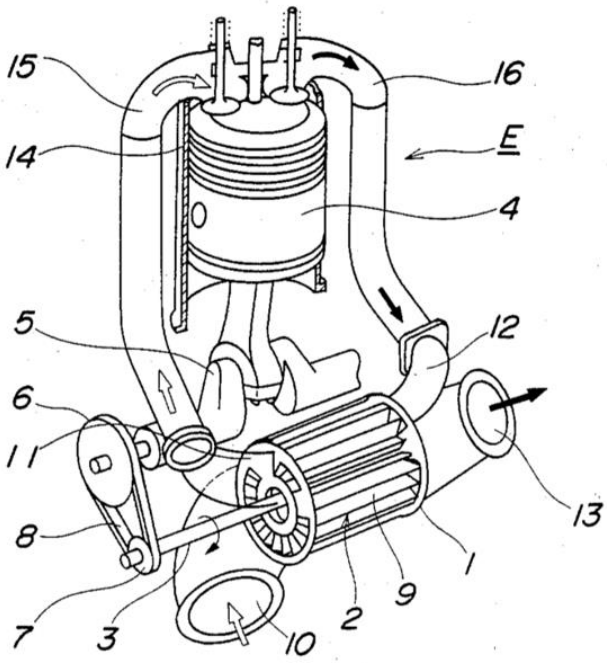

Figure 3.5. Pressure wave supercharger. [56]

1: rotor housing; 2: rotor; 3: rotary shaft; 4: piston of engine; 5: crankshaft; 6: crankshaft pulley; 7: rotary shaft pulley; 8: belt; 9: rotor cells; 10: air inlet; 11: air outlet; 12: exhaust gas inlet; 13: exhaust gas outlet; 14: cylinder of engine; 15: intake passenger; 16: exhaust passage; E: piston engine

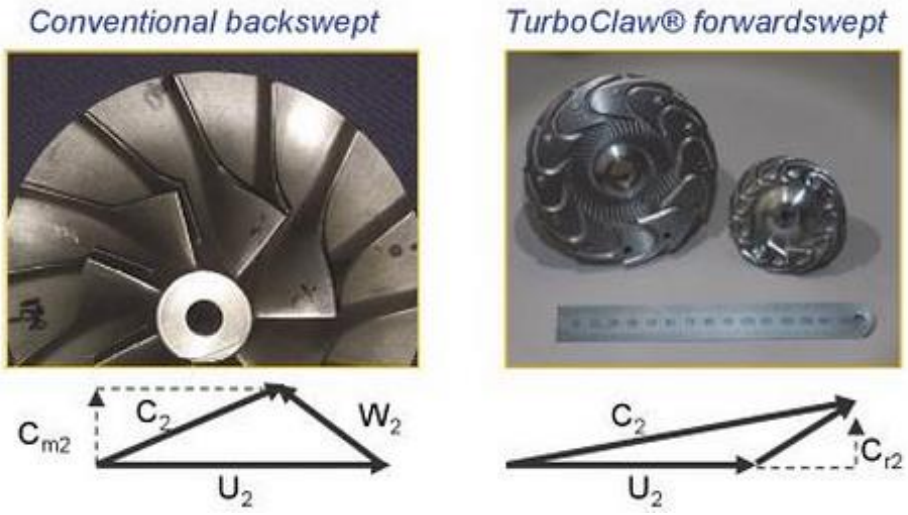

Figure 3.6. Turbocompressors and velocity triangles: Left: conventional backswept; right: TurboClaw forwardswept. [147]

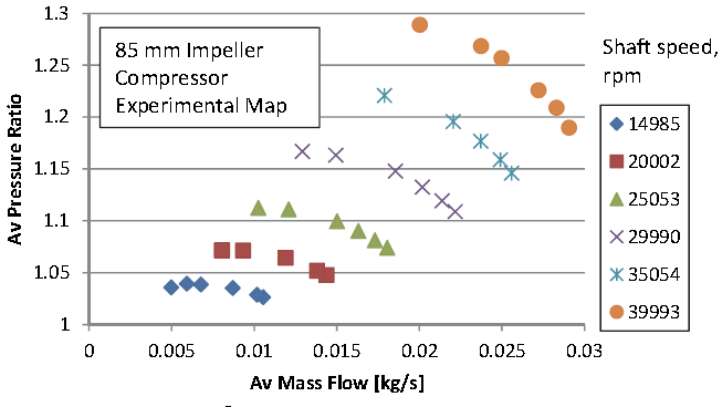

Figure 3.7. TurboClaw compressor map for an 85mm rotor. [147]

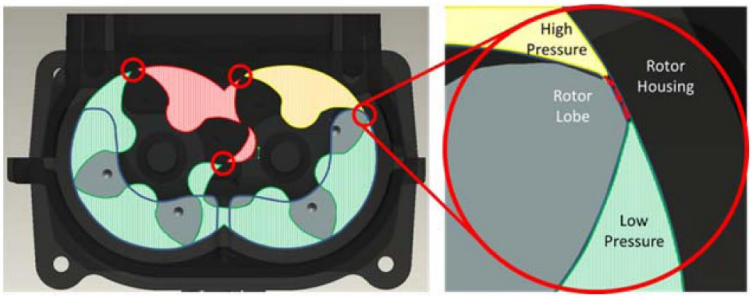

Figure 3.8. Diametral rotor leakage locations (left) and air leakage between the rotor lobe tip and rotor housing (right). [130]

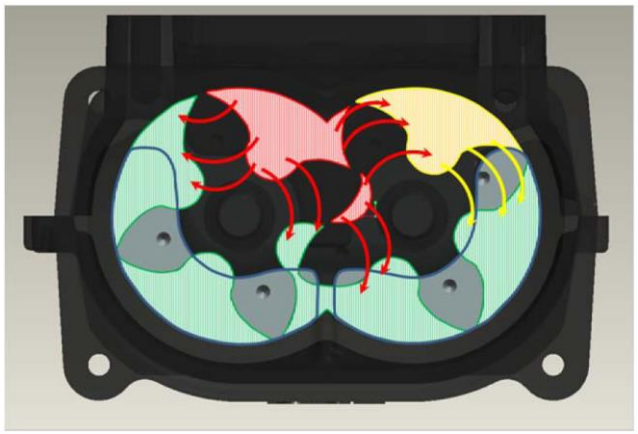

Figure 3.9. Leakage between rotors and end plates. [130]

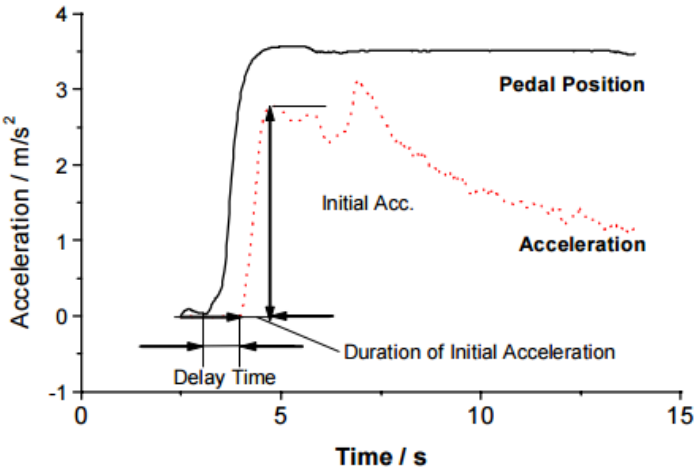

Figure 3.10. Illustration of the characteristic values. [152]

Delay time: the time between the first change in pedal position and the first change in the acceleration trace;

Acceleration: the peak value of the initial acceleration phase;

Jerk: the value of the initial acceleration divided by the duration of the initial acceleration.

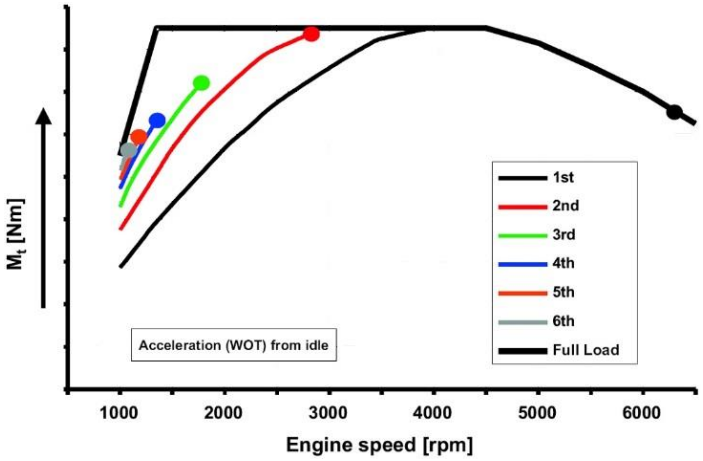

Figure 3.11. Comparative analysis of transient vs steady state engine torque delivery for a turbocharged engine: M_t achieved after 5 seconds in different gears vs steady state. [154]

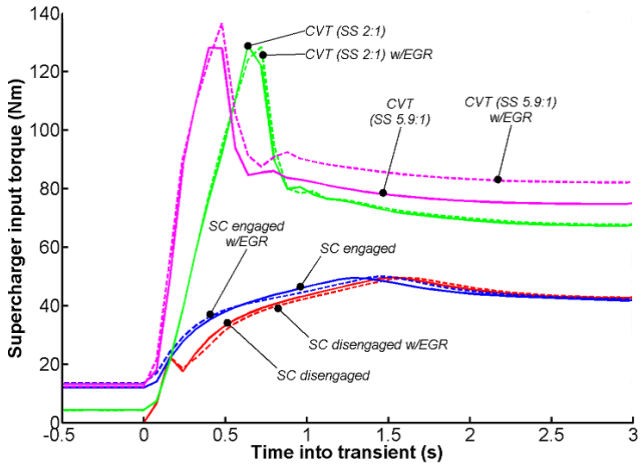

Figure 3.12. Supercharger input torques for tip-in simulations in the supercharger-engaged regime, the supercharger disengaged regime and for a CVT-driven supercharger regime. [163]

CVT: continuously variable transmission; SS: steady-state ratio; w/EGR: without exhaust gas recirculation; SC: supercharger.

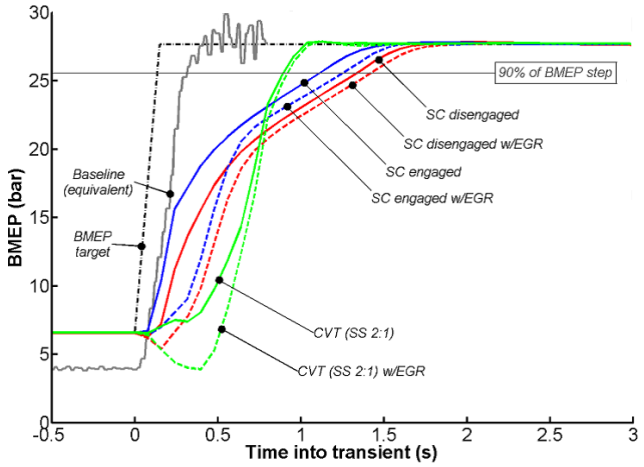

Figure 3.13. BMEP response for tip-in simulations of the supercharger engaged regime and the CVT-driven supercharger regime, showing the effect of the initial steady-state CVT ratio. [163]

For reference, the BMEP target, 90% of the BMEP step demand (i.e. full load), and the equivalent BMEP for the baseline experimental results are also shown.

BMEP: brake mean effective pressure; CVT: continuously variable transmission; SS: steady-state ratio; w/EGR: without exhaust gas recirculation; SC: supercharger.

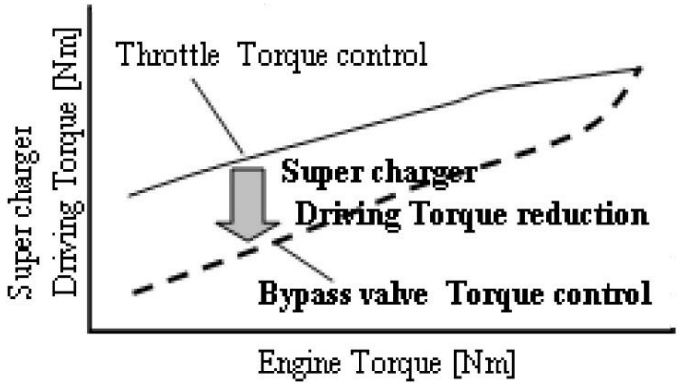

Figure 3.14. Effect of bypass valve control. [162]

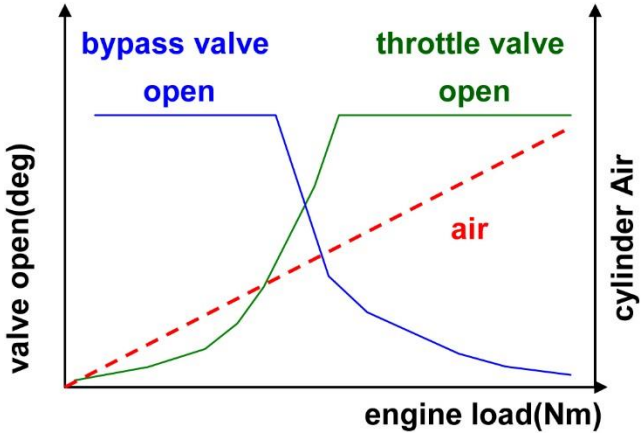

Figure 3.15. Throttle valve and bypass valve motion. [162]

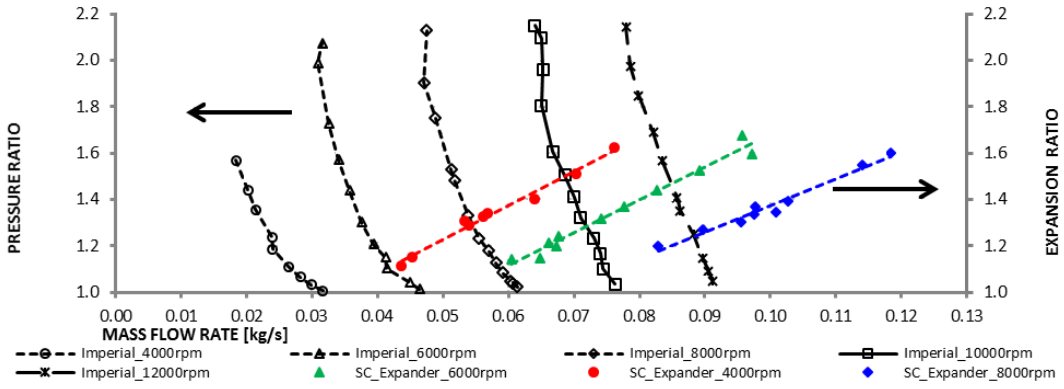

Figure 3.16. Pressure and expansion ratio of the Eaton R-Series R410 supercharger versus mass flow. [59]

RPM: revolutions per minute; SC: supercharger.

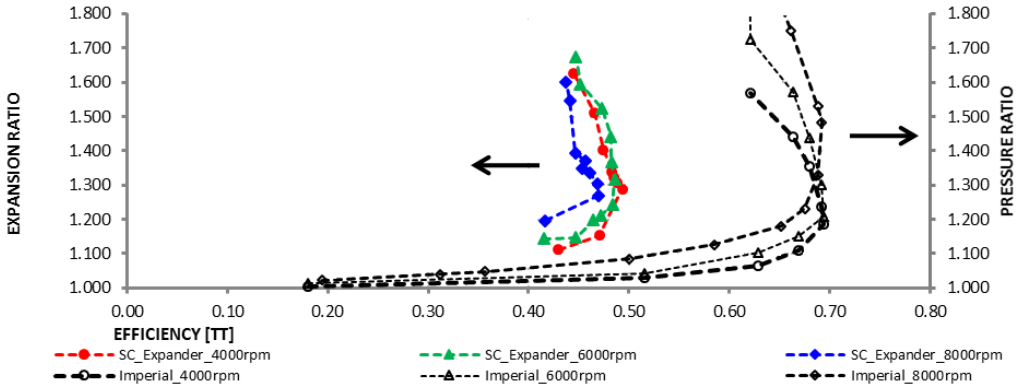

Figure 3.17. Total to total isentropic efficiency of the supercharger operating as a compressor and expander. [59]

RPM: revolutions per minute; SC: supercharger.

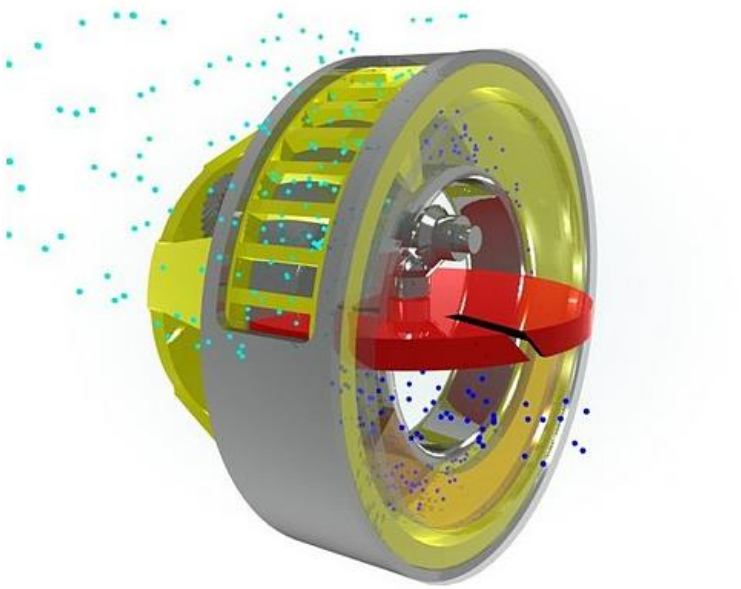

Figure 3.18. Lontra Blade Supercharger. [73]

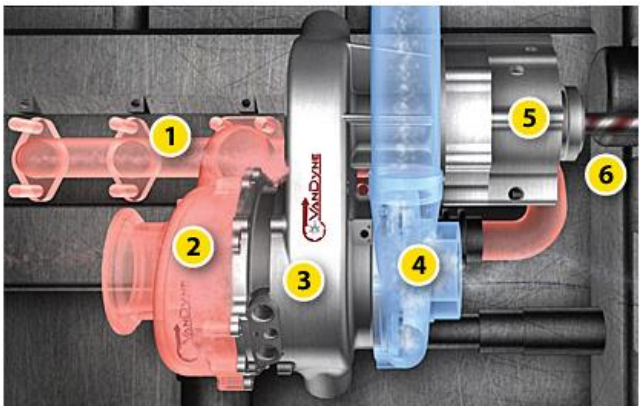

Figure 3.19. The VanDyne SuperTurbo [168]

1: exhaust manifold; 2: uniquely designed turbine; 3: high speed drive; 4: matched compressor; 5: continuously variable transmission; 6: engine interface

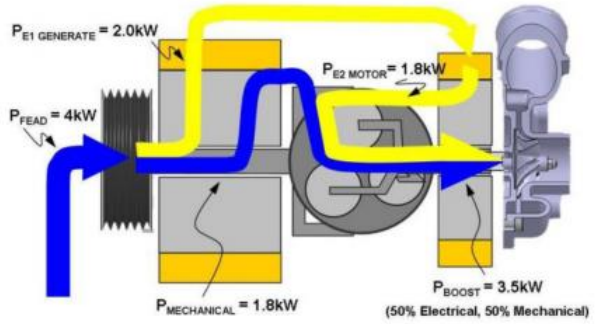

Figure 3.20. Power-split electromechanical transmission system of the SuperGen supercharger. Approximate power flow is shown for a mid-load condition. [135]

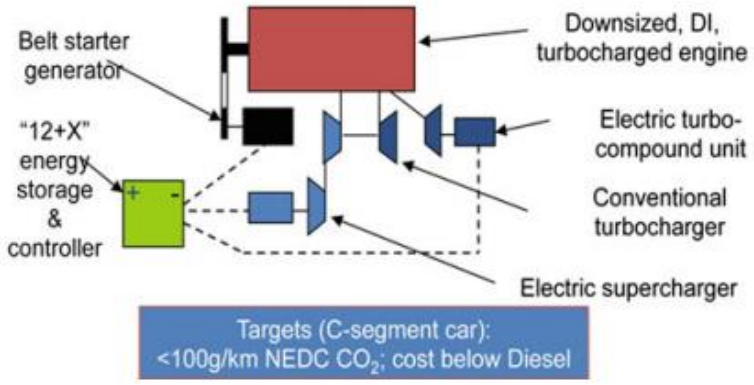

Figure 3.21. HyBoost concept scheme. [157]

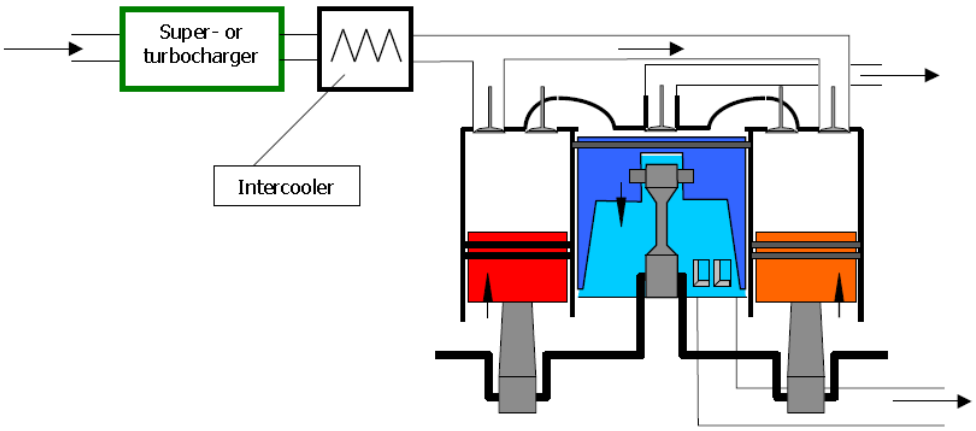

Figure 3.22. Three cylinder 5-stroke engine. [175]

Chapter 4 – *Modelling methodology*

This chapter will present a modelling and calibration theory foundation for study in the following chapters. It mainly includes three sub-sections, namely engine modelling introduction and calibration, engine control theory and tuning, and in-vehicle modelling, each of which has been put into practice by demonstrating a case study.

Parts of the comparison, discussion and conclusion in this chapter have been published in the form of a review article in the Proceedings of Institution of Mechanical Engineer, Part D: Journal of Automobile Engineering.

4.1. Engine modelling

4.1.1. Introduction

Engine modelling is widely adopted in the engine design and development process. It can either speed up the time frame from conception to birth for a specific technology in an engine or predict some engine parameters (such as residual gas fraction and trapping ratio) that are difficult or impossible to measure in experiments. Several types of engine modelling approaches are available, which include black box model, mean value model, 1-D model, fast-running model and multi-dimensional model. These tools, which form a spectrum of computational time and prediction accuracy, can be used for different objectives [11]. In this work, only the 1-D model and fast-running model (FRM) will be detailed, considering that (a) a high-fidelity 1-D engine model has been supplied in this project, and (b) an FRM model can be easily converted from a 1-D model. The mean value model will also be introduced, mainly for the purpose of comparison with the 1-D model.

A mean value model uses only simplified look-up maps to characterise the cylinder air flow and distribution of fuel energy without predicting the breathing and combustion processes. This approach is usually used for in-vehicle simulation or control system design when a fast computational time is required, and when a detailed characterisation of engine processes is considered not as important. Typically, three quantities are needed in the mean value model, including: volumetric efficiency, which is used to calculate the air mass flow rate that enters into the cylinder; indicated efficiency, which mainly describes the proportion of the fuel that can be converted to the work; and exhaust energy fraction. The maps-based characteristic of a mean value model and its fast computational time are ideal for an artificial neural network that allows the user to define outputs as a function of multiple inputs by training a large number of data sets (usually conducted by a design of experiment (DOE)). When a mean value is determined to be used, several aspects need to be considered. The range of engine parameter inputs, such as air fuel ratio, that are used to determine the characteristics of a mean value model need to cover the whole operating range, especially if a transient operation is to be conducted [181]. In addition, due to the fact that a valve model is not needed, and also because the intake and/or exhaust system is usually lumped into a larger equivalent volume in a mean value model, the pressure loss and heat transfer in the intake and exhaust system is required to be re-tuned. For the engine operating points with large scavenging (usually at high load, low engine speed), a trapping ratio is also required to be

estimated, or measured in experiments; this accounts for the blow-through flow that otherwise would not have been considered in the mean value model. Finally, if the mean value model involves a turbocharger, the pulse flow in a detailed dynamic engine model or in a test will not be captured, due to the maps-based characteristics of the model. Thus, a pulse efficiency multiplier and pulse mass multiplier need to be calculated and defined in the mean value model.

A 1-D engine code (such as GT-Power) solves the Navier-Stokes equations – namely, the conservation of continuity, momentum, and energy equations - in one dimension for the flow in the piping system of the engine, and uses simplified models, maps and look-up tables for other critical parts such as valves, turbocharger, cylinder, friction, and combustion. Due to the assumptions and extrapolation approaches made, the 1-D engine model usually requires extensive calibration against the measured data in a test cell [24]. In GT-Power, the whole system is discretised into many volumes that are connected by boundaries. In each volume, the rate of the change of mass equals the sum of mass flux in and out; the rate of change of energy equals to the sum of energy transfer in and out; and the rate of change of momentum is equal to the net pressure forces and wall shear forces in a system plus the net flow of momentum in and out. The scalar variables, such as pressure, temperature, density, internal energy, enthalpy, and species concentration are assumed to be uniform over each volume. The vector parameters, such as mass flux and velocity, are calculated for each boundary [181].

Fast-running models are designed to run the simulation in the order of real-time, without largely affecting the predictive capabilities in the model. They are intended to be used on system-level simulations, such as coupling a relatively detailed engine model with an integrated vehicle to study the fuel consumption in a specific driving cycle, or comparing the transient response for different boosting systems. Essentially, this approach is accomplished by reducing the complexity of a detailed engine model, by combining pipes and flow-splits into flow-splits with larger volumes, while retaining the cylinder, valve, and ports parts. Since only a few sub-volumes remain in the model, and since a larger time steps are usually a default setting, the engine run-time will be significantly reduced. Although this method cannot capture higher frequency wave dynamic content, a high level of fidelity of the low frequency and primary engine order dynamics is maintained, which is normally of interest to transient simulations.

4.1.2. Combustion description and validation

The proper calibration of the combustion model is critical and is usually the first step to achieving a well-calibrated and predictive engine model. In GT-Power, two-zone combustion applies to almost all combustion models. The burned and unburned air-fuel mixtures are trapped in the burned and unburned zones, respectively. The pressure distribution in the whole combustion chamber is homogeneous, whereas the temperatures in the two zone are modelled separately. In the two-zone model, the following energy equations are solved separately for each time step in each zone:

Unburned zone:

$$\frac{d(m_u e_u)}{dt} = -p\frac{dV_u}{dt} - Q_u + \left(\frac{dm_f}{dt}h_f + \frac{dm_a}{dt}h_a\right) + \frac{dm_{f,i}}{dt}h_{f,i} \quad \textbf{4.1}$$

Where:

m_u	Unburned zone mass
V_u	Unburned zone volume
m_f	Fuel mass
Q_u	Unburned zone heat transfer rate
m_a	Air mass
h_f	Enthalpy of fuel mass
$m_{f,i}$	Injected fuel mass
h_a	Enthalpy of air mass
p	Cylinder pressure
$h_{f,i}$	Enthalpy of injected fuel mass

Burned zone:

$$\frac{d(m_b e_b)}{dt} = -p\frac{dV_b}{dt} - Q_b - (\frac{dm_f}{dt}h_f + \frac{dm_a}{dt}h_a) \quad \textbf{4.2}$$

Where subscript ‘b’ denotes burned zone.

Basically, three types of combustion model are available in GT-Power: non-predictive, semi-predictive, and predictive. Although they all can be applied to a given engine, it is important to understand when and how to use these models.

A non-predictive combustion model simply defines a burn rate as a function of crank angle regardless of the conditions, such as pressure and temperature, in the cylinder, as long as

there is enough fuel available to support the burning. This model may be appropriate if the intended use is to investigate a parameter of an engine that has little or no effect on the burn rate. To a spark-ignition engine, specifically, a non-predictive combustion model is prescribed in the simulation, either in combustion profile or Wiebe model format, both of which can be calculated from the cylinder pressure. In the following, a spark-ignition Wiebe model is detailed, followed by the methodology of calculating burn rate from measured cylinder pressure.

The spark-ignition Wiebe function approximates the shape of an SI burn rate using a Wiebe function. This approach is reasonable for most situations if measured cylinder pressure is not available, and can be used to set up a semi-predictive combustion model if the combustion data of a range of engine operating points are available. The Wiebe equations are given below:

$$BMC = -\ln(1 - BM) \quad \text{Burned midpoint constant} \qquad \textbf{4.3}$$

$$BSC = -\ln(1 - BS) \quad \text{Burned start constant} \qquad \textbf{4.4}$$

$$BEC = -\ln(1 - BE) \quad \text{Burned end constant} \qquad \textbf{4.5}$$

$$WC = \left[\frac{D}{BEC^{1/(E+1)} - BSC^{1/(E+1)}}\right]^{-(E+1)} \quad \text{Wiebe constant} \qquad \textbf{4.6}$$

$$SOC = AA - \frac{(D)(BMC)^{1/(E+1)}}{BEC^{1/(E+1)} - BSC^{1/(E+1)}} \quad \text{Start of combustion} \qquad \textbf{4.7}$$

Where:

AA	Anchor angle
D	Duration
E	Wiebe exponent
CE	Fraction of fuel burned
BM	Burned fuel percentage at anchor angle
BS	Burned fuel percentage at duration start
BE	Burned fuel percentage at duration end

Burn rate calculation

$$Combustion(\theta) = (CE)\left[1 - e^{-(WC)(\theta - SOC)^{(E+1)}}\right] \qquad \textbf{4.8}$$

Where:

θ	Instantaneous crank angle

Calculating a burn rate from a cylinder pressure trace is referred to as a 'reverse run' in this work, compared to the normal operation, which is determining the cylinder pressure using the burn rate as an input. Both forward and reverse run calculations use all the same equations described in the two-zone combustion methodology, and there are no assumptions that are only applied to the reverse run. In GT-Power, two approaches are available to calculate the burn rate from a measured cylinder pressure trace. The first one is termed 'stand-alone burn rate calculation', and the second is often named 'three pressure analysis (TPA) burn rate calculation'.

The stand-alone burn rate calculation methodology essentially determines the burn rate by using only the cylinder pressure data, either from a single cycle or an assembled average and a few cycle-averaged parameters, together with the engine cylinder geometry. This approach, compared to the TPA discussed below, is advantageous to save computational time and can be cost-effective, due to the fact that only one measured instantaneous pressure trace is required. However, this approach requires the estimation of some parameters that are difficult or impossible to measure in experiment, such as trapping ratio and residual gas fraction. In this work, the combustion calibration will be mostly based on this methodology, considering that a high-fidelity 1-D engine model has been supplied in this project which can be used to predict the trapping ratio and residual gas fraction, and also because, at the time of writing, only a cylinder pressure trace is available.

A TPA burn rate calculation requires three measured pressure traces, including intake, cylinder, and exhaust - hence the name three pressure analysis. This approach uses a relatively detailed engine model (including valve and port) compared to the stand-alone burn rate calculation methodology discussed above; thus, there is no need to estimate the trapping ratio and residual gas fraction. Note that in a standard TPA model, when the valves are closed, pressure fluctuations may be 'spuriously' generated within the ports. It is desirable to reduce the magnitude of these fluctuations caused by reflections during the valve-closed period, so that the predicted pressure behaviour within the port is as close to the measured behaviour as possible [182]. In addition, the discretisation length should be reduced to minimise the possibility of unwanted noise in the pressure signal generated.
Before imposing the raw measured pressure data on the model described above, it is usually required that some pegging routines are conducted. This is mainly due to the shift of measured combustion phasing and the error that occurs to convert the measured signal into

an absolute pressure in experiment. For the incorrect pressure phasing problem, the crank angle difference between the measured and calculated cylinder peak pressure is often used as a shift offset. In terms of the cylinder pressure correction, the recommended pegging routine to correct the cylinder pressure is by setting the cylinder pressure at IBDC equal to the average intake pressure.

It is often the case that the measured and calculated cylinder pressure trace differs, even though a standard combustion data calibration procedure is performed. This might be attributed to the incorrected compression ratio in the supplied model, due to the stack-up of the tolerances in each component (even if they are all within specified tolerances). The method to check this inconsistency is to look at the cylinder pressure in the compression stroke to see whether the measured and calculated pressure traces are overlapped. The cylinder heat transfer could also have a significant effect on the calculated burn rate, especially if an incorrect estimation of the heat transfer coefficeint is applied during the power stroke.

Semi-predictive combustion models utilise a set of non-predictive burn rates as a function of some engine significant variables (i.e. engine speed, intake manifold pressure, residual gas fraction, etc.). This will allow the combustion model to change the 'shape' of the burn rate in different operating conditions, without significant central processing unit (CPU) penalty when compared to some predictive models. For a spark-ignition engine specifically, if only full-load simulation is to be conducted, the three terms of the Wiebe function (50% burn duration, 10-90% duration and exponent) will be interpolated from the look-up tables, which calculate the corresponding terms based on the engine speed. However, if a larger range of engine operating points is considered, an artificial neural network may have to be introduced to train the behaviour of the engine characteristics, using a representative set of data.

Predictive combustion models will take the cylinder's geometry, spark locations and timing, air motion, and fuel properties into consideration and an extensive calibration is usually needed to tune the model. Nevertheless, once the model is well-calibrated, based on the measured data, the effects of cylinder geometry and spark timing on the combustion behaviour can be analysed.

Considering that the engine hardware is available in this project, the burn rate could be calibrated by obtaining the combustion data from the experiments and also due to the fact that the control parameters only vary in a limited range, some non-predictive combustion models are utilised in this work to set up a semi-predictive combustion model. This should give some reasonable accuracy to the model, which allows it to have some capability to predict without a significant computational time penalty.

4.1.3. Turbocharger modelling

Turbomachinery performance maps:

Zero-dimensional turbocharger performance maps are often utilised by some advanced 1-D gas dynamic engine simulation code (like GT-Power in this work). Typically, the 'speed line' map should consist of several sets of mass flow rate, pressure ratio, and thermodynamic efficiency. It might be worth noting that the data point with the lowest mass flow rate for each speed line of a compressor map is assumed to be on the surge line, and peak efficiency data must be included at each turbine speed line so that the data can be fitted to a curve that will allow the extrapolation of the test data (as detailed later in this section).

Each compressor and turbine map data set must be corrected to account for changes in temperature, pressure and compositions. Typically, a compressor map is corrected to a common reference temperature and pressure (usually 298K and 1bar). The equation to correct the engine speed and mass flow rate can be seen below:

$$RPM_{corrected} = {RPM_{actual}} \Big/ \sqrt{\frac{T_{inlet-total}}{T_{reference}}} \quad \textbf{4.9}$$

$$\dot{m}_{corrected} = \dot{m}_{actual} \times \sqrt{\frac{T_{inlet-total}}{T_{reference}}} \Big/ \frac{P_{inlet-total}}{P_{reference}} \quad \textbf{4.10}$$

Figure 4.1 shows a typical corrected compressor map with 'ideal' straight bell-mounted inlet and vehicle inlet system. This indicates that when a dyno or vehicle inlet and charge air system is fitted, the compressor characteristic can be dramatically changed, which will affect the engine/turbocharger performance and their interactions.

Turbine maps, due to the significantly different reference conditions, are usually 'reduced' to 'remove' the effects of the inlet temperature and pressure on their performance. This

approach is quite convenient, as any two turbine maps could be compared without looking at the reference conditions. The formula to reduce the turbine maps can be seen in the following:

$$RPM_{reduced} = \frac{RPM_{actual}}{\sqrt{T_{inlet-total}}} \quad \textbf{4.11}$$

$$\dot{m}_{reduced} = \frac{\dot{m}_{actual}\sqrt{T_{inlet-total}}}{P_{inlet-total}} \quad \textbf{4.12}$$

It might be worth noting that the ratios of specific heats and gas constants should also be considered if different compositions at different inlet temperatures are passing through the turbine. For spark-ignition engines specifically, when the engine is operating at large scavenging (i.e. rich air/fuel ratio), or a low-pressure turbine in a two-stage turbocharging configuration is considered, corrections for the ratios of specific heats and gas constants should be conducted by using the following terms multiplied by the reduced speed and reduced mass flow rate, respectively.

$$\sqrt{\frac{\gamma_R R_R}{\gamma_a R_a}} \quad \textbf{4.13}$$

$$\sqrt{\frac{\gamma_a R_R}{\gamma_R R_a}} \quad \textbf{4.14}$$

Where:

γ_R	Reference ratio of specific heats
γ_a	Actual ratio of specific heats at the inlet of the turbine
R_R	Reference gas constant
R_a	Actual gas constant at the inlet of the turbine

Turbocharger shaft modelling:

The most two important attributes for a turbocharger shaft are inertia and mechanical efficiency. The shaft inertia should represent a total of rotational inertia of the turbine wheel, compressor wheel, and shaft, and this attribute has a larger effect on the transient response than the steady-state performance. However, in order to run the steady-state simulation with the least number of engine cycles, artificially manipulating the turbocharger inertia is allowed in GT-Power. The recommended routine to optimise a turbocharger's inertia is to make the inertia multiplier quite high (usually around 100) for the first three to four engine cycles, so that the speed of the turbocharger does not drop while the velocity in the manifolds is developing. Then, the inertia multiplier could be made very low (usually around 0.01) to allow it to reach the convergence as quickly as possible within 10 to 15 engine cycles.

After that, the inertia multiplier should be returned to 1, in order to avoid diminishing returns and excess speed fluctuations.

Most turbocharger suppliers lump the bearing friction in the turbine efficiency map, though sometimes this is not explicitly stated [181]. This is mainly due to the fact that a recommended gas stand test procedure (such as the one from SAE) describes the process wherein the turbine efficiency is using the actual total enthalpy rise of the compressor stage divided by the isentropic enthalpy drop across the turbine stage multiplied by mechanical efficiency (see equation below). By doing this, the bearing friction is combined into the turbine isentropic efficiency map. This method should be valid when the turbine inlet temperature is reasonably close to the condition of the gas stand test. The SAE specification recommends the inlet temperature for an SI engine is 900 degrees Celsius +/- 20. At part load, where the inlet temperature is significantly lower, some explicit model should be utilised to account for the temperature change on the friction.

$$\eta_t = \frac{C_{P,comp} \times (T_{0,out} - T_{0,in})_{comp}}{\eta_{mech} \times \left(1 + \frac{1}{A/_F}\right) \times C_{P,Turb} \times T_{0,in,turb} \times \left[1 - \left(\frac{1}{PR_t}\right)^{\frac{\gamma-1}{\gamma}}\right]} \quad \textbf{4.15}$$

Compressor map extrapolation:

The measured compressor map is extrapolated by some built-in algorithm in GT-Power. To be more specific, the surge line is linearly interpolated with the measured lowest mass flow rate for each speed line, and then extrapolated between a newly-added 0.0 RPM speed line with a pressure ratio of 1.0 and a mass flow rate of nearly 0.0 and the imposed lowest speed line, by complying with the scaling laws of turbomachinery wherein the mass flow rate is proportional to the speed and the pressure ratio is proportional to the square of the speed. In addition, GT-Power extrapolates each speed line to a pressure ratio of 1.0 by linearly extrapolating the mass flow rate, but taking choke into consideration to avoid unrealistic extrapolated mass flow. The efficiency on the line of 1.0 pressure ratio is usually set to be 20% with the other extrapolated efficiency developed using a built-in algorithm in GT-Power.

Turbine map extrapolation:

The turbine map fitting method in GT-Power is much more complicated than the extrapolation method used for a compressor. It is based on normalisation of efficiency, blade

speed ratio (BSR), and mass flow parameters by their values at maximum efficiency for all speed lines (see **Figure 4.2**). The rationale behind this is that the data points of mass flow and efficiency for all speed lines will end up being on a single line, thus allowing the extrapolation to be done by fitting a single curve on respective mass flow and efficiency against blade speed ratio plots [184].

The fitting approach firstly identifies the pressure ratio, blade speed ratio and, mass ratio of the maximum efficiency point for each speed line. The blade speed ratio and the mass ratio equation are shown below.

$$BSR = \frac{U}{C_s} \quad \textbf{4.16}$$

$$U = \frac{\pi DN}{60} \quad (Blade\ tip\ speed) \quad \textbf{4.17}$$

$$C_s = \left[2C_pT_{in}\left(1 - PR^{\frac{1-\gamma}{\gamma}}\right)\right]^{1/2} \quad \text{(Isentropic speed)} \quad \textbf{4.18}$$

$$Mass\ Ratio = \frac{\emptyset_{max}}{Max\emptyset_{max}} \quad \textbf{4.19}$$

Pressure ratio and mass ratio curves are fitted against the speed parameter, so that they give every pressure ratio an estimated speed parameter and mass ratio. Hence, $\emptyset_{max}$ is made available for each data point in the turbine map. This will be used to calibrate the mass flow ratio (MFR) defined below.

$$MFR = \frac{\emptyset}{\emptyset_{max}} \quad \textbf{4.20}$$

Similarly, BSR ratio could be obtained by the following fitting and calculation process. The normalised efficiency is determined by the equation below.

$$BSR\ Ratio = \frac{BSR_{max}}{MaxBSR_{max}} \quad \textbf{4.21}$$

$$BSR_{norm} = \frac{BSR}{BSR_{max}} \quad \textbf{4.22}$$

$$\eta_{norm} = \frac{\eta}{\eta_{max}} \quad \textbf{4.23}$$

At this stage of the procedure, the mass flow ratio and the normalised efficiency should be lining on single lines against normalised blade speed ratio, in order for the extrapolation to be carried out. A curve is fitted to the mass flow ratio against the normalised blade speed ratio plot using the following equation.

$$MFR = cm + BSR_{norm}^{m}(1 - cm) \quad \textbf{4.24}$$

The normalised efficiency is fitted to two curves for normalised low-blade speed ratios ($BSR_{norm)} < 1$) and normalised high blade speed ratios ($BSR_{norm} \geq 1$) as follows:

$$\eta_{norm} = 1 - (1 - BSR_{norm)}{}^{b} \quad (BSR_{norm} < 1) \qquad \textbf{4.25}$$

$$\eta_{norm} = 1 - c(BSR_{norm})^2 \quad (BSR_{norm} \geq 1) \qquad \textbf{4.26}$$

$$Z_0 = 1 + \frac{1}{\sqrt{c}} \qquad \textbf{4.27}$$

Where

N	Turbine speed (RPM)
D	Diameter (m)
T_{in}	Inlet temperature (K)
C_p	Specific heat at constant pressure (J/kg/K)
γ	Ratio of specific heats
$\emptyset_{max}$	The mass flow rate at maximum efficiency point
$Max\emptyset_{max}$	The largest of mass flow rate for all speed lines
cm	Intercept of the curve at 0.0 BSR_{norm}
m	Exponent coefficient
b	Constant to control the curve of the low BSR_{norm} efficiency fit
Z_0	Intercept

Tracing back to the methodology used to extrapolate the turbine performance map, it is safe to say that extending the range of the experimental data may be needed, in order to ensure the accuracy of the simulation. Any data which is out of the test data range should be used with caution, as this might cause turbocharger or engine performance to deviate from the real world.

4.1.4. Supercharger modelling

The compressor modelling of a supercharger is similar to that of a turbocharger. The most significant difference between the two is the manner of the friction that occurs. Unlike the traditional turbocharger compressor whose shaft mechanical efficiency is often lumped into the turbine efficiency map, the supercharger compressor shaft mechanical efficiency should be explicitly modelled, either by imposing a power or torque template which extracts the mechanical loss from the supercharger system, or via estimating a mechanical efficiency. In the recent GT-Power version, a new compressor template could be utilised to account for

the mechanical losses in a supercharger system. It, unlike a standard compressor performance map, which consists of four sets of data (speed parameter, mass flow rate, pressure ratio, and isentropic efficiency), features additional total shaft power data, which is used to determine the total power needed to drive the supercharger at the corresponding speed and pressure ratio. It might be worth noting that this template is useful when an 'overblown' effect (i.e. when the inlet pressure is larger than the outlet) is to be investigated.

4.1.5. Scavenging modelling

Although the cylinder scavenging modelling had only been carried out for two-stroke engines, in some cases, it might still be required for four-stroke engines, to represent the real flow characteristics. Typically, for a four-stroke engine model, there is no scavenging model used by assuming the gases in the cylinder are homogeneously mixed. Nevertheless, from experiments or from some computational fluid dynamics (CFD) calculations, it is seen that the gas flow characteristics during the intake and exhaust valve overlap could be visualised using **Figure 4.3**. A mathematical model is built on this by using the relationship between cylinder residual ratio and exhaust residual ratio during the intake and exhaust valve overlap. The cylinder residual ratio is the ratio of burned gas mass in the cylinder to all gas mass in the cylinder, and the exhaust residual ratio is the ratio of burned gas mass exiting the cylinder to all gas mass exiting the cylinder. **Figure 4.4** shows a pre-defined 'S-shape' scavenging function to mimic a real scavenging process, by allowing the exhaust residual ratio to decrease slowly during the first part of the scavenging and then to drop rapidly when the time progresses to the end of the scavenging. This approach is useful to model the scavenging effect at low engine speed and high load and can improve the accuracy of a knock model, as the residual gas fraction could have a significant effect on the knock sensitivity. However, in order to simulate the real scavenging process, a considerable amount of time is needed to fit the 'S-shape' function by conducting the CFD calculations. This might not be possible for the early stage of the development process, especially with the consideration that for every single engine operating point, the scavenging process is different.

4.1.6. Case Study: V-Charge engine model validation

In the following, the V-Charge engine model (see **Figure 4.5**) will be validated using the experimental data from test cell 3 at the University of Bath. The selected engine operating point in this work is 1000RPM and 130Nm, but a similar process has been conducted in other

operating points. A high-fidelity engine model was supplied in this project, but as the supercharger and turbocharger maps were not the same as in the original model, and due to the engine operating points being outside of the validated range, a relatively extensive calibration is still required.

Firstly, the engine combustion model was calibrated using the stand-alone burn rate calculation methodology discussed above. This approach was performed over a standard TPA method, as only the cylinder instantaneous pressure sensor was installed in the engine. However, as the air trapping ratio and the residual gas fraction could be predicted using the supplied engine model, the calibration should still be valid.

The required averaged engine parameters - including air volumetric efficiency, injected mass per cycle, and injection timing, etc. - and the cylinder geometry data were derived from the test. The air trapping ratio and the residual fraction at intake valve closing (IVC) were predicted from the supplied engine model. The measured data was pegged before imposing onto the measured cylinder pressure analysis object. **Figure 4.6** shows the measured and simulated cylinder pressure at the corresponding engine operating point. It can be seen that the cylinder pressure trajectory at both the compression stroke and the power stroke fits well.

The combustion profile was then imposed on the original model with only the boundary conditions (the supercharger and the turbocharger template were deleted) in order to calibrate the valve timing, valve lash, and valve discharge coefficient. After the mass air flow was matched, the supercharger and the turbocharger compressor were added to calibrate its behaviour, followed by the calibration of the exhaust system. Note that no coefficient multiplier was used for the boosting systems, which indicates the robustness of this engine model on predicting.

Figure 4.7 and **Figure 4.8** show the supercharger and the turbocharger maps, which are well within the data imposed. The simulated turbocharger was on the surge line, which was in line with the observations in the experiment. **Table 4.1** following, shows the comparison between the test and the simulation for some important parameters in the engine.

Table 4.1. The comparison between the test and the simulation

*1000RPM 130N*m*	Test	Simulation
Mass air flow (kg/h)	67.9	67.9
Injected mass per cycle (mg/cycle)	48.9	48.9
Supercharger PR	1.10	1.13
Turbocharger PR	1.48	1.47
Turbocharger shaft speed (PRM)	123,200	124,902
Engine torque (N*m)	130.3	130.1

4.2. Control modelling and calibration

4.2.1. Control introduction

Proper control logics in the engine's electronic control unit (ECU) are of importance to achieving the requirements of fuel efficiency, emission standards, and driveability performance. In this section, control modelling in a spark-ignition engine will be introduced, followed by a detailed model build-up for the boost pressure control of a supercharger-turbocharger two-stage gasoline system.

The tasks of an ECU are receiving signals from a number of sensors (such as pedal and speed sensors), interpreting the information, and determining a suitable control actions based on pre-defined codes or maps. Typically, the control strategy varies significantly for different engine platforms, and most of them are quite complex, which could involve thousands of pages of code just for interpretation purposes [185]. Nevertheless, the control principle for a spark-ignition engine is not that difficult to understand, and the control algorithm behind the code is not so 'advanced' that it requires the knowledge of some sophisticated control theories. In the following, some general control methodologies are introduced.

For a gasoline engine, the two most important variables that define the engine operating points are engine speed and load. The engine speed can be directly measured by a speed sensor, but the engine load can only be expressed by air mass flow rate (or volumetric efficiency, relative air charge) or by some models that take intake pressure, temperature, and engine breathing characteristics into consideration. It might be worth noting that, unlike diesel engines, whose loads are controlled by fuel quantity, the loads of gasoline engines are

regulated by the airflow into the cylinder. This is because a full homogeneous mixture of fuel and air is required before combustion, in order to fully take advantage of the three-way catalyst to protect the environment.

Traditionally, a number of engine control actions (such as fuel injection and thermal management) have been seen as a passive system. However, in recent years, with the push for better fuel economy/improved emissions and the development of the component technology, a number of actuators that can actively modulate the engine performance have emerged. Among all the active components that have already been installed in a production gasoline engine, direct injection should be emphasised due to its benefits in fuel consumption and system stability. The DI technology, unlike its carburettor predecessor, has the capability to precisely control the fuel injected, thus improving fuel efficiency. It can also combine with some other technologies, such as the augmentation of the geometric compression ratio and the stratified approach, to further enhance an engine's fuel performance at frequently used areas of low-load engine operation. The disadvantages of utilising active components are its cost along with the possibility that the increased control complexity might need extensive tuning in the later calibration process.

4.2.2. Feedback control

Although there are many feedback control theories available, for an automotive application, the most widely used control strategy is Proportional-Integral-Derivative (PID) control, due to the fact that this control strategy is well understood by powertrain calibrators and is therefore, in principle, easy to implement.

PID controllers are based around minimising the error between a given set-point value and a measured feedback term by applying a control action to the system, which is determined based on the error (**see Figure 4.9**). It might be worth noting that the derivative loop in a standard PID controller is typically not required for an automotive application for the following two reasons:

- The function of a derivative loop is usually replaced by a feed-forward map control;
- Tuning of the derivative term can be quite challenging and an improper calibration will amplify the noise in the feedback that may tend to cause oscillatory behaviour.

Proportional-Integral (PI) control in practice is not that simple to implement, especially if two or more PI controllers that regulate two or more interdependent engine parameters are applied in one engine system. To avoid two controllers fighting each other and causing unstable operation of the engine, some enhancements are required (an example is detailed in the second case study below). Also, an optimal gain in a PI controller that is ideal for one engine operating point might be inappropriate for another, resulting in slow response of an oscillatory behaviour. A common approach to deal with this is called gain scheduling, where the controller gains are altered according to the engine speed and load operating point.

Integral wind-up is also a problem in a PI controller. An example (see **Figure 4.10**) is given to illustrate this effect on the control behaviour. Imagine the scenario where the target is higher than that can be achieved by the actuator. The integrator will wind-up and produce poor response on the subsequent change of set-point.

In this work, both the back-calculation method and clamping approach have been considered in terms of avoiding integral wind-up. **Figure 4.11** shows a PID controller block with the back-calculation method. It can be seen that by enabling the back-calculation, the block has an internal tracking loop that is able to discharge the integrator output. However, the control parameter Kb is difficult to determine, and an improper setting will lead to worse results than that without an anti-windup loop. Clamping is another commonly used anti-windup approach that sets the integral path of a PID controller to zero, in order to avoid wind-up when detecting an integrator overflow (see **Figure 4.12**). Compared to the back-calculation method, the clamping approach is 'always' working, but an extensively tuned back-calculation anti-windup approach could enable better dynamics.

4.2.3. Feed-forward loop

In theory, a proper feedback controller (such as PI controller, discussed above) can reach the target as long as the time is sufficient. However, for an automotive application, especially when an engine is studied, fast and robust response behaviour is required. This is commonly achieved by adding a feed-forward loop into the existing feedback controller. This approach can be seen as implementing a best estimation of what the controller action should be, and mapping this value to engine set points with direct control action. By doing that, the response

time could be reduced significantly and the gains in the feedback could be relaxed, making the system more stable.

However, an anti-windup method is not appropriately suitable to the control strategy with a feed-forward loop, unless the contribution of the feed-forward signal has been subtracted in such a way that allows the PID controller block to know its share of the effective control signal applied to the actuator. An anti-windup PID control demonstration with a feed-forward control is seen in **Figure 4.13**.

Figure 4.14 shows a control strategy schematic for an engine boosting system with a VGT. Similar control strategies could also be seen in other sub-systems of a gasoline engine. Please note that linearization tables for sensors and actuators are often implemented in the ECU to alleviate the work by the calibration and improve the control stability.

4.2.4. GT-Suite and Matlab/Simulink co-simulation

GT-Suite models can be coupled with models developed in Matlab/Simulink Environment. This is a common practice in the industry where engine, powertrain, and vehicle dynamics are modelled in GT-Suite, and electronic controllers are modelled in Matlab/Simulink. There are two methods that are currently adopted for the GT-Suite and Matlab/Simulink co-simulation:

- Running a GT-Suite model from the Matlab/Simulink interface
- Compiling Matlab/Simulink models into .dll/.so files and importing them into a GT-Suite model.

For all the co-simulation work in this thesis the first option above was used, and in the following an example was given to illustrate how a Matlab/Simulink embedded optimization strategy (which is genetic algorithm) is utilized to optimize a GT-Power engine model.

In order to optimize a non-linear engine system (take the optimization of the DEP valve timing for example), a genetic algorithm can be employed to avoid the problems of the embedded optimization tools in GT-Suite (in GT-Suite, the output variable must have a unique minimum or maximum, see **Figure 4.15**).

GT-Suite applications can be run in conjunction with Simulink, and a Matlab code may be utilized to achieve the optimization goals for a Simulink block. To be clearer, **Figure 4.16** illustrate the co-simulation between a GT-Suite engine model and a Simulink module. In addition, the function of a genetic algorithm (see in **Figure 4.17**) is fulfilled in a Matlab interface, in order to minimize BSFC for different exhaust timings for a downsized gasoline engine. Using this co-simulation technique, the strength of each software can be combined and enhanced.

In the genetic algorithm, a population of individuals (different exhaust valve timings) was simulated in GT-Suite and ranked by a custom fitness function. Selection of the parents based on their fitness was then conducted (stochastic uniform). After that, reproduction process consisting of the elite choice, crossover and mutation was carried out (see **Figure 4.18**). The algorithm terminated when the maximum number of iterations was exceeded or the stopping criteria was fulfilled.

In order to give reader confidence in the genetic algorithm approach, a 'peaks' problem which has a couple of local maximums and minimums are shown in **Figure 4.19.** A genetic algorithm was carried out to look for the global minimum of this function and all the evaluated points (red dots in the figure) were recorded. It can be seen that the genetic algorithm is able to find the global minimum, whilst the embedded GT-Power algorithm (see **Figure 4.15**) could have ended in the local minimum, depending on the starting point of the optimization.

4.2.5. Case Study: V-Charge Boost control

The proposed control sequence is basically composed of a driver input which is the pedal position and how the input affects the actuator actions in the engine system. For details, see **Figure 4.20.** The ECU will first receive the pedal position and engine speed signals from the driver, and will then calculate the demand total boost pressure, followed by the determination of the boost split (feed-forward loop). Finally, a feedback control loop is required to correct the demand boost pressure to the target, under different boundary conditions (or, in other words, a different altitude) or component ageing.

In order to build a robust control strategy and gain some knowledge of tuning the behaviour of this two-stage boosting system, a GT-Power model was initially used to simulate the gas dynamic response, while the control strategy was generated from Simulink. This approach was also beneficial later, when a near-to-complete control strategy was transferred from Simulink to an open ECU developer platform in the experimental phase, due to the fact that the open ECU that is adopted in this project can be compiled in a Simulink environment.
The proposed CVT control module (see in **Figure 4.21)** is made of several sub-systems, including a feedforward steady-state look-up table and a feedback loop on manifold pressure.

The feed-forward loop, which is basically a look-up table, is designed to help the controller to achieve the target quickly and robustly. This map is characterised by the strategy of the boost split. In the simulation below, it is decided to primarily make use of the turbocharger boost, with the supercharger providing a boost only when the turbocharger boost is insufficient.

The feedback control includes an anti-windup function and a gain scheduling strategy. The feedback controller here, essentially, has two targets here: adjusting the CVT ratio so that the total boost pressure can be achieved if the feed-forward loop is not working precisely (due to component ageing or different boundary condition); and detecting a transient signal in order for the supercharger to 'pre-boost' the engine system.

It might be worth noting that two look-up maps (i.e. upper and lower CVT ratio rate limiter) were used to optimize the transient trajectory shaping for the best V-Charge performance, which was from the perspective of physical response behaviour, and also the driveability consideration. At the time of writing, it is found in simulation that the largest achievable CVT change rate might not be appropriate to implement during a transient event, due to the 'dip' phenomena, as there may be too much acceleration torque generated. This might affect the driveability if a similar torque response was repeated in the experiments, depending on whether the simulation model is predictive or not. In addition, whether the torque dip (if there is any) could be 'felt' by the driver is another question, which also needs to take into consideration the damping effect of the whole powertrain system (and is thus beyond of the scope of this research).

In order to accurately control the boost split in the two-stage system, the standard closed-loop pneumatic mechanism was replaced by a 'smart' pneumatic wastegate mechanism with electronic control, as seen from **Figure 4.22**. **Figure 4.23** shows the wastegate control module that was proposed for the V-Charge project. It is, like the CVT ratio control discussed above, was comprised of two main sub-sections of controlling: feed-forward and feedback loop. There is also an anti-windup loop in the wastegate control module. Note that the PI controller input for the wastegate control is the turbocharger pressure ratio difference between the target and the actual, and that for the CVT ratio control is the total boost pressure difference between the target and the actual. This is scheduled in order for the two interdependent PI controllers not to fight each other.

In the following, a transient simulation of 20 - 100% full load was conducted. A transient GT-Power model was modified around the full-load model, with the valve timing kept fixed. Although it was very simplistic, it actually made very little difference on most of the transients, where the engine's transient response was dominated by the dynamic behaviour of the turbocharger and supercharger. It might be noted that the combustion model (which is also fixed in this simulation) can also have a significant effect on a transient response. Consequently, it is admitted that the simulation results might have a large deviation compared to the test results. Nevertheless, the tuning trends should be very similar to those in the test phase, which is why the control strategy was initially constructed in the simulation phase.

In this work, the transient response simulation was carried out with a standard procedure whereby the model was run at each speed for five seconds at a load of 20% full-load for stabilisation, prior to a step load demand input to full load. The full load was then held to the end of the simulation. The time-to-torque in this work was taken for the engine torque to increase to 90% of the target full load (T90). The epicylic ratio and pulley ratio were initially set to be 12.67 and 3, respectively. The turbocharger and supercharger map were supplied by Borgwarner and Honeywell, respectively. Note that there are other configurations that are considered in the later experimental phase, but the calibration process should be very similar.

From **Figure 4.24**, it can be seen that the transient response of the V-Charge engine is similar to that of an NA engine, although there is slight 'dip' during the first phase of the acceleration

and a mild overshoot at the end of the transient. Both deficiencies could be mitigated by optimising the CVT rate limit and the PI gains in the CVT module. **Figure 4.25 (a)** shows the CVT ratio trajectory during the transient, which functioned as predicted. The CVT was ramped to the largest level that pre-boosted the engine as soon as a transient signal was detected, and then the boost was handed over from the supercharger to the turbocharger by reducing the CVT ratio. The wastegate behaviour in simulation can be seen in **Figure 4.25 (b)**, which shows that the wastegate was fully opened during the steady-state low load, and then quickly shut down when a transient signal was detected.

Figure 4.25 (c) and **Figure 4.25 (d)** illustrate the supercharger and turbocharger compressor response in the transient. The supercharger pressure ratio trace was in line with the CVT ratio trajectory in **Figure 4.25 (a)**. It might be worth noting that there is a pressure ratio 'dip' for the turbocharger compressor, as can be seen in **Figure 4.25 (d)**. This is mainly due to the fact that the supercharger response is much faster than the turbocharger; thus, a lot more pressure is blocked between the supercharger and the turbocharger.

4.3 In-vehicle modelling

There are two approaches currently in the literature that utilise steady-state engine look-up maps to simulate driving-cycle fuel economy, including the engine-level consolidated point methodology and the vehicle-level kinematic mode.

4.3.1. Consolidated point methodology

This uses a least-squares method to reduce the number of engine speed and load operating points that an engine operates during a driving cycle, from typically hundreds to only a few points (see **Figure 4.26)**. The point is then given a time weighting based on the total driving cycle time [186]. The calculated fuel economy, using the engine steady-state look-up tables, has been proven to be within a 3% error of running the full vehicle, but with approximately 40 times less computational time [153].

4.3.2. Kinematic mode

This is a backward-looking method directly imposing the driving-cycle speed to back-calculate the engine speed and the load, by using the aerodynamic, rolling resistance, and the road

characteristics, without considering the transient differences in charge air handling systems [182, 187]. The instantaneous engine speed and load are used for look-up tables in speed-load dependent engine maps to calculate the instantaneous rates of fuel consumption, emissions, etc. In addition, since the engine speed and torque are directly calculated, these may not reflect the driver's perception of the vehicle's performance. However, this method is relatively simple, requires less knowledge of the vehicle control system, and is still considered to be a valid methodology to simulate and compare the performance of a NA vehicle.

An example is given here to explain why the consolidated point method (termed Minimap methodology in some of the literature, including [7,61,135,159,163] and the kinematic mode cannot reproduce the boost system response and cannot exhibit a real fuel economy in a driving cycle for comparing boosted engines with different transient performances [153]. During a vehicle acceleration event, the transient performance of the engine influences the driver's pedal demand, which can further cascade to the transmission shifts event. If continuously pressing the pedal still cannot produce the expected torque performance due to the slow boost response, a down shift may be operated, which causes the engine to run in a higher-speed and lower-torque region, where the efficiency drops. Thus, suitable numerical simulations should incorporate a dynamic driver model to control the engine parameters in a forward-direction manner. However, most of the currently performed vehicle simulations do not incorporate this.

4.3.3. Half-dynamic mode

Most driving-cycle fuel economy simulation had been carried out kinematically because the dynamic solution was extremely time-consuming and a robust solution was available only for kinematic simulations. Typically, a proportional and integral (PI) controller was used to target vehicle speed in a driving cycle, but this required laborious tuning of different gains for a particular vehicle over a particular driving cycle, in order to avoid control noise. A recent trend in vehicle simulation is to adopt a model-based feed-forward dynamic solution with corrective feedback loop (PI gains) to follow driving-cycle speed targets accurately [188]. Because the PI controller of a dynamic solution is used to correct only those small errors that exist, the simulation speed is significantly increased. It should be noted that a fully-developed dynamic model should incorporate dynamic modules for both a vehicle and the

driveline. Currently, the most widely adopted approach for vehicle simulation utilises only the dynamic mode for the vehicle, without a detailed dynamic analysis for the engine. This method, as opposed to the kinematic mode mentioned above and the full-dynamic mode below, is termed the half-dynamic mode, which features a more highly-developed vehicle control model to determine the necessary accelerator and brake pedal position, in order to follow the required driving cycle target, but only with engine steady-state look-up tables.

4.3.4. Full-dynamic mode

Unlike the two approaches discussed above, a full-dynamic mode refers to those with a detailed engine model and a more highly developed driver control unit. By doing this, the dynamic response of the engine can be reproduced and the driver behaviour can also be simulated. It should be noted that this methodology is extremely CPU intensive when trying to simulate a drive cycle. An FRM might need to be used in this case, to save some simulation time [188]. This is, in essence, achieved by lumping pipe objects together on the intake and exhaust side of a detailed engine model. Although this method cannot capture higher frequency wave dynamic content, a high level of fidelity of the low-frequency and primary engine-order dynamics is maintained, which is normally of interest to transient simulations.

This mode allows the development of the physical control system for both the vehicle and the engine [182]. In addition, the down-speeding and transmission shift frequency effect on fuel efficiency may only be able to simulate in this mode for different boosting solutions [156], which, in contrast with the conventional engine-map-based vehicle models, has the capability to model transient phenomena, such as turbo-lag during drive away and gear shifts [188].

4.3.5. Case Study: V-Charge in-vehicle simulation

In order to assess the vehicle response for the V-Charge system compared with the fixed-ratio positive-displacement counterpart, in-vehicle simulation was conducted using the vehicle data from Ford. There are four manoeuvres which are of interest to Ford, including:

1: 60-100km/h in 4^{th} and 5^{th} gear

2: 80-120km/h in 4^{th}, 5^{th}, and 6^{th} gear

3: WOT tip-in in 1^{st} gear from 840RPM

4: WOT tip-in in 2^{nd} gear from 1850RPM

As the torque curve is only available between 1100RPM and 4000RPM from the original full-load GT-Power model, the achievable torque above 4000RPM was assumed to be proportional to the classic Fox engine, coming from a Ford paper (see **Figure 4.27**) [189].
Figure 4.28 shows a tractive torque diagram calculated and plotted from the engine performance curve and the gear ratio. Since there is no point of intersection between each gear, the fastest vehicle acceleration manoeuvres should be using each gear to the highest engine speed and then shifting up.

The simulation was conducted by coupling the detailed transient model with a simplified vehicle system in GT-Power. Some unknown parameters (such as inertia of each axle and transmission efficiency) came from a GT-Power example file. Unlike the fixed-speed transient simulation, the engine mode was changed from speed to load, which means that the engine speed will be calculated depending on the actual engine load. The simulation was run for 30 seconds at the corresponding initial engine speed for stabilisation prior to a step load demand input to the target full load. It might be noted that, for this simulation, the fixed-ratio positive-displacement configuration was assumed to be equipped with a clutch, while for the V-Charge system a clutch was not needed and the epicyclic ratio and pulley ratio were set to be 12.67 and 2.5, respectively. The following are the results of the manoeuvres mentioned above.

It is safe to say that the V-Charge system has a similar vehicle response when compared with the fixed-ratio positive-displacement configuration, even though the V-Charge system has better engine transient response. This is mainly due to the fact that the full-load target was fixed for both the V-Charge and the Eaton configuration in simulation. However, when the supercharged configuration (both V-Charge and fixed-ratio positive-displacement) is compared with the turbo-only system, it is seen that there was a perceptible lag (so called turbo-lag), especially when the gear and the engine speed were low (see **Figure 4.34** and **Figure 4.35**). This is mainly due to the fact that the target full load was not reached by the turbo-only configuration, because of the turbo lag, when the target was already achieved by the supercharged version.

Note that for the turbo-only configuration, there are two sets of simulation that have been performed. One simulation assumes that the target torque is the same as that of the V-Charge and the fixed-ratio positive-displacement configuration. The other simulation lowers

the target torque to see how that affects the transient performance of both the engine and the vehicle. This could also be seen as different strategies for supercharger matching to an existing turbocharged gasoline engine.

- A supercharger is only used to assist transient response;
- A supercharger is used for the torque curve augmentation and improving the transient behaviour.

Figure 4.36 shows the effect of the supercharging on improving the transient response of both the engine and the vehicle in a manoeuvre of 60-100km/h in 5th gear. It also indicates that the augmentation of torque curve will have a larger effect on the transient behaviour over that achieved by only adopting a supercharger to improve the transient response without enhancing the torque curve. However, as the lower target torque curve was still not achieved in **Figure 4.34** and **Figure 4.35**, the wide open throttle (WOT) tip-in performance in 1st gear from 840RPM and 2nd gear from 1840RPM would not be improved, indicating that the torque augmentation might only be beneficial for the higher engine or vehicle speed transient performance.

Figures in Chapter 4

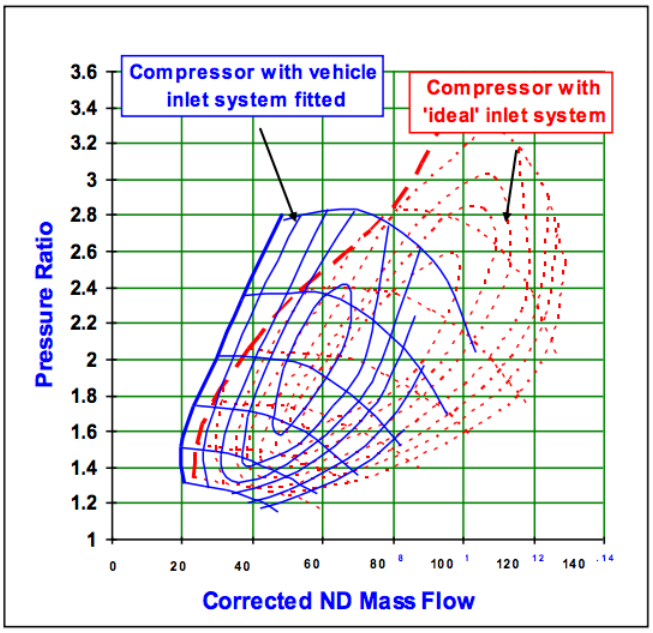

Figure 4.1. Corrected compressor maps with 'ideal' straight bell-mounted inlet and vehicle inlet system. [183]

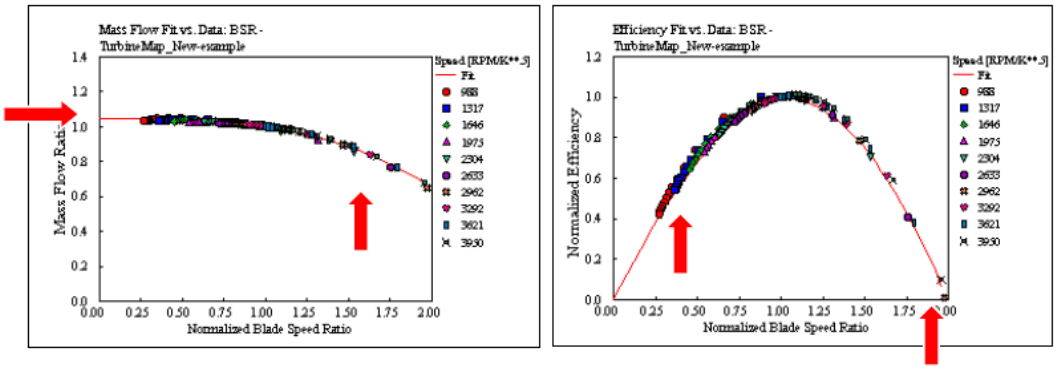

Figure 4.2. Turbine map fitting method

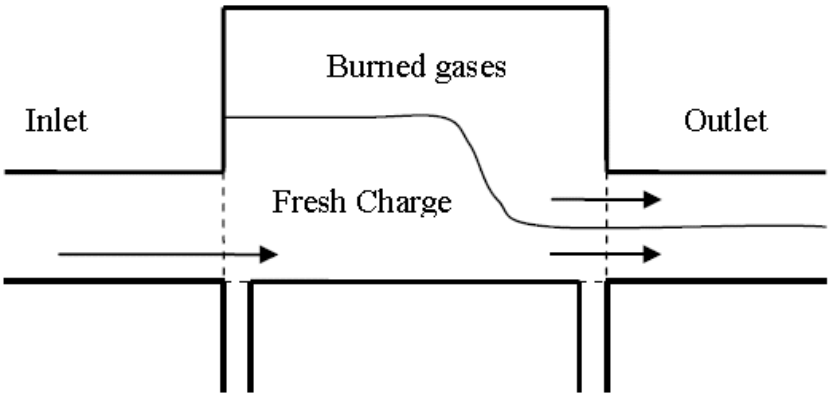

Figure 4.3. Scavenging process in a realistic engine [181]

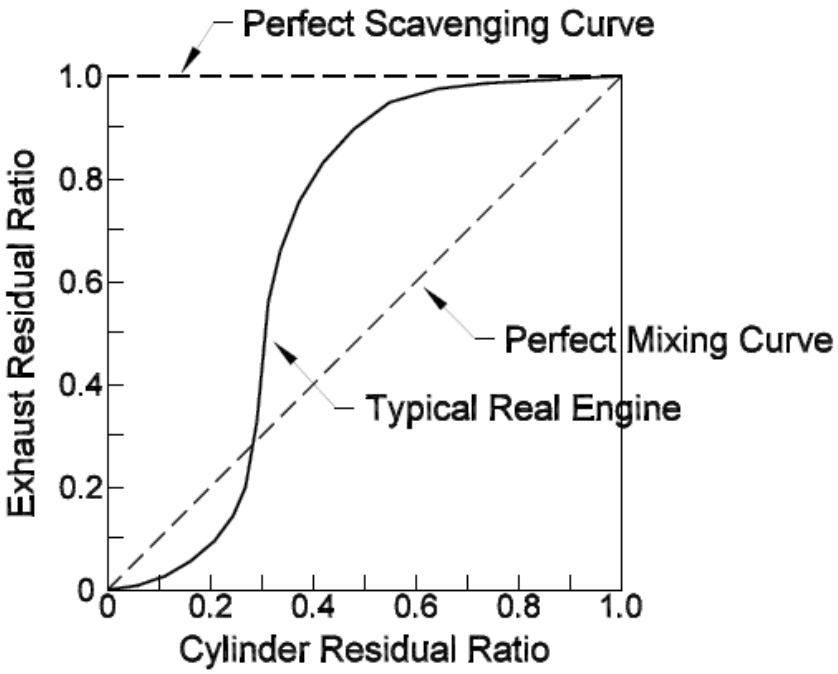

Figure 4.4. 'S-shape' scavenging function [181]

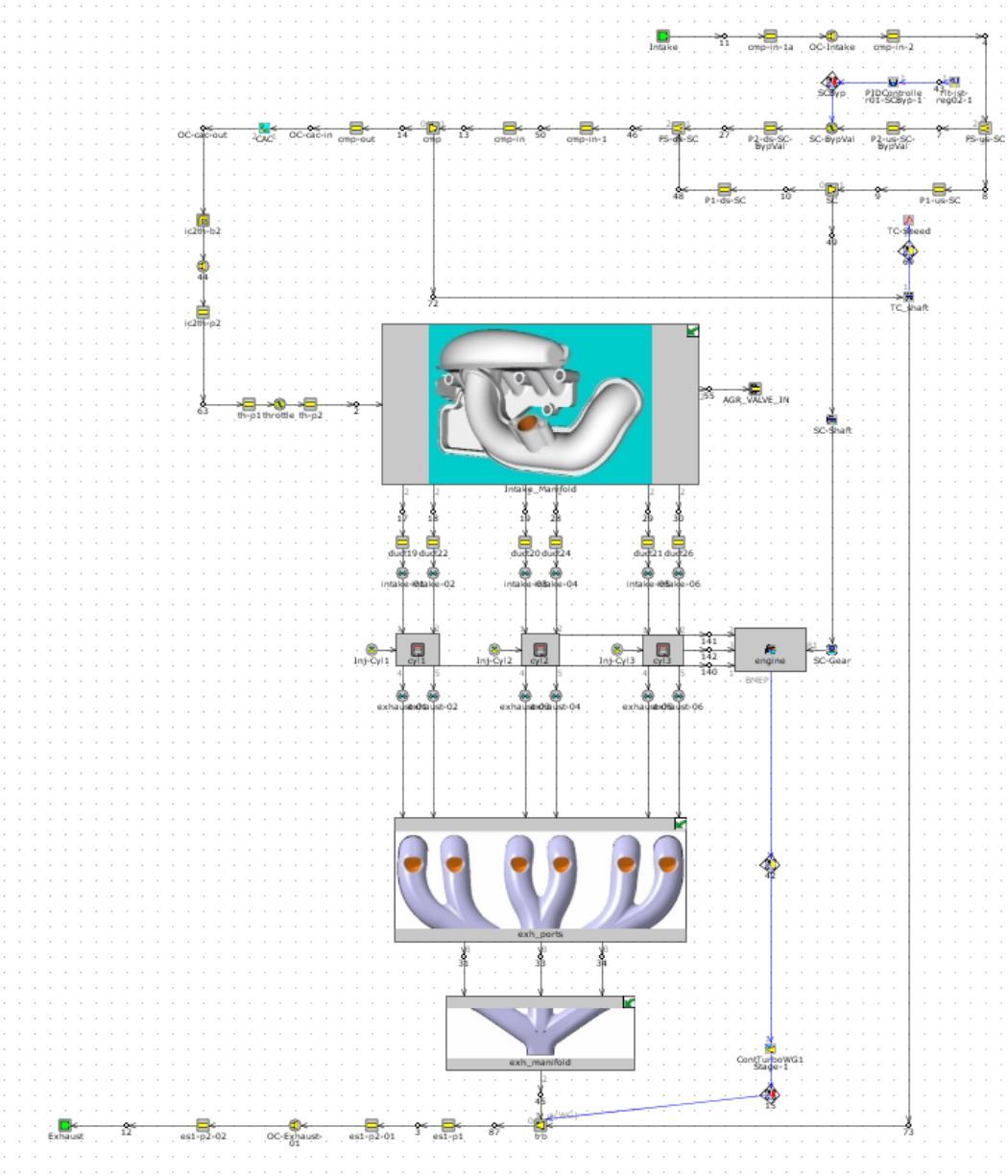

Figure 4.5. The engine GT-Power model supplied in this project

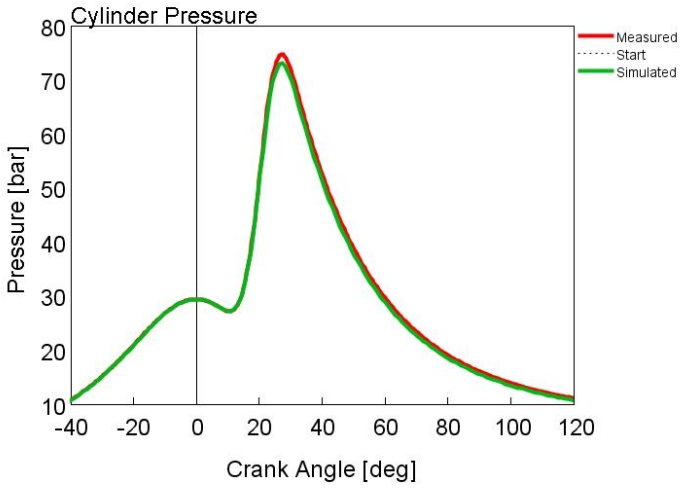

Figure 4.6. Measured and simulated cylinder pressure at 1000RPM and 130Nm

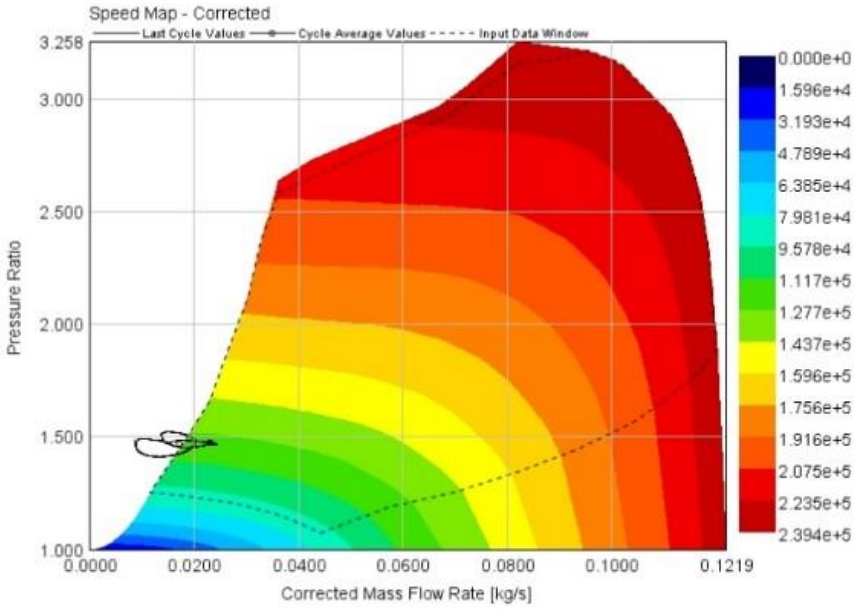

Figure 4.7. Turbocharger compressor operating point

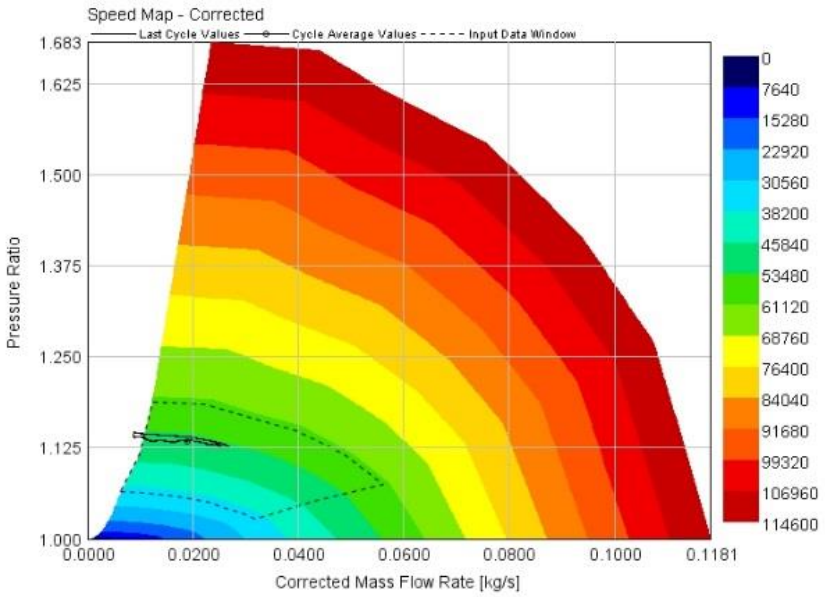

Figure 4.8. Supercharger compressor operating point

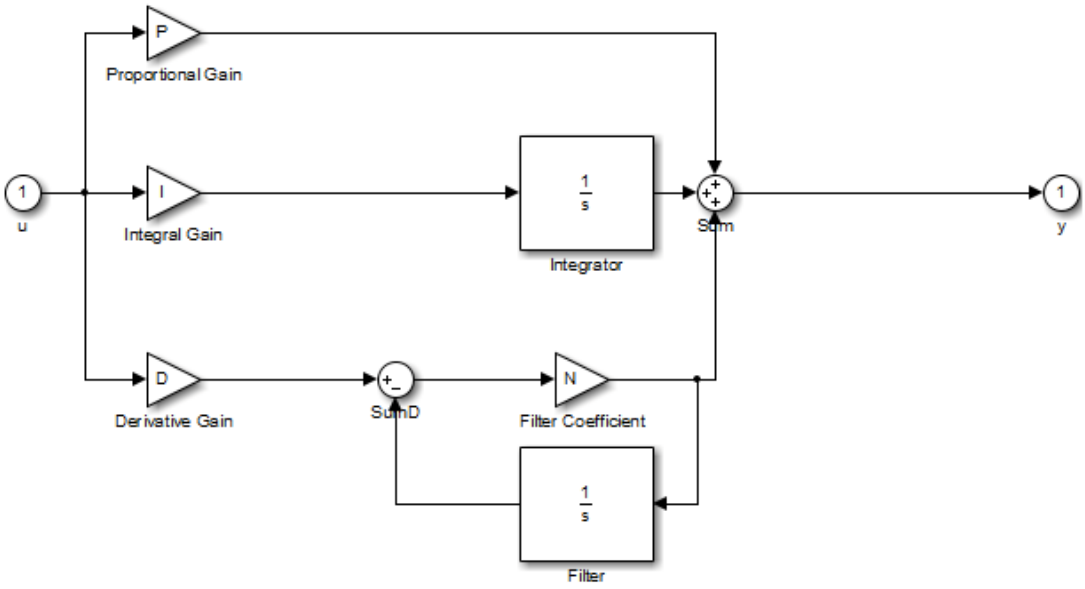

Figure 4.9. PID controller Simulink block

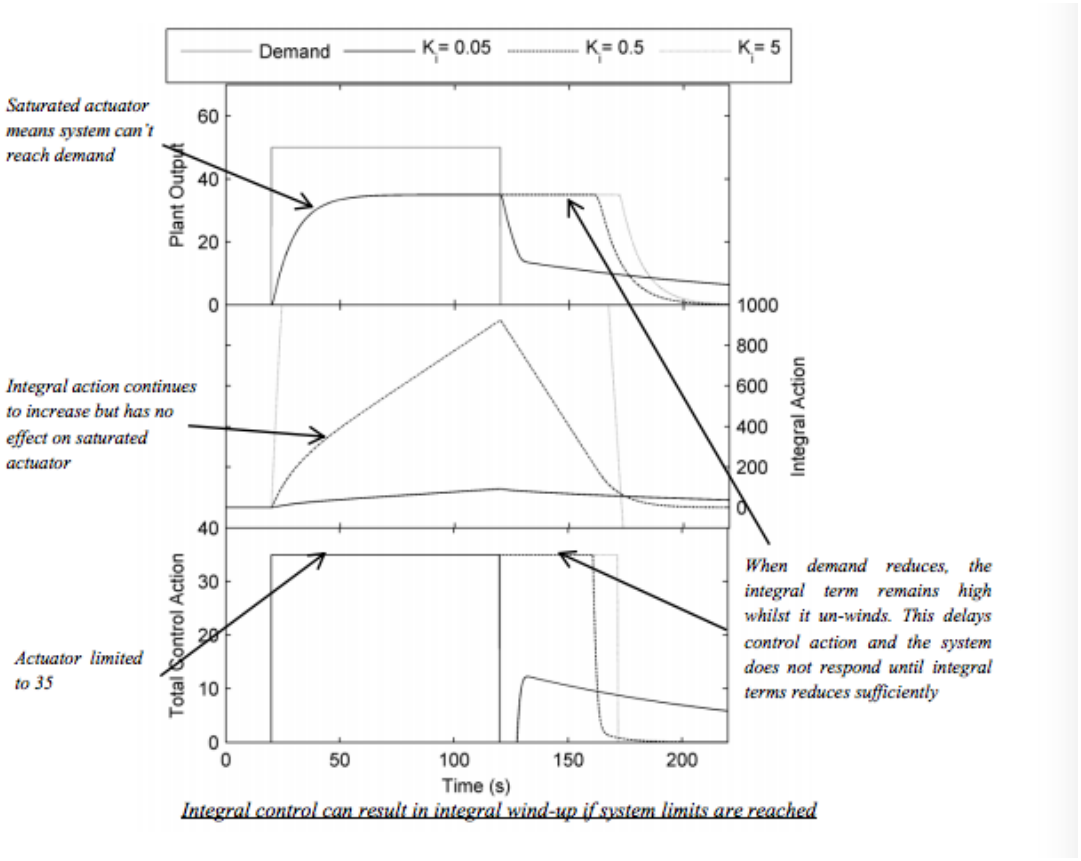

Figure 4.10. Integral wind-up for a PID control [169]

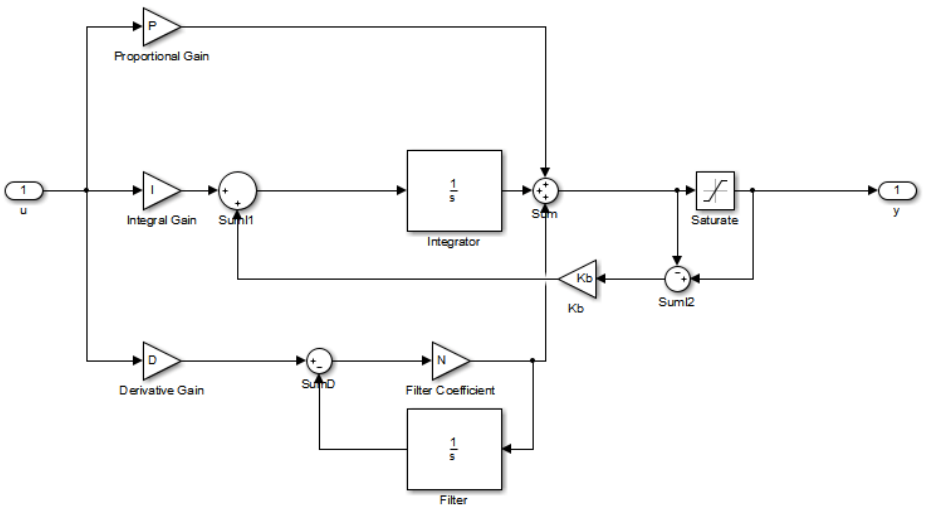

Figure 4.11. Back-calculation anti-windup method

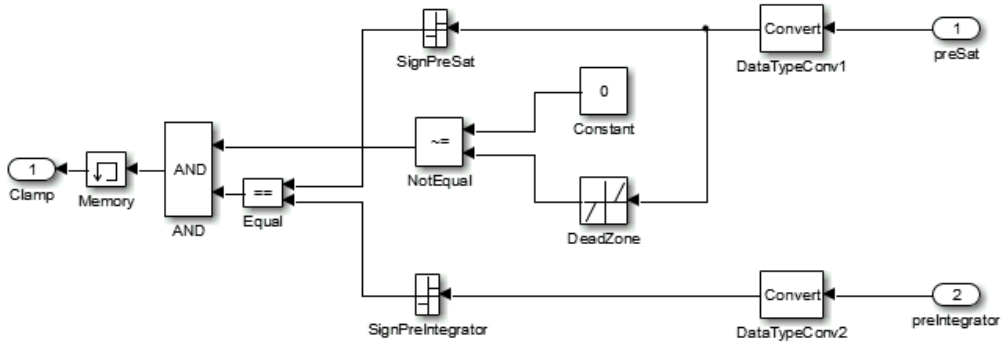

Figure 4.12. Clamping anti-windup method

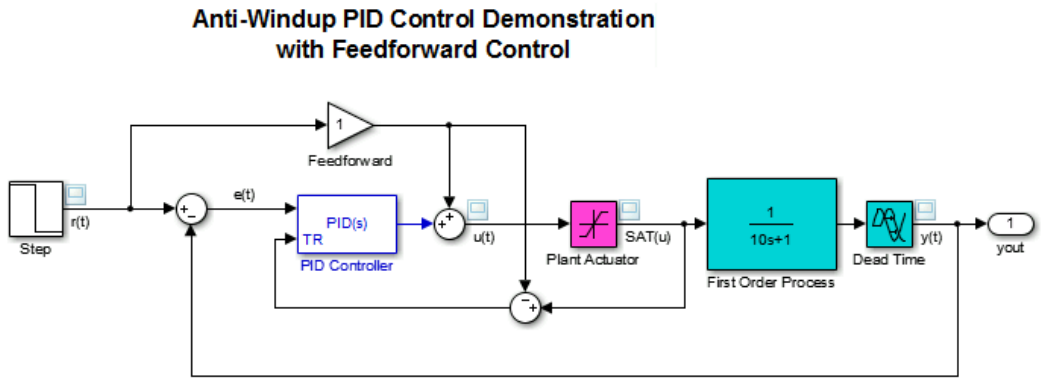

Figure 4.13. Anti-windup PID control demonstration with feedforward control

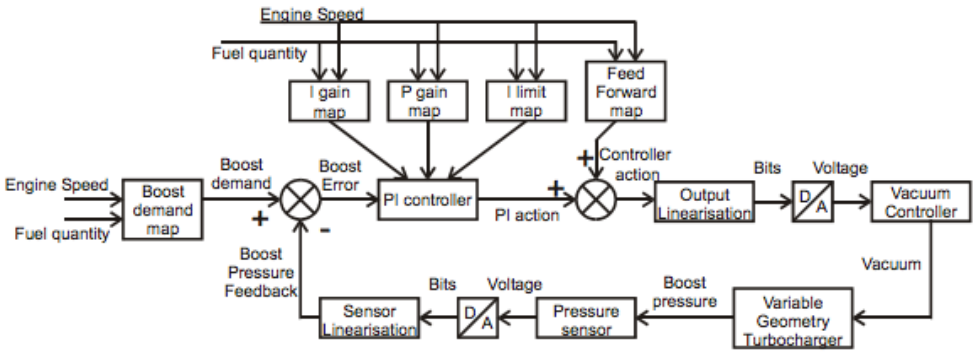

Figure 4.14. Control strategy schematic for a variable geometry turbocharger in an engine [169]

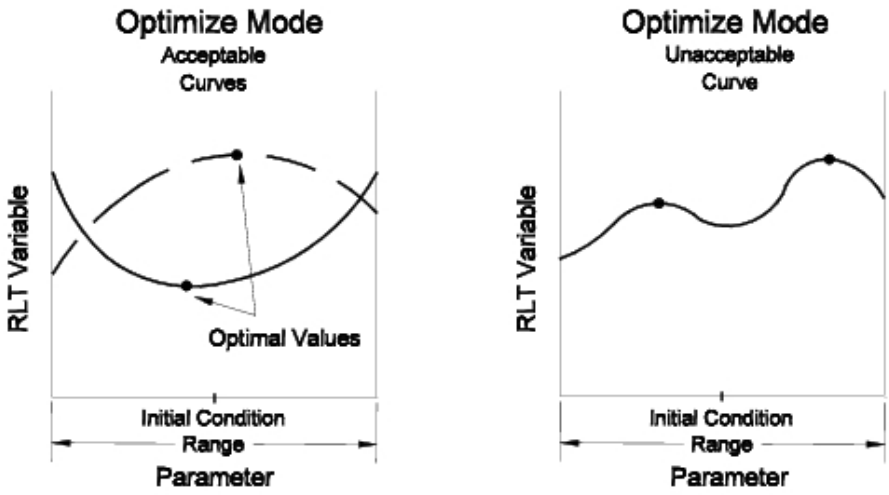

Figure 4.15. Illustration of the GT-Suite embedded optimization strategy

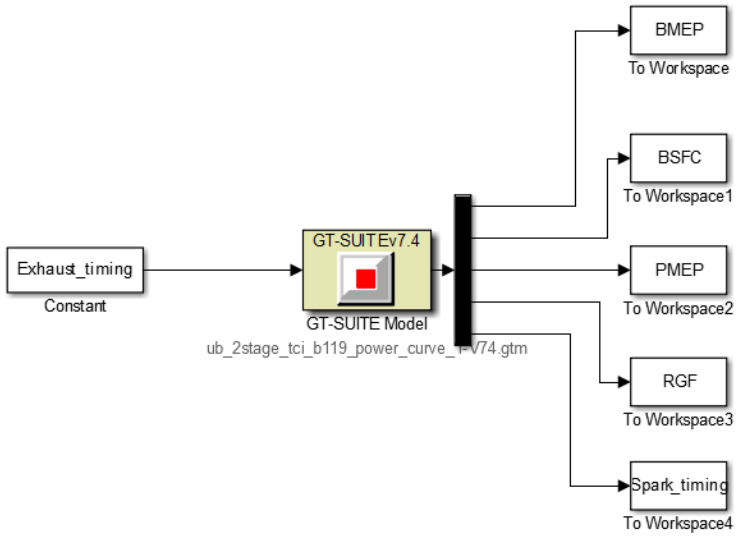

Figure 4.16. Illustration of a GT-Power engine model in Simulink interface

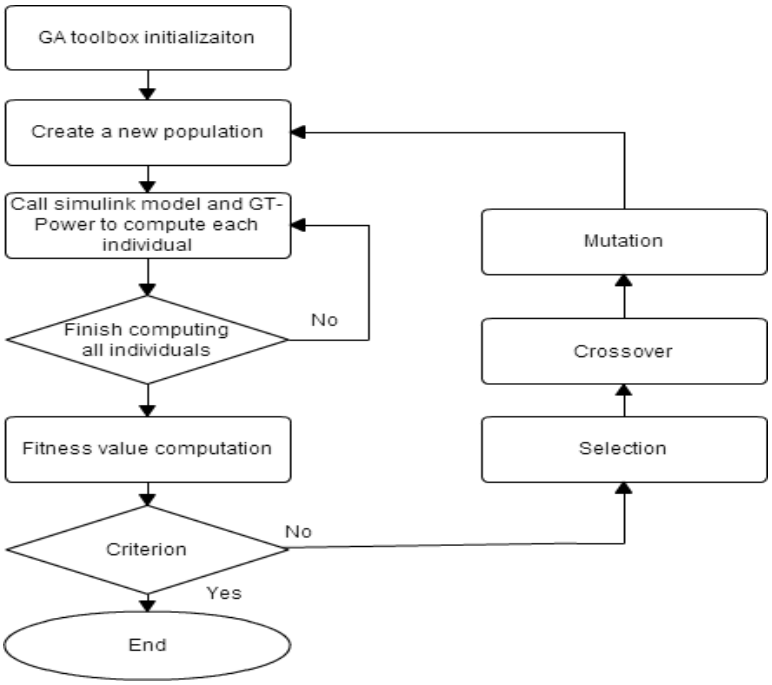

Figure 4.17. Genetic algorithm procedure

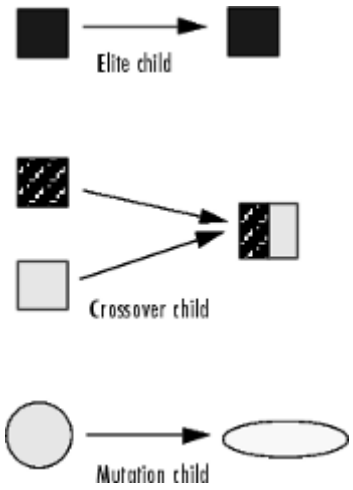

Figure 4.18. Illustration of three types of children

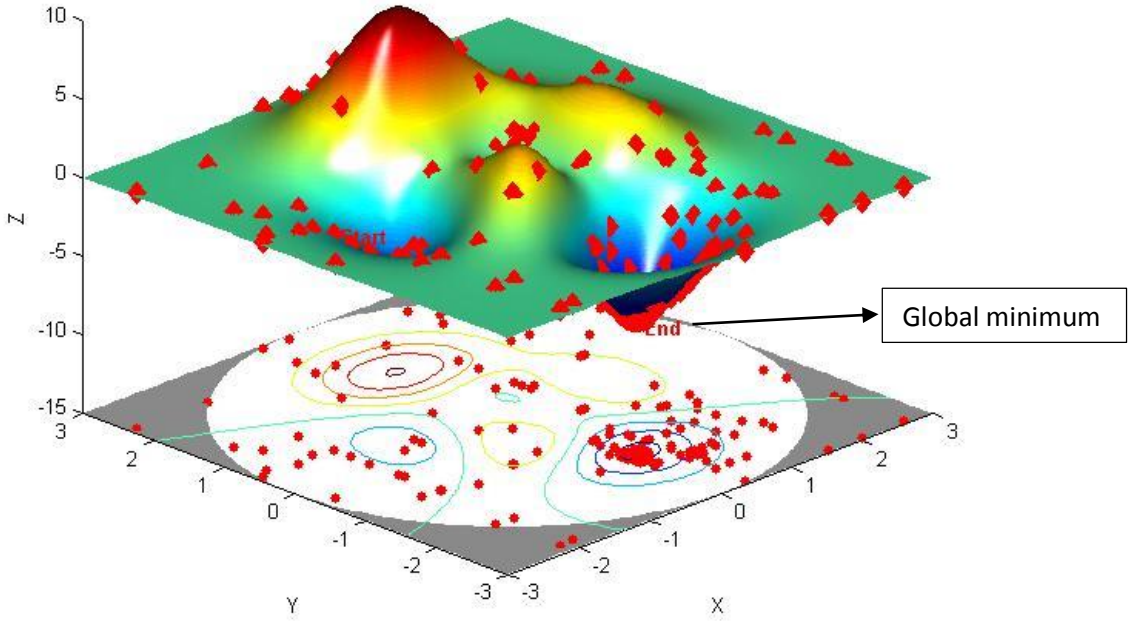

Figure 4.19. Genetic algorithm testing

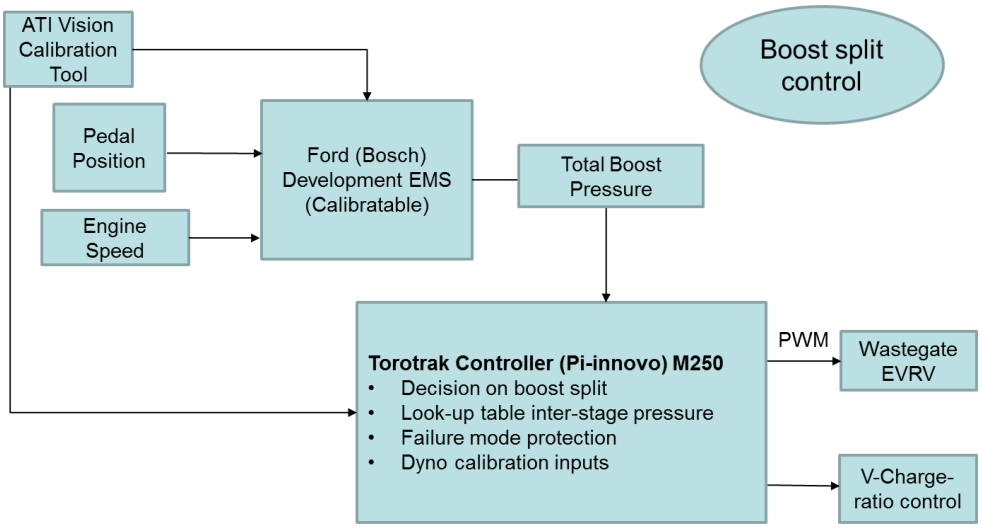

Figure 4.20. Boost split control module

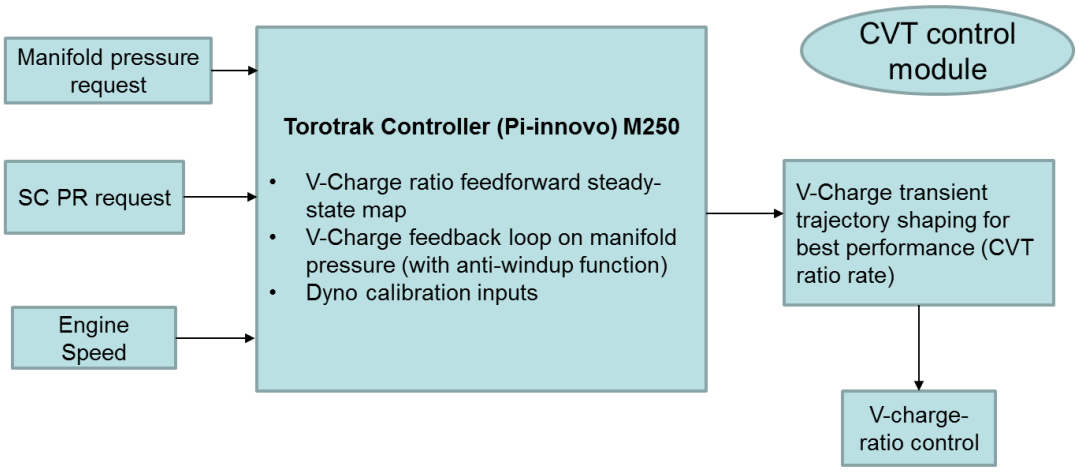

Figure 4.21. CVT control module

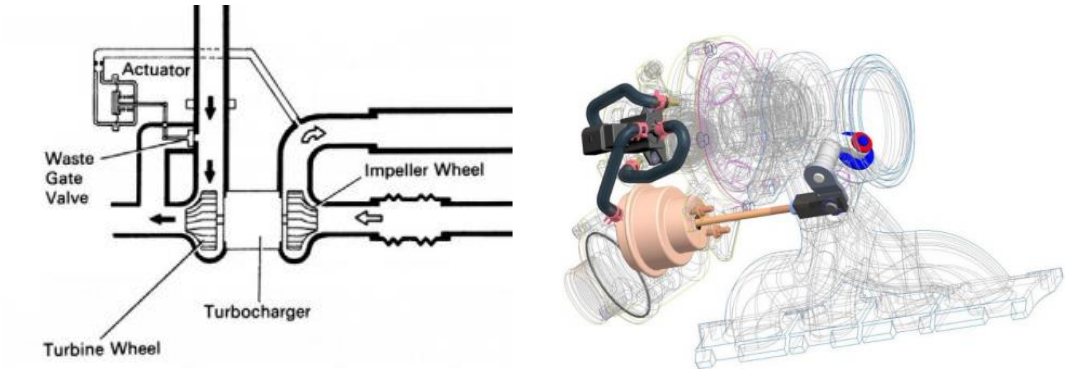

Figure 4.22. Standard closed-loop pneumatic wastegate control (left) and smart pneumatic wastegate with electronic control (right)

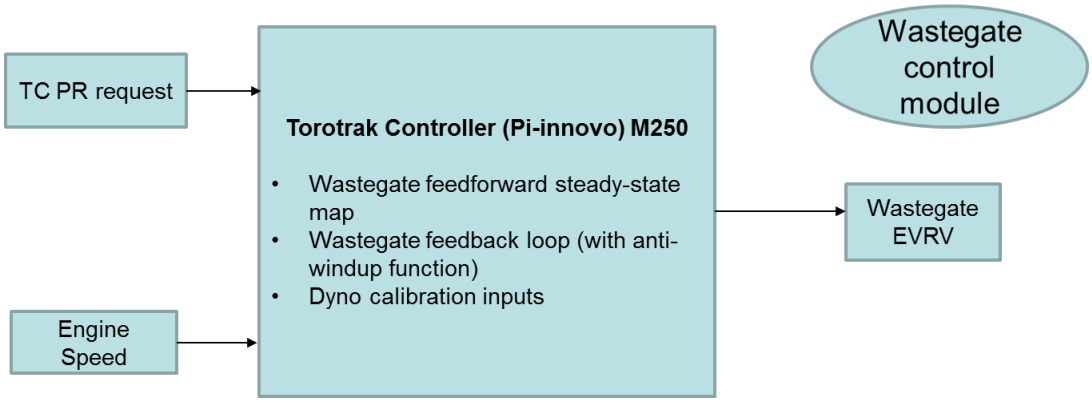

Figure 4.23. Wastegate control module

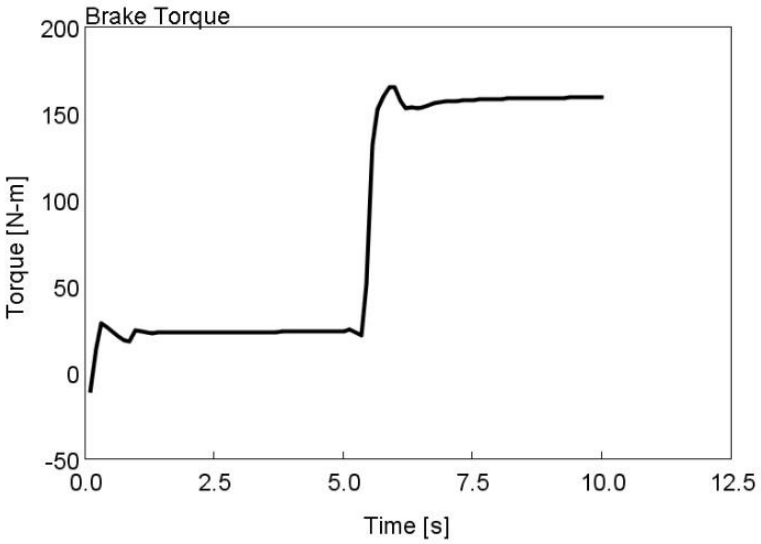

Figure 4.24. Torque performance during a transient event at 1100RPM

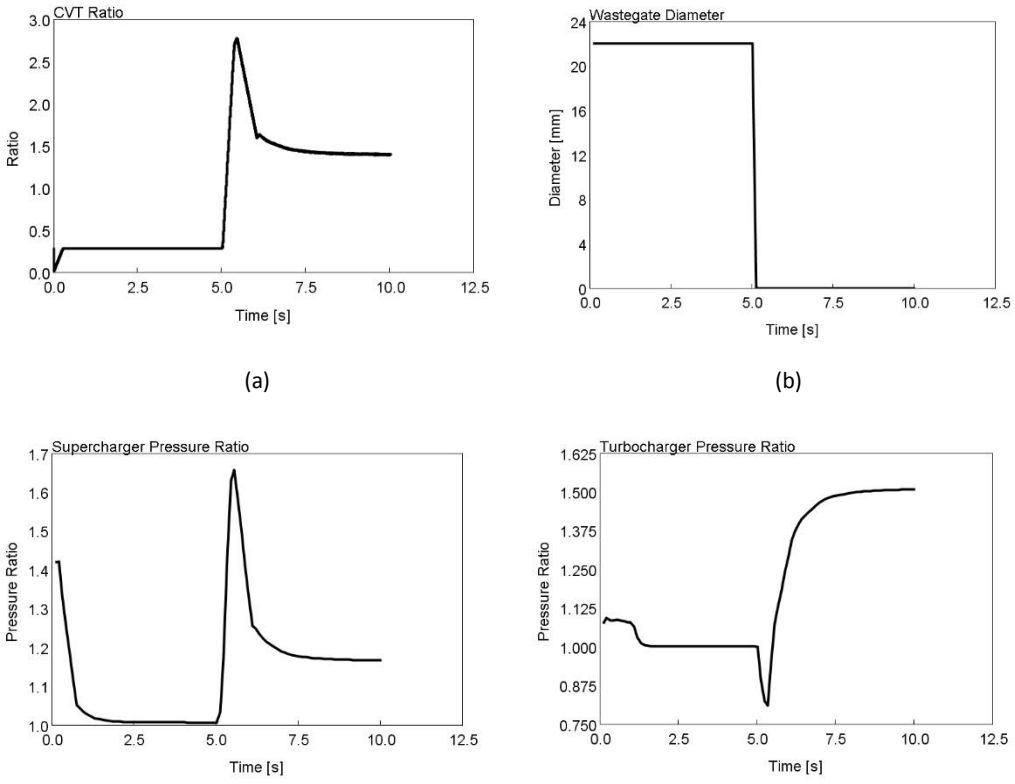

Figure 4.25. The V-Charge system trajectory during a transient event at 1100RPM

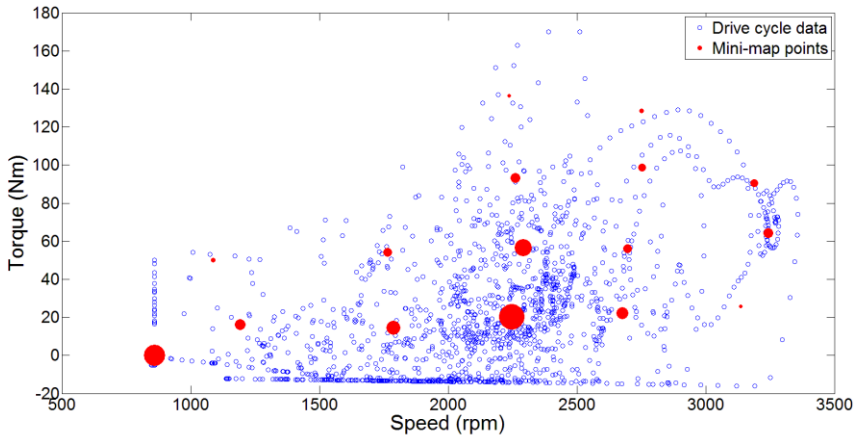

Figure 4.26. Consolidated point methodology

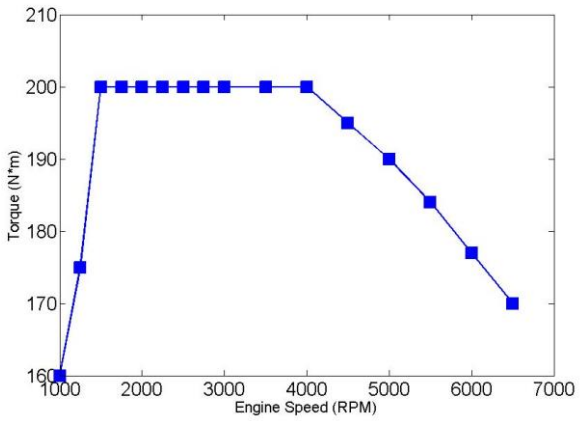

Figure 4.27. Engine performance curve for a Ford GTDI engine

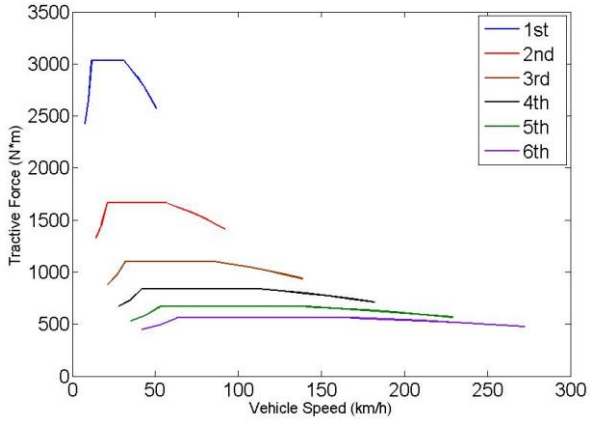

Figure 4.28. Tractive torque diagram for a Ford vehicle with different transmission gear

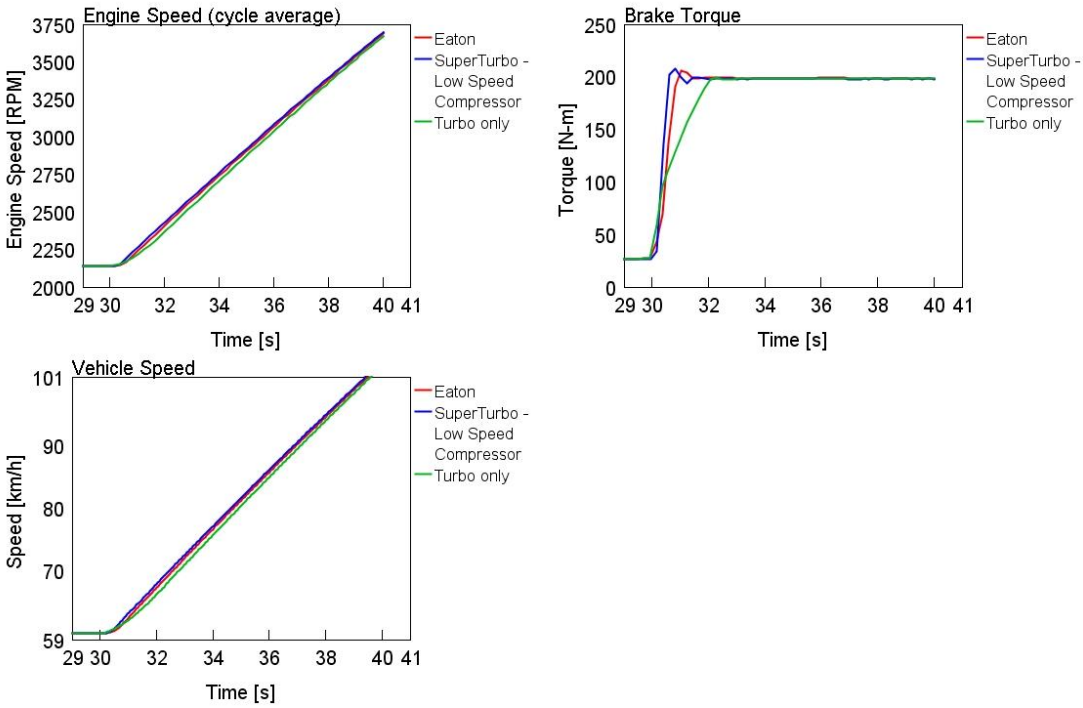

Figure 4.29. 60-100km/h in 4th gear

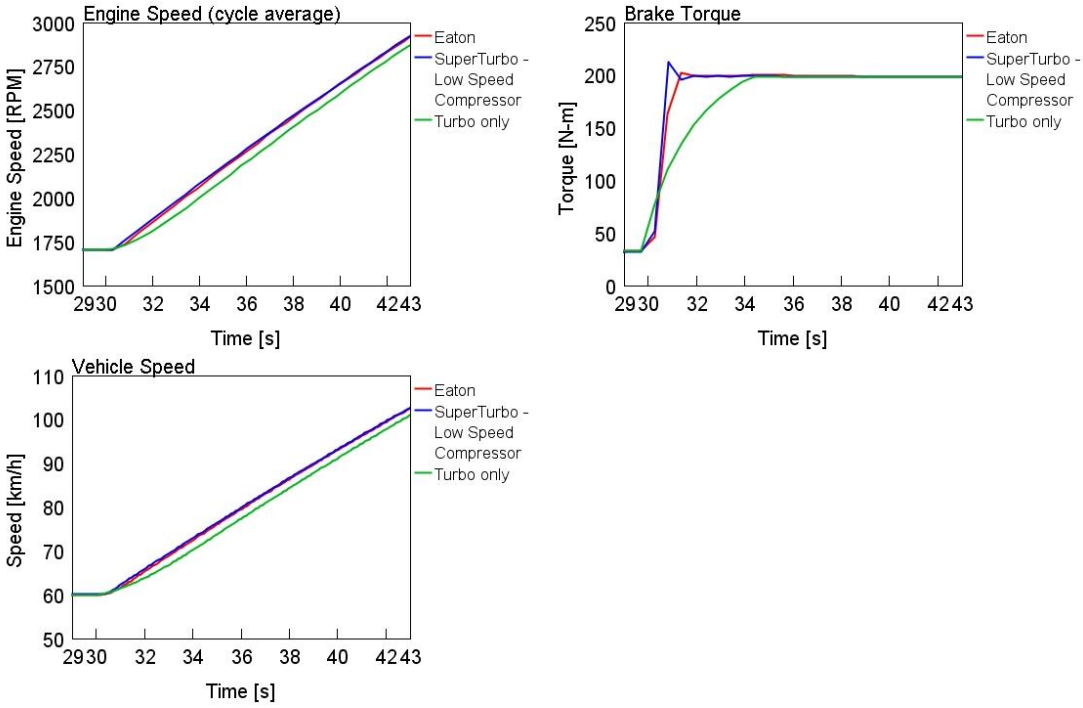

Figure 4.30. 60-100km/h in 5th gear

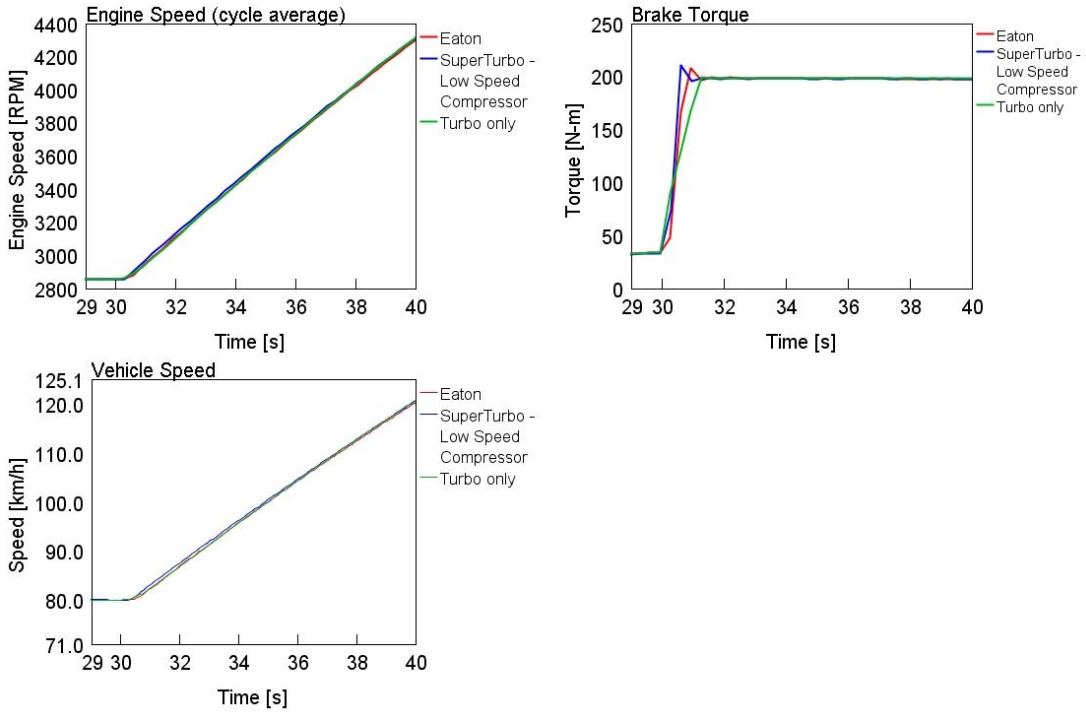

Figure 4.31. 80-120km/h in 4th gear

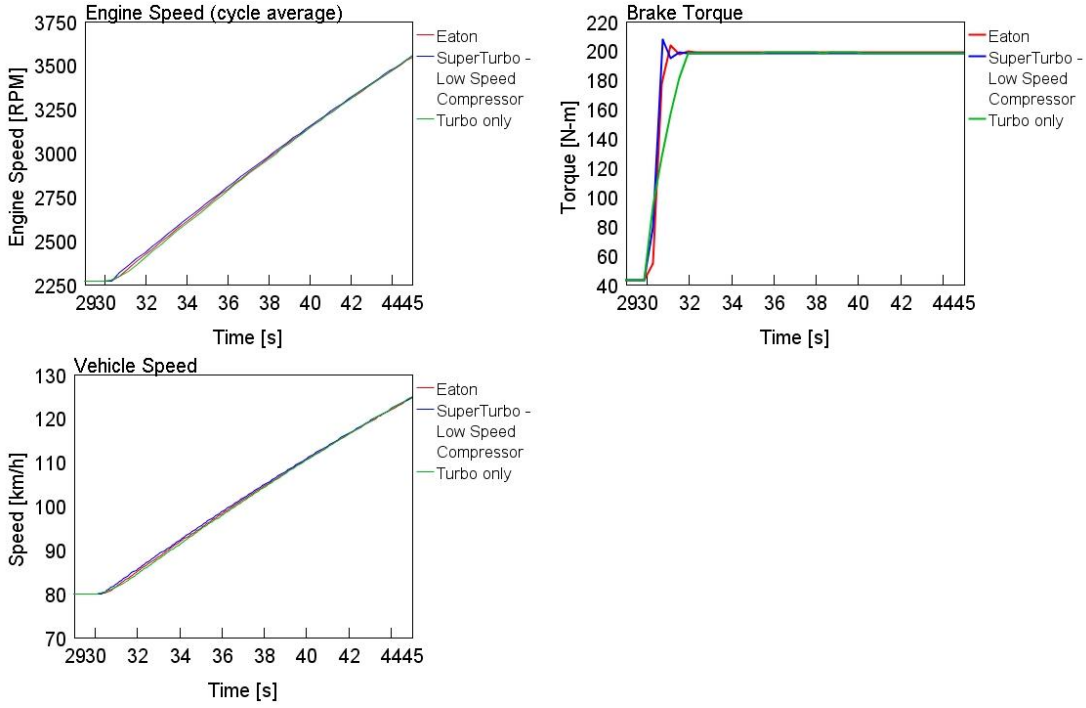

Figure 4.32. 80-120km/h in 5th gear

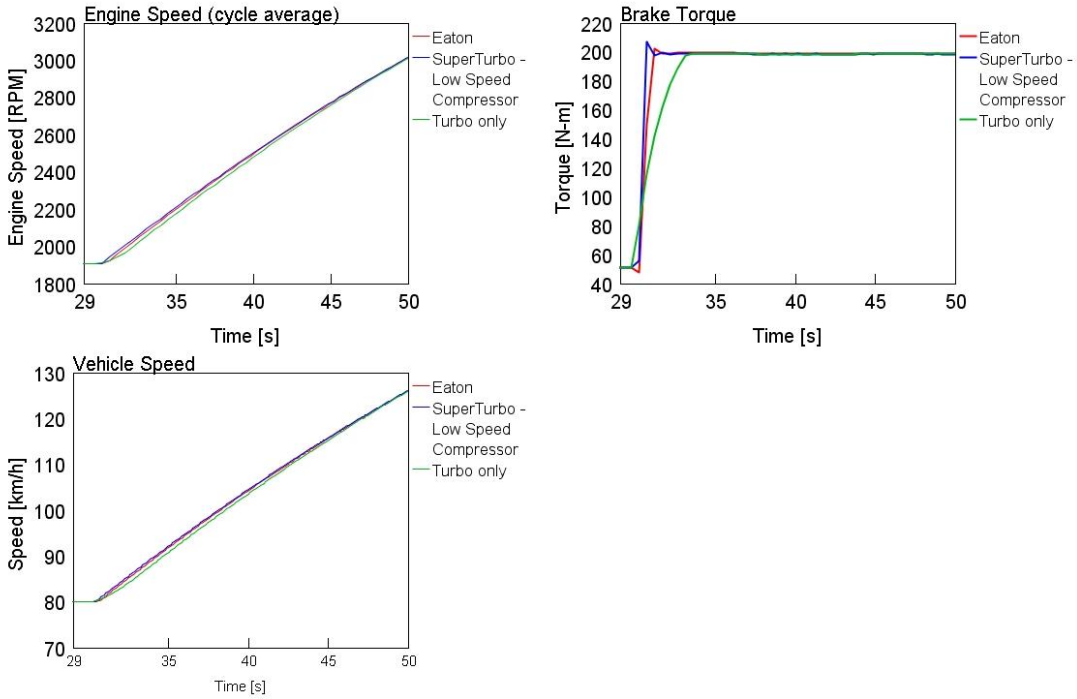

Figure 4.33. 80-120km/h in 6th gear

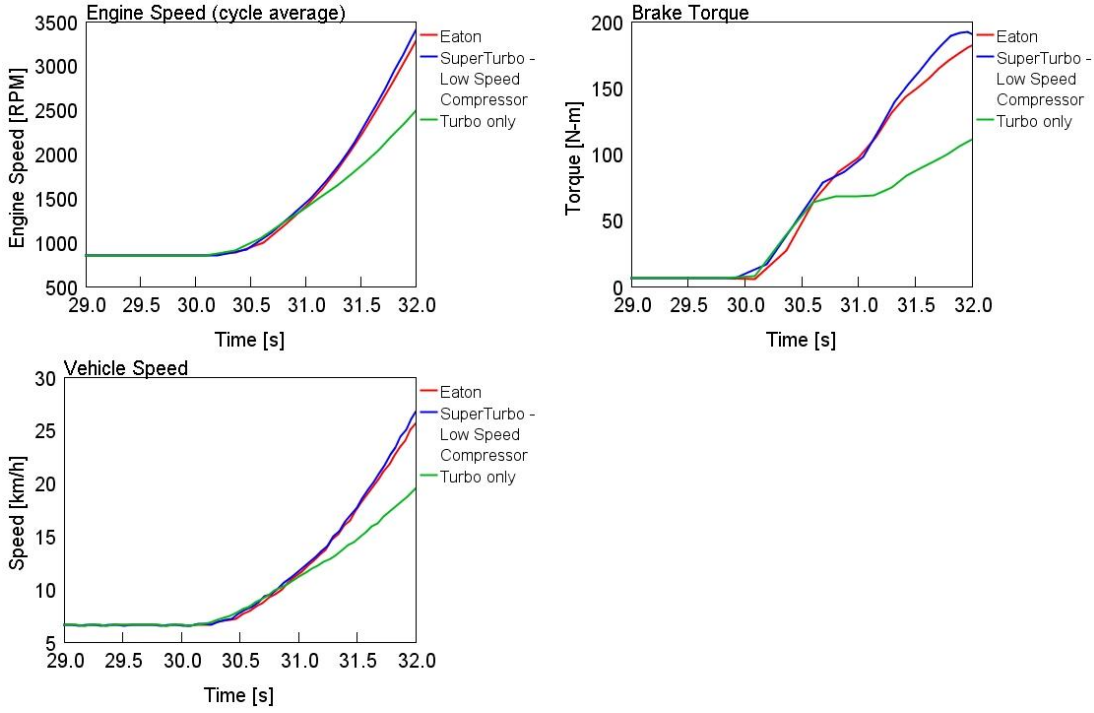

Figure 4.34. WOT tip-in in 1st gear from 840RPM

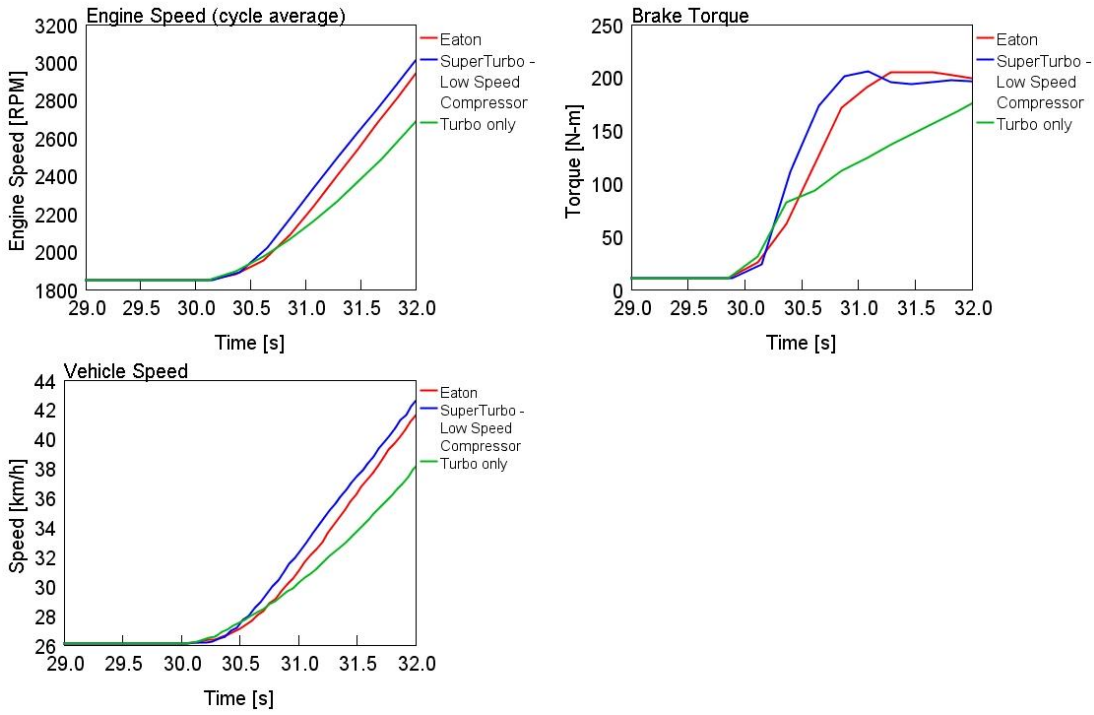

Figure 4.35. WOT tip-in in 2nd gear from 1840RPM

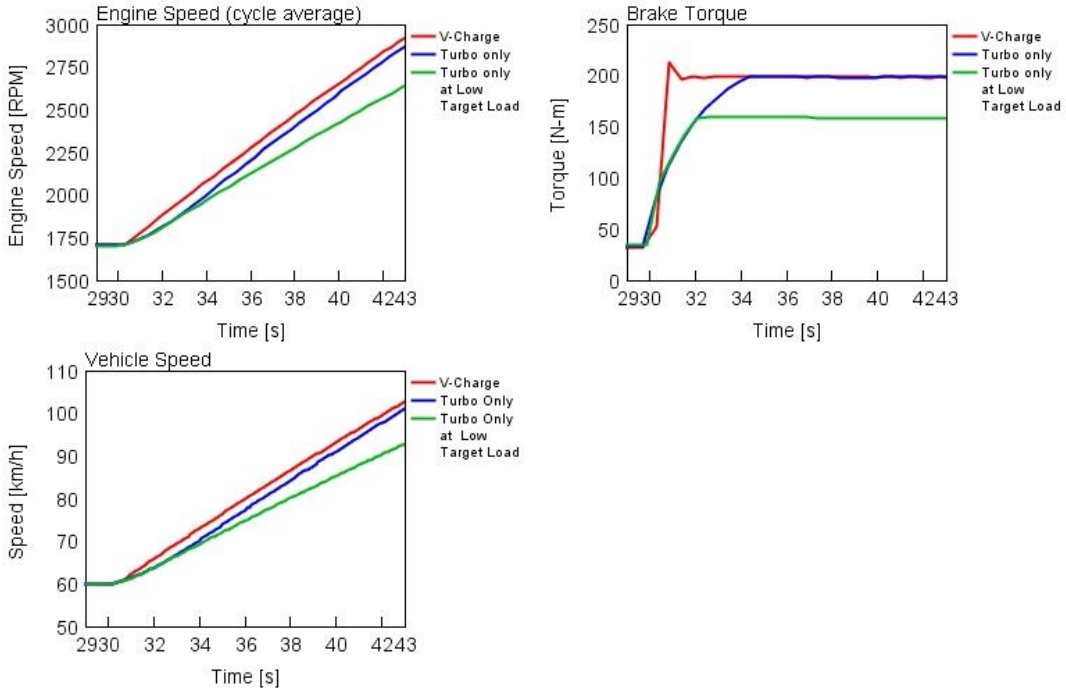

Figure 4.36. 60-100km/h in 5th gear with a lower target full load curve for turbo-only configuration

Chapter 5 – Modelling the conventional DEP concept

DEP is an alternative gas exchange concept, where two exhaust ports from each cylinder are separated into different manifolds. The blow-down pulse is directed through one valve that leads to the turbocharger turbine, in order to boost the intake charge, while the other valve path (termed the scavenging valve) bypasses the turbine to scavenge the remainder of the exhaust mass flow. By combining the characteristics of the downsized turbocharged engine and the scavenging process of a more normal, naturally aspirated engine, the gas exchange process of a downsized engine could be enhanced.

In this chapter, the conventional DEP concept will be investigated in simulation, using a validated highly-downsized 2.0 Litre SI engine model. The final results showed that the full-load BSFC, the engine combustion stability and the transient performance were all improved due to the fact that the DEP concept features a better gas exchange process and improved combustion phasing.

The comparison, discussion and conclusion in this chapter have been presented at the SIA Spark Ignition Engine International Conference, ImechE 11th International Conference on Turbochargers and Turbocharging, and SAE 2014 World Congress & Exhibition. The SAE 2014 World Congress & Exhibition conference paper has been selected to be a journal paper.

5.1 Introduction

For the turbocharged SI engine, high-enthalpy exhaust mass flow can be further expanded in a turbine that drives a compressor and boosts the engine, allowing a smaller engine to propel a larger vehicle. However, the turbocharger also incurs larger backpressure, which either subtracts energy from the crankshaft or traps hot residual gas in the cylinder, resulting in poorer pumping work and degraded combustion phasing, respectively.

It is known that the exhaust stroke basically comprises two phases: the blow-down and displacement phase (see **Figure 5.1**). The blow-down phase is between the end of the power stroke (when the exhaust valve opens) and the first part of the exhaust stroke, when the cylinder pressure is higher than the exhaust manifold pressure. The blow-down energy is the driving force for the turbine, and it is considered that the maximum utilisation of this portion of energy can increase the engine's specific power.

The displacement phase is when the cylinder pressure is equal to the exhaust manifold, and it is the displacement of the piston to the TDC which pushes the remaining exhaust gas out of the cylinder. This phase provides significantly lower energy for the turbine and evacuates a larger fraction of the residual gas out of the cylinder. However, at high engine load, the high averaged backpressure (usually above 1.5bar) hinders the gas exchange from the cylinder to the ambient (resulting in poor pumping work), and leads to relatively higher trapped residuals in comparison with NA counterparts. Furthermore, pulsation interference often occurs during the displacement phase, where the blow-down pulse of the next-firing-order-cylinder forces some of the exhaust gas back into the cylinder. This also results in some unnecessary pumping losses and leads to higher trapped hot residuals. To make it clearer, **Figure 2.3** in Chapter 2 shows the blow-down phase, the displacement phase, and the pulsation interference effect.

It is conceived that if the blow-down energy of a gasoline engine could be utilised to boost the intake charge, just like the function of a conventional turbocharged engine, and the remaining hot residual could be somehow directly evacuated through a low-resistant exhaust manifold, the strengths of traditional turbocharged engines and NA engines could be combined. Such a concept, if it were possible, could achieve improved breathing characteristics (reduced pumping loss and improved pulsation interference), due to the

significant reduction of the backpressure achieved in the displacement phase, and better combustion phasing, mainly attributable to the significantly reduced RGF and the reduced requirement of gross IMEP.

5.2 Conventional one-stage DEP concepts

The DEP concept is a novel way of accomplishing the gas exchange process in turbocharged engines, with the aim of combining the positive effects of using a turbocharger while removing some of the negative aspects by using a VVT system on the exhaust system. **Figure 5.2** shows the schematic view of the DEP concept. Unlike the standard layout of the engine exhaust system, two exhaust valves are separated to feed the turbine and the exhaust pipe, respectively. The blow-down valve functions just like a standard exhaust valve, discharging the first portion of exhaust gas into the turbine to boost the intake air. While the scavenging valve, which evacuates the latter exhaust portion directly into the exhaust pipe (lower backpressure), aims at better gas exchange. By combining the characteristics of standard turbocharged and NA engines, it is anticipated that the gas exchange process and the combustion phasing could be improved, while maintaining the required BMEP. The specific reasons to enhance the gas exchange process and combustion phasing are detailed below:

As the high backpressure between the turbine inlet and the exhaust port is isolated from the engine piston during the latter portion of the exhaust stroke, an increased PMEP (a reduced pumping loss) could be attained. For the fixed BMEP condition, increased PMEP indicates less gross IMEP, thus better BSFC.

Meanwhile, by bypassing the turbine, a positive pressure gradient across the intake and exhaust system could be achieved. This is beneficial for the cylinder scavenging process, resulting in a large decrease for RGF. It is known that RGF is strongly related to the knock intensity and engine test variability. For example, one author has stated that at knock-limited points, less RGF would cause the engine to be less prone to knock, which would then lead to the advance of the spark timing [190]. Hence, the DEP concept could also benefit from an improved combustion phasing. Improved combustion phasing from reduced RGF also results in reduced exhaust gas temperature, and thus may reduce the need for other exhaust gas temperature control actions, such as over-fuelling, the adoption of water-cooled exhaust manifolds, or increased EGR.

5.3 Modelling methodology

In this section, seven degrees of freedom in the actuation of the DEP concept engine, including the timing of the intake, blow-down and scavenging valves, and the lift and duration of the blow-down and scavenging valves were investigated. In order to understand the underlying gas exchange process, the timing of the scavenging valve (one degree of freedom mechanism) effect on BSFC was investigated first. Optimisation of the fully-flexible mechanism was then undertaken, and is presented later in the section. For the one degree of freedom study, the profile of the intake and the exhaust valves were retained, in order to investigate the BSFC improvement potential with minimum change to the whole system.

One degree of freedom mechanism:

By adjusting the timing of the scavenging valve, the relationship between the blow-down and the scavenging valve varies in feeding a specific amount of the exhaust mass flow into the turbine. Meanwhile, the overlap between the scavenging valve and the intake valve alters accordingly, which influences the amount of blow-through or short circuit air flow. Overlap A and overlap B, as can be seen in **Figure 5.3,** are necessary to avoid choked flow and to control the blow-through or back-flow, respectively.

The operation strategy depends on the requirements of the system.* If **fuel efficiency** is pursued, the scavenging valve should be set to a maximum advance that attains the BMEP target. By advancing the scavenging valve, less pumping work is needed, thus fuel efficiency is increased. This strategy can also benefit from less blow-through, which leads to less fuel injected.

To make it clearer: A DoE has been conducted at 4500RPM full load. **Figure 5.4** shows the timing of each valve to maintain the target BMEP. From **Figure 5.5** it can be seen that the minimum BSFC occurs at a maximum advance of the scavenging valve that attains the BMEP target. **Figure 5.6** also suggests that, by advancing the scavenging valve, less pumping work is required.

Multiple degrees of freedom mechanism:

Due to the possible large blow-through and the limitation of only one controllable degree of freedom, the results might not be fully optimised, as can be seen in the following section. It is therefore necessary to introduce fully-flexible mechanisms of the intake and exhaust valves (see **Figure 5.7**), in order to exploit the maximum potential of the DEP concept engine.

As all the degrees of freedom are strongly interrelated, changing one would cause the others to change their action on the engine system. Thus, some mathematical approaches for optimising multi-variables systems and multi-objective responses need to be investigated. A genetic algorithm has the capability to mimic the process of natural evolution, and is thus considered to be one of the most useful approaches to solve this kind of problem. To be more specific, each degree of freedom represents a gene in the chromosome, and BSFC forms the fitness function. More detail about the structure of the GA system can be seen in **Figure 4.18**.

It should be noted that, in this section, the timing of the scavenging valve is also the control parameter to maintain or achieve the target BMEP, the function similar to a traditional wastegate. The value of the other parameters will be based on the optimisation for different purposes and will form a map in the ECU, which is more like a traditional calibration. Theoretically different variable valve mechanisms VVT or variable valve lift (VVL) could be adopted in the DEP concept. Selecting the timing of scavenging valve to be the control parameter is due to the following reasons:

- The VVT mechanism is more easily manufactured than VVL and variable valve duration mechanisms.
- The scavenging valve is subjected to less thermal and pressure shock than the blow-down valve.
- The research engine features DI, thus a larger scavenging can be tolerated.* But for a PFI engine, variable blow-down valve timing is a reasonable solution where large scavenging is significantly undesirable.

** The decision of scavenging ratio is also dependent on catalyst characteristics and emission requirement.*

It is also noted that potential PMEP gains, due to the implementation of the DEP concept, could offset some of the turbocharger power loss, due to the smaller amount of exhaust mass flow into the turbine. However, for some operating points, the initial BMEP or desired higher

BMEP is still not attainable. Thus, a smaller sized turbocharger may need to be selected to optimise the whole system. The matching of the IC engine and the turbocharger was performed by scaling the mass flow axis of the standard engine's turbocharger maps. Without a considerable effort, a smaller sized turbocharger was selected by using the mass multiplier in GT-Power [181].

5.4 Results

This study was carried out on a validated 2.0 Litre extremely downsized SI engine model using GT-Power. It is worth mentioning that the target BMEP of this engine can be in excess of 32bar, and it is anticipated that the gas exchange process is potentially significantly different to that of the engines investigated in previous studies, given their lower BMEPs. The diameter of the valves was increased by 4mm to avoid choking when only one valve is involved in the gas discharging process. Although the increase of the exhaust valve could improve the pumping work as well, it was verified in simulation that this only affected around 10% of the pumping work that the DEP concept brought (For example, at 6500RPM full-load seen in **Table 5.1**, with the original exhaust valve size, the pumping work of the DEP concept would be -1.3bar compared to -1.2 bar with increased exhaust valve size). The wastegate control strategy was replaced by the timing of the scavenging valve to maintain the target BMEP. The Douaud & Eyzat knock model was implemented in GT-Power in an effort to predict knock onset for individual cycles [191].

In this section, the one degree of freedom effect was presented first, with detailed explanation. Then, multiple degrees of freedom interactions were presented, with some explanations of the process occurring.

The aim of this study is to reduce fuel consumption, residual gas content, and to improve boost control. Steady-state operating points of 6500RPM/26.2bar, 4500RPM/30.9bar, 2500RPM/17.9bar and 1500RPM/12.7bar were presented. The reason why these four sets were chosen is because they represented four different gas exchange processes, detailed in the following.

1) One degree of freedom mechanism
6500RPM/26.2bar:

Table 5.1. Cycle averaged results for 6500RPM

	BMEP (bar)	BSFC (g/kW*h)	RGF	CA50	PMEP (bar)	Turbine Power (kW)
Original	26.2	258.7	2.74	17.3	-2.2	43.9
DEP	26.2	254.3	1.75	17.5	-1.2	39.2

From **Table 5.1**, it can be seen that the BSFC may be reduced by 1.72% while keeping BMEP fixed. This was largely due to the improvement of the pumping work, as negative PMEP was increased by 44.7%. The combustion phasing, on the other hand, did not change too much, which did not correlate with the reduction of RGF [9]. A possible reason could be the poorer choking condition when only one exhaust valve is involved, which adversely affects the temperature and pressure in cylinders.

Lower pumping losses can also be implied from the reduced turbine power; the DEP concept engine only needed 39.2kW power to boost the intake pressure in order to attain the required BMEP, while the base engine required as much as 43.9kW, which indicated that more power was wasted in overcoming the pumping resistance for the baseline engine.

4500RPM/30.9bar:

Table 5.2. Averaged results for 4500RPM

	BMEP (bar)	BSFC (g/kW*h)	RGF	CA50	PMEP (bar)	Turbine Power (kW)
Original	30.9	249.0	3.49	23.3	-0.450	35.0
DEP	30.9	242.9	0.94	19.0	0.074	29.9

At 4500RPM, as can be seen in **Table 5.2**, BSFC dropped a lot: from 249.0 to 242.9. Unlike the 6500RPM situation, both the reduction of the pumping losses and the improvement for combustion efficiency contributed to the reduction of BSFC. The anchor angle (CA50) advanced by about four degrees from 23.3 to 19.0, which contributed more than the improvement of PMEP although it was not verified quantitatively. This correlated with RGF very well, with RGF reducing from 3.49 to 0.94. It is also anticipated that the DEP concept engine would also benefit from more stability, due to the significant RGF decrease. This would further improve an engine's efficiency.

Table 5.3. Averaged results for 2500RPM &1500RPM

2500RPM/17.9bar:

	BMEP (bar)	BSFC (g/kW*h)	RGF	CA50	PMEP (bar)	Turbine Power
Original	18.1	239.4	4.36	14.7	-0.10	5.6
DEP	18.2	239.4	3.23	13.3	-0.03	5.2

1500RPM/12.7bar:

	BMEP (bar)	BSFC (g/kW*h)	RGF	CA50	PMEP (bar)	Turbine Power
Original	12.7	246.2	5.14	11.4	0.04	0.9
DEP	12.7	247.3	4.31	10.9	0.00	0.7

BSFC at 2500RPM and 1500RPM did not change too much, which indicated that the DEP concept did not have significant BSFC benefit within a lower engine speed. At 1500RPM, the increased BSFC was attributed to the decrease of the pumping work. It should be noted here, that the original model is equipped with a supercharger as well, but, in order to investigate the DEP concept on turbocharged SI engines, the supercharger was removed and the torque target was reduced to the level it was at when the wastegate was fully closed. Therefore, the limited BSFC improvement could also be attributed to the fact that the turbocharger was not producing large backpressure at these operating points, which was also indicated by the PMEP value.

Pumping Loop:

Fuel consumption reduction between the standard and the DEP model can also be presented using the pumping loop in a P-V diagram. It can be seen from **Figure 5.8** that, during the end of the exhaust stroke, the original engine continued to push the remaining exhaust gas from the cylinder to the turbine, which increased the backpressure further (this was also due to the pulsation interference), and as the exhaust valve started to close there was a large peak in the cylinder pressure. However, for the DEP concept engine, as the blow-down valve was closed while the scavenging valve started to open, the cylinder pressure dropped dramatically to nearly atmospheric level, which removed the backpressure to the piston. Pumping work can also be implied from the enveloped area; it is clear that the DEP concept benefits from less pumping loss than that of the original model.

From the results above, it can be summarised that, for the fixed BMEP condition, BSFC improvement depends on the trade-off between the benefits of the reduction in pumping work and the combustion efficiency gain.

2) Multiple degrees of freedom mechanism

Table 5.4. Averaged results for multiple degrees of freedom mechanism

	6500RPM		4500RPM		2500RPM		1500RPM	
	Original	DEP	Original	DEP	Original	DEP	Original	DEP
BMEP (bar)	26.2	26.2	30.9	30.9	18.1	18.1	12.7	12.7
BSFC (g/kW*h)	258.7	252.9	249.0	239.3	239.4	235.6	246.2	245.6
RGF	2.74	1.19	3.49	1.50	4.36	2.72	5.14	4.93
Anchor Angle	17.3	16.2	23.3	19.3	14.7	11.4	11.4	12.25
PMEP (bar)	-2.2	-1.2	-0.45	0.26	-0.11	0.16	0.05	0.06
Turbine Power (kW)	43.9	38.1	35.0	29.0	5.6	5.0	0.9	0.85

Table 5.4 shows the averaged results for the multiple degrees of freedom mechanism. Due to the improved gas exchange process and better combustion phasing, the BSFC performance for all speed ranges was improved, with a large decrease of BSFC occurring around the higher speed.

However, due to the complexity of utilising the seven degrees of freedom mechanism for series production engines, it is almost impossible to achieve such improvement. Engines equipped with the DEP concept in the future are most likely to be in between the one degree freedom and the seven degree freedoms; thus, the behaviour or the performance of the engine should also be in the between.

5.5 Discussions

It should be noted that, even though the baseline engine model is validated using the prototype engine testing data, the modified model for the DEP concept does not calibrate. The potential of this novel theory could be better proved with some testing results. In addition to that, the knock model for running the simulation which decides the anchor angle might not be suitable for the DEP concept; this will be verified in the future.

Transient performance is one of the major challenges to address in order to see widespread adoption of turbocharging in most production engines. Although further research work in this area is needed, it is expected that the DEP concept bring benefits to the transient performance of a turbocharged engine. This is, to a great extent, due to the fact that smaller inertia of the modified turbocharger is adopted. In addition, during a cold start, a shut-down valve could be used in the blow-down path to force the total mass flow to bypass the turbine. By doing so, the catalyst could be warmed up more quickly; thus, the cold start performance could be improved.

Higher blow-down exhaust temperature and choking are the two major drawbacks for DEP concept engines. As the majority of high-enthalpy mass flow is evacuated during the first portion of the exhaust stroke, and a relatively low-enthalpy mass flow which directly links to the exhaust pipe does not balance some of the blow-down pulse temperature, higher blow-down but a lower scavenging pulse temperature should be anticipated. It should be noted that, for this study, the limit of the inlet turbine temperature was not considered. High temperature-resistant material should be used, or a fuel-enrichment strategy needs to be involved. This would either increase the cost of the system or affect the fuel efficiency. **Figure 5.9** shows the comparison of the original, blow-down and scavenging exhaust temperatures when one degree of freedom was involved.

From **Figure 5.10**, it can be seen that, even though the diameter of the exhaust valves were increased, a choking condition still existed, and was even poorer than the original engine. This is due to the fact that, for the first phase of the blow-down phase and the last phase of the displacement phase, only one of the exhaust valves was involved. This can also partly explain why PMEP drops for the higher speed range when the timing of the scavenging valve retards. The choking condition could be largely improved by optimisation of the timing, lift, and duration of the exhaust valves.

Since the boost pressure and RGF can be reduced, together with better combustion phasing for a DEP concept engine, it is anticipated that the compression ratio could be increased for further BSFC improvement at part load.

5.6 Chapter summary and conclusions

The following summary and conclusions are drawn from the study in this chapter:

1: The general trend under fixed BMEP condition is that, at lower engine speed, the backpressure is low and there is less to gain from the DEP concept, whilst at higher speeds the backpressure is higher, and the potential to reduce this backpressure is higher. Thus, the BSFC reduction is more noticeable at higher speeds. But it should be noted that this conclusion may only be valid for this specific engine with the installed supercharger removed.

2: The DEP-based engine can achieve up to 4% improved BSFC performance due to better gas exchange and combustion processes, without changing the settings of the intake and exhaust valve profile. However, introducing fully-flexible intake and exhaust valve mechanisms could further optimise the results above.

3: The complexity of the system, higher blow-down exhaust temperature and choking are the major drawbacks for DEP concept engines.

Figures in Chapter 5

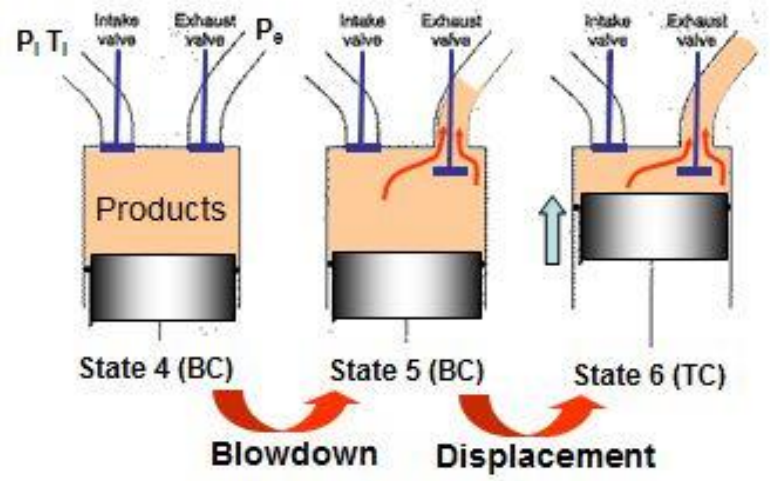

Figure 5.1. Blowdown and displacement phases

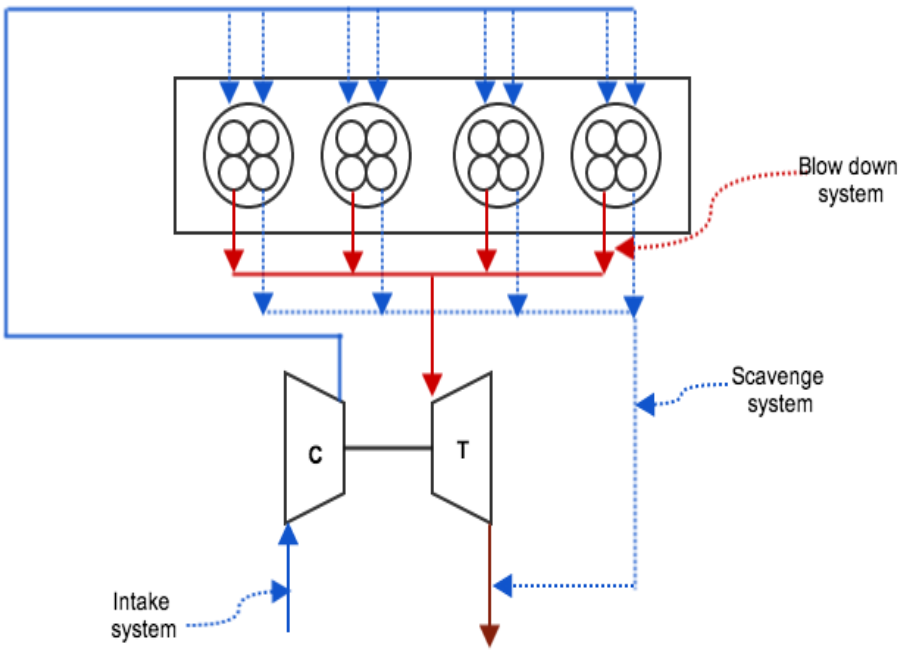

Figure 5.2. Schematic view of the exhaust system layout in DEP concept

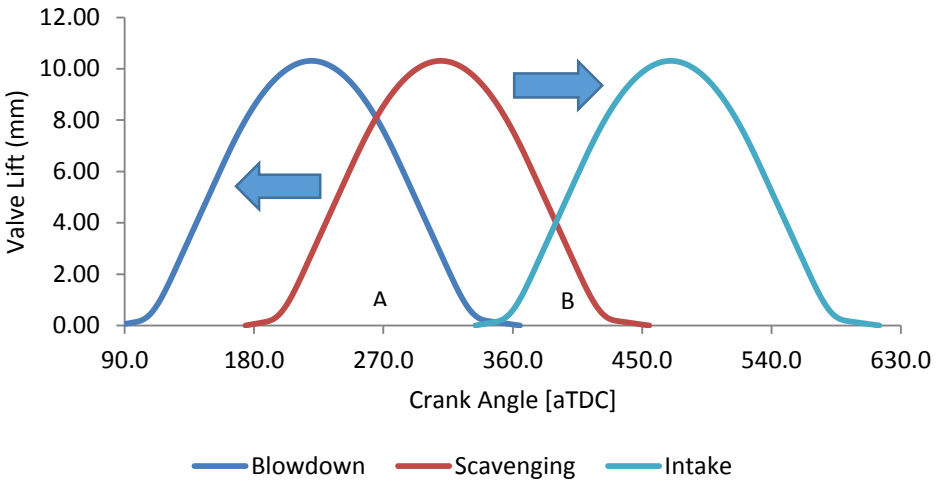

Figure 5.3. Exhaust and intake valve – one degree of freedom

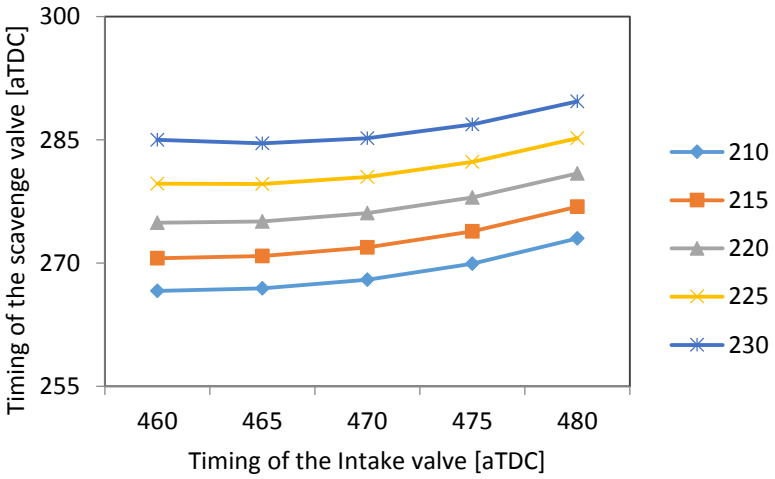

Figure 5.4. Timing of the exhaust valves to maintain the target BMEP at 4500RPM

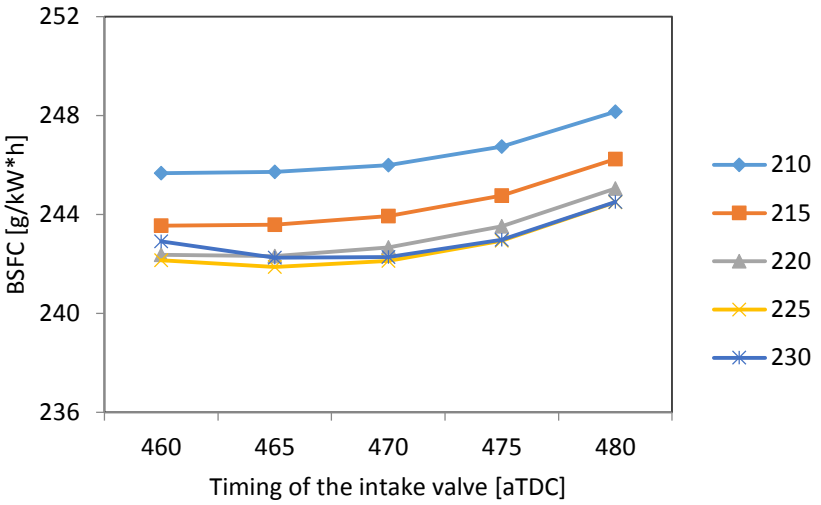

Figure 5.5. BSFC for different timing of the intake and blow-down valve at 4500RPM

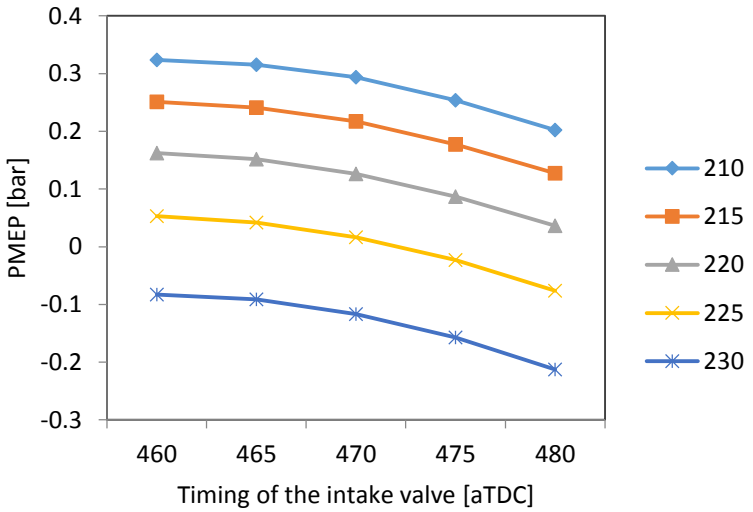

Figure 5.6. PMEP for different timing of the intake and the blow-down valve

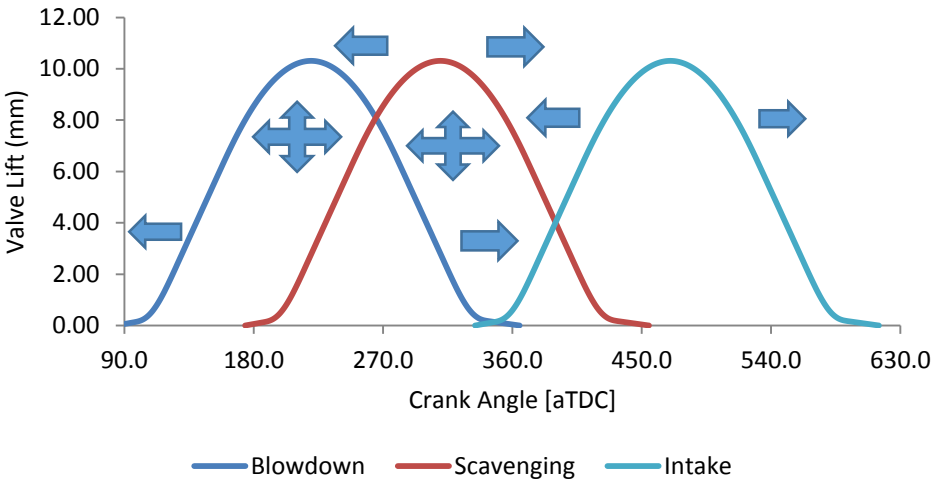

Figure 5.7. Exhaust and intake valve – multiple degrees of freedom

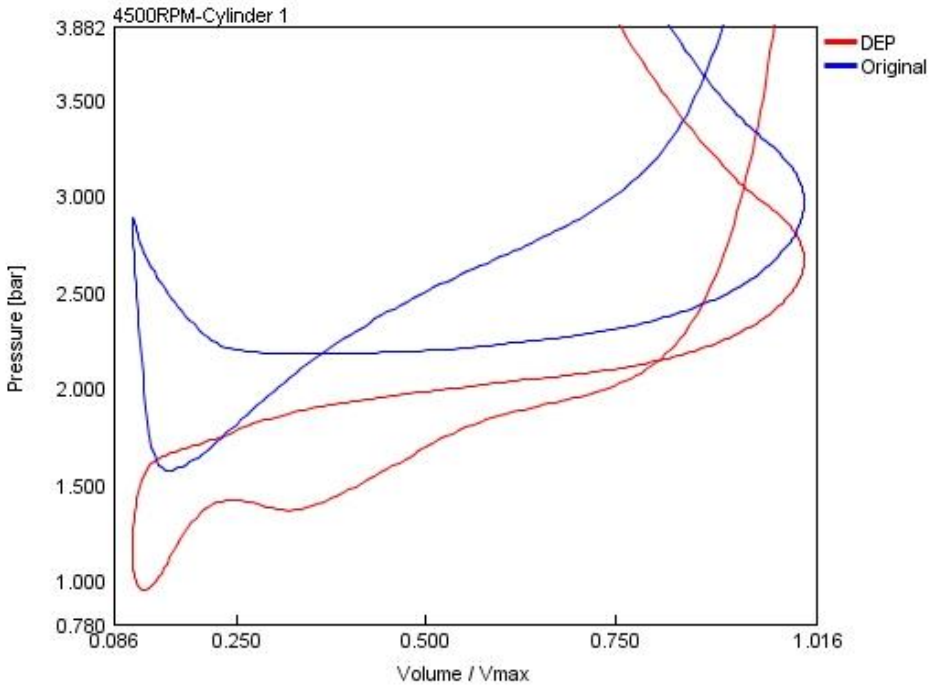

Figure 5.8. Pumping loop in P-V diagram at 4500RPM

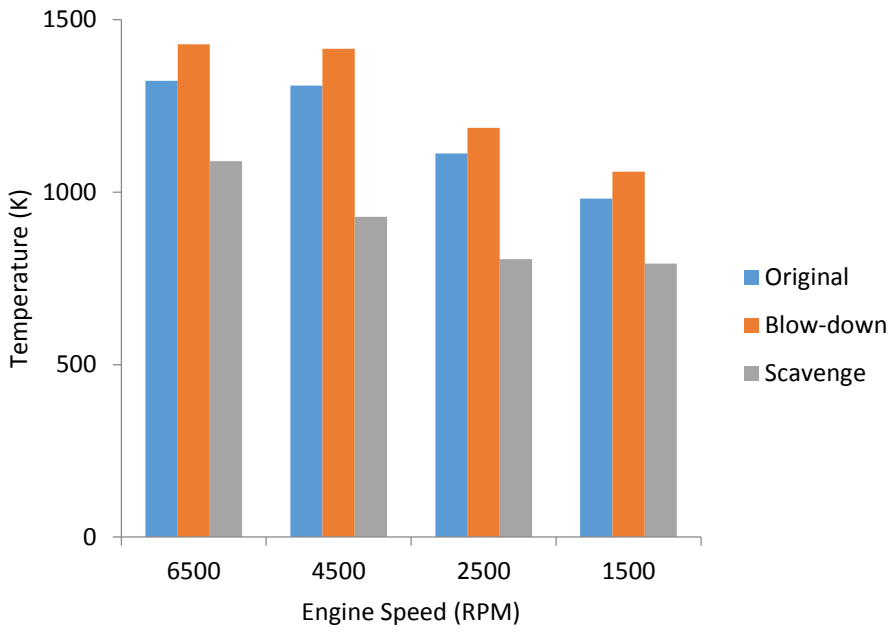

Figure 5.9. The comparison of the original, blow-down and scavenging exhaust temperature

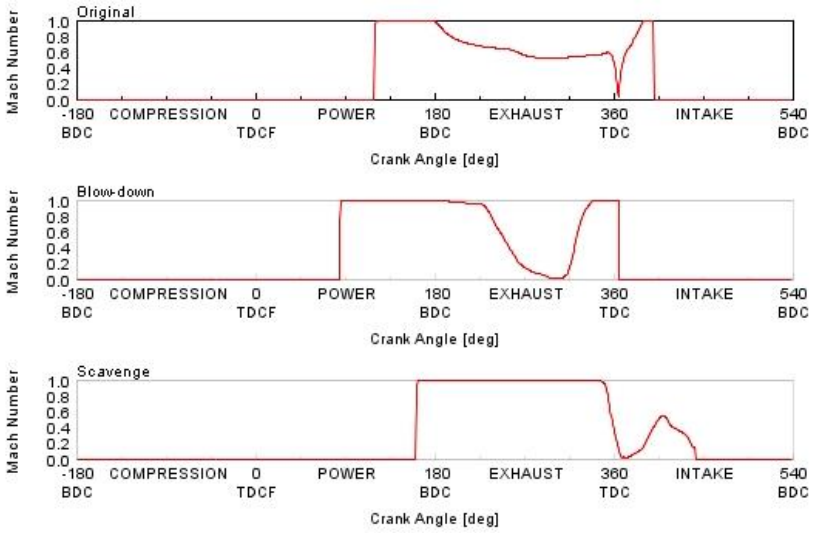

Figure 5.10. Mach number for Original and DEP concept engine at 6500RPM

Chapter 6 – *Modelling the DEP two-stage concept*

The DEP concept has only been applied to single-stage turbocharged engines so far. However, it, in its basic form, is in no way restricted to a single-stage system. This chapter, for the first time, will apply the DEP concept to a two-stage downsized SI engine. By controlling the timing of the exhaust valves separately, to feed the exhaust mass flow to the high-pressure turbine or the low-pressure turbine or the exhaust pipe, it is anticipated that such a system could achieve even better breathing characteristics.

The comparison, discussion, and conclusion in this chapter have been presented at SAE 2014 International Powertrain, Fuels & Lubricants Meetings and ASME Turbo Expo 2015. The ASME Turbo Expo 2015 conference paper has been selected to be a journal paper.

6.1 Introduction

DEP is an alternative way of accomplishing the gas exchange process in turbocharged engines. The DEP concept engine features two exhaust valves with separated functions. The blow-down valve acts like a traditional turbocharged exhaust valve to evacuate the first portion of the exhaust gas to the turbine, while the scavenging valve feeds the later portion of the exhaust gas directly into the lower back-pressure exhaust pipe, behaving in a way similar to valves in a naturally-aspirated engine. By combining the characteristics of both turbocharged and NA engines, high back pressure between the turbine inlet and the exhaust port is maintained in the blow-down phase, while a significant reduction of the back pressure can be achieved in the later displacement phase [13].

The DEP concept has, up to now, only been applied to single-stage turbocharged engines. However, it, in its basic form, is in no way restricted to a single-stage system. In addition, two-stage downsizing has been proved to be one of the most viable solutions to achieve BSFC improvement [7]. Applying such a novel gas exchange process to a two-stage system could enhance the advantages which two-stage turbocharged engines have already obtained, while offsetting the deficiencies inevitably inherited. This chapter will, for the first time, apply the DEP concept to a two-stage downsized SI engine.

6.2 DEP Two-stage Concept

A new gas exchange concept will be proposed in this section. In this system, two exhaust valves in each cylinder separately function, with one valve feeding the exhaust mass flow into the HP manifold while the other valve evacuates the remaining mass flow directly into the low-pressure (LP) manifold. By adjusting the timing of the exhaust valves, the target boost can be controllable, while improving the engine's pumping work and scavenging which results in better fuel efficiency from the gas exchange perspective. It is also anticipated that the DEP two-stage system could also benefit from better combustion phasing, due to the improved RGF and reduced requirement of gross IMEP. To be more specific in terms of gross IMEP, if assuming fixed FMEP, an engine's BMEP only comprises gross IMEP and PMEP. The DEP two-stage concept benefits from improved PMEP, thus the required gross IMEP is reduced.

In order to implement the DEP functionality, the two exhaust valves were re-routed as shown in **Figure 6.1**. The wastegate function of the conventional fixed geometry turbocharger was

replaced by adjusting the timing of the HP or LP valve to maintain the target BMEP. It should be noted here that the HP valve timing was optimised using a genetic algorithm, while the LP valve was controlled by a PID controller, which aims to attain the target torque requirement.

6.3 Modelling methodology

Model modification:

For the simulation work presented in this chapter, a 1-D model of a highly-downsized SI engine was used as a starting point (the schematic can be seen in **Figure 6.2**). The engine, the basic parameters of which are detailed in **Table 6.1,** has a BMEP designed to facilitate a 60% downsizing factor when compared with an equivalent NA engine.

The research engine on which this work is based is an ambitious project aiming to deliver a 2.0 L, four cylinder gasoline downsized demonstrator engine capable of up to 35bar BMEP, air pressure charging of up to 3.5bar absolute, and offering up to approximately 35% potential for the reduction of fuel consumption and CO2 emissions, while still matching JLR's 5.0 Litre V8 NA engine performance figures [7]. There are several boosting systems - including TurboSuper, Twin-Turbo and Supergen-Turbo - which are considered to be the potential layout for the project [150]. This chapter is based on the Twin-Turbo configuration. It might be noted that TurboSuper is the final selection for the project and, at the time of writing, is being tested at University of Bath.

Knock model:

For reason of simplicity, only the Douaud & Eyzat knock model was considered to showcase the potential combustion phasing improvement by adoption of the DEP two-stage system. It might be noted that although the Douaud & Eyzat model showed good predictive capability for identifying knock-limited spark advance, some corrections might still be needed for engines with a higher residual gas fraction (especially for engines with EGR loops) and for those with a non-stoichiometric air fuel ratio. The occurrence of knock was predicted based on empirical induction time correlations.

$$I(\alpha) = \frac{1}{6(RPM)} \int_{-100}^{\alpha} \frac{1}{5.72\times10^{6} M_1 \left(\frac{ON}{100}\right)^{3.402} p^{-1.7} exp\left(\frac{3800}{M_2 T}\right)} d\alpha \qquad \textbf{6.1}$$

Where: I = induction time integral

α = crank angle

RPM = engine speed

ON = Fuel Octane Number

p = instantaneous cylinder pressure (Pa)

T = instantaneous unburned gas temperature (K)

M_1= knock induction time multiplier

M_2 = Activation Energy Multiplier

Table 6.1. Basic parameters of the simulated engine

Engine Type	-	Inline-4-cylinder
Capacity	cc	1991
Bore	mm	83
Stroke	mm	92
Compression ratio	-	9.0:1
Firing Order	-	1-3-4-2
Combustion System	-	Gasoline GDI
Valvetrain	-	DOHC, Cam Phasers and Cam Profile Switch on Intake and Exhaust Camshafts
Spec. Power	kW/L @ min	142 @ 6500
Spec. Torque	Nm/L @ min	255 @ 3500
Max. BMEP	bar @ min	35 @ 3500 and 25 @ 1000 &6500
Air Charging System	-	Two-stage

The knock index is a phenomenologically-based parameter that was developed by Gamma Technologies, Inc. and can be scaled to the loudness of knock as heard in the laboratory using the knock index multiplier. The knock index is defined as a time-dependent quantity as follows [181]:

$$\mathrm{KI} = 10000\mathrm{Mu}\frac{\mathrm{V_{TDC}}}{\mathrm{V}}\exp\left(\frac{-6000}{\mathrm{T}}\right)(\max(0,1-(1-\varphi)^2)\mathrm{I_{avg}} \qquad \textbf{6.2}$$

Where: KI = Knock index

M = Knock Index Multiplier

u = percentage of cylinder mass unburned

V_{TDC} = cylinder volume at top dead centre

V = cylinder volume

T = bulk unburned gas temperature (K)

φ = equivalence ratio of the unburned zone

I_{avg} = induction time integral, averaged over all end gas zones

In the modelling, a Wiebe combustion model was adopted; the value of CA10-90 and the Wiebe exponent were taken from a similar output SI engine and the CA50 was controlled by a PID controller to keep the knock index under the prescribed index. The intake valve timing was retained and the exhaust valve timing was optimised for both the DEP concept model and the original two-stage model for an easy comparison, using a genetic algorithm that will be detailed in the next section. The exhaust valve diameter was increased to the same size as the intake valve, in order to ease the mass flow choking when only one valve is involved for the DEP based engine model.

Genetic algorithm:

The capability of a genetic algorithm to mimic the process of natural evolution is considered to be one of the most useful approaches to optimise the engine performance. The schematic diagram for optimising the results is shown below. In the modelling, only the exhaust valve timings were optimised using a genetic algorithm to achieve minimum BSFC while attaining the target BMEP. To be more specific, the exhaust valve timing (in the original model) and the blow-down valve timing (in the DEP concept model) each represents a gene in the chromosome, and BSFC together with the BMEP target-related constraint forms the fitness function. More details about the structure of the GA system can be seen from **Figure 4.18**.

It should be noted that a genetic algorithm cannot be considered to be a simple way of performing design work, as considerable effort needs to be involved in designing a workable fitness function. If the fitness function is designed badly, the algorithm will either converge on an inappropriate solution or will have difficulty converging at all. The main aim for the optimisation process was to gain fuel economy subject to specific constraints, and therefore the fitness function was defined as **Equation 6.3**.

$$Fitness\ (x) = BSFC(x) + P \times |1 - \frac{BMEP(x)}{BMEP_{target}}| \qquad \textbf{6.3}$$

where x refers to an individual containing the information of valve timing, P is a penalty factor. The value of P quantifies the penalty for individuals who do not satisfy the constraint. The larger the value of P, the higher the penalty factor imposing on the objective function, leading to more powerful confinement but worse selection efficiency.

Compared with a more complex fitness definition, a static penalty function is more robust and rapid. After trying a considerable number of times, P was quantified to be 1000 for the original model and was adjusted to 5000 for the DEP concept model.

Minimap:

For ease of analysis and comparison, the performance of the baseline V8 engine over the NEDC has been discretised into a number of steady-state 'Minimap' operating points (see in **Table 6.2**), as described by Carey et al [186]. Each of these points represents a portion of the driving cycle, and holds a weighting equivalent to the proportion of the time that the engine is run at this speed, and load during the NEDC. Using this method, improvements in the fuel economy over the driving cycle can be estimated much more quickly. For the purpose of simplicity, only Minimap point number 9 (corresponding to 1000RPM 4.99bar BMEP) was selected for investigating the benefits of the DEP two-stage concept considering the following facts:

- The necessity for a throttle plate in the original downsized engine
- Relatively high weighting

Table 6.2. Minimap operating points

Minimap point number	Engine speed	BMEP MEP	BSFC NEDC weighting
-	(rpm)	(bar)	(-)
1	600	1.75	0.291
2	1500	2.50	0.013
3	1500	6.54	0.099
4	1500	12.48	0.025
5	2000	4.99	0.001
6	2000	12.46	0.008
7	1250	1.00	0.109
8	1000	1.00	0.079
9	1000	4.99	0.089
10	1250	9.99	0.023
11	1350	14.97	0.023
12	1500	18.72	0.014
13	1250	7.49	0.043
14	1250	3.74	0.124
15	1500	8.74	0.046

6.4 Results and Discussions

To be specific, three different modes can be achieved via distributing different portions of the mass flow into the different exhaust manifold.

<u>High-speed full load (the LP turbocharger can provide enough boost for the required torque target):</u>

At high engine speed, only the LP turbocharger is involved with the HP turbocharger deactivated by opening the intake bypass, HP bypass and LP bypass. This is a standard one-stage DEP layout. The two exhaust valves separately function, with the HP valve feeding the blow-down pulse to the LP turbine, while the LP valve targets the scavenging by bypassing the LP turbine. A PID controller is used to control the timing of the two exhaust valves to maintain the target BMEP. However, it should be noted that the lift and duration of the LP

valves should be resized here otherwise the target engine performance cannot be attained. As this layout has been demonstrated by a number of previous studies [13, 15, 17-24], a detailed investigation is therefore ignored here. The following is a brief review/conclusion for the standard one-stage DEP concept.

The engines equipped with this configuration could achieve significantly low backpressure at the end of the exhaust stroke during the displacement phase which, from the gas exchange view, could improve the pumping work and facilitate the scavenging. It should be noted that the reduced (or sometimes even eliminated) pulsation interference also contributes to the improved pumping work. This is different from the twin-scroll turbocharger, which hinders the exhaust gas back into the cylinder [192]. In the standard DEP concept, an even larger portion of the exhaust mass flow backflows into the cylinder through the HP valve, but the back-flowed exhaust residual, together with some of the hot residual from the cylinder, is then evacuated from the LP valve, due to the larger pressure difference between the cylinder and the LP exhaust manifold. It is also anticipated that such a layout benefits from advanced spark timing, mainly due to the significantly reduced hot residual and the reduced requirement of gross IMEP. However, as at the beginning of the blow-down phase and the end of the displacement phase only one valve is involved, the exhaust valves might suffer choke, which could negatively affect the pumping work. Higher HP exhaust manifold temperature is also an issue, as the majority of high-enthalpy mass flow is evacuated during the blow-down phase and a relatively low-enthalpy mass flow, which directly links to the LP exhaust manifold does not balance some of the blow-down pulse temperature.

Medium speed full load (3000RPM):

At medium speeds, the exhaust energy is sufficient for the two-stage turbocharger system to provide enough boost, but not as sufficient for only the LP turbocharger to boost the engine. Both the HP and LP turbocharger systems are involved by separately being separately fed by the distributed mass flow from the two exhaust valves via closing the intake bypass, HP bypass and LP bypass. As the HP turbocharger adopted is significantly smaller than the LP turbocharger, the LP valve opens prior to the HP valve, to reduce the backpressure at the beginning of the exhaust stroke. The HP valve opens afterwards, targeting the required engine performance. Compared to the conventional two-stage model, which utilises a HP bypass to evacuate the excessive mass flow into the LP turbine, the DEP two-stage system can directly divert the cylinder mass flow into the LP manifold without passing the gas

through the relatively HP manifold, resulting in better pumping work. **Figure 6.3** shows the corresponding pumping loops in a standard P-V diagram at 3000RPM, which illustrates that the pumping loss was decreased due to the reduced backpressure at the beginning of the exhaust stroke. The averaged PMEP was improved from -2.19bar to -1.63bar with approximately 0.5bar PMEP increase.

Such a scheme could also benefit from reduced pulsation interference. This is similar to the configuration at high engine speed wherein, although it pushes a larger proportion of exhaust residual back to the cylinder through the HP valve, the majority of the exhaust gas is then evacuated through the LP valve to the LP manifold (see **Figure 6.4**). To have an easy comparison, the mass flow rate of the original system is shown in **Figure 6.5**. It can be seen that the original model did not feature back-flow, but the magnitude of the mass flow rate was smaller than that of the LP valve in DEP two-stage configuration.

More details on the comparison of the different engine characteristics can be seen in **Table 6.3.** It can be seen that the combustion system of the DEP two-stage configuration does not need to produce as much power as in the original model, due to the reduced power needed to overcome the pumping resistance. This will lead to a smaller turbocharger power requirement, resulting in reduced average intake pressure and temperature. Under knock-limited spark advance (KLSA), the combustion phasing will be advanced and the combustion efficiency will be improved.

Table 6.3. Averaged results for 3000RPM full load

	Original	DEP	gradient
Engine speed (RPM)	3000	3000	-
BSFC (g/kW*h)	273.6	266.7	2.5%
BMEP (bar)	31.50	31.50	-
Gross IMEP (bar)	35.20	34.63	-0.57 bar
PMEP (bar)	-2.19	-1.63	0.56 bar
RGF	3.49	3.48	-
CA50 (degree)	32.3	31.5	-0.8 degree
HP Turbocharger Power (kW)	5.14	4.61	-0.53 kW
LP Turbocharger Power (kW)	31.71	30.38	-1.33 kW
Average Intake pressure (bar)	3.38	3.27	-0.11 bar
Average Intake temperature (K)	305.2	304.7	-0.5 K

However, although such a layout could achieve better pumping work, the hot residual might not decrease as much as in the high-speed layout. This is because such a layout can only facilitate the scavenging at the beginning of the exhaust stroke, while not improving the scavenging process during the displacement phase, where a larger scavenging of the exhaust residual is required.

According to the calculation from GT-Power, the DEP two-stage model only achieved around 1% of hot residual decrease. The combustion phasing was observed to be improved, and this is mainly due to the reduced gross IMEP requirement, which reduces the cylinder maximum pressure and temperature, resulting in less likelihood to knock when compared to the same engine operating point for the conventional two-stage counterpart. CA50, which represents spark timing in the GT-Power model suggested, that the DEP two-stage model could achieve an approximately 0.8 CA advance, which is beneficial for fuel efficiency and also advantageous to the turbine inlet temperature. The overall net fuel efficiency was improved by around 2.5%.

Low speed full load (1500RPM):

At low speed, when the exhaust mass flow is insufficient, both the HP and LP turbocharger system are operating. All the bypass valves are closed as at the medium speed. However, the HP valves open ahead of the LP valves to fully take advantage of the smaller turbocharger. From the perspective of the gas exchange process, the distribution of the exhaust mass flow at low engine speed is similar to that at high engine speed, by feeding the blow-down pulse into the HP manifold and bypassing the remaining displacement pulse directly into the LP manifold. It should be noted that the low-pressure manifold refers to the post-LP-turbine and pre-LP-turbine manifold, respectively, for high and low engine speed. From **Figure 6.6**, it can be seen that the DEP two-stage system could achieve lower cylinder pressure when compared to the original two-stage system during the whole exhaust stroke, due to the significantly lower backpressure caused by the divided exhaust manifold. This will improve the pumping work, making the turbochargers do less work and, most importantly, reduce the requirement of the gross IMEP and reduce the hot residual gas fraction, resulting in better combustion phasing. The averaged PMEP was increased by around 0.5bar and the value of RGF was decreased from 3.73 to 2.14. CA50, which represents spark timing in the modelling, advanced by around 1 degree. The net fuel efficiency was improved by 1.5%.

The pulsation interference effect can also be reduced or even eliminated at this operating point. However, it should be noted that there is still pulsation interference from the HP manifold to the cylinder but such effect is offset by the scavenging effect from the cylinder to the LP manifold, which can be seen from **Figure 6.7**. **Figure 6.8** shows the mass flow rate for the conventional two-stage counterpart, for a direct comparison.

More details on the comparison of the different engine characteristics can be seen in **Table 6.4**. As in the medium-speed full-load condition, the reduced backpressure caused by the DEP makes the combustion system of the DEP two-stage configuration do less work when compared to the original model. This will reduce the power requirement of the turbocharger system resulting in decreased intake temperature and pressure. Under KLSA, the combustion phasing will be advanced and the combustion efficiency will be improved.

Table 6.4. Averaged results for 1500rpm

	Original	DEP	gradient
Engine speed (RPM)	1500	1500	-
BSFC (g/kW*h)	250.4	246.2	1.7%
BMEP (bar)	27.67	27.67	-
Gross IMEP (bar)	29.06	28.53	-0.53 bar
PMEP (bar)	-0.22	0.30	0.52 bar
RGF	3.73	2.14	-42.6%
CA50 (degree)	27.7	26.9	-0.8 degree
HP Turbocharger Power (kW)	5.78	5.29	-0.49 kW
LP Turbocharger Power (kW)	3.89	3.62	-0.27 kW
Average Intake pressure (bar)	2.68	2.52	-0.16 bar
Average Intake temperature (K)	305.4	305.0	-0.4 K

Low load operating points (e.g. 1000RPM, 4.99bar):

It is known that internal EGR benefits at low and part loads due to the reduced pumping losses and re-heat of the intake charge [74]. Conventionally, the overlap of the exhaust and intake valve needs to be increased to capture more back-flow (internal EGR). For the fixed-duration valve mechanism, retard of exhaust valve timing might be necessary. However, this might cause the re-compression of the exhaust residuals during the first phase of the exhaust stroke, resulting in an even larger pumping loss. In addition, some pumping loss might also exist when the exhaust valve opens early, as the exhaust valves would be closed near to TDC, causing the re-compression at the end of the exhaust stroke. **Figure 6.9** illustrates such an effect using different mean opening position (MOP) of the exhaust valves for the original model. The red curve represents the early exhaust valve opening condition and the blue line indicates the late exhaust valve opening situation. It is considered that if the duration of the exhaust valve was increased, the pumping loss would be largely reduced.

At part or low loads, when the valve choke is not a problem, the DEP which operates the HP and LP valves separately, could be utilised to extend the 'duration' of the exhaust valves. This is not only beneficial to avoid the re-compression effect during the first phase of the exhaust stroke but also advantageous to reduce, or even eliminate, the re-compression effect when

the valve is about to close near TDC. To be more specific, one valve can capture the exhaust mass flow from the end of the power stroke to the beginning of the exhaust stroke. The other valve could be used as a mechanism to increase the overlap between the exhaust and intake valve, in order to gain more internal EGR. By adopting this approach, the pumping loss could be significantly reduced. **Figure 6.10** shows the valve timing (including intake, HP and LP valves) and the corresponding mass flow rate across each valve for this proposed engine operating point.

In order to make it clearer, the P-V diagram of the original model was drawn together with that of the DEP model (see **Figure 6.11**). It should be noted that the exhaust valve timing of both the original and the DEP model was optimised to achieve the minimum BSFC. It can be seen that the pumping loss of the DEP two-stage concept was nearly zero, while the original model suffered from the negative re-compression effect during the end of the exhaust stroke and lower intake charge pressure. In addition, the DEP two-stage model seems to have better expansion work compared to the original counterpart. The net BSFC was improved by 6.9% under this engine operating point.

Table 6.5. Averaged results for low-load Minimap points

Engine speed (RPM)	BMEP (bar)	Weighting	Weighting - low load	BSFC - Original (g/kW*h)	BSFC DEP (g/kW*h)	Difference (%)
1000	1	0.079	0.126	549.2	436.7	20.5
1000	4.99	0.089	0.142	288.4	268.6	6.9
1250	1	0.109	0.174	544.8	453.7	16.7
1250	9.99	0.023	0.037	249.3	249.0	0.1
1250	7.49	0.043	0.069	260.9	254.7	2.4
1250	3.74	0.124	0.198	306.6	281.9	8.1
1500	2.5	0.013	0.021	350.0	317.3	9.4
1500	6.54	0.099	0.158	265.8	258.0	2.9
1500	8.74	0.046	0.073	252.3	250.2	0.8
2000	4.99	0.001	0.002	283.3	274.7	3.0
Total	-	0.626	1.000	-	-	9.0

All the operating points in the low-load Minimap points (the high-load Minimap points were not evaluated in this work) have demonstrated BSFC improvement, due to the reduced re-compression and the effect of internal EGR. It is shown that the DEP two-stage system can have better fuel consumption performance over the low-load NEDC drive cycle and, on

average, 9% fuel consumption improvement could be achieved (the averaged fuel consumption benefit in the whole driving cycle might be less if the high-load Minimap points were also considered) .

6.5 Chapter summary and conclusions

Fuel efficiency optimisation for a DEP regulated two-stage downsized SI engine has been conducted using a genetic algorithm, and it was found that the DEP two-stage system could achieve better fuel efficiency across the engine speed at full load, due to the better engine breathing characteristics and improved combustion phasing. The following summary and conclusions are drawn from the study in this chapter:

1: At full load, the DEP two-stage system can achieve three different gas exchange processes at high, medium and low engine speed, respectively. At high engine speed, by the controlling of the three bypass valves, the system can be regarded as a standard DEP concept, with one exhaust valve evacuating the first portion of the exhaust gas to the LP turbine, acting like a traditional turbocharged engine, and the other exhaust valve feeding the latter portion of the exhaust gas directly into the LP exhaust pipe, which behaves like a NA engine. By combining the characteristics of both turbocharged and NA engines, high backpressure between the turbine inlet and the exhaust port is maintained in the blow-down phase, while significant reduction of the backpressure could be achieved in the later displacement phase. This is directly beneficial for the pumping work and residual gas scavenging. Combustion phasing is also considered to be improved, due to the reduced gross IMEP requirement and significantly reduced RGF.

2: At medium engine speed, via the optimised distribution of the exhaust mass flow into the HP turbine and LP turbine, low backpressure could be achieved at the beginning of the exhaust stroke. Such a scheme could also benefit from reduced pulsation interference, but the reduced backpressure at the beginning of the exhaust stroke might not significantly facilitate the scavenging, as such a layout does not facilitate the scavenging during the end of the exhaust stroke where a larger portion of the exhaust residual needs to be scavenged. The corresponding combustion phasing improvement in the GT- power model was due to the reduced gross IMEP requirement with the value of RGF kept the same level.

3: At low engine speed, by opening the HP valve significantly earlier than the LP valve, the DEP two-stage system could attain the target BMEP whilst achieving improved pumping work. The backpressure was stated to be lower for the whole exhaust stroke when compared to the conventional two-stage counterpart, with less pulsation interference observed during the cycle. The reduced hot residual, together with the reduced gross IMEP requirement, was demonstrated to be beneficial for the improvement of the combustion phasing.

4: At part loads (frequently used operating points over NEDC), the DEP two-stage system could be used as a mechanism to extend the 'duration' of the exhaust valve. This will reduce the re-compression effect of the exhaust residuals during the beginning and the end of the exhaust stroke, compared to the original two-stage model, with late exhaust valve opening and early exhaust valve opening. In addition, increased internal EGR, due to the increased overlap between the LP and the intake valve, is beneficial for the improved PMEP, as the throttle can be further opened to reduce the corresponding throttling loss. The average net BSFC improvement is approximately 6-7%.

Figures in Chapter 6

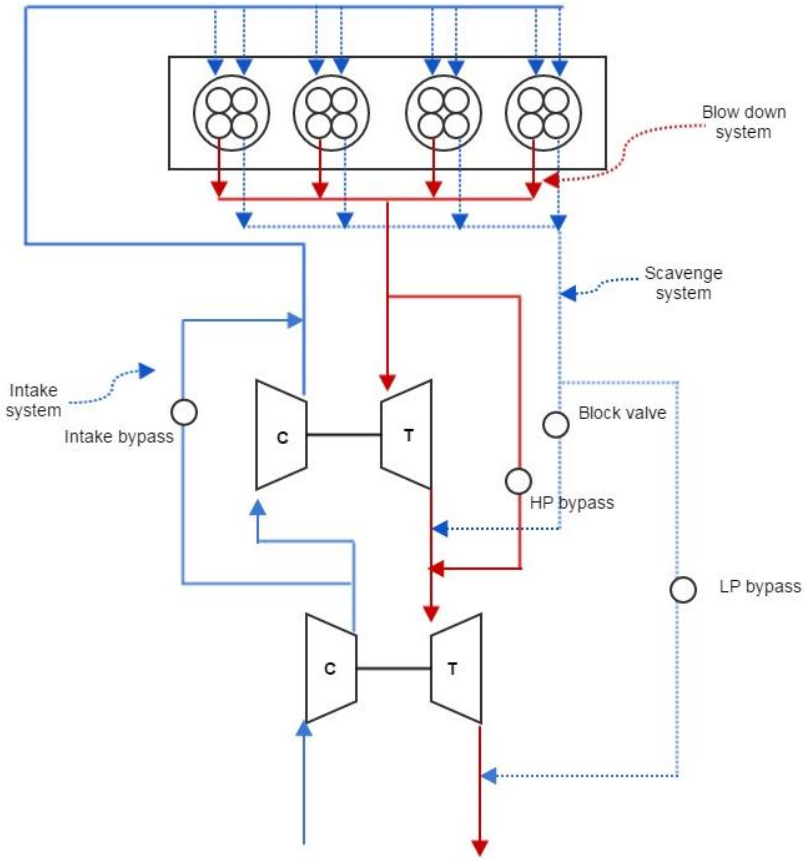

Figure 6.1. Schematic of a DEP two-stage system

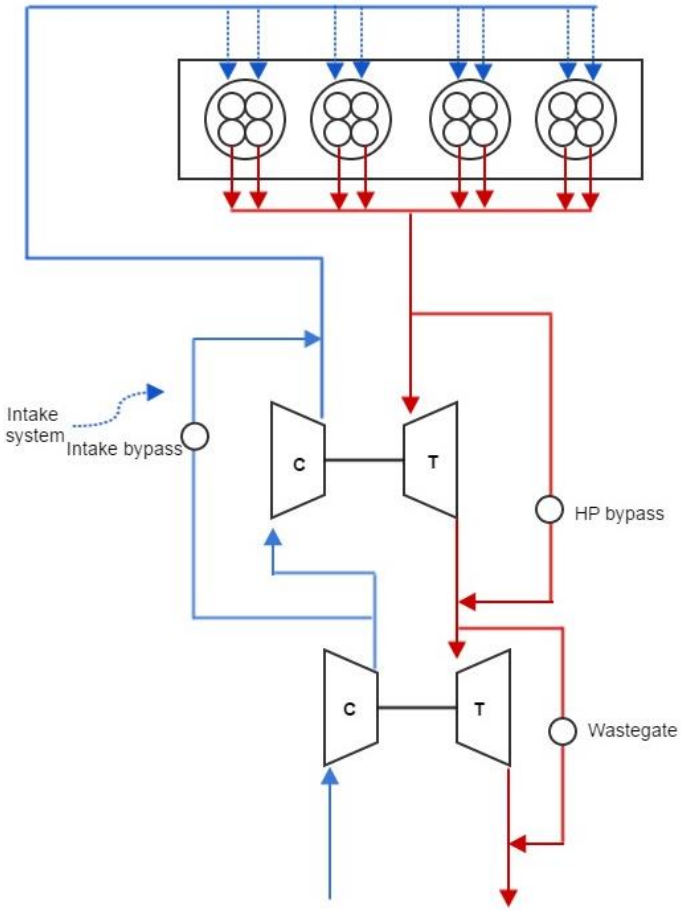

Figure 6.2. Schematic of an original two-stage system

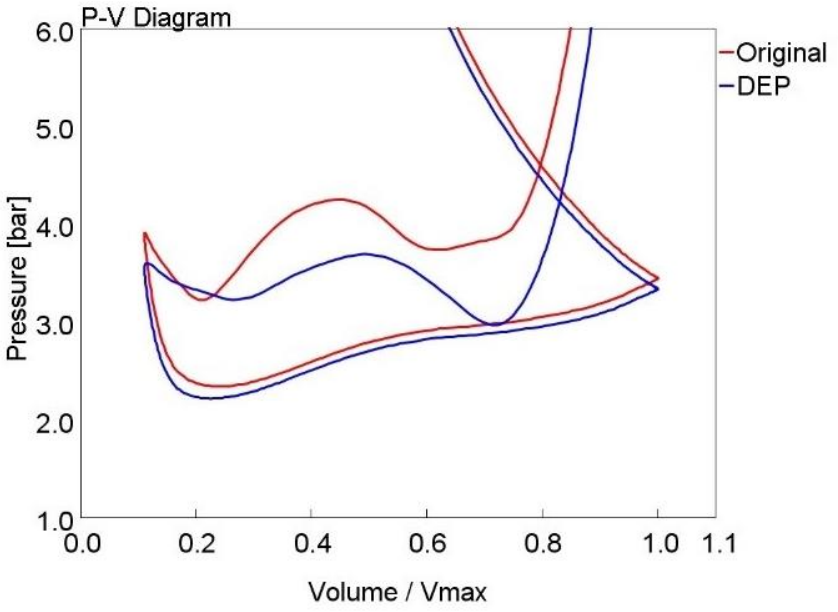

Figure 6.3. Pumping loops in a standard P-V diagram at 3000RPM

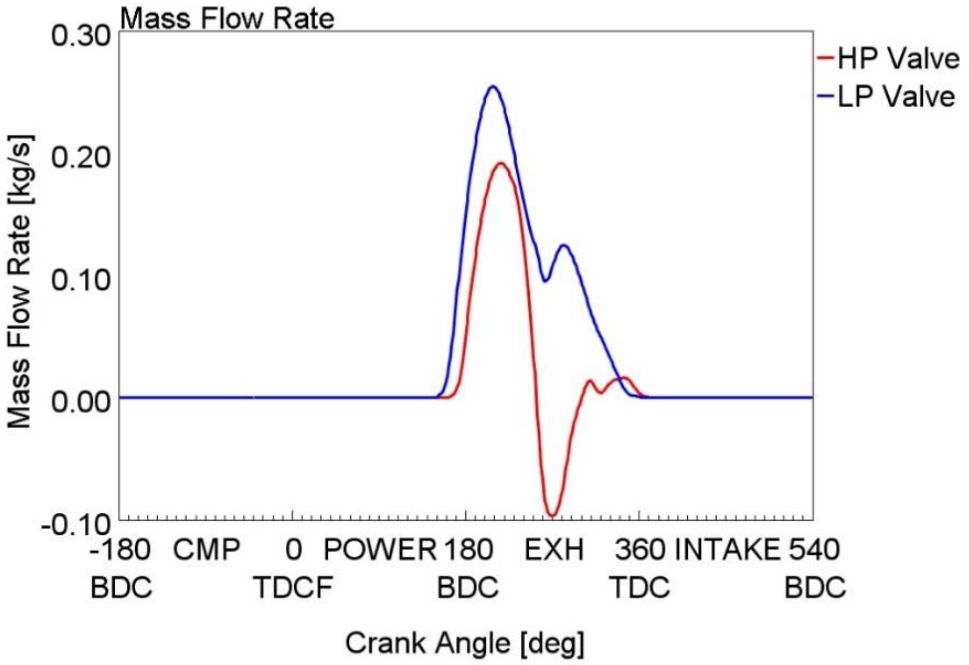

Figure 6.4. Mass flow rate across the valves for the DEP two-stage system at 3000RPM

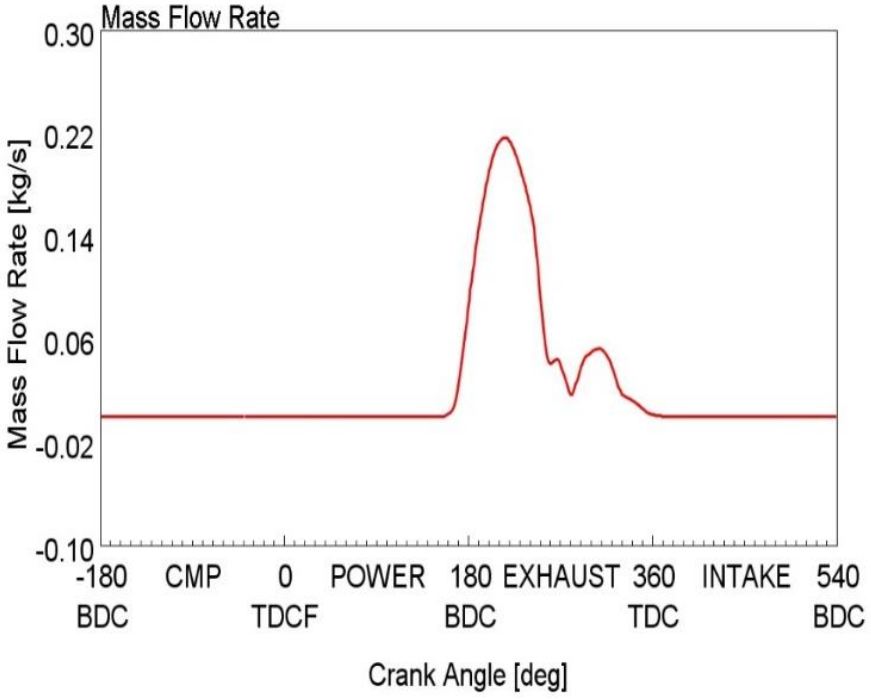

Figure 6.5. Mass flow rate across the valves for the original system at 3000RPM

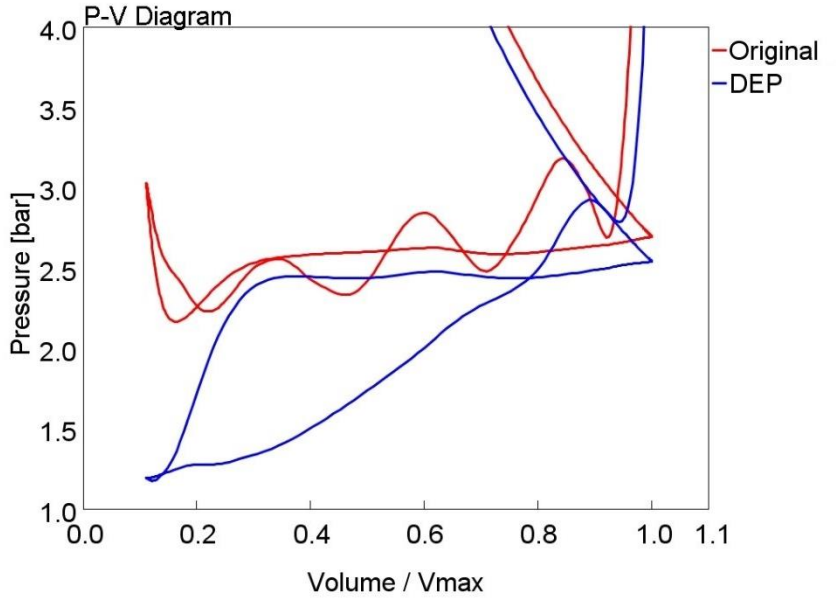

Figure 6.6. Pumping loops in a standard P-V diagram at 1500rpm

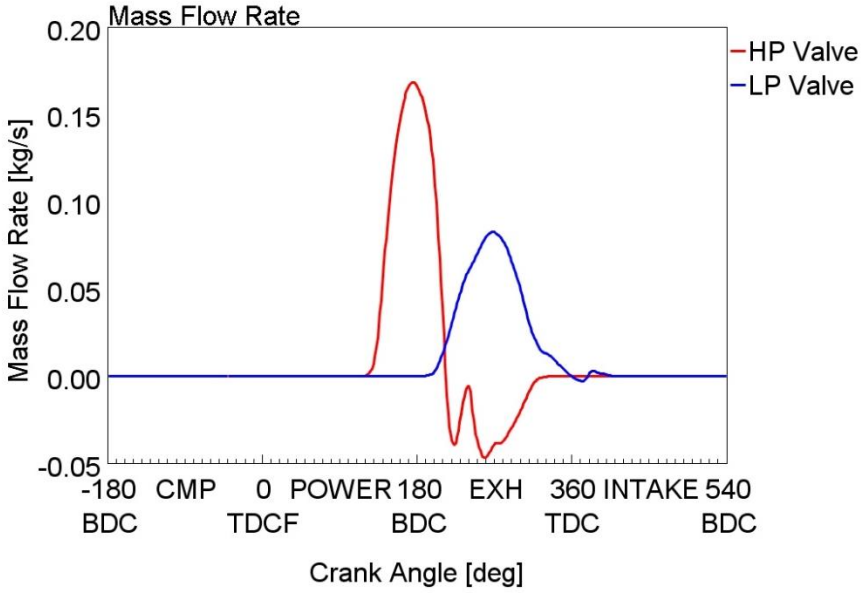

Figure 6.7. Mass flow rate across the valves for the DEP two-stage system at 1500RPM

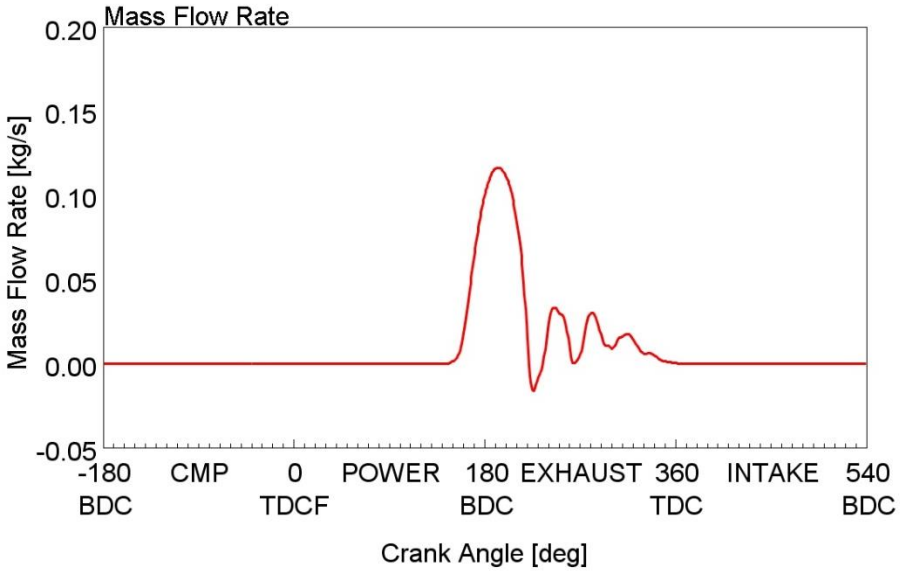

Figure 6.8. Mass flow rate across the valves for the original system at 1500RPM

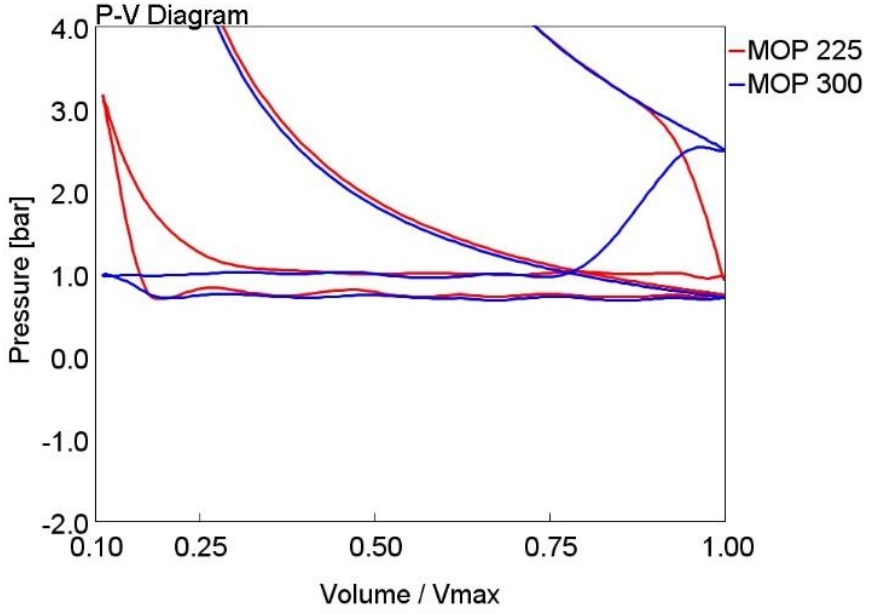

Figure 6.9. Pumping loops in a standard P-V diagram at 1000rpm 4.99bar BMEP

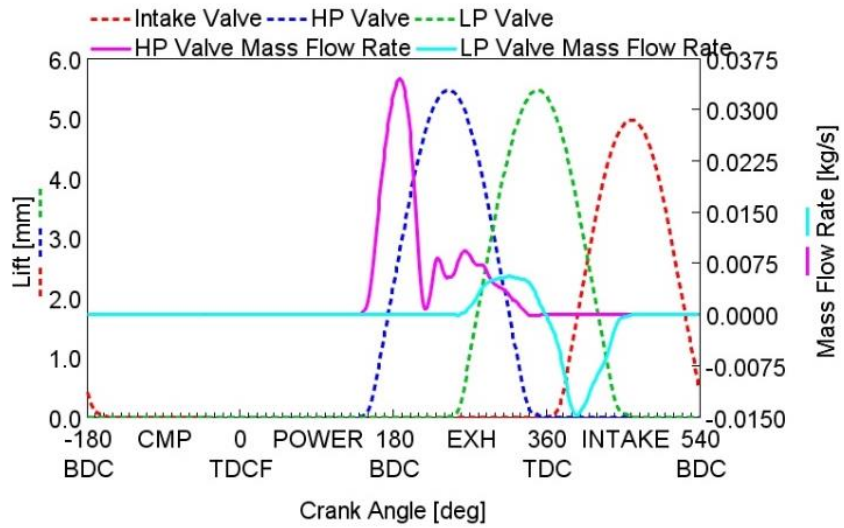

Figure 6.10. Valve profile and mass flow rate across each valve

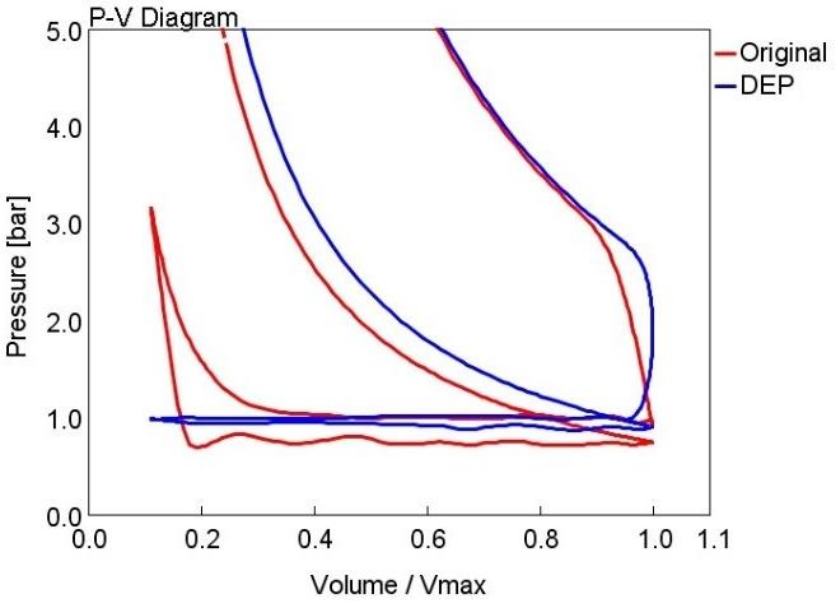

Figure 6.11. Pumping loops in a standard P-V diagram at 1000rpm 4.99bar BMEP

Chapter 7 – *Modelling the turbo-expansion concept*

Engines equipped with pressure charging systems are more prone to knock, partly due the increased intake temperature. Meanwhile, turbocharged engines when operating at high engine speeds and loads cannot fully utilise the exhaust energy as the wastegate is opened to prevent over-boost. Thus, the turbo-expansion concept is conceived in order to reduce the intake temperature by utilising some otherwise unexploited exhaust energy.

This concept can be applied to any turbocharged engines equipped with both a compressor and a turbine-like expander on the intake loop. The turbocharging system is designed to achieve the maximum utilisation of the exhaust energy, from which the intake charge is over-boosted. After the intercooler, the turbine-like expander expands the over-compressed intake charge to the required plenum pressure and reduces its temperature whilst recovering some energy through the connection to the crankshaft. It is anticipated that such a concept has benefits for knock resistance and energy recovery, despite suffering higher pumping losses.

Analogically, the turbo-expansion concept can also be adopted to behave like a conventional throttle for SI engines at part load, in order to reclaim some throttling energy by expanding the close-to-ambient pressure (1bar) to the required intake manifold pressure (normally <0.5bar).

This chapter will present the simulation results using the turbo-expansion concept at both high load and low load. The comparison, discussion and conclusion in this chapter have been presented at SAE 2014 International Powertrain, Fuels & Lubricants Meetings and published in the SAE International Journal of Engines (first presented at the SAE 2015 World Congress & Exhibition).

7.1 Introduction

Downsizing and turbocharging are believed to be the mega trend for SI engines in future decades in terms of addressing fuel economy and environmental issues. However, some inherent characteristics, such as turbo lag and low-end torque, significantly affect the driving comfort performance. The combination of supercharger and turbocharger system seems to be one of the viable solutions to take into account both fuel efficiency and driving fun.

In a standard Turbo-Super system (see **Figure 7.1**), the supercharger provides complementary boost at low to medium engine speed and full load and is declutched at high engine speed and low-load region, where the exhaust energy is sufficient for the turbocharger to provide the required boost and where the engine is 'off boost', which is indicated in **Figure 7.2**. For passenger car gasoline engines, the most frequently used superchargers are the positive displacement type, and centrifugal devices are often seen in the turbocharger system.

At high load for low engine speed, both the supercharger and the turbocharger are involved to provide the target boost. However, at high engine speed, the supercharger does no work since it is declutched. Meanwhile, at some operating points, especially under WOT condition, some of the exhaust energy is wasted by opening the turbine wastegate to prevent over-boost and high pumping loss. From the perspective of energy conservation, this may not be desirable. The question here is how the exhaust mass flow can be fully utilised.

One possible solution, which is termed turbo-expansion, is proposed by Turner et al. [52]. **Figure 7.3** and **Figure 7.4** show the schematic and the T-S diagram for this concept. The air is initially over-compressed by the conventional turbocharging process to point X, cooled to point Y via an intercooler, and then passed through the expander to point Z, in which state it enters the engine. When **Figure 7.1** and **Figure 7.3** are compared, it can be seen that the only difference is the device type downstream of the turbocharger. In a Turbo-Super configuration, the unit after the turbocharger is basically a compressor, whilst in the turbo-expansion concept a turbine-like expander should be utilised.

This only difference was overcome in an experimental research by Romagnoli et al. [59] where they conducted a study on supercharger as an expander. It was considered to be the

first available performance test data in the public domain of an Eaton supercharger (positive displacement) acting as an expander [59]. The authors found that in order to deliver a similar mass flow range to the engine when it is operated as an expander, the supercharger must spin at a slower rotational speed. For example, if an expansion ratio of 1.4 was desired, in order to deliver a similar engine mass flow, the supercharger would have to spin at approximately half the speed compared to the operation as a compressor (see **Figure 3.16**). In addition, when the supercharger was used as an expander, the isentropic efficiency dropped significantly to be around 45%, as can be seen in **Figure 3.17**. It is thus suggested that the supercharger could function either as a compressor or an expander if a CVT was installed.

This chapter will propose a new turbo-expansion concept for a Turbo-Super engine system, using data from Imperial College London. The turbocharging system is designed to achieve maximum utilisation of the exhaust energy, from which the intake charge is over-boosted. After the intercooler, the supercharger acts like a turbine, expanding the over-compressed intake charge to the required plenum pressure and reducing its temperature whilst recovering some energy through the connection to the crankshaft (see **Figure 7.5**).

The turbo-expansion concept will feature a lower intake charge temperature, which might result in improved combustion phasing and will also benefit from the reclaimed energy from the supercharger when functions as an expander. However, since some of the otherwise unexploited exhaust mass flow is forced into the turbine, a larger backpressure should be anticipated, which could lead to a larger engine pumping loss. The net BSFC improvement by adopting such a concept should depend on the balance of PMEP, combustion phasing and energy recovered.

In order to show the effect of lower intake charge temperature on the combustion phasing, the constant air density test was conducted at 1500RPM and the results, in terms of KLSA, are presented in **Figure 7.6** below. This shows clearly that for each set of constant charge air density data, as the air temperature was reduced, KLSA increased correspondently.

It is also conceived that by lowering the intake charge temperature, the engine's geometric compression ratio could be increased under fixed-knock index condition, thus improving the thermodynamic efficiency of the engine across the whole of the operating points. **Equation**

7.1 shows the SI engine's ideal thermodynamic cycle efficiency, which is dictated by engine's compression ratio (r) and the ratio of specific heats of the working fluid (γ). To make it clearer, ideal Otto cycle efficiency versus compression ratio is plotted in **Figure 7.7** [193].

$$\eta_{idea} = 1 - \frac{1}{r^{\gamma-1}} \quad \textbf{7.1}$$

The turbo-cooling concept [55-56] can also achieve cooling-intake effect. In a TCS, both additional compressor and turbine are utilised to compress and expand the intake charge. By removing the heat with an intercooler and making the expansion ratio greater than the compression ratio, sub-ambient temperature could be achieved (see **Figure 7.8**). However, unlike the turbo-expansion concept, the turbo-cooling concept does not reclaim energy but, instead, leads to lower pumping loss.

There are some similarities between the new turbo-expansion concept and turbocharged Miller cycle. They both have larger backpressure and larger after-turbocharger-compressor pressure. The aim of both configurations is to lower the cylinder temperature at the point of ignition in order to mitigate knock at high load. However, the Miller cycle allows a reduction in effective compression ratio and transfers the compression work from the cylinder to the turbocharger compressor, with the charge cooled as an intermediate stage. While the new turbo-expansion concept differs from the Miller cycle, by reducing the charge temperature via the high-pressure stage expander, it does not change the compression stroke, and has a plenum pressure similar to its conventional turbocharged counterpart.

The CVT driven supercharger in the new turbo-expansion concept features the characteristic of recovering some over-compressed intake energy by lowering the intake pressure at high load. Analogically, the CVT supercharger can also be adopted to replace the conventional throttle for SI engines at part load, to recover some throttling energy by expanding the close-to-ambient pressure (1bar) to the required intake pressure (normally <0.5bar). It is conceived that by reclaiming some throttling loss through the supercharger, part-load fuel efficiency could be improved. In addition, the cooling effect of the supercharger expansion could lighten the load of the after-cooler, which is beneficial for knock resistance and volumetric efficiency for the following possible high-load cycle.

This chapter will only investigate the BSFC benefit at high engine speed or low-load region when the supercharger functions as an expander. Thus, the performance of the supercharger

when operated as a normal compressor is not considered in this piece of work. While this dual purpose is not possible with a fixed-ratio drive, model-based research into the use of a CVT drive supercharger has been carried out by other authors [163]. Thus, such a switch between compressor and expander operation could be conceived using such a variable-ratio drive system.

This work will first investigate the net fuel efficiency benefit from the turbo-expansion concept at full load. Following that, the methodology of the new de-throttling concept utilising the turbo-expansion concept is proposed and simulated.

7.2 Methodology

For the simulation work presented in this chapter a 1-D model of a highly downsized SI engine detailed in **Table 7.1** was used as a starting point (the schematic can be seen in **Figure 7.1**). In addition, some experimental data has been gathered at Imperial College on the performance of an Eaton supercharger when operated as an expander. The corresponding data can be seen in **Figure 3.16** and **Figure 3.17**.

Table 7.1. Basic Parameters of the simulated engine

Engine Type	-	Inline-4-cylinder
Capacity	cc	1991
Bore	mm	83
Stroke	mm	92
Compression ratio	-	9.0:1
Firing Order	-	1-3-4-2
Combustion System	-	Gasoline GDI
Valvetrain	-	DOHC, Cam Phasers and Cam Profile Switch on Intake and Exhaust Camshafts
Spec. Power	kW/l @ min	142 @ 6500
Spec. Torque	Nm/l @ min	255 @ 3500
max. BMEP	bar @ min	35 @ 3500 and 25 @ 1000 &6500
Air Charging System	-	HP: Eaton R410, LP: Honeywell GT30

From **Figure 3.16**, it can be seen that, for a given pressure ratio, the relationship between the mass flow and the rotational speed was nearly linear. It should be noted that the mass flow here was much lower than that required at WOT condition (over 200g/s) and higher than that needed at low load.

It is conceived that by bypassing some intake mass flow directly into the plenum (see **Figure 7.9**) or extrapolation of the existing data could be a viable solution, considering that the experimental data for higher and lower rotational speed is not feasible in a short time. For the simulation results in the next section, firstly the bypassing approach was adopted to investigate the net BSFC improvement by using the new turbo-expansion concept. Then, the extrapolation method was employed to examine the benefits obtained from higher rotational supercharger speed. For the low-load region, only the extrapolation method was used.

Figure 3.17 shows that the isentropic efficiency for the supercharger as an expander was limited between 40% and 50% which is much lower than the efficiency when the supercharger is utilised as a standard compressor. This is due to fact that the original supercharger was not designed to operate as an expander. It should be noted here that the definition of expansion efficiency was simply taken from a turbine definition, as shown in **Equation 7.2**. In section of 7.4 in this chapter, the net BSFC benefit from improved supercharger (expander mode) efficiency will also be investigated.

$$\eta_{TT} = \frac{1-\left(\frac{T_{T,OUT}}{T_{T,IN}}\right)}{1-\left(1/(ER)^{\gamma-1/\gamma}\right)} \qquad \textbf{7.2}$$

$$\text{where} \quad \mathrm{ER} = {}^{\mathrm{P_{T,IN}}}\Big/_{\mathrm{P_{T,OUT}}}$$

GT-Power has templates for a positive displacement compressor but does not have such a template for a turbine-like expander. In addition, a turbine template such as “TurbineMap” is normally used for centrifugal turbines, which embed pre-defined fitting algorithms developed only for centrifugal turbines (detailed in **Chapter 4**). Thus, the template named “TurbineMapGrid” was adopted here to only perform a raw fitting of the experimental data. Of course, this would require more data in order to provide an accurate representation, but would potentially model the supercharger as an expander concept quite well.

7.3 Simulation results at high load

Existing data simulation

In this section, the existing experimental data will be used to investigate the net BSFC benefit when adopting the new turbo-expansion concept. The idea is to use a supercharger bypass to keep the mass flow rate in the range of the existing experimental data whilst controlling the wastegate of the turbine, in order to target the required BMEP.

For the purpose of simplicity, only the WOT operating point at 6500RPM was simulated. In addition, in order to provide sufficient mass flow rate, an 8000 rev/min supercharger speed was used.

Table 7.2. Averaged results for the original and the new turbo-expansion concept

Engine Speed: 6500RPM	Original	Expansion-cooling
BMEP (bar)	26.24	
BSFC (g/kW*h)	258.7	259.6
Average Pressure (bar)	2.78	2.83
Average Temperature (K)	324.4	324.8
PMEP (bar)	-2.19	-2.31
Spark Timing (ATDC degree)	17.4	18.0
Energy Recovered (kW)	-	1.32
Supercharger Efficiency	-	40.78%
Wastegate Diameter (mm)	15.8	12.6

It can be seen in **Table 7.2** that BSFC performance was not improved as predicted, due to the fact that both the engine breathing characteristics and the combustion phasing were degraded. Pumping loss was predictably increased as the wastegate was closed further to provide energy to cool the intake charge. The increased intake temperature was clearly undesirable, seeing that the principle of the new turbo-expansion concept was to decrease intake temperature, in order to improve the combustion phasing. This is probably because the poor isentropic efficiency of the supercharger when functioning as an expander, and is also attributed to the fact that some exhaust mass flow did not enter into the supercharger for cooling. It is considered that by increasing the isentropic efficiency of the supercharger as

an expander or forcing more mass flow into the supercharger, there would be some net BSFC improvement.

It can be concluded here that by using the exiting data (bypassing some exhaust mass flow directly into the intake plenum), no BSFC improvement was observed, although some of the otherwise unexploited waste exhaust energy was recovered indirectly through the supercharger to the engine. More efforts should be focused on the intake temperature decrease to accomplish the task of expansion cooling.

Extrapolation of the existing data

In this section, a process of extrapolation from the existing data was conducted. It can be seen from **Figure 3.16** that the relationship between the mass flow and the supercharger (expander-mode) rotational speed is nearly linear. Thus, a simplified linear model was adopted to predict the mass flow at high supercharger rotational speed. By doing the extrapolation method, it is conceived that GT-Power can calculate the efficiency and pressure ratio when all the mass flow is entered into the supercharger, thus making more use of the expansion-cooling effect. The wastegate was also used to control the target BMEP as in the original model, and **Table 7.3** shows the averaged results for the original and the new turbo-expansion concept, when maps have been extrapolated as explained.

Table 7.3. Averaged results for the original and the new turbo-expansion concept

Engine Speed: 6500RPM	Original	Turbo-expansion
BMEP (bar)	26.2	
BSFC (g/kW*h)	258.7	258.6
Average Pressure (bar)	2.78	2.82
Average Temperature (K)	324.4	322.0
PMEP (bar)	-2.19	-2.31
Spark Timing (degree)	17.4	17.9
Energy Recovered (kW)	-	2.16
Supercharger (expander mode) Efficiency	-	45%
Wastegate Diameter	15.79	12.48

It can be seen that, although the expansion-cooling effect was fulfilled, there was very little BSFC improvement. This is, of course, partly due to the larger pumping loss, which was an inherited characteristic of the new turbo-expansion concept, and is partly attributed to the retarded combustion phasing, which was not predictable. In the following section, the reason why the combustion phasing was not improved is investigated by looking at the Douaud & Eyzat knock model in GT-Power [191]. The detailed of this model is seen in **Section 6.3**.

It can be seen from both **Equation 6.2** and **Equation 6.3** that the induction time integral and the knock index are strongly related to the cylinder end-gas pressure and temperature. End-gas temperature and pressure is related to the temperature and pressure of the mixture at the start of the combustion process, which is related to the averaged boost pressure and intake temperature. The new turbo-expansion concept has the benefit of reducing the averaged intake temperature but also features increased boost pressure, thus, at fixed knock index point, combustion phasing might be improved or degraded depending on the combination effect of the intake temperature and boost pressure.

In addition, RGF is also an important parameter, which significantly affects knock index. The new turbo-expansion concept features larger backpressure, thus RGF would be increased, resulting in larger knock index or, in other words, under fixed knock index condition the combustion phasing needed to be retarded.

It is hereby concluded that when the supercharger (expander mode) operates at a lower efficiency, the new turbo-expansion concept using the experimental data may not feature improved combustion phasing, but can benefit from an indirect energy recovery. Larger pumping loss was also an important factor, which negatively affects the BSFC performance.

7.4 Discussions at high loads

Supercharger speed sensitivity study:

It is known that at high engine speed the turbocharger could provide a larger boost, while the supercharger supplies a larger expansion to make the intake manifold pressure approximately the same level. The larger boost supplied by the turbocharger could be achieved by further closing the wastegate, and a larger expansion could be targeted through further slowing the supercharger speed. Described in the following section, a supercharger

speed sensitivity study was conducted to see how the supercharger speed impacts the engine's BSFC performance.

From **Figure 7.10** to **Figure 7.14**, it can be seen that the engine's BSFC performance is not sensitive to the supercharger speed. Although at lower supercharger rotational speed the energy that could be reclaimed increased, the pumping losses would be degraded and the sparking timing retarded, due to the larger RGF.

Supercharger isentropic efficiency sensitivity study:

In the previous section, only very limited BSFC improvement was demonstrated, which is attributed to the degraded combustion phasing and poor engine breathing characteristics. Such results seem to be reasonable as the supercharger device, as designed, was not intended to be used as an expander. In the following section, the isentropic efficiency of the supercharger (expander mode) was increased from 45% to 90%, in order to test the influence of improved performance. As before, the diameter of the wastegate was used to control the target BMEP. For simplicity, only the rotational speed of the supercharger 14000 rev/min was studied.

It can be seen from **Figure 7.15** that when the efficiency of the supercharger was increased, the BSFC performance improved, and it provided better fuel economy than the original engine model when the efficiency was above 50%. More details on the engine breathing characteristics, combustion phasing, and energy recovery can be seen from **Figure 7.16** to **Figure 7.19**.

It is shown in **Figure 7.16** that the pumping loss was decreased for the increased supercharger (expander mode) isentropic efficiency. This would result in an increased diameter of the wastegate, as less boost pressure was needed to overcome the resistant pumping work. But even when the efficiency was 90%, compared to the original model, the new turbo-expansion concept still suffered larger pumping loss. This is due to the fact that some of the exhaust mass flow was forced into the turbine to provide the required energy to cool the intake charge.

The combustion phasing was also improved with the increased supercharger (expander mode) isentropic efficiency (see **Figure 7.17**). As explained in the section on extrapolation of

the existing data, combustion phasing is affected not only by the intake temperature and boost pressure but also the residual gas fraction. However, even if the isentropic efficiency of the supercharger as an expander could achieve approximately 90%, the combustion phasing of the engine adopting the new turbo-expansion concept would still be not improved in comparison with the original model. In **Figure 7.18**, it can be seen that the expansion-cooling effect was fulfilled. However, it also shows that, although for increased isentropic efficiency of the supercharger (expander mode) the corresponding value of the boost pressure decreased, the new turbo-expansion concept cannot achieve reduced boost pressure when compared to the original model.

The energy recovered by the supercharger with different supercharger (expander mode) efficiency is shown in **Figure 7.19**. It can be seen that, with increased efficiency, the energy recovered increased significantly, from around 2.2 kW to approximately 3.9 kW. But it should be noted that the assumption of 100% mechanical efficiency was made here whereas, in reality, less energy would be recovered, resulting in a smaller BSFC improvement.

7.5 Simulation results at low load

Extrapolation method:

In order to provide sufficient data to GT-Power with the consideration that the experimental data for lower rotational speed and higher pressure ratio is not feasible in a short time, some viable extrapolation method needs to be employed. As this is only a research exercise, some simplified assumptions are made here.

- For a given supercharger rotor speed, the relationship between the pressure ratio and the corresponding mass flow rate is nearly linear
- For a given pressure ratio, the relationship between the mass flow and the supercharger rotational speed is ascending, and the curve goes through the point (0, 0).
- The isentropic efficiency of the supercharger functioning as an expander is assumed to be a constant 45%, which is a fair representation of the data shown in **Figure 3.17**.

Figure 7.20 and **Figure 7.21** show the extrapolated data using the assumptions mentioned above; **Figure 7.22** is the re-organised standard performance map for the supercharger functioning as an expander. When compared to the performance map of the supercharger under compression mode (see **Figure 7.23**), the supercharger map under 'expansion mode' looks sufficiently reasonable.

Throttling losses model:

The power that is lost in the throttling process and thus available to the expander is called the wasted work or lost work, which could be represented by the following equation:

$$b_1 - b_2 = h_1 - h_2 - T_0(s_1 - s_2)$$

where b_1, h_1, s_1 are the exergy, enthalpy and entropy before the throttle, b_2, h_2, s_2 are the exergy, enthalpy and entropy after the throttle, and T_0 is the ambient temperature. **Figure 7.24** shows the exergy destructed in the throttling process at engine speed from 1000RPM to 3000RPM and engine BMEP from 1bar to 5bar.

Minimap: For simplicity, only Minimap point numbers 8 and 9 (see **Table 6.2**) were selected for investigation into the benefits of the new de-throttling concept, considering the following facts:

- The necessity for a throttle plate in the original downsized engine;
- Relatively high weighting.

Control strategy and calibration:

In order to achieve the required BMEP target, the LP turbine wastegate was set to be fully closed. With fully-closed wastegate, the fuel consumption of the throttled engine will be slightly higher, due to the increased exhaust backpressure. However, as the simulation was run at very low engine load, the fuel economy is very similar between the wastegate fully closed and the fully-open configuration.

In the engine calibration, the wastegate could also be fully closed or fully open for different purposes (sporty or economy) at part load. The reason why both the throttled model and the de-throttled counterpart are calibrated with the wastegate fully closed is the consideration to show the maximum fuel consumption improvement potential by utilising the new de-throttling concept. The valve timing and the combustion profile of the model were retained as in the throttled counterpart. The rotational speed of the supercharger was optimised to attain the target engine BMEP with the throttle plate fully opened.

At a start point for this investigation, Minimap point 9 (1000RPM, 4.99bar BMEP) was selected, owing to its high NEDC weighting value and reasonable load requirement. **Figure 7.25** shows the supercharger speed map under 'expansion mode' in GT-Power with the cycle

average value. It can be seen that the averaged pressure ratio is above 1, which could reduce the inlet temperature.

From **Table 7.4**, it can be seen that the required low BMEP can be achieved by altering the supercharger rotational speed without the need for the conventional throttle control. BSFC was improved by 1.4% due to some of the throttling energy recovery. It should be noted here that the supercharger downstream temperature dropped significantly from 305K to 281K, which is beneficial for the volumetric efficiency and, most importantly, is advantageous to cool the after-cooler, resulting in enhanced knock resistance for the following possible high-load cycle. However, cold intake air will increase the intake pumping work, although the effect of the temperature on the intake pumping work is very limited. In the following table, a lower BMEP point at the same engine speed (1000RPM, 1bar) was selected in order to investigate the effect of the supercharger de-throttling concept under a similar high weighting operating point in the NEDC cycle.

Table 7.4. Parameters of the de-throttling concept and the throttled counterpart at Minimap point 9

	De-throttling Concept	Throttled Counterpart
BMEP (bar)	4.99	4.99
Engine Speed (RPM)	1000	1000
Brake Power (W)	8279	8279
Supercharger Rotational Speed (rev/min)	495	0
BSFC (g/kW*h)	294.9	299.1
Supercharger Downstream Temperature (K)	281	305
Throttling Energy Recovery (W)	181.7	0

Table 7.5 shows the averaged results of the de-throttling concept and the throttled counterpart at 1000RPM and 1bar BMEP. Compared to **Table 7.4**, it can be seen that BSFC improvement was incremented from 1.4% to up to 3.3%. This is mainly due to the increased proportion of the recovered energy. The supercharger downstream temperature was also

reduced a lot to sub-ambient. The condensation effect needs to be considered in this situation, and will be demonstrated in the discussion section.

Table 7.5. Parameters of the de-throttling concept and the throttled counterpart at Minimap point 8

	De-throttling Concept	Throttled Counterpart
BMEP (bar)	1	1
Engine Speed (RPM)	1000	1000
Brake Power (W)	1673	1673
Supercharger Rotational Speed (rev/min)	156	0
BSFC (g/kW*h)	550.8	569.8
Supercharger Downstream Temperature (K)	258	307
Throttling Energy Recovery (W)	149.4	0

Figure 7.26 and **Figure 7.27** show the throttling loss recovery and the supercharger speed across the engine speed, respectively. It can be seen that with increased engine speed and increased engine torque, the achievably reclaimed throttling loss and the supercharger speed increased, which is mainly due to the mass flow requirement.

Figure 7.28 shows the BSFC improvement in percentage across the engine speed under low load. It can be seen that the maximum BSFC improvement occurred under low engine speed and low engine torque with decreased trend to the higher engine speed and higher engine torque. The supercharger outlet temperature can be seen in **Figure 7.29** which illustrated that, with lower engine torque and engine speed, the supercharger outlet temperature tended to be lower (even to sub-ambient).

Controllability:

Since the supercharger rotational speed could be optimised to provide the required target BMEP, the control of the throttle valve in an SI engine can be replaced by the control of the supercharger rotational speed via a CVT. **Figure 7.30** shows BMEP vs supercharger rotational

speed which indicates the CVT supercharger de-throttling concept has a good controllability over the frequently part load.

7.6 Discussion at High Loads

Transient performance:

The CVT-driven supercharger is potentially beneficial for an engine's transient performance due to the overshoot characteristics of the supercharger [163]. However, the time-to-torque performance of the new de-throttling concept will depend on the CVT change ratio and the largest CVT reaction torque (sum of the CVT input and output torque) limit. To the authors' knowledge, due to the large inertia of the positive displacement supercharger system and the current CVT design, the time-to-torque transient performance of the new de-throttling concept might not be as good as in its de-throttled counterpart.

By adopting supercharger de-throttling concept, it is anticipated that a conventional clutch might not be needed, which is beneficial from the cost performance viewpoint. In addition, the NVH issues caused by the engagement of the clutch during the transient will be eliminated, which, compared to the clutched counterpart, improves the driving comfort.

CVT ratio range:

In the simulation conducted above, it is not considered whether typical existing CVT systems can achieve the required low torque. According to Rose et al. [163] typical Milner CVT, full-toroidal/half-toroidal CVT and belt-drive CVT have CVT ratio ranges of 4.5, 6.0 and 6.0, respectively. However, this data is at least three years old, given the date of the publication. Without considerable review of the current typical CVT ratio range, it is anticipated that a CVT ratio range of 8 may be achieved with current technology.

For the research model of the two-stage downsized engine, a fixed-gear ratio between the supercharger and the engine needs to be at least 5.9 to attain the required full-load BMEP. If the value of 5.9 is set to be the largest possible CVT ratio, then the lowest possible CVT ratio would be 0.74 (at 1000RPM, supercharger rotational speed can only be down to 740rev/min) if a CVT ratio range of 8 was adopted. This means that both the target BMEP of Minimap point 8 and Minimap point 9 cannot be attained if the CVT is the only control parameter of the engine. In this situation, an additional throttle valve might be needed to

provide additional pressure drop, which will lead to raised supercharger downstream temperature and relatively higher BSFC, due to the throttling effect of the throttle valve.

Condensation effect:

It is considered that one of the phenomena to cause condensation corresponds to the supercharger de-throttling concept in which the intake air parcel expands and cools. Eichhorn et al. state that the energy released through the condensation effect increased linearly with the temperature drop [50]. In the results section, it is found that operating points with lower BMEP characteristics lead to higher temperature drop; thus, condensation is a very important feature during these conditions. As GT-Power does not feature condensation effect in its default setting, thus no condensation effect could be assumed for the purpose of simplicity.

However, in an experiment, the inlet mass flow could release some heat after the supercharger, due to condensation resulting in a relatively higher downstream temperature. This could either influence the cooling effect of the outlet charge to the after-cooler or influence the calculation of the expansion recovery power, due to the smaller difference of the temperature.

The trade-off between the combustion efficiency and the recovered throttling energy:

The new de-throttling concept aims to reclaim some throttling energy and reduce the power required in the combustion system at fixed-engine operating point. However, for the de-throttling concept, the combustion efficiency will drop as the cylinder pressure and gross IMEP is reduced (combustion under high pressures is thermodynamically more efficient). The brake engine efficiency therefore depends on the combustion efficiency drop and the energy reclaimed by the supercharger. In this work, it can be seen that the recovered energy is above the efficiency loss in the combustion system. For example, in GT-Power, at 3000RPM and 16.1Nm, the de-throttling concept has an indicated efficiency of 26.88% and brake efficiency of 14.09%, compared to the throttled counterpart with an indicated efficiency of 27.47% and brake efficiency of 14.03%.

However, for this specific work, it is seen that recovered energy is way above the efficiency loss in the combustion system.

Supercharger operating points extension:

Since the supercharger could have a normal compression mode and an unconventional 'expansion mode', the operating range of the supercharger could be significantly extended for a turbo-super configuration SI engine (see **Figure 7.31**). To be more specific, the supercharger can supply an additional boost at low speed/high load when the turbocharger energy is not sufficient. At high speed/high load, when the exhaust energy is sufficient for the turbocharger to provide the required boost, the supercharger could function as an expander, presenting an indirect means to recover some of the exhaust energy. At part load, the supercharger could serve as a de-throttling mechanism to recover some of the otherwise wasted throttling loss, through a direct connection to the crankshaft. Thus, with different CVT ratio, the supercharger could fulfil different tasks, which could push the fuel efficiency of the downsized two-stage SI engine further.

7.7 Chapter summary and conclusions

A novel turbo-expansion concept has been proposed using a Turbo-Super twin-charger 1-D simulation model. The turbocharging system is designed to achieve the maximum utilisation of the exhaust energy, from which the intake charge is over-boosted. After the intercooler, the turbine-like supercharger expands the over-compressed intake charge to the required plenum pressure and reduces its temperature, while recovering some energy through the connection to the crankshaft. A new de-throttling concept has also been proposed utilising the CVT driven supercharger to 'throttle' a Turbo-Super configuration SI engine rather than adopting a conventional throttle valve. The following summary and conclusions are drawn from the study in this chapter:

1: At high load, when the model was first simulated, it was found that the expander model using the existing experimental data could not supply enough mass flow, due to the range of tested supercharger (expander mode) speed data and the fact that the expander template can only perform a raw fitting of the data. The approach of using the bypass of the supercharger was adopted to keep the mass flow into the supercharger within the range of the tested data. It was found that such a layout did not achieve the purpose of expansion-cooling, due to the poor efficiency of the supercharger and because some mass flow did not enter into the supercharger for cooling. In addition, with increased boost pressure and RGF, the combustion phasing was degraded. Pumping loss of the engine adopting the new turbo-expansion concept was also poorer than in the original model. However, such a layout

benefited from the energy recovered from the supercharger. In total, the BSFC performance was not improved.

In order to investigate the effect when all the intake mass flow enters into the supercharger, the experimental data was extrapolated to higher rotational speeds. The relationship between the mass flow and the rotational speed was assumed to be linear and the isentropic efficiency was assumed to be 45%. The results showed that the expansion-cooling task was accomplished, but the poor isentropic efficiency of the supercharger functioning as an expander resulted in a limited improvement in BSFC.

The poor improvement in BSFC is reasonable since the Eaton supercharger was not designed to operate efficiently under expansion. The isentropic efficiency was therefore manually increased from 45% to 90%, in order to investigate the net BSFC improvement from a more suitable-imaginary supercharger. The results seemed different from those of previous studies, showing that, even with isentropic efficiency as high as 90%, the combustion phasing was not improved significantly, due to the higher boost pressure and larger RGF. Pumping loss and energy recovered were, as predicted, decreased and increased, respectively. The final BSFC was improved by approximately 1%. This might suggest that the new turbo-expansion concept is not suitable for this specific simulated engine model, although this novel gas exchange concept could be used in some other engines for its own interest.

2: At low load, by recovering some throttling loss through the supercharger, part-load fuel efficiency could be improved by up to 3%, depending on the operating points. In addition, the cooling effect of the supercharger expansion could lighten the load of the after-cooler, which is beneficial for the knock resistance and volumetric efficiency for the following possible high-load cycle. However, the issues of limited supercharger operating range with an existing production CVT, condensation, fuel evaporation and worse pumping work need to be addressed before taking the supercharger-throttling gas exchange process from concept to reality.

The rotational speed of the supercharger could also be used as a control mechanism to attain the required part-load target. However, more investigation in this area needs to be conducted.

Since the supercharger could have a normal compression mode and an unconventional ‘expansion mode’, the operating range of the supercharger could be significantly extended for a Turbo-Super configuration SI engine.

Figures in Chapter 7

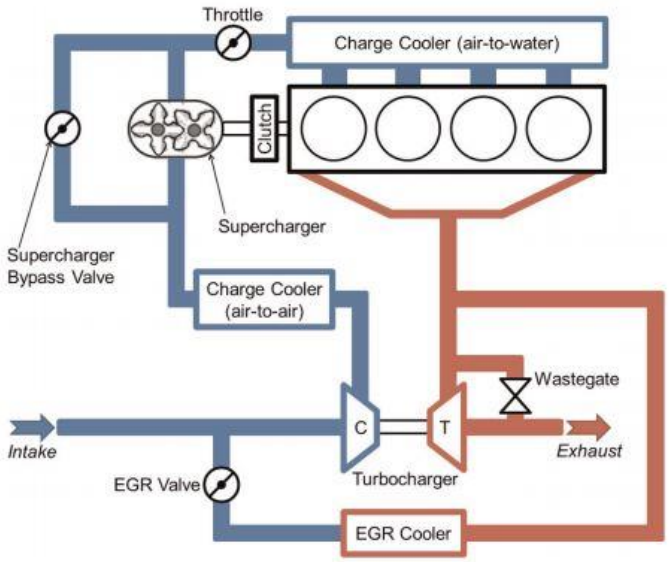

Figure 7.1. Schematic of a standard Turbo-Super system [163]

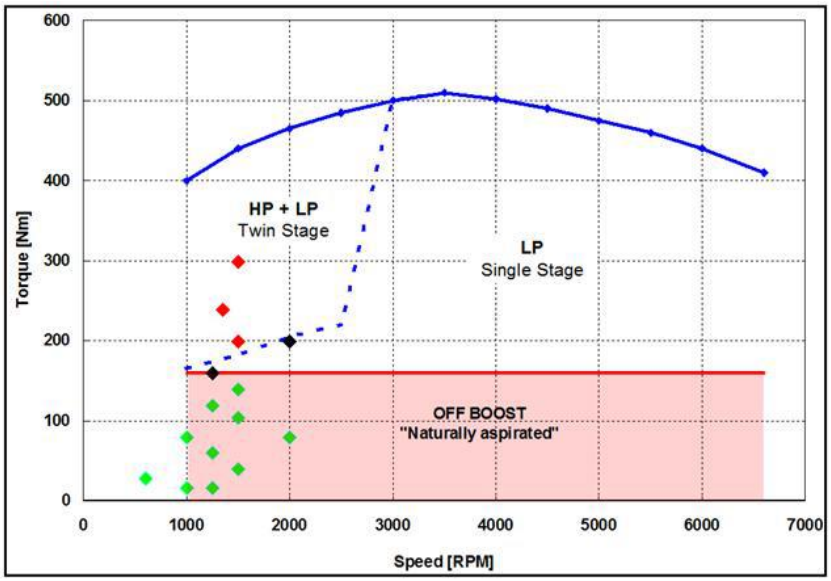

Figure 7.2. Operating range of a conventional supercharger

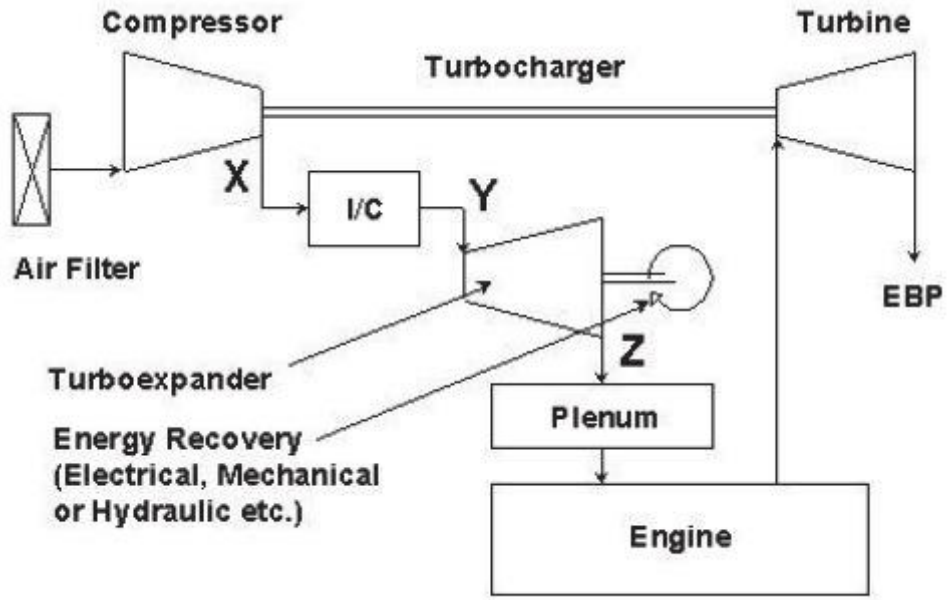

Figure 7.3. Schematic of simplified turbo-expansion system. [52]

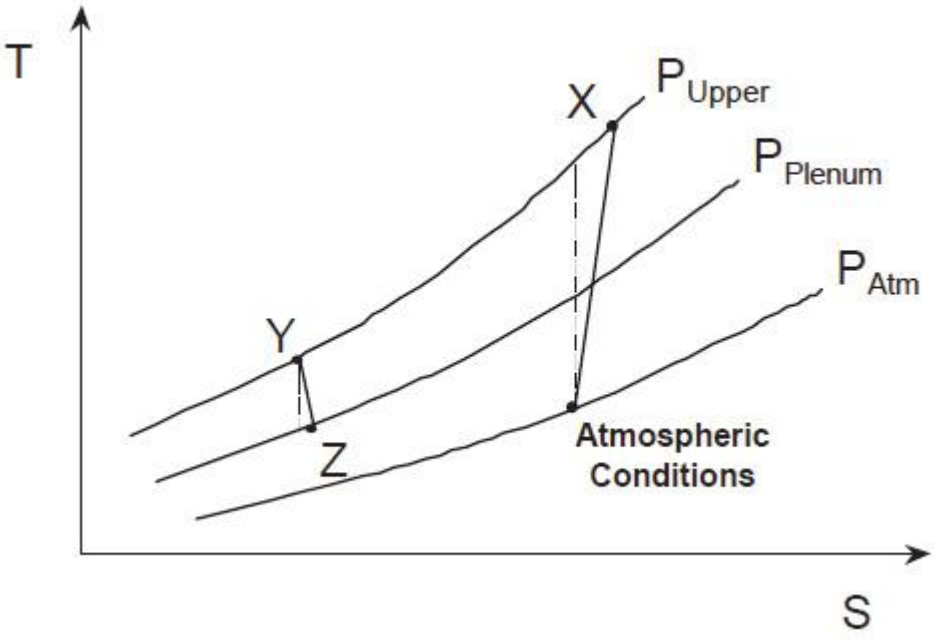

Figure 7.4. T-S diagram for turbo-expansion system. [52]

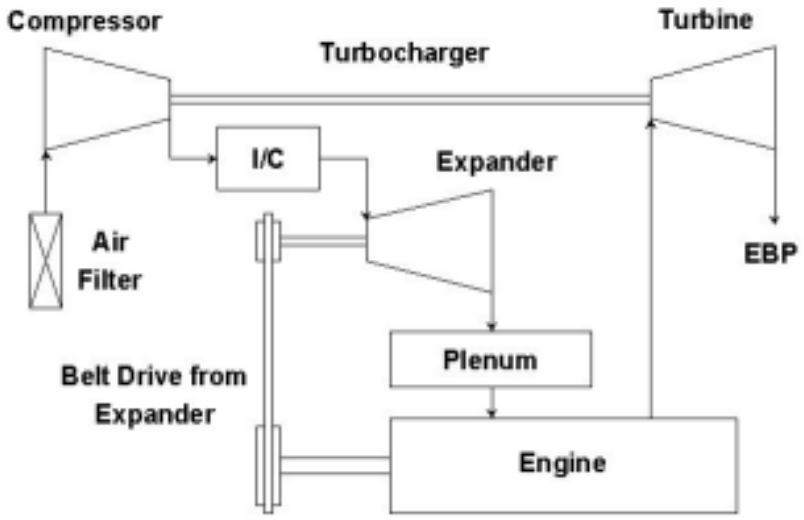

Figure 7.5. Proposed Turbo-Super system using Eaton supercharger

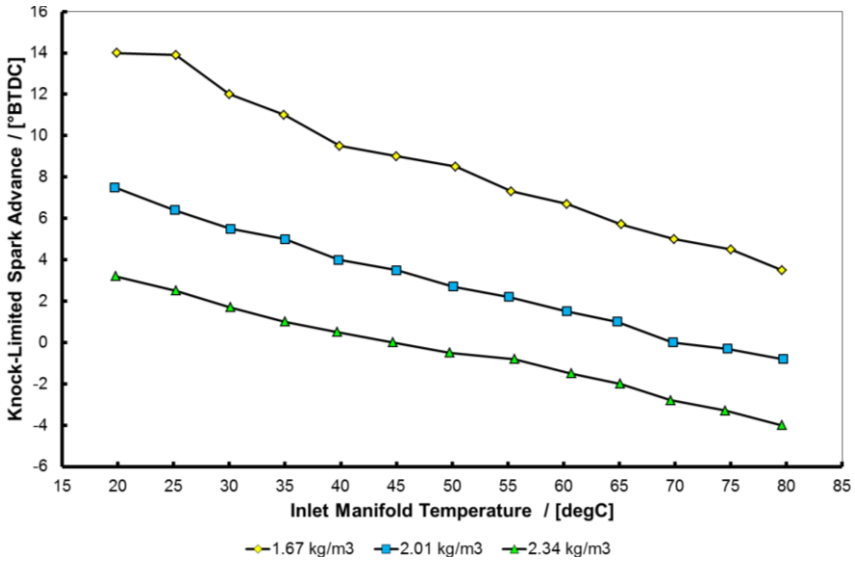

Figure 7.6. KLSA versus change air temperature for constant charge air density tests

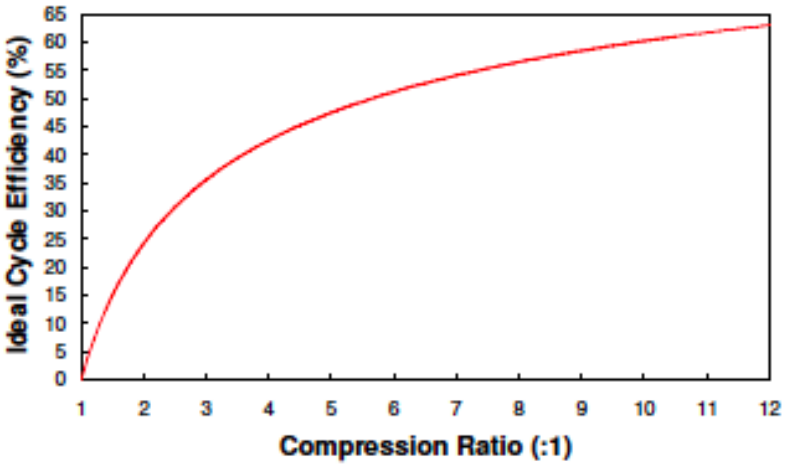

Figure 7.7. Ideal Otto cycle efficiency versus compression ratio

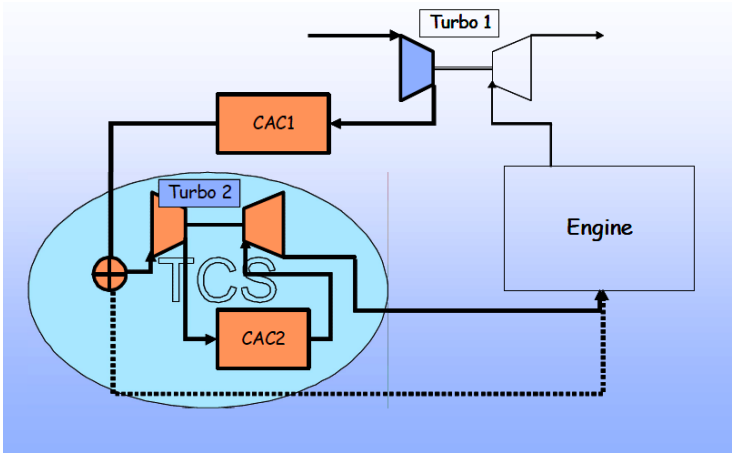

Figure 7.8. Schematic of turbo-cooling concept. [56]

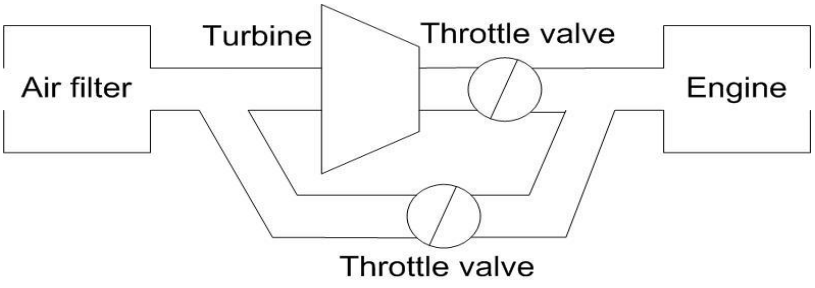

Figure 7.9. Air flow paths in the WEDACS system [6] *

* The turbine here refers to the supercharger which behaves like a turbine rather than a compressor

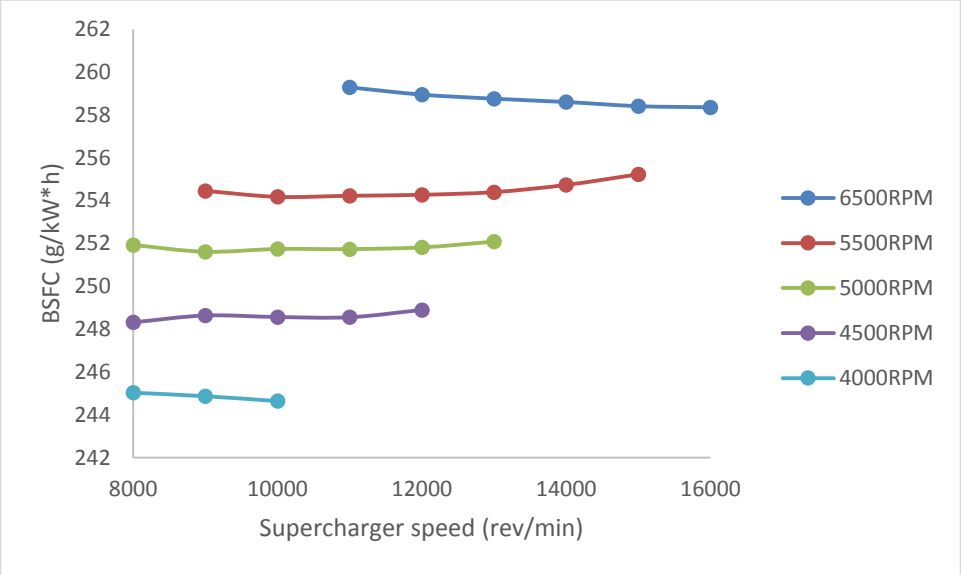

Figure 7.10. Impact of supercharger speed on engine BSFC performance

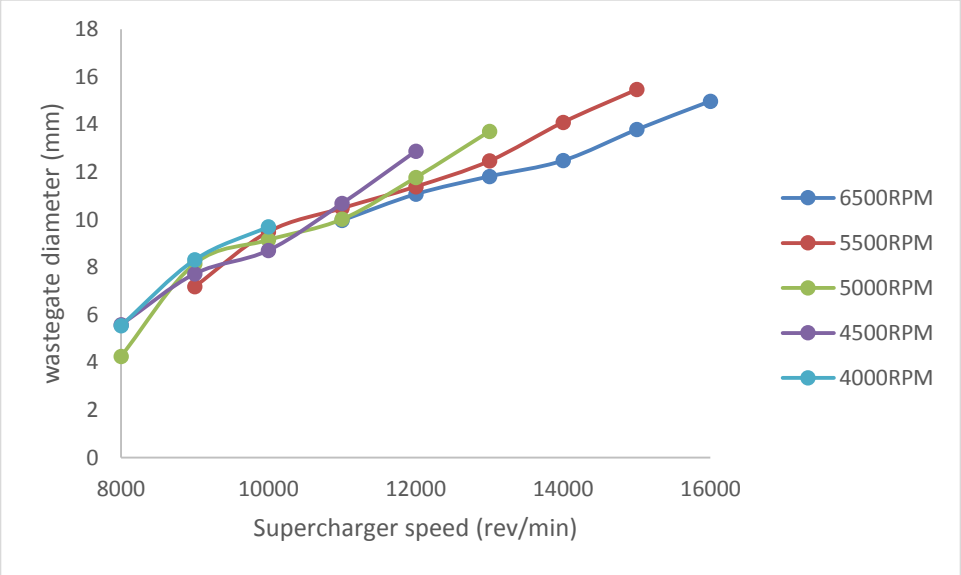

Figure 7.11. Impact of the supercharger speed on the turbine wastegate

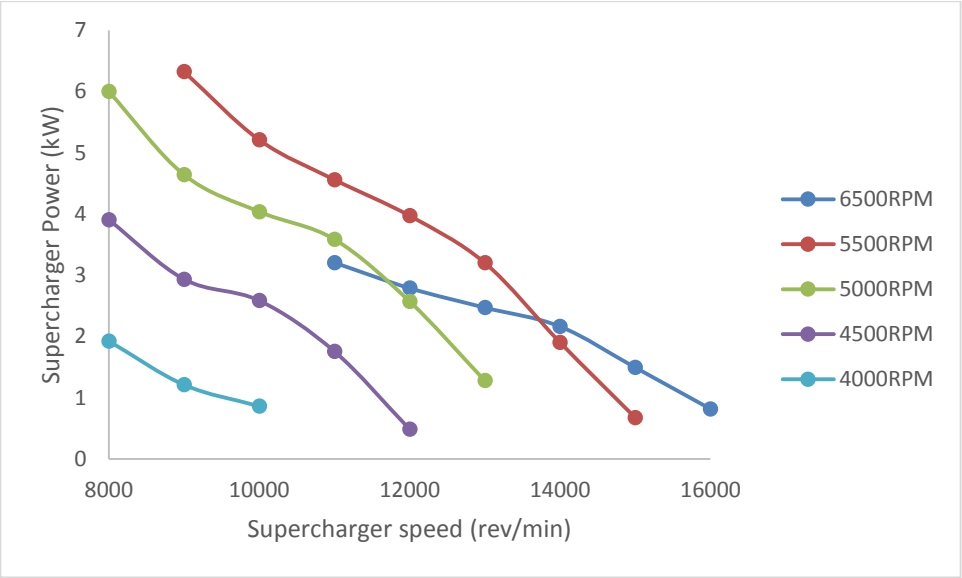

Figure 7.12. Impact of supercharger speed on the supercharger power

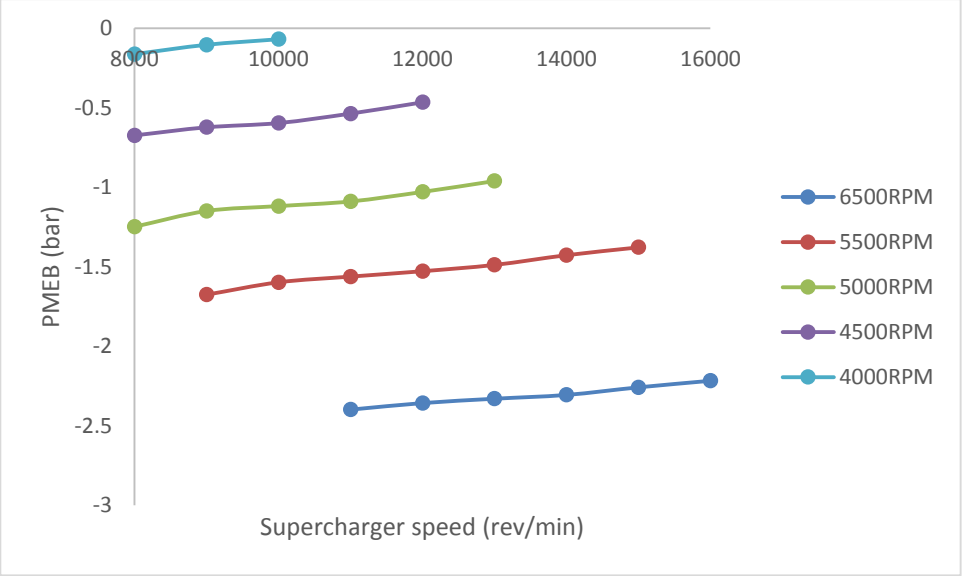

Figure 7.13. Impact of supercharger speed on PMEP

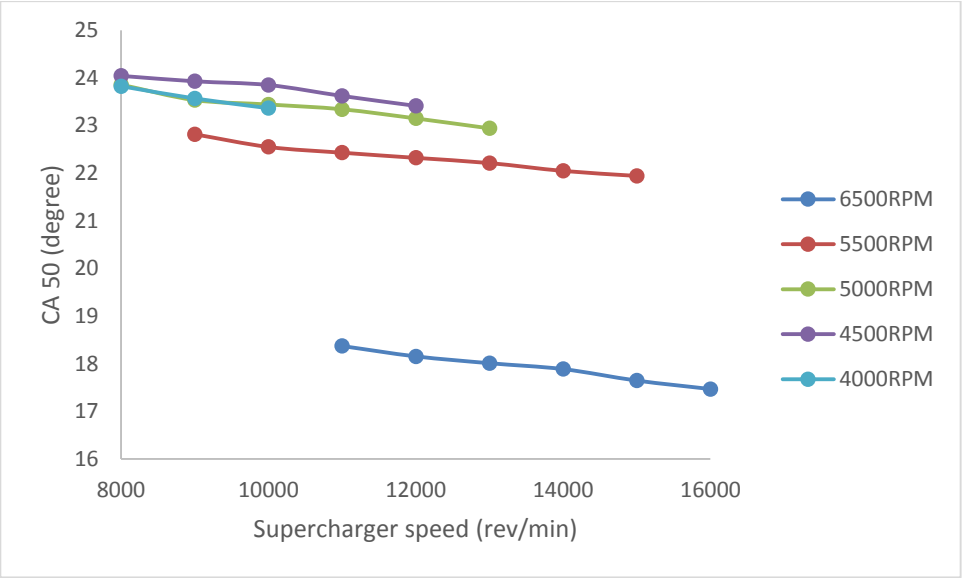

Figure 7.14. Impact of supercharger speed on CA50

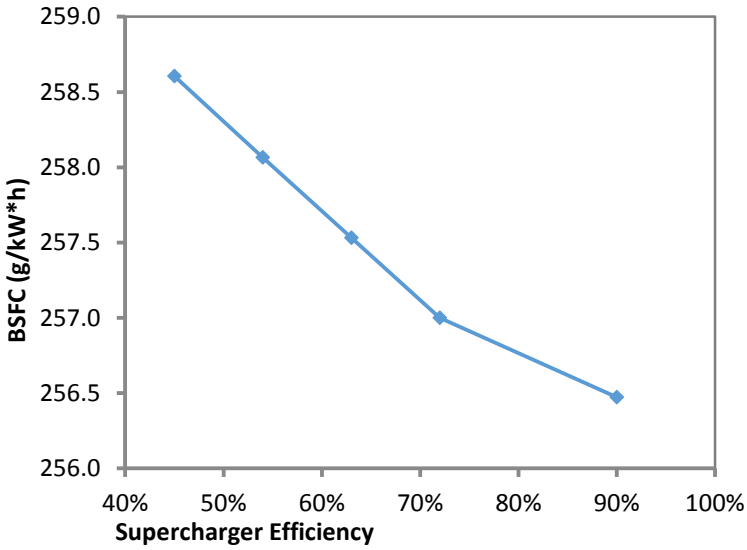

Figure 7.15. BSFC performance at increased efficiency point

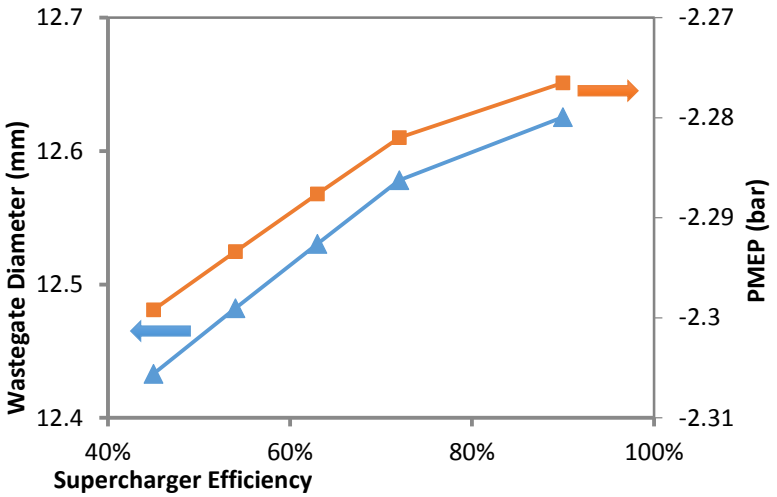

Figure 7.16. PMEP and wastegate diameter at increased efficiency point

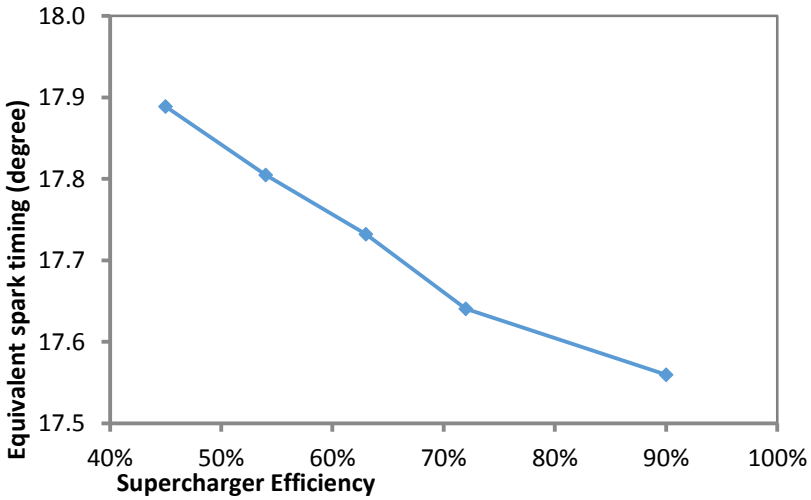

Figure 7.17. Combustion phasing performance at increased efficiency point

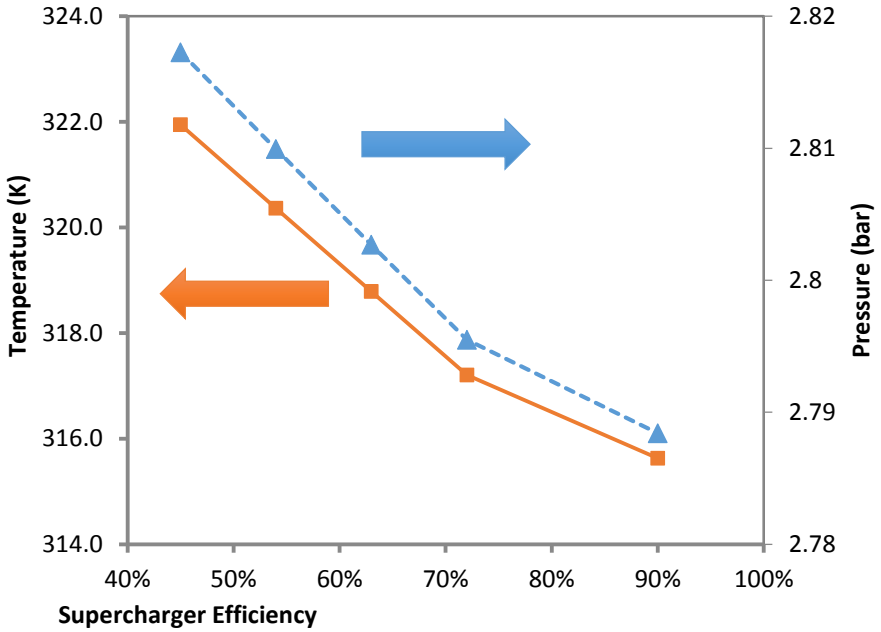

Figure 7.18. Intake temperature and boost pressure at increased efficiency point

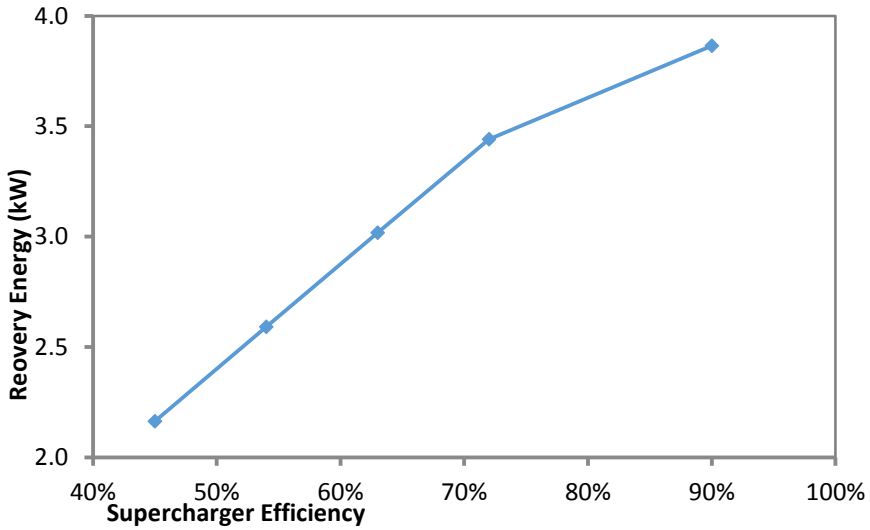

Figure 7.19. Energy recovered performance at increased efficiency

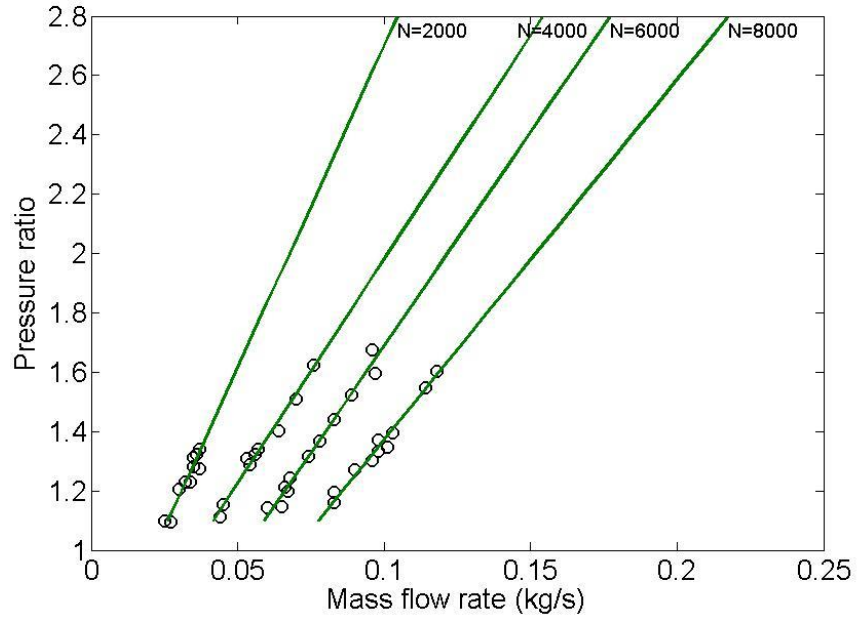

Figure 7.20. Pressure ratio vs. mass flow rate at given supercharger rotational speed

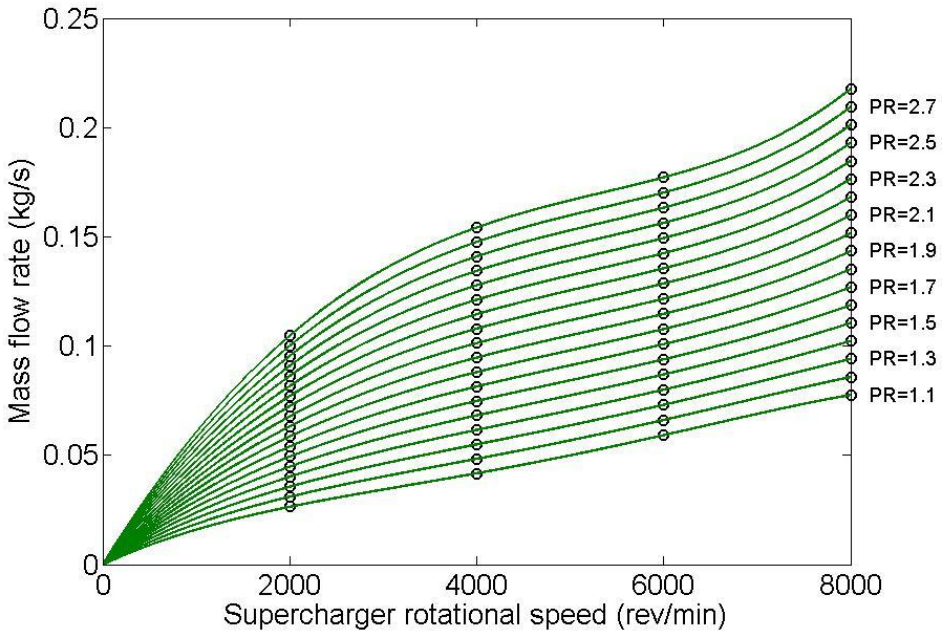

Figure 7.21. Mass flow rate vs. supercharger rotational speed at given pressure ratio

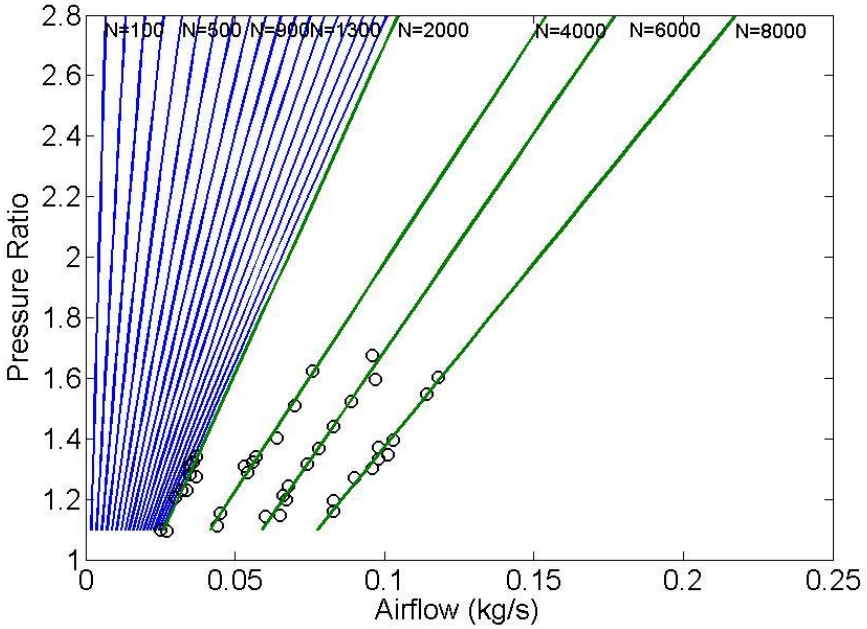

Figure 7.22. Supercharger performance map under expansion mode

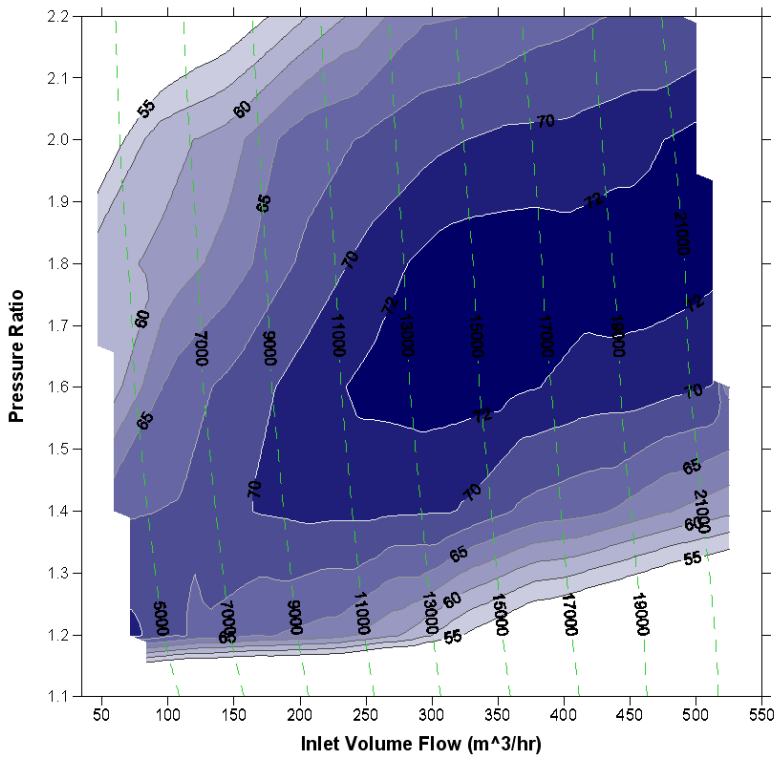

Figure 7.23. R410 TVS supercharger performance map under compression mode. [9]

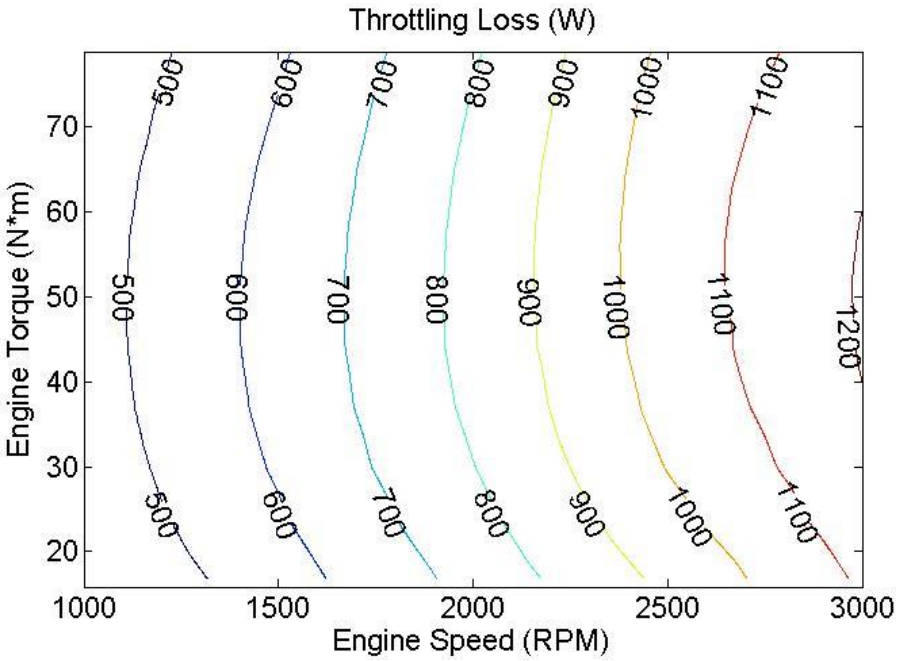

Figure 7.24. Exergy destructed in the throttling process for a twin-charged downsized engine

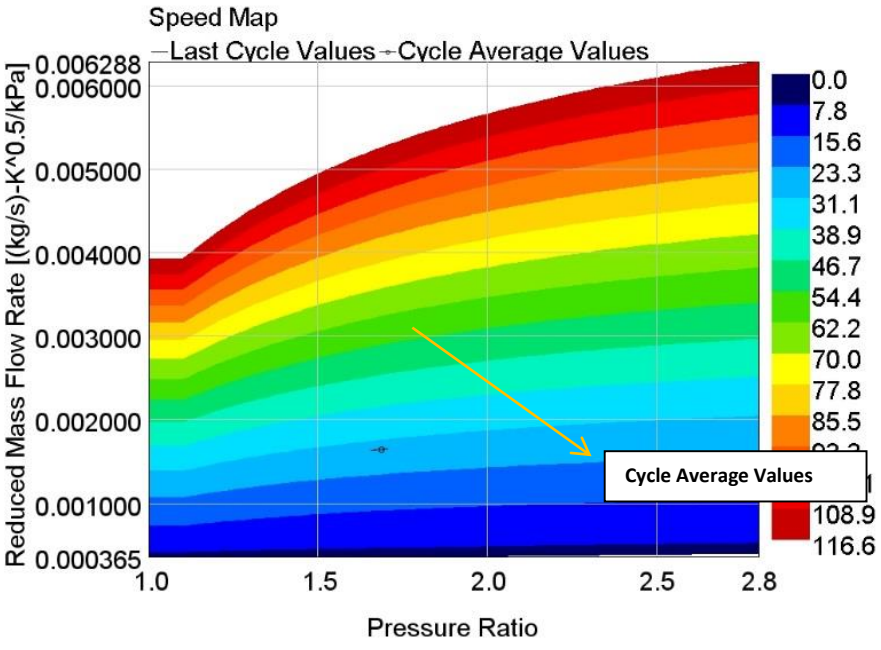

Figure 7.25. Supercharger speed map under expansion mode

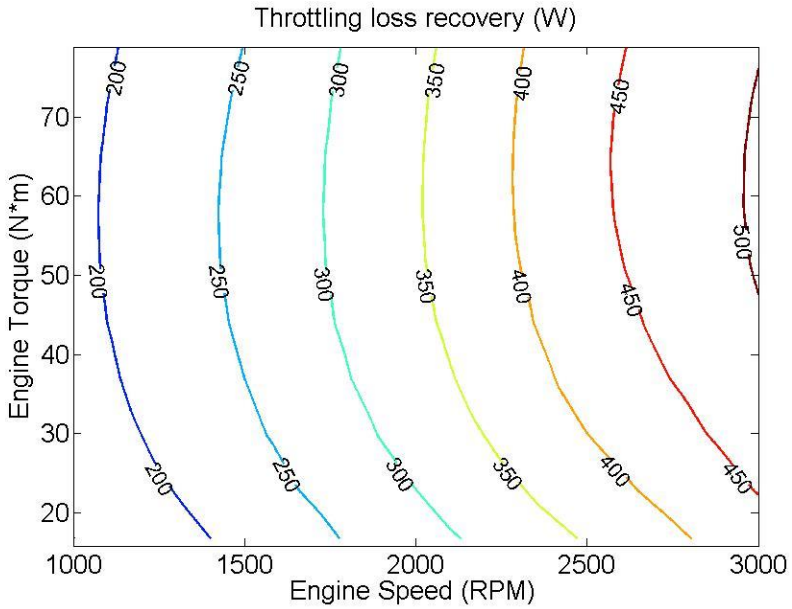

Figure 7.26. Throttling loss recovery across the engine speed under low load

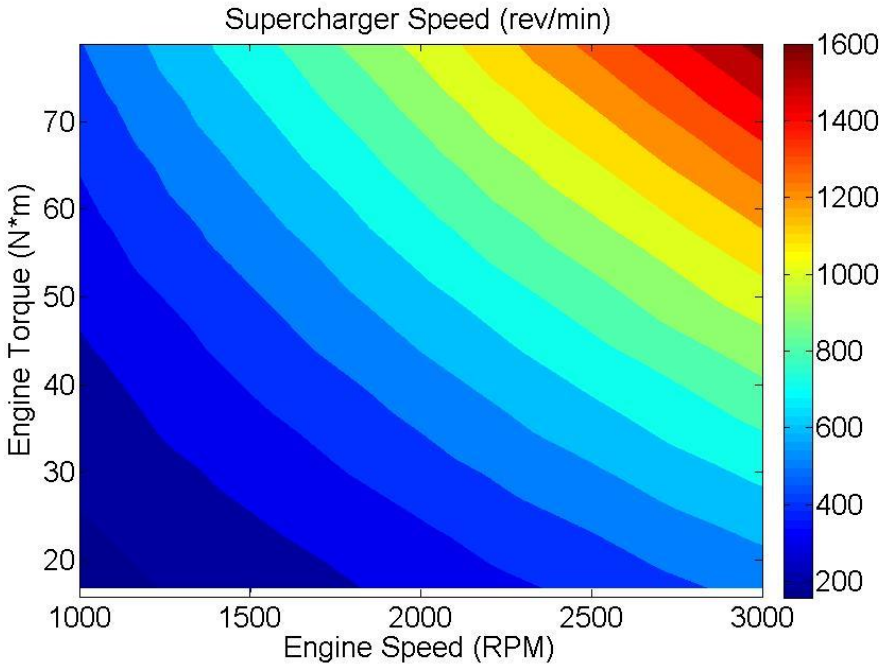

Figure 7.27. Supercharger speed across the engine speed under low load

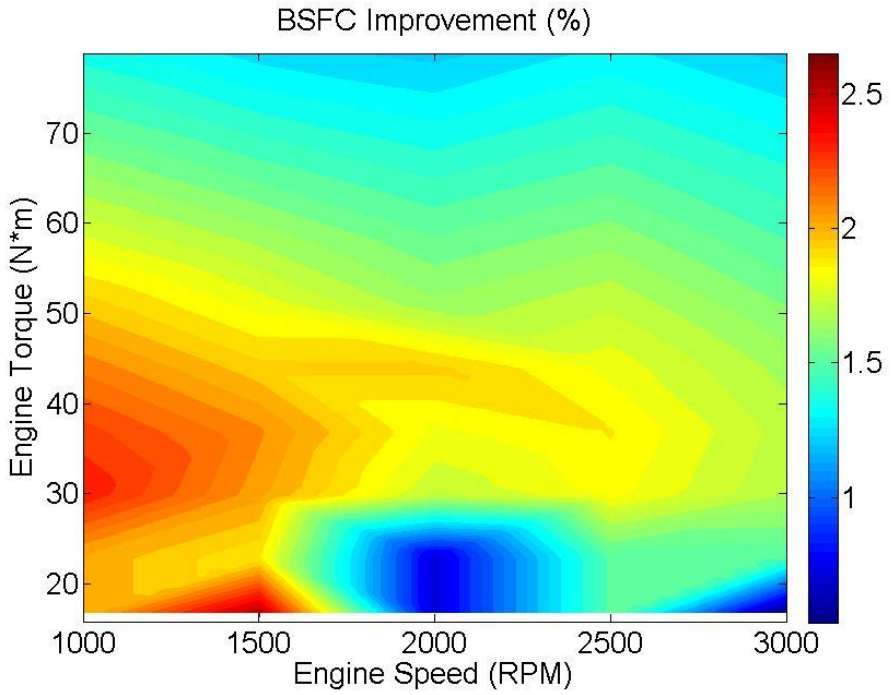

Figure 7.28. BSFC improvement across the engine speed under low load

Figure 7.29. Supercharger outlet temperature (K) across the engine speed under low load

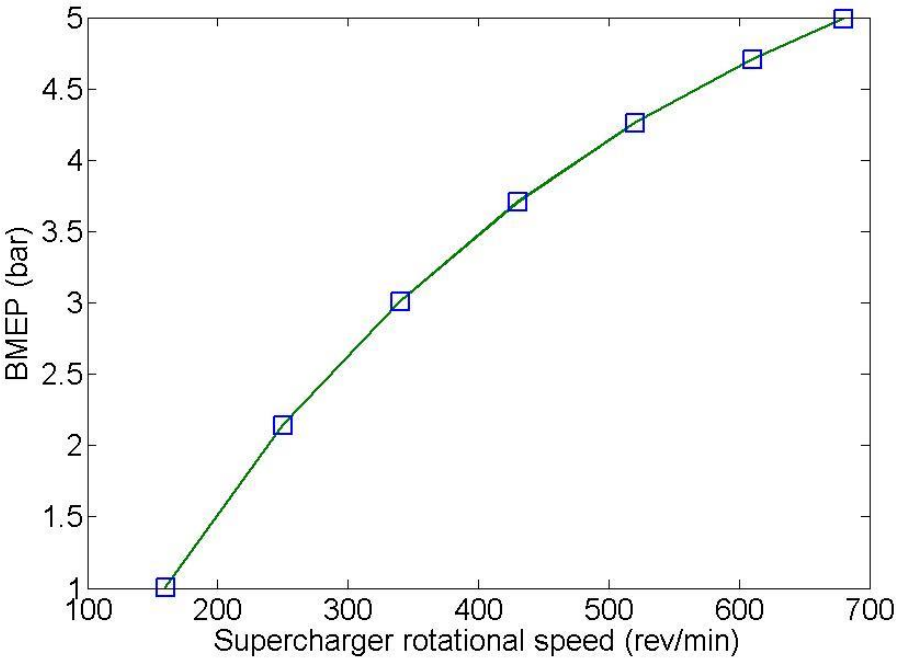

Figure 7.30. BMEP vs Supercharger rotational speed at 1000RPM

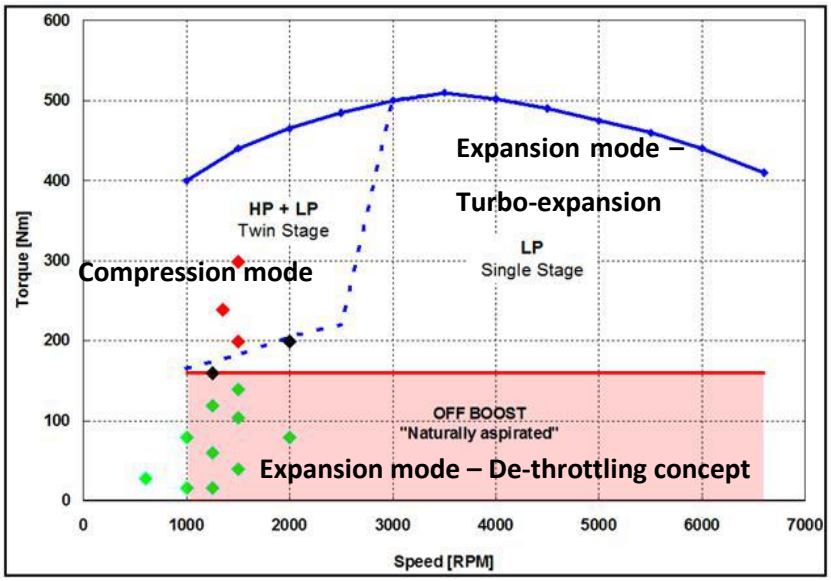

Figure 7.31. Supercharger operating range of a twin-charged gasoline engine

Chapter 8 – *Modelling and testing the variable-drive supercharging concept*

A supercharger system which boosts the engine via a direct drive from the engine crankshaft has been identified as a possible solution to improve low-end torque and transient response for a conventional turbocharged SI engine. However, the engine equipped with a fixed-ratio supercharger is not as fuel-efficient, especially at high load and low speed, due to the fact that a large portion of the intake mass air flow has to recirculate through a bypass valve causing inevitable mechanical and flow losses. In addition, the fixed-drive ratio of the supercharger, which is mainly determined by the full-load requirements might not be able to provide sufficient over-boost during a transient. The fact that a clutch may be necessary for high engine speed operation on the fixed-ratio supercharger system is another issue from the perspective of cost and NVH performance.

This chapter will present a simulation and experimental investigation to look at alternative boosting systems applied to a Ford 1L EcoBoost engine, in order to achieve an enhanced target torque curve The objective was to assess the performance of a centrifugal-type supercharger system driven via a Torotrak CVT against a fixed-ratio positive-displacement supercharger solution. Both concepts feature a fixed-geometry waste-gated turbocharger.

Part of the comparison, discussion and conclusion in this chapter have been presented and published at the 2015 JSAE/SAE Powertrains, Fuels and Lubricants International Meeting held in Kyoto, Japan.

8.1 Introduction

Downsizing and down-speeding are the enablers for passenger car SI engines to reduce fuel consumption and CO_2 emissions. These reductions are mainly achieved by reduced pumping loss, improved gas heat transfer and better friction condition at part-load operation. The rated power and torque are conventionally recovered by means of turbocharging. However, the low-end torque performance and transient response of such engines is affected by the static and dynamic characteristics of the turbo-machinery [194]. A supercharger system which boosts the engine via a direct drive from the engine crankshaft has been identified as a possible solution to address the aforementioned issues for a conventional turbocharged SI engine. The potential of a fixed-ratio positive-displacement supercharger on a passenger car SI engine has been investigated by a number of researchers [7, 149-150]. For production engines, Volkswagen has already successfully implemented such a technology into its twin-charged 1.4 litre gasoline TSI engine. Pairing of a positive-displacement supercharger with a turbocharger is also adopted by Volvo in its new 2.0 litre four-cylinder T6 engine. However, the difficulties in the boost pressure control, the necessity of a clutch, cost, packaging and NVH issues are identified as the major challenges facing fixed-ratio positive-displacement supercharged SI engines.

This chapter will, for the first time, propose a CVT driven centrifugal supercharger for a Ford 1.0 litre EcoBoost engine using the Torotrak V-Charge system. The performance of this system will be compared to an alternative boosting solution, which was equipped with a fixed-ratio positive-displacement supercharger. The results comprise three parts: full-load performance; part load fuel consumption; and transient response. In addition, the benefits of adopting a novel compressor have also been investigated and discussed.

8.2 Simulation Methodology

BASELINE ENGINE:

The type of engine used in this work is a Ford 1.0 litre EcoBoost engine [195] featuring a fixed-geometry turbocharger.

FIXED-RATIO POSITIVE DISPLACEMENT SYSTEM:

An alternative boosting solution was modelled around the baseline engine system by adding a fixed-ratio positive-displacement supercharger (see **Figure 8.1**) at the low-pressure stage. The enhanced torque and power curve can be seen in **Figure 8.2**. In order to provide superior transient response whilst maintaining the same part-load fuel consumption, a combination of a high drive ratio and a clutch was implemented.

TOROTRAK V-CHARGE SYSTEM:

The Torotrak V-Charge system is comprised of a pulley step-up gear, a CVT mechanism and an epicyclic gear as indicated in **Figure 8.3** and **Figure 8.4**. For this simulation work, the step-up ratio and epicyclic ratio were initially selected to be 3 and 12.67, respectively. The Torotrak CVT ratio has the capability to vary from 0.281 to 2.82, with CVT ratio range being 10. The corresponding mechanical losses on the CVT and epicyclic mechanism have been tested and incorporated into the look-up efficiency maps in GT-Power. The corresponding inertia data was also imported in order to simulate the transient performance of the system.

With the consideration of surge elimination at low engine speed and the requirement of sufficient pressure ratio margin for transient performance, a conventional centrifugal compressor has been selected for use in the Torotrak V-Charge system. In addition, a TurboSuper configuration has been initially determined to use in the following simulations considering the fact that the TurboSuper and SuperTurbo configurations have a similar performance output in terms of full load, part load and transient response (the TurboSuper layout is shown in **Figure 8.5**).

CONTROL STRATEGY:

For the fixed-ratio positive-displacement supercharger model, the supercharger is engaged below 2000RPM full load and disengaged by a clutch at higher engine speed, to avoid over-speeding (the engine performance can be seen in **Figure 8.2**). In order to provide sufficient over-boost during the transient, the supercharger is doing significantly less work compared to the turbocharger at steady-state full-load condition by using an active supercharger bypass to control the target torque performance (the wastegate is fully closed). Thus, a large amount of intake mass air flow is recirculated back into the compressor intake, resulting in higher supercharger inlet temperature. At part load, such as 2bar BMEP, the clutch is most likely to

be disengaged or the corresponding BSFC is significantly high. **Figure 8.6** shows the BSFC performance comparison between clutched and declutched model at 2bar BMEP.

For the Torotrak V-Charge model, by adopting the proposed CVT a clutch might not be needed at higher engine speed, due to the capability for the supercharger to down-speed and be passively bypassed. Also, via controlling the CVT ratio, the exact required mass flow rate could be delivered by the supercharger; thus, the associated mechanical and flow losses due to the recirculation of the mass flow will be eliminated. This is also beneficial for reducing the inlet temperature of the supercharger, resulting in higher compressor corrected speed. In addition, as the ratio between the crankshaft and the supercharger is variable, the CVT driven supercharger is able to provide additional over-boost capacity during the transient.

It might be noted that for the Torotrak V-Charge configuration, the active bypass valve, which is a necessity in the fixed-ratio positive-displacement supercharger model, can be replaced by a passive valve, due to the elimination of the recirculated mass flow around the supercharger. This will have some benefits from the perspective of control complexity and cost.

MATCHING, COST AND PACKAGE:

In many respects, a positive displacement supercharger may be a more easily integrated device than a centrifugal counterpart. It is a lower speed machine and can therefore have a belt-drive system to the crankshaft; it also has air consumption characteristics very similar to a typical internal combustion engine. However, positive displacement superchargers are usually more expensive and difficult to package.

Centrifugal superchargers are generally more efficient, smaller and lighter than their positive-displacement counterparts. The drawback is that boost increases with the square of the rotational speed, resulting in a low boost at low engine speeds. However, it has been suggested that a centrifugal supercharger can be driven through a variable transmission to allow the boost to be optimised throughout the entire engine speed range [123, 163]. In order to provide sufficient boost, centrifugal superchargers usually need to be driven by some step-up devices, which will inevitably incur some mechanical loss.

SIMULATION METHODS:

In order to assess the performance of the alternative boosting solutions, a validated full-load GT-Power model was used as a starting point. An SI Wiebe combustion model was used and the corresponding valve timing was calibrated at full-load condition.

A transient model was modified around the full-load model with the combustion model and valve timing kept fixed. Although it was very simplistic, it actually made very little difference on most of the transients where the engine's transient response was dominated by the dynamic behaviour of the turbocharger and supercharger. It might be noted that the combustion model can also have a significant effect on a transient response, but as both configurations were modelled from the full-load model, the combustion effect could be ignored.

In this work, the transient response simulation was carried out with a standard procedure whereby the model was run at each speed for five seconds at a load of 2bar BMEP for stabilisation, prior to a step-load demand input to full load. The full load was then held to the end of the simulation. The time-to-torque in this work was taken for the engine torque to increase to 90% of the target full load (T90).

8.3 Simulation Results

The results are presented in three sections, discussing first the system behaviour of the full-load operation, then that of the part-load region, and finally that of the transient performance. It should be noted that the Torotrak V-charge system discussed below is not equipped with a clutch, unless specifically mentioned.

Full-load Performance:

For the fixed-ratio positive-displacement model, the supercharger bypass was used to control the target torque performance, while for the V-Charge system the bypass control can be eliminated and the exact mass flow rate, which is solely controlled by the optimised CVT ratio, can be supplied by the supercharger, resulting in reduced mechanical and flow losses.

It can be seen from **Figure 8.7** that BSFC of the Torotrak V-Charge system was improved by approximately 1% at full load when compared to the fixed-ratio positive-displacement supercharger. Despite the V-Charge system having higher mechanical losses with its

integrated CVT, it can eliminate the recirculated mass flow around the supercharger, resulting in lower power consumption than the positive-displacement supercharger system.

In addition, only engine speeds from 1100RPM to 1750RPM were simulated, as at 2000RPM or above, the turbocharger alone could supply sufficient boost pressure. At high engine speed, the V-Charge system down-speeding feature only suffers a minor reduction of full-load fuel consumption compared with its de-clutched fixed-ratio positive-displacement counterpart. It was demonstrated in the simulation that only approximately 0.2% of the engine power was used to overcome the transmission losses if a bypass valve was used.

Low-load Performance:

The Torotrak V-Charge system low load performance was compared with the de-clutched and clutched positive displacement systems in this section. Twenty engine operating points across 2 to 8bar BMEP, engine speed from 1100RPM to 2000RPM were simulated. For simplicity, only 2bar BMEP fuel consumptions are shown here.

Figure 8.8 shows the low-load BSFC performance between positive-displacement de-clutched, positive-displacement clutched and Torotrak V-Charge models. It can be seen that the fuel consumption of the Torotrak system only increased by approximately 2% compared to the fixed-ratio positive-displacement supercharger de-clutched configuration. The V-Charge system can achieve this due to its capability to down-speed, resulting in reduced mechanical and flow losses. This indicates that a clutch might not be necessary in the Torotrak system, which will bring some benefit in transient and NVH performance. It should be noted that if a clutch was used in the Torotrak system, the low-load BSFC performance would be the same as in the positive displacement supercharger de-clutched configuration.

Transient Performance:

In order to investigate the theoretically best time-to-torque performance and the maximum capacity of the boosting systems, the wastegate control was removed from both the fixed-ratio positive-displacement configuration and the Torotrak engine model. For the engine equipped with a positive-displacement supercharger, the clutch engagement time for the supercharger was 500ms, to prevent excessive inertial loading. For the Torotrak V-charge system, the CVT ratio was linearly varied from 0.281 to 2.82 within 360ms.

A limit variator reaction torque (sum of input and output CVT torques) arises as a result of minimising the size of the V-Charge system. Hence the transient control strategy is optimised to avoid violating this limit.

In the simulation, it is seen that the variator reaction torque was exceeded at 1500RPM and 2000RPM (see **Figure 8.10** for example) for the given CVT change ratio. Thus, some strategies should be adopted to reduce the maximum reaction torque while maintaining a similar time-to-torque performance. In the following, the control strategy to keep the reaction torque within the prescribed limit is presented first. After that, the transient response comparison is conducted between the fixed-ratio positive-displacement and the optimised Torotrak system.

It is considered that if the variator reaction torque is only exceeded during the time when the CVT is accelerating, the CVT change rate should be reduced at the point when the reaction torque is reaching the limit. However, if the reaction torque is exceeded after the CVT acceleration time and before T90, then the CVT largest ratio needs to be reduced. This strategy will affect the transient response, but if the change is minor the final engine behavior is almost imperceptible, which is beneficial to facilitate a smaller CVT package. For simplicity, only the control strategy at 1500RPM is shown in **Figure 8.9**. Compared with the non-optimised condition in which the variator reaction torque was exceeded, the optimised strategy reduced the CVT change rate at the point when the reaction torque was reaching the limit. By doing that, the variator reaction torque was limited, and there will be two torque extremes during the CVT acceleration (see **Figure 8.10**). It should be noted here that the CVT ratio was only varied linearly for both the first part of the CVT acceleration and the second part of the CVT acceleration, where the CVT change rate was reduced. By further optimising the CVT change rate and allowing non-linear change curve, the line between the two torque extremes could be flat.

Figure 8.11 shows the transient engine torque response at 1500RPM for both the non-optimised and optimised strategies. It can be seen that there is only a very limited decline in terms of T90 for the optimised strategy. The optimised strategy, however, is beneficial for the smoothness of the transient response during the second part of the transient.

In the following, the transient response comparison is conducted between the fixed-ratio positive-displacement configuration and the optimised Torotrak system. **Figure 8.12-8.14** shows the transient response under the engine speed from 1100RPM to 2000RPM. The dashed line represents the T90 (time-to-torque) target and the solid line represents the full-load torque target. It can be seen that the Torotrak V-Charge system has a better transient response at 1500 and 2000RPM, while maintaining a similar transient performance at 1100RPM. This is mainly due to the characteristics of the centrifugal compressor, the boost of which increases with the square of the rotational speed, resulting in a lower boost at low engine speeds.

In addition, it can be seen that the Torotrak V-Charge system is able to produce larger brake torque than the fixed-ratio positive-displacement system. This is potentially beneficial to improve the low-end torque if the supply of the sufficient air mass flow is the main issue rather than the restriction of engine knock and Pmax. This will be verified in the later experimental test.

8.4 Simulation Discussions

<u>The trade-off between the part load BSFC and transient performance:</u>

There are three trade-offs: clutched and de-clutched; high and low drive ratio; and sporty and economic mode. The latter two trade-offs only occur when the clutch is not used. In the following section, first the clutched and de-clutched trade-off will be discussed, followed by the optimisation of the drive ratio and the trade-off between the sporty and economic mode.

It was demonstrated that the Torotrak V-Charge system suffers a minor decline of part-load BSFC if a clutch is not utilised. However, such a configuration is beneficial for the transient performance in terms of the time-to-torque response and NVH issues. Thus, the adoption of a clutch will determine the trade-off between the part-load BSFC and transient performance. A Torotrak configuration with a clutch will have better part-load and full-load (>=2000RPM) BSFC, and a Torotrak configuration without a clutch benefits from quicker and smoother transient response.

The second trade-off occurs around the optimisation of the drive ratio, which includes step-up ratio and epicyclic ratio when a clutch is not used. The larger the multiple value of the step-up ratio and epicyclic ratio, the higher the parasitic losses that will incur at part load.

However, a larger drive ratio will have higher supercharger pressure ratio during the transient, which will also be beneficial to accelerate the turbocharger, resulting in improved transient performance.

As the boost supplied by the centrifugal supercharger is controllable, different strategies could be used to satisfy the needs of sport and economy. For the sporty mode, in which the transient performance is of higher priority, the CVT mechanism could be engaged at higher ratio at part load. This will reduce the time for the CVT mechanism to sweep from the lowest ratio to the highest ratio during the transient. For the economic mode, in which fuel efficiency is of higher priority, CVT is always engaged at its lowest ratio at part load, in order to reduce the corresponding mechanical and flow losses. In this chapter, all the simulation results were based on economy mode.

Novel compressor simulation:

It is known that CVT and epicyclic efficiency are strongly related to the associated input speed. Any methods which could reduce the input speed while maintaining or exceeding the demonstrated full-load and transient response performance are beneficial for the reduction of associated parasitic losses at part load. In the following, a novel compressor supplied by Honeywell is simulated using the same assumptions and settings as in the conventional centrifugal compressor shown above. The proposed novel compressor is a compressor which can provide the same pressure ratio at lower rotational speed. The drawback of such a compressor is its lower maximum PR.

Figure 8.15 shows that the engine model equipped with the novel compressor has the lowest BSFC at full load. This is partly due to the higher isentropic efficiency of the compressor and is partly attributable to the reduced mechanical losses resulting from the reduced transmission speed.

For low-load operation, theoretically, the proposed novel compressor engine model will have a poorer BSFC performance than the conventional compressor system. This is due to the fact that for both configurations the transmission speed is the same (engaged at the lowest CVT ratio), thus the transmission losses are very similar. The supercharger power is increased for the novel compressor configuration when the corresponding PR is larger at the fixed rotational speed. **Figure 8.16** shows the part-load BSFC comparison between fixed-ratio

positive-displacement compressor, conventional compressor and the novel compressor at part load.

However, it is considered that the transient response time of the novel compressor configuration is not as sensitive as that of the conventional compressor if the drive ratio is reduced. This is mainly due to the fact that only a smaller portion of the CVT range is utilised for the novel compressor configuration, considering its maximum speed limit. Thus, the step-up or the epicyclic ratio could be optimised for the novel compressor configuration in order to reduce the corresponding parasitic losses at part load, while still maintaining a similar transient performance.

In the transient simulation, for the novel compressor, the largest CVT ratio was controlled to maintain the maximum compressor speed around its physical limit. For this specific simulation, the CVT mechanism cannot attain its physically largest ratio, thus some of the transient potential cannot be achieved. To be more specific, at 2000RPM and 1500RPM, the largest CVT ratio can only be 1.5 and 2.0, respectively.

Figure 8.17 - 8.19 show the transient response comparisons between the fixed-ratio positive-displacement configuration, the Torotrak V-charge system with a conventional compressor and the Torotrak V-charge system with a novel compressor (also see **Table 8.1** for the time-to-torque response). It can be seen that the novel compressor configuration has a similar transient response compared with the conventional compressor configuration at 1500RPM and 2000RPM, and exceeds the transient performance at 1100RPM when compared to the conventional compressor configuration.

Table 8.1. Transient time-to-torque (T90) performance for three different configurations

Engine Speed / Configuration	1100RPM	1500RPM	2000RPM
Fixed-Ratio Positive-Displacement System	1.24s	1.39s	0.93s
Torotrak V-Charge – Conventional Compressor	1.05s	0.77s	0.69s
Torotrak V-Charge – Novel Compressor	0.73s	0.80s	0.59s

8.5 Experimental set-up

It is usually the case that the computational simulation results may not accurately reflect the real test performance. In order to investigate the benefits that the V-Charge system could actually obtain, a test rig has been built. In addition, the simulation tool will also be utilised to predict or analyse the results that would be impossible or difficult to test in a rig.

The test was carried out in an engine test cell at the University of Bath (see **Figure 8.20**). The schematic of the engine system and the measure locations can be seen in **Figure 8.21**. In the facility, the ECU calibration software ATI Vision communicated with the host system CP Cadet via an ASAP3 link. ATI Vision also communicated with the ECU via a CAD Calibration Protocol (CCP), and selected channels could be transferred to CP Cadet for ease of recording and monitoring.

The experiments were conducted on a Ford 1.0 L, three-cylinder, gasoline turbocharged direct injection (GTDI) engine with variable intake and exhaust-valve timing system [195]. The Torotrak V-Charge system, which comprises a pulley step-up gear, a CVT mechanism and an epicyclic gear as shown in **Figure 8.4**, was directly connected to the engine crankshaft with a sprag clutch. A check valve (seen in **Figure 8.22)** was mounted around the V-Charge compressor to act as a passive bypass valve, in order to bypass the compressor when the V-Charge compressor is not able to provide the required mass flow rate.

In order to have a wide operating range and precise control of the engine boundary conditions, the cooling circuit for the engine coolant and oil were replaced with an external water-to-coolant heat exchanger. In addition, an aftercooler was replaced by a water-to-air heat exchanger. Therefore, the temperatures of the engine coolant, oil and engine intake air could be controlled by varying the water flow rate in each heat exchanger. In this test, before logging the test data, the engine coolant, oil and aftercooler temperatures were kept around 90 degC, 100 degC and 45 degC, respectively.

8.6 Experimental Procedure

The engine testing was split into two main sections, with the aim to understanding how the V-Charge may best influence the engine performance and fuel economy, and to build a

robust control strategy using the steady-state testing data. The first section is to study the conventional two-stage compound charging configuration with a passive bypass valve across the supercharger compressor. The second section is to investigate the 'wind-milling' effect of the V-Charge compressor. This is when the inlet pressure of the V-Charge compressor is above the outlet and the energy reclaimed across the compressor offsets some of the parasitic transmission losses [196]. It might be worth noting that although the 'wind-milling' effect has the potential to mitigate the parasitic losses it is, at the moment, difficult to quantify its role on fuel economy in experiments. This is because the resolution of the fuel sensor in the test cell might not capture the difference.

8.7 Experimental Methodology

This research will focus on the steady-state performance both in experiment and in simulation. The transient performance will only be briefly introduced in simulation, with further observations and optimisation presented in due course. The aim of this project is to understand when the V-Charge technology will provide better performance than its fixed-ratio positive displacement counterparts. The work will focus on the low-speed region, which is considered the most important a limiting in terms of maximum steady-state BMEP and transient response.

Firstly, a full-load V-Charge model was validated using the measured data. The work will then investigate the full-load performance of a fixed-ratio positive-displacement counterpart that is also tandem with the fixed-geometry turbocharger. A trade-off between part-load fuel efficiency and transient response was then studied, with the aim of identifying optimisation development in the future. Finally, the partial- and low-load performance were compared.

Steady-state engine model calibration:

The combustion behaviour of the engine model was firstly calibrated using the fast response pressure data from the test. After that, the valve timing, valve lash, valve discharge coefficients and pressure drop in the intake and exhaust manifold were modified to match the mass air flow. The turbocharger performance was then calibrated using the measured turbocharger speed by modifying the mass and efficiency multiplier. Finally, the supercharger with its tested transmission efficiency was added and the brake torque was compared and calibrated.

Note that the transmission efficiency for the V-Charge system comprises three parts: pulley efficiency; CVT efficiency; and epicyclic efficiency. Also, the power ratio, as defined in the literature [59], was used to estimate the transmission losses occurring between the crankshaft and the fixed-ratio positive-displacement supercharger (see **Figure 8.23**). The transmission efficiency of the V-Charge system was tested and imported in the simulation model. The power ratio (combining the pulley efficiency and the supercharger mechanical efficiency) of the positive-displacement device was assumed to be 70% considering the average operating points of the supercharger within its map at full load, and 50% if the PR of the compressor is near 1.

For both boosting systems, the wastegate was fully closed and the torque target was only controlled by altering the boost pressure of the supercharger system, unless a turbocharger surge was detected. The V-Charge device modulates the boost pressure via controlling the CVT ratio; thus, the exact boost can be provided by the V-Charge system. The control parameter for the fixed-ratio positive-displacement is the active bypass across the supercharger, which recirculates some of the intake mass flow back to the supercharger inlet, as can be seen in **Figure 8.24**.

Two drive ratios for both configurations were used to study the trade-off between the steady-state fuel efficiency and transient response. The drive ratio for both the V-Charge and the positive-displacement counterpart refer to the pulley ratio, as it is the most easily manufactured component.

Transient Response Simulation:

A transient model was modified around the full-load model with the valve timing kept fixed. Although it was very simplistic, it actually made very little difference on most of the transients, where the engine's transient response was dominated by the dynamic behaviour of the turbocharger and supercharger. To prove it, an engine measured transient performance was compared with an engine simulation transient result (see **Figure 8.25** and **Figure 8.26).** It can be seen that both the engine torque and turbocharger speed are predicting well, considering the combustion phasing, valve timing are kept fixed.

In this work, the transient response simulation was carried out with a standard procedure whereby the model was run at each speed for five seconds at a load of 2bar BMEP for

stabilisation, prior to a step-load demand input to full load. The full load was then held to the end of the simulation. The time-to-torque in this work was taken for the engine torque to increase to 90% of the target full load (T90). In order to investigate the theoretically best time-to-torque performance and the maximum capacity of the boosting systems, the wastegate control was removed from both the fixed-ratio positive displacement and the Torotrak engine model.

8.8 Experimental Results

According to the target torque, engine speeds from 1000RPM to 2000RPM were tested and simulated. Note that most of the V-Charge configurations were tested and validated in the simulation, while all of the fixed-ratio positive-displacement solutions were only simulated. However, as the baseline engine was working at a similar boundary condition, the simulation results of the positive-displacement configuration should still be valid.

In this work, both supercharger systems assessed are mainly utilised to improve the transient performance rather than largely enhancing the low-end torque, so, even at full load, the power consumed for driving the supercharger compressor is relatively low. The turbocharger can provide the full load target from 1400RPM; thus, the main function of the supercharger is to augment the torque from 1000RPM to 1400RPM and improve the transient response.

Small pulley ratio:
At 1000RPM, the highest torque achieved in the test was approximately 130Nm, due to the turbocharger compressor surge, although there was still some potential for the supercharger to boost more. A detailed engine model validation was performed then in order to predict the engine performance if a fixed-ratio positive-displacement counterpart was installed.

Because there was some intake mass flow recirculating through the bypass valve, causing some mechanical and flow losses for the positive-displacement system, it had approximately 0.3% worse fuel consumption. At the engine operating point of 1250RPM and 167Nm, a different situation was observed with approximately 1% fuel consumption benefit for the positive-displacement configuration. This is mainly because the transmission losses of the V-Charge system were larger.

However, it should be noted that the recirculation of the intake mass air flow might cause the turbocharger compressor to surge, which means that the engine could not achieve the torque that would be reached by the V-Charge system.

Large pulley ratio:

For the V-Charge system, a large pulley ratio, which is 3.3, is available considering the geometry of system configuration. Similarly, the Eaton rival could also be installed with a large pulley ratio, which is 7.3. Due to the CVT capability to alter the total drive ratio, the full-load BSFC performance should be very similar to that achieved with the small pulley ratio. However, for the fixed-ratio positive-displacement counterpart, a larger flow and mechanical losses will occur, which will degrade the fuel efficiency.

The simulation results suggested that at 1000RPM the V-Charge system will gain advantage by 3% fuel consumption benefit, and at 1250RPM it will have a 0.5% fuel consumption benefit over the fixed-ratio positive-displacement counterpart.

Partial load simulation (just boosted condition):

Small pulley ratio:

At just-boosted engine operating points, the positive-displacement configuration still needs to be engaged at a fixed-drive ratio and regulated by the active bypass valve, while the V-Charge system could provide the right amount of boost capable of eliminating the transmission and flow losses that occurred for the fixed-ratio positive-displacement configuration. Thus, the V-Charge should have some fuel efficiency benefit. In addition, as the compressor of the positive-displacement configuration has to be transiently engaged during the period when the boost request is from no boost to just-boosted condition, some NVH issues will occur. However, the compressor of the V-Charge system, due to its capability to be constantly engaged even at the low load, will have much mitigated NVH issues.

The results show that there was approximately 8.6% fuel consumption benefit for the V-Charge system at 1000RPM, whilst at 1250RPM the fixed-ratio positive-displacement has a similar fuel consumption with the V-Charge system. This is mainly due to the fact that at 1250RPM the flow losses for the positive-displacement configuration were similar to the transmission loss for the V-Charge system.

Large pulley ratio:

As discussed above, only the BSFC performance of the positive-displacement configuration will be different if a large pulley ratio was mounted. The simulation results suggested that at 1000RPM as much as approximately 17.5% fuel consumption benefit could be achieved by the V-Charge system. In addition, at 1250RPM the V-Charge system will have a 2.9% fuel consumption benefit.

Low load performance (within the NA):

Small pulley ratio:

As mentioned in the work [132], the compressor of a fixed-ratio positive-displacement configuration usually needs to be disengaged at low load, especially if a large drive ratio is installed. However, the V-Charge system could trade some fuel efficiency at low load for better transient behaviour by constantly connecting the compressor to the engine crankshaft with its minimum ratio.

It is known that when the engine mass air flow is lower than that being supplied by the V-Charge compressor for the same inlet condition, then the V-Charge compressor will be above 1 and the passive bypass valve closed. However, when the engine mass air flow is larger than that being supplied by the V-Charge for the same inlet condition, then the PR of the compressor will be around 1 and the bypass path will share some of the mass air flow.

According to the test data, even at a low engine load (thus, low engine mass air flow) with the minimum CVT ratio, the V-Charge compressor PR were all around 1, indicating that there was a bypass flow. For changing engine load (in the throttled region) at the same engine speed, given that the PR and the speed of the V-Charge compressor are normally the same, the parasitic losses of the V-Charge should be around the same.

As there was no mass air flow sensor mounted in the supercharger path, the power consumed will be calculated in the validated simulation in this work. The simulation showed that at 1000RPM only approximately 60W was wasted to constantly connect the supercharger compressor to the crankshaft, the ratio of the consumed power to the engine power being around 1-2% at the frequently-used low-load area. At higher engine speed, a similar situation was observed.

In order to reduce these parasitic losses, a novel approach was proposed that just takes the bypass valve out of the system. This so called 'wind milling' effect will force the PR of the supercharger to be below 1 at low loads, resulting in the energy flow to be reversed, in order to offset some of the parasitic transmission losses. Due to the low resolution of the fuel sensor in the test and the lack of compressor model theory when the PR is below 1, the parasitic losses in this work were only estimated. It is considered that the smallest parasitic losses (only pulley friction loss) will occur when the reclaimed energy is reversed from the supercharger to the sprag clutch and lets the measured CVT input speed above be calculated.

However, if the V-Charge control calibration is considered, the use of a passive bypass valve will be beneficial. This is mainly due to the fact that, at low load within the throttled region, the configuration with a bypass can constantly keep the CVT ratio at its minimum, while for the system without a bypass valve, the CVT ratio might need to be tuned to supply the required mass air flow (the parasitic losses will also be increased along with the durability of the CVT).

Large pulley ratio:

A large pulley will increase the compressor speed, but according to the test results, the PRs of the supercharger compressor were still around 1. This indicates that the parasitic losses will still be low, and the simulation results suggested that the ratio of the consumed power to drive the supercharger to the engine power were still within 2% in the frequently-used low-load area.

Transient Performance at 1000RPM:

From **Figure 8.27**, it can be seen that at 1000RPM the V-Charge system has a transient performance similar to the positive-displacement counterpart if the pulley ratios were to be 2.4 and 5.8, respectively. If a large pulley ratio is adopted, the V-Charge system will have better time-to-torque performance, while the positive displacement counterpart has a larger boost capacity.

The drawback of centrifugal compressors lies in the fact that the supplied boost increases with the square of the rotational speed, resulting in a low boost at low engine speeds. However, by using the variable drive system (as in this work) the challenges could be addressed.

8.9 Experimental Discussion

Engine torque enhancement at low engine speed

As aforementioned, the V-Charge engine still has some capacity to enhance the engine torque if the turbocharger compressor surge issue is mitigated. In the following simulation, the CVT of the V-Charge system was set to maximum, while the turbine wastegate was utilised to maintain the torque requirement. It should be noted that the engine torque target was not increased here, because at higher engine torque the combustion situation might differ.

Comparing **Figure 8.28** and **Figure 8.29** with **Figure 4.8** and **Figure 4.9,** it can be seen that by boosting the supercharger harder, the turbocharger surge margin increases, indicating the potential to enhance the engine's specific power.

The trade-off between part-load BSFC performance and transient response

From the discussion above, it is clear to see that there is a trade-off between the part-load BSFC performance and the transient response.

For a positive-displacement device, a larger pulley ratio will enhance the engine's transient response while compromising some of the partial-load BSFC, especially at just-boosted condition. In addition, a larger pulley ratio could also make the compressor over-speed at lower engine speeds, thus affecting the driveability consistency at high engine speeds.

For a variable drive centrifugal supercharger system, the choice of the drive ratio is also important. A larger drive ratio will, like the positive-displacement counterpart above, improve the time-to-torque transient response. However, this will also degrade the part-load fuel efficiency. It might also be noted that if the drive ratio was chosen to be too high, the 'wind-milling' might not be working at all.

8.10 Chapter summary and conclusions

This chapter details a simulation and experimental investigation to look at alternative boosting systems applied to a Ford 1L EcoBoost engine, in order to achieve an enhanced target torque curve. The objective was to assess the performance of a centrifugal-type

supercharger system driven via a Torotrak V-Charge system against a fixed-ratio positive-displacement supercharger solution. The following summary and conclusions are drawn from the simulation study in this chapter:

1: The V-Charge system comprises a step-up pulley, a CVT, an epicylic assembly and a compressor (conventional centrifugal or novel compressor). It was initially decided to adopt the TurboSuper configuration in the simulation, considering the similar output results for both TurboSuper and SuperTurbo configurations.

2: The results show that BSFC was improved by approximately 1% at full load, due to its capability to eliminate the use of supercharger bypass, resulting in reduced mechanical and flow losses. The BSFC performance could be improved further by another 1% if a novel compressor was used, which is mainly attributed to the reduced transmission losses and increased compressor isentropic efficiency.

3: Under part load, both clutched and non-clutched configurations were assessed and discussed. It was demonstrated that a clutch might not necessarily be needed for the Torotrak V-Charge system, and only a minor decline of the part-load BSFC performance was observed if a clutch was not used. For the novel compressor configuration, if the drive ratio was retained, part-load BSFC of the novel compressor configuration would have slightly degraded BSFC performance in comparison with the conventional compressor configuration, due to the higher PR at fixed compressor rotational speed. However, it was considered that the drive ratio could be reduced for the novel compressor configuration to improve the part-load BSFC performance while still maintaining a similar transient response.

4: In transient, the simulated results suggest that the Torotrak V-Charge system with a conventional compressor could provide better transient response when compared to the fixed-ratio positive-displacement supercharger drive counterpart. The novel compressor configuration can provide even better transient performance at low engine speed, while maintaining a similar performance response at high engine speed.

The following summary and conclusions are drawn from the experimental study in this chapter:

1: Two alternative supercharger systems - a variable drive centrifugal device and a fixed ratio positive displacement unit - have been applied to a turbocharged GTDI engine, in order to improve the transient response and low-end torque.

2: At steady-state partial-load engine operating points, the fixed-ratio positive-displacement system characterises a larger recirculated flow loss, while the Torotrak V-Charge system features a larger transmission loss. The total parasitic loss for each boosting system depends on the pulley ratio adopted. In addition, for low-load operation, approximately 1-2% fuel consumption will be used to constantly connect the V-Charge system to the crankshaft.

3: For the transient time-to-torque performance, it seems that the Torotrak V-Charge system could match the fixed-ratio positive-displacement counterpart. However, the Torotrak V-Charge system will have much fewer NVH issues than the positive-displacement counterpart as no clutch engagement will be required during a transient event.

Figures in Chapter 8

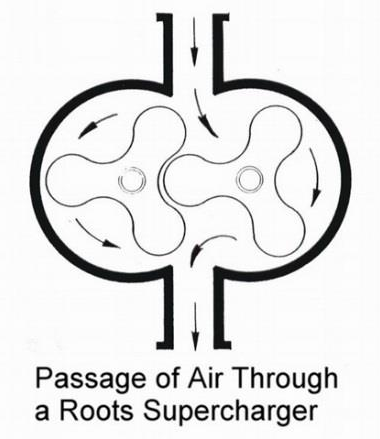

Figure 8.1. Positive-displacement supercharger (roots type for example)

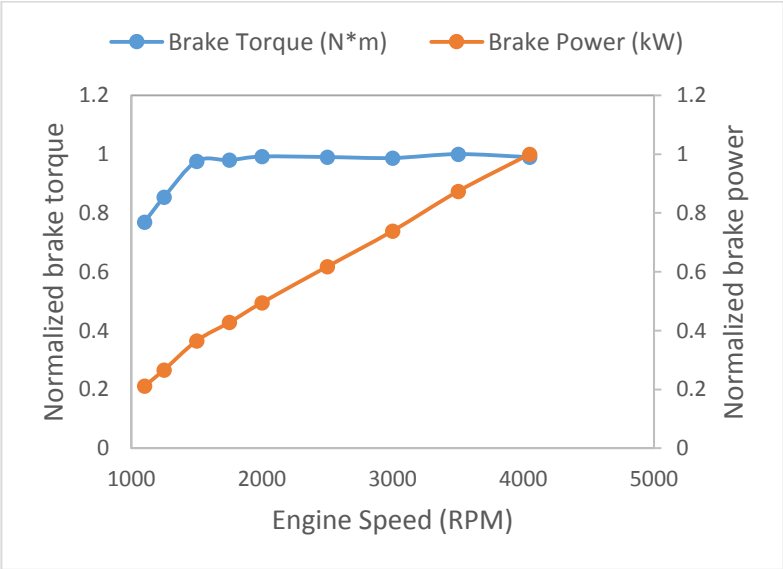

Figure 8.2. Engine performance for the downsized SI engine

Figure 8.3. Torotrak V-Charge system

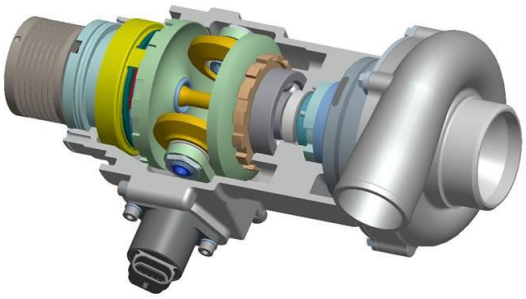

Figure 8.4. Torotrak V-Charge mechanism

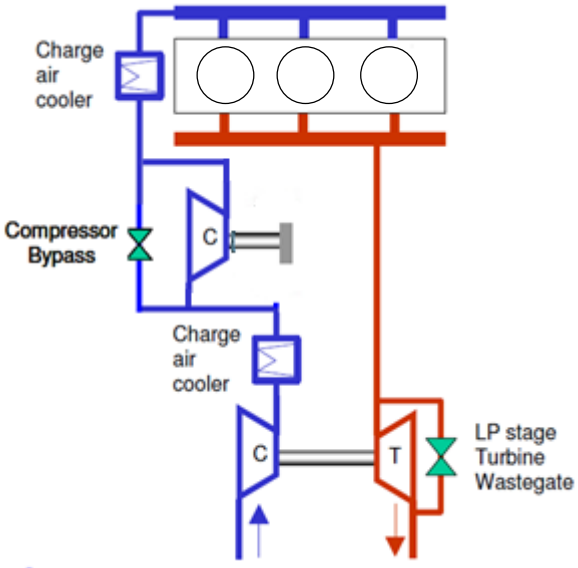

Figure 8.5. Schematic of the proposed engine equipped with V-Charge system

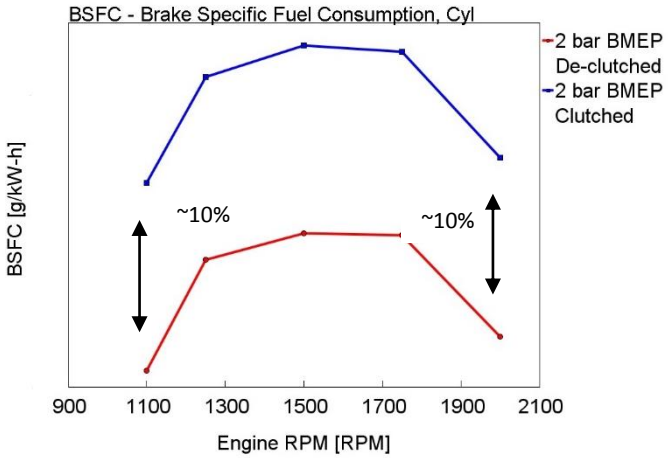

Figure 8.6. BSFC under low load for clutched and de-clutched configuration for fixed-ratio positive-displacement supercharger configuration

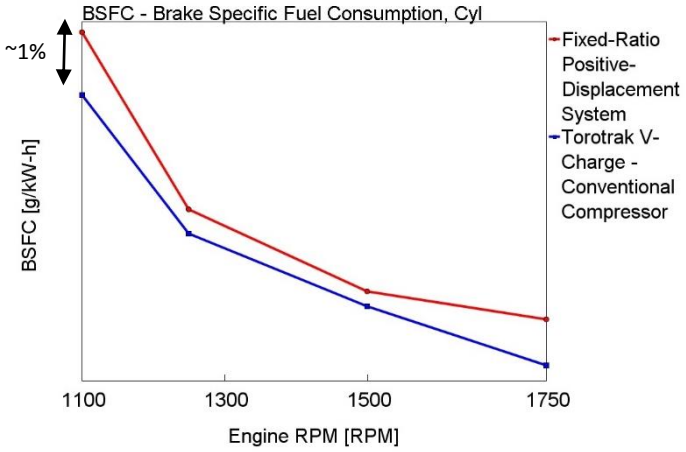

Figure 8.7. Full load BSFC performance

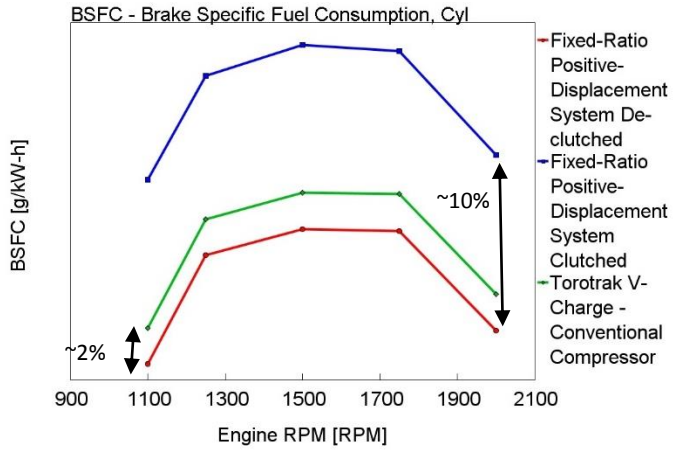

Figure 8.8. 2bar BMEP BSFC performance

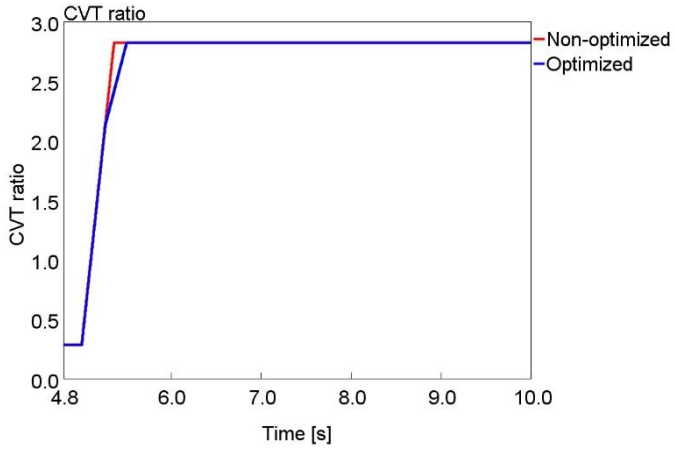

Figure 8.9. Transient CVT ratio at 1500RPM

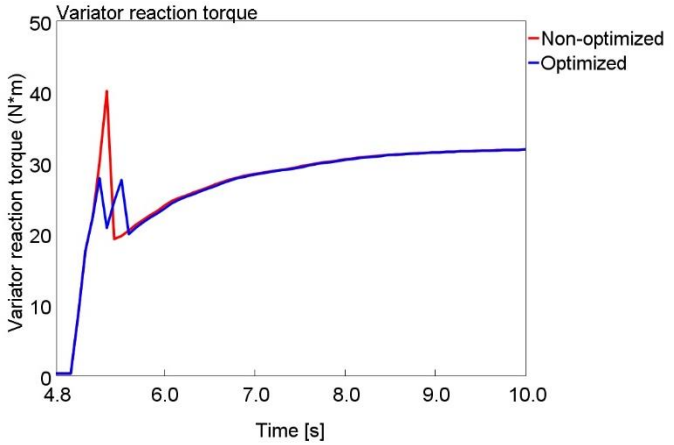

Figure 8.10. Transient variator reaction torque at 1500RPM

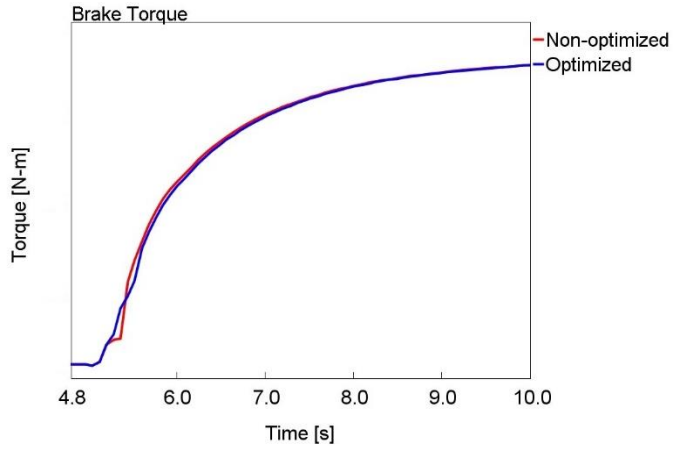

Figure 8.11. Transient engine torque response at 1500RPM

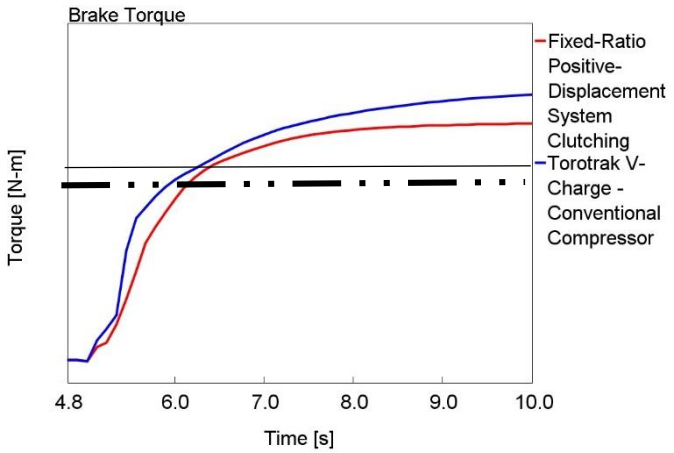

Figure 8.12. Transient engine torque response at 1100RPM

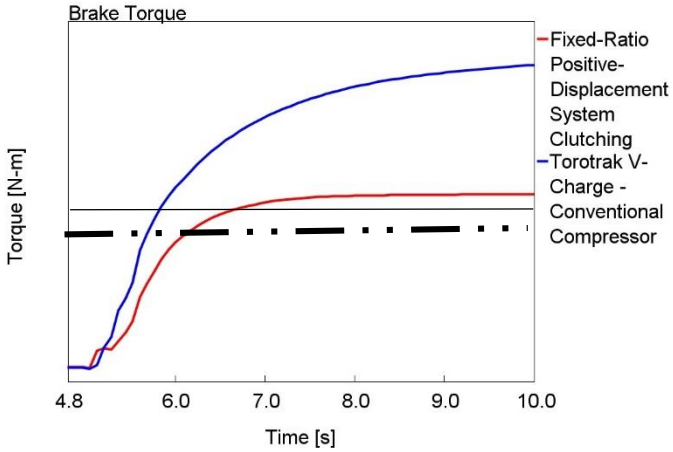

Figure 8.13. Transient engine torque response at 1500RPM

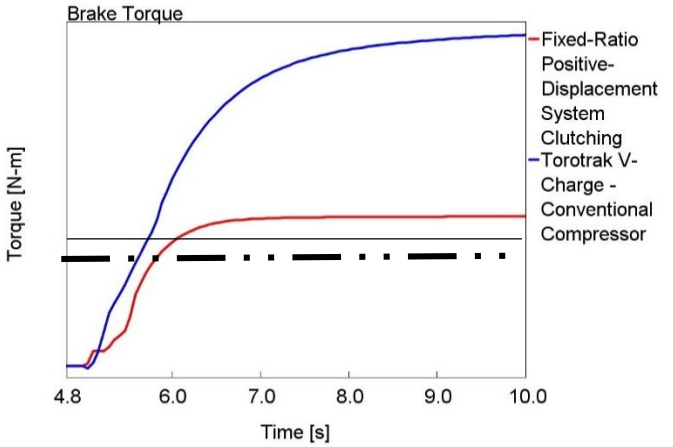

Figure 8.14. Transient engine torque response at 2000RPM

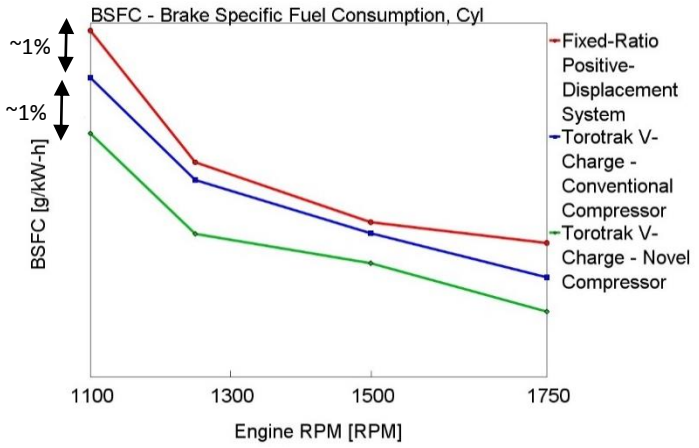

Figure 8.15. Full load BSFC performance

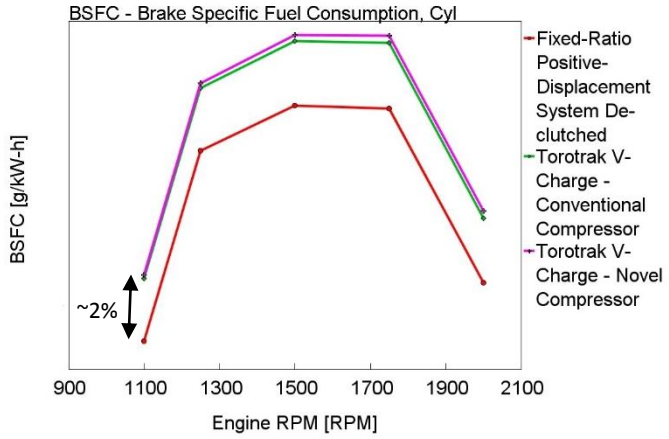

Figure 8.16. 2bar BMEP BSFC performance

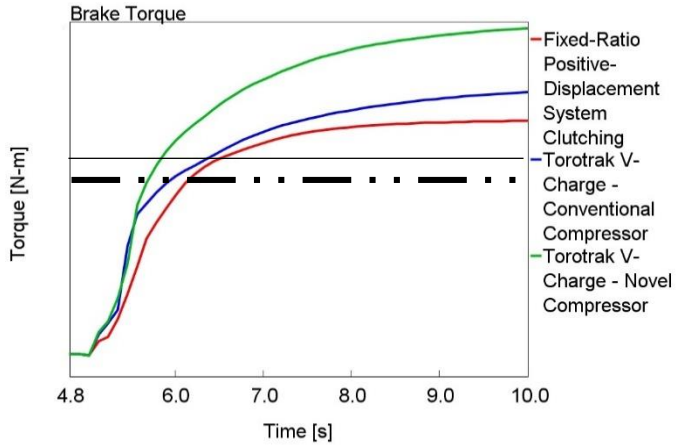

Figure 8.17. Transient engine torque response at 1100RPM

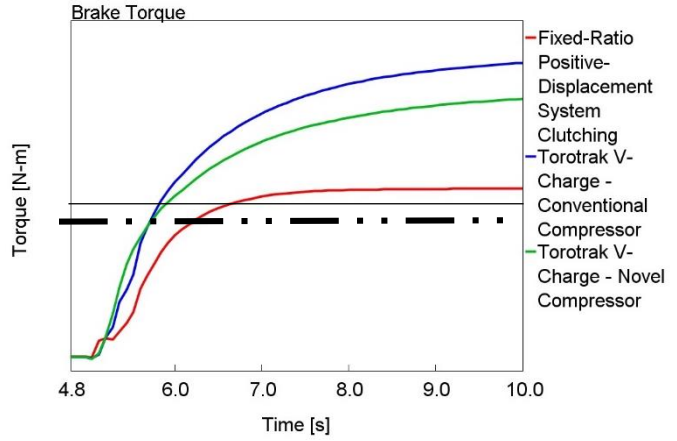

Figure 8.18. Transient engine torque response at 1500RPM

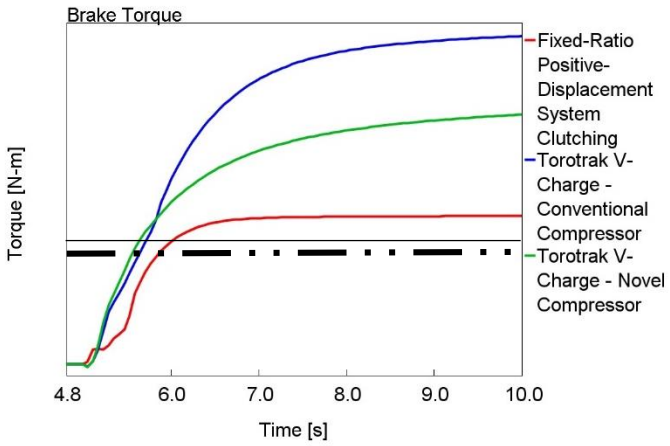

Figure 8.19. Transient engine torque response at 2000RPM

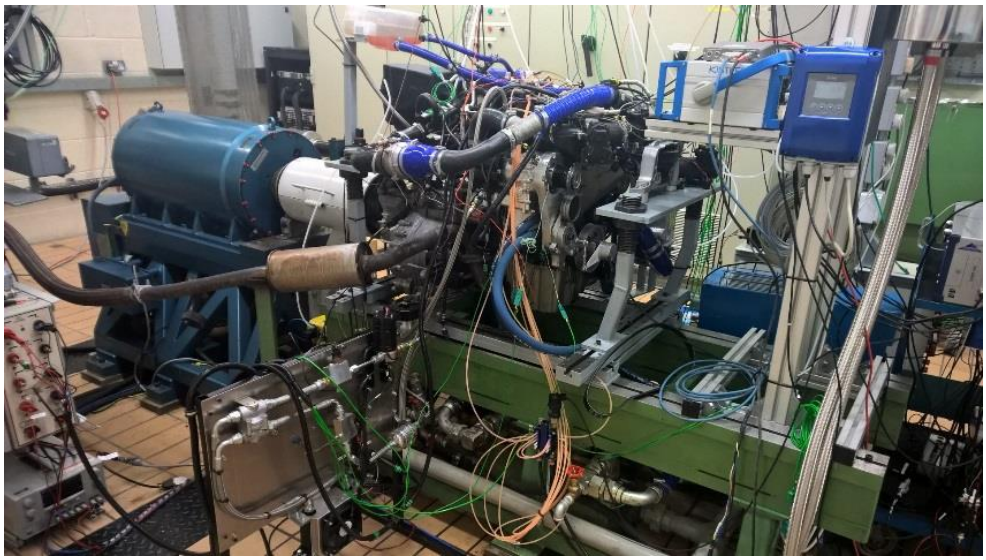

Figure 8.20. Test cell at University of Bath

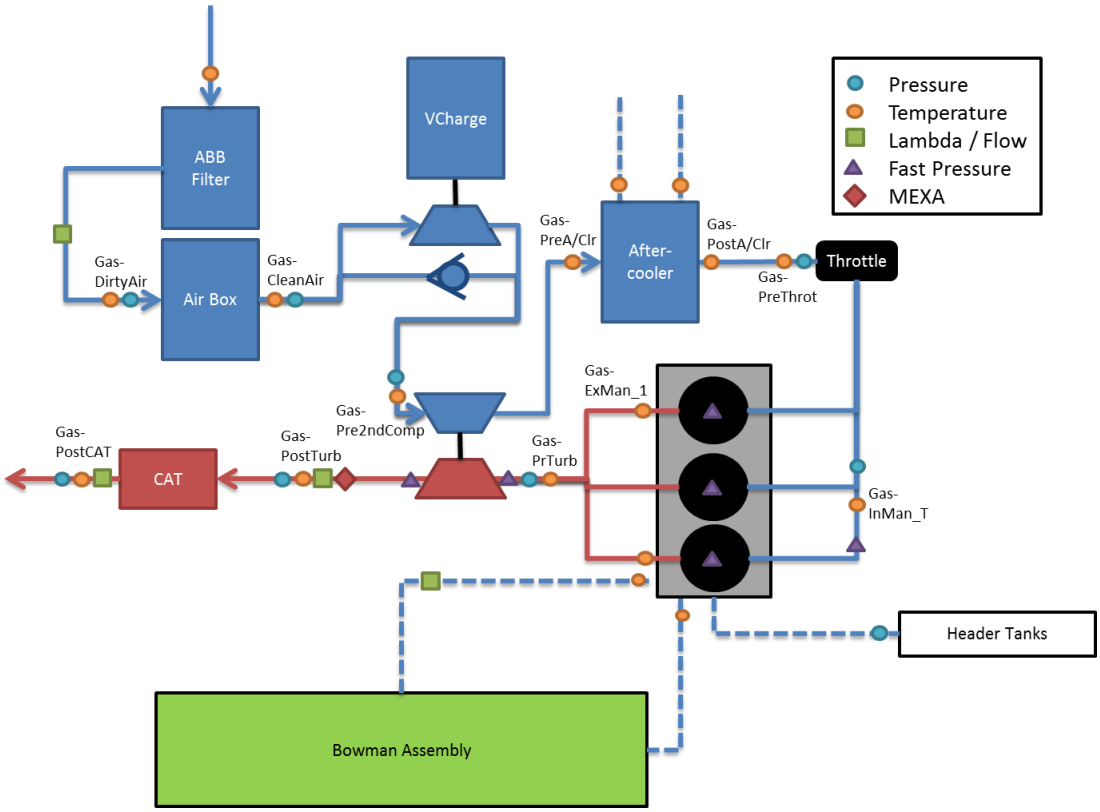

Figure 8.21. Measure locations

Figure 8.22. Check valve configuration

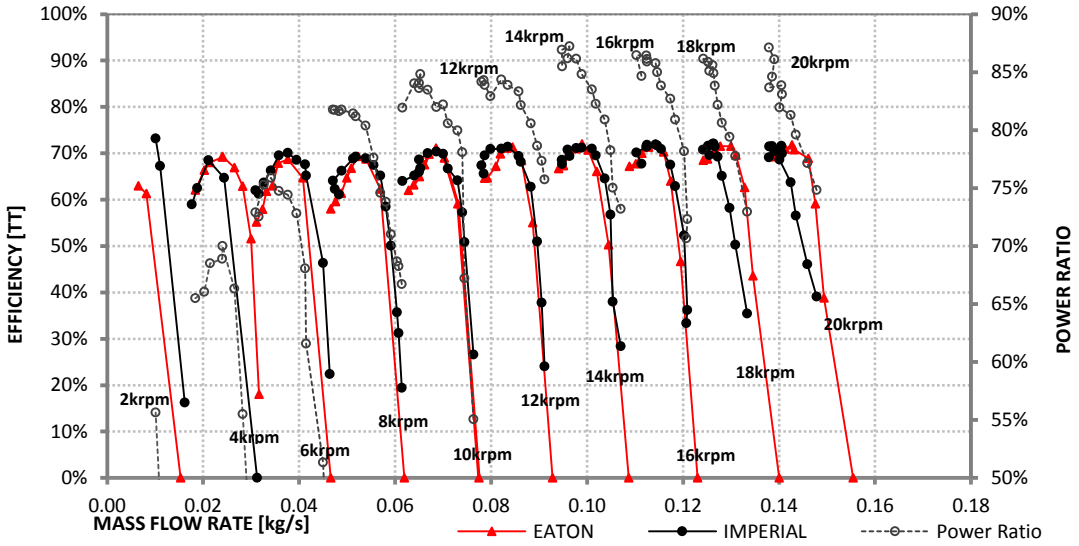

Figure 8.23. Validation for supercharger efficiency measurements (primary axis) and plot of the power ratio (second axis)

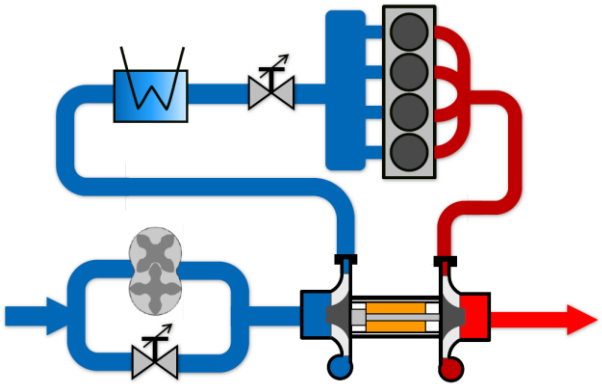

Figure 8.24. Schematic of the fixed-ratio positive displacement supercharger system [164]

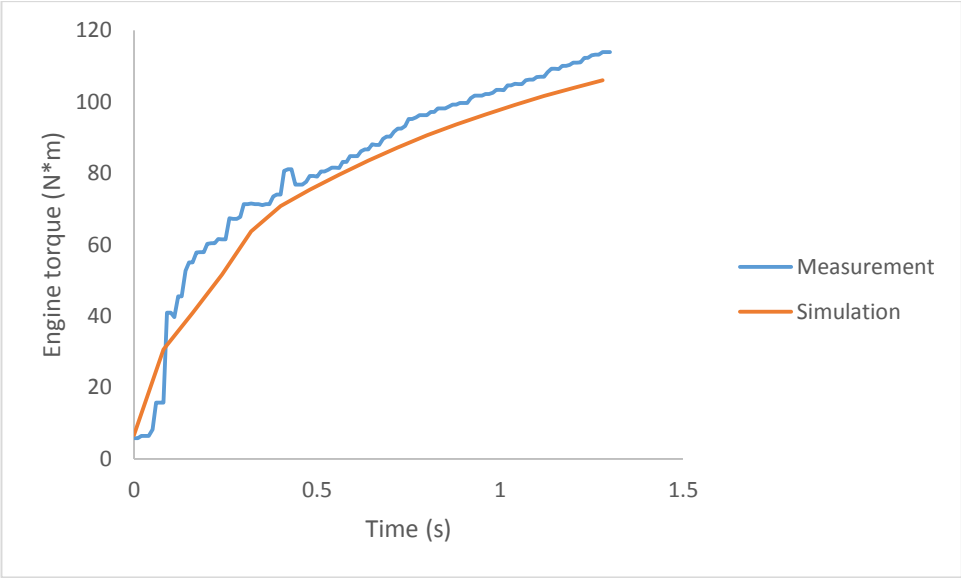

Figure 8.25. Measurement and simulation transient engine torque comparison

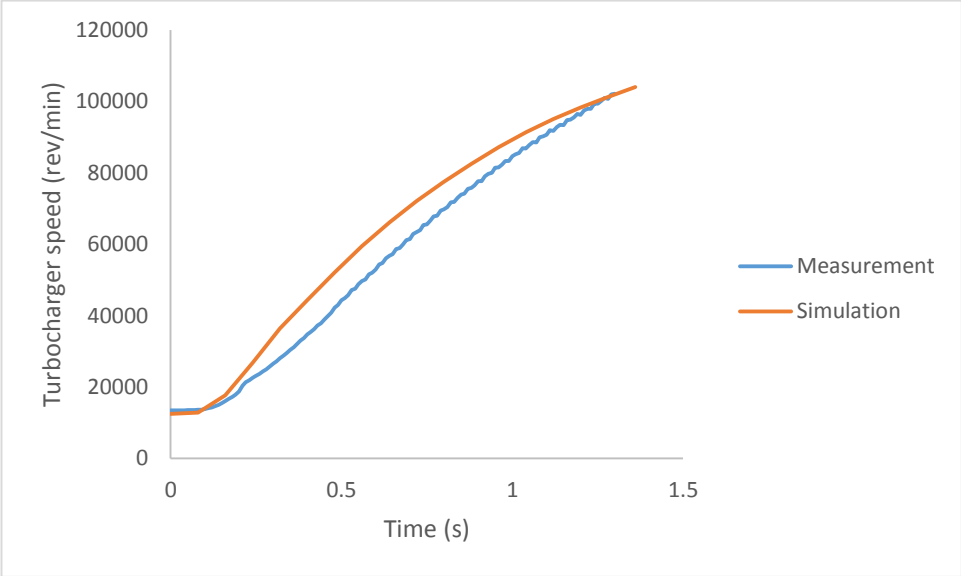

Figure 8.26. Measurement and simulation transient turbocharger speed comparison

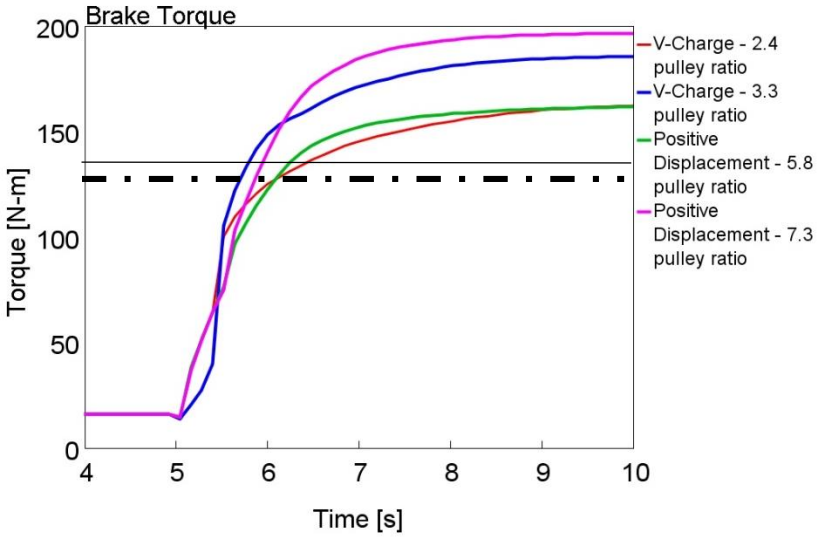

Figure 8.27. Brake torque transient response at 1000RPM

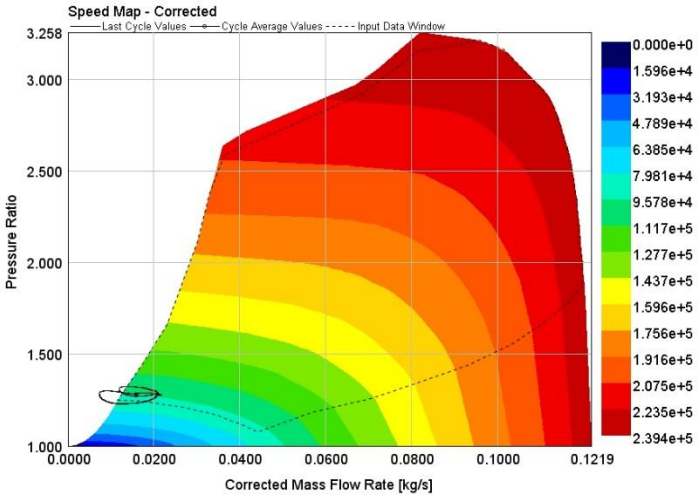

Figure 8.28. Turbocharger compressor operating point

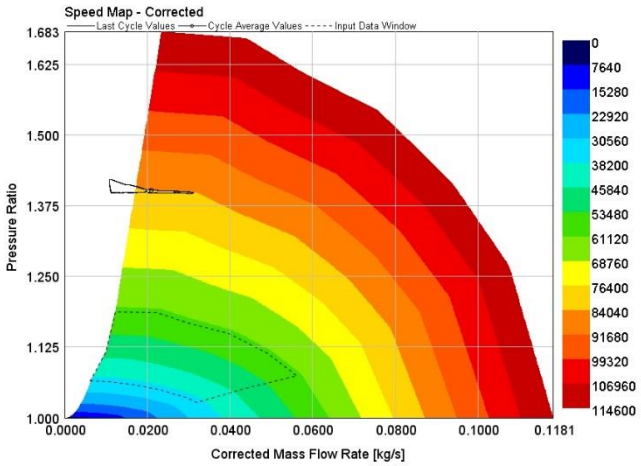

Figure 8.29. Supercharger compressor operating point

Chapter 9 - *Conclusions*

In this final chapter, the contributions, impacts and conclusions of the work presented in this thesis are summarised. This will be followed by some suggestions and recommendations for future work.

9.1 Summary, contributions and impacts

In this thesis, the application of DEP and the variable-drive supercharging concept for a downsized gasoline engine has been presented. To be more specific, the achievements in this work will be discussed with reference to the project aim and objectives laid out in Chapter 1.

- *Review the novel approaches to improve the gas exchange process of downsized turbocharged gasoline engines.*

The major findings to improve the gas exchange process that emerge from this review comprise four aspects (depending on the location where the novel technologies are implemented): charge air pressurisation/de-pressurisation improvement; combustion efficiency enhancement within the chamber; valve event associated development; and exhaust system optimisation. Although the interaction between these technologies on different aspects of the gas exchange process was found to be highly complex, the optimisation or the combination of these technologies is anticipated to further improve a downsized turbocharged SI engine's performance.

- *Review the current methods and potential trends for mechanically supercharging a downsized gasoline engine*

After reviewing the literature, it seems that low-end torque enhancement, transient driveability improvement and low-load parasitic-loss reduction are the three main development directions for a supercharger system, among which the adoption of a CVT to decouple the supercharger speed from the engine speed, compressor isentropic and volumetric efficiency improvement and supercharger mechanism innovation seem to be the potential trends for mechanically supercharging a passenger car engine.

- *Develop the simulation techniques, including the build and calibration of a 1-D engine model, engine control construction, and in-vehicle simulation analysis*.

Chapter 4 has presented a modelling and calibration theory foundation for the study in the following chapters. It mainly includes three sub-sections: engine model introduction and

calibration; engine control theory and tuning; and in-vehicle modelling. Each of these has been put into practice by demonstrating a case study.

- *Model the conventional DEP concept to understand the benefits of dividing blow-down and displacement phase in the exhaust stroke.*

The conventional DEP concept has been investigated in simulation using a validated highly-downsized 2.0 Litre SI engine model. The final results showed that the full-load BSFC and the engine combustion stability were both improved due to the fact that the DEP concept features a better gas exchange process and improved combustion phasing.

- *Apply the DEP concept to a two-stage system to try to enhance the advantages which two-stage turbocharged engines have already obtained while offsetting the deficiencies inevitably inherited.*

This chapter, for the first time, has applied the DEP concept to a two-stage downsized SI engine. By controlling the timing of the exhaust valves separately, to feed the exhaust mass flow to the high-pressure turbine or the low-pressure turbine or the exhaust pipe, such a system can achieve even better breathing characteristics and improved combustion phasing. In addition, part-load BSFC could also be reduced by using the scavenging valve to extend the 'duration' of the exhaust valve (thus reducing the re-compression effect) and to achieve internal EGR through reverse flow. However, this depends on the authorities of the scavenging valve timing (and piston clearance) and the combustion stability (EGR tolerance).

- *Model the variable drive positive-displacement supercharging system in a compound charging system*

A novel turbo-expansion concept has been proposed using a Turbo-Super twin-charger 1-D simulation model. The turbocharging system is designed to achieve the maximum utilisation of the exhaust energy, from which the intake charge is over-boosted. After the intercooler, the turbine-like supercharger expands the over-compressed intake charge to the required plenum pressure and reduces its temperature whilst recovering some energy through the connection to the crankshaft. According to the simulation results, the final BSFC was improved by approximately 1%. This might suggest the new turbo-expansion concept is not

suitable for this specific simulated engine model, but this novel gas exchange concept could be used in some other engines for its own interest.

In addition, a new de-throttling concept has also been proposed utilising the CVT driven supercharger to 'throttle' a Turbo-Super configuration SI engine rather than adopting a conventional throttle valve. By recovering some throttling loss through the supercharger, part-load fuel efficiency could be improved by up to 3%, depending on the operating points. However, the issues of limited supercharger operating range with an existing production CVT, condensation, fuel evaporation and worse pumping work need to be addressed before taking the supercharger-throttling gas exchange process from concept to reality.

- *Simulate and test the variable-drive centrifugal supercharging system in a compound charging system*

The simulation results show that BSFC was improved by approximately 1% at full load due to its capability to eliminate the use of supercharger bypass, resulting in reduced mechanical and flow losses. The BSFC performance could be improved further by another 1% if a novel compressor was used, which is mainly attributed to the reduced transmission losses and increased compressor isentropic efficiency. Under part load, both clutched and non-clutched configurations were assessed and discussed. It was demonstrated that a clutch might not necessarily be needed for the Torotrak V-Charge system, and only a minor decline of the part-load BSFC performance was observed if a clutch was not used. For the novel compressor configuration, if the drive ratio was retained, part-load BSFC of the novel compressor configuration would have slightly degraded BSFC performance when compared to the conventional compressor configuration, due to the higher PR at fixed compressor rotational speed. However, it was considered that the drive ratio could be reduced for the novel compressor configuration to improve the part-load BSFC performance while still maintaining a similar transient response. In transient, the simulated results suggest that the Torotrak V-Charge system with a conventional compressor could provide better transient response when compared to the fixed-ratio positive-displacement supercharger drive counterpart. The novel compressor configuration can provide even better transient performance at low engine speed while maintaining a similar performance response at high engine speed.
In experiments, at steady-state partial-load engine operating points, the fixed-ratio positive-displacement system characterises a larger recirculated flow loss while the Torotrak V-

Charge system features a larger transmission loss. The total parasitic loss for each boosting system depends on the pulley ratio adopted. In addition, for low-load operation, approximately 1 - 2% fuel consumption will be used to constantly connect the V-Charge system to the crankshaft. For the transient time-to-torque performance, it seems that the Torotrak V-Charge system could match the fixed-ratio positive-displacement counterpart. However, the Torotrak V-Charge system will have much fewer NVH issues than the positive-displacement counterpart, as no clutch engagement will be required during a transient event.

9.2 Outlook

The work performed in this project has led to a number of impacts on the continuation of this project and other projects at the University of Bath and with industrial partners.

1. Two peer-reviewed review journal papers on novel approaches to achieving turbocharging and supercharging have received high comments from the reviewers, and will potentially have a large impact on enriching the knowledge base in the field of internal combustion engine boosting.

2. The DEP research could potentially be further developed for a JLR project. In addition, the findings and discussions from modelling the concept have led to some other papers within the University.

3. The concept of using a positive-displacement supercharger as an expander, by adopting a variable-drive unit, has been validated and published by another JLR project [159]. The findings of this investigation have also inspired the author to study this concept in the following Torotrak V-Charge project, in order to eliminate the bypass valve and offset some of the parasitic losses.

4. The recommendations for selecting the drive ratio for a compound charging system have been suggested for the V-Charge project, considering the trade-off between the part-load BSFC and the transient response. This could be useful for some other supercharging projects.
5. The structure of the transient control for the V-Charge engine developed in this project can be applied to other complex two-stage compound charging systems. In addition, the in-vehicle simulation methodology developed in this thesis could be used in other projects

where the consolidated point or the kinematic method cannot capture the transient response, and cannot exhibit a real fuel economy in a driving cycle.

9.3 Further work

1. The DEP and the turbo-expansion concept can be validated further with some experimental test. In addition, the knock model, which is used to control the combustion phasing in those simulations, can be validated against the test data in a later research.

2. Although some experimental work has been conducted for the variable-drive supercharging concept, some more experimental study is needed to optimize the whole engine system. The control strategy, which is only briefly described in this work, needs to be calibrated in the rig in the near future, in order to give an optimized performance, especially in a transient operation.

3. The vehicle test using the variable-drive supercharging concept is being conducted at the University of Bath, and the vehicle driveability analysis shall be investigated in comparison with a standard vehicle fitted with a GTDI counterpart in the near future.

4. The potential additive benefit that might arise from VGTs (due to its capability to optimize the turbocharger performance) combined with the DEP and variable drive supercharging concept can be pursued in order to further improve the gas exchange process in a downsized gasoline engine.

References

[1] Salamon C, McAllister M, Robinson R, et al. Improving fuel economy by 35% through combined turbo and supercharging on a spark ignition engine. In: *21st Aachen Colloquium Automobile and Engine Technology*, Aachen, Germany, 07 October -10 October 2012.

[2] Stone R. *Introduction to Internal Combustion Engines*. 3rd ed. London: MacMillan; 1999

[3] Ross T and Zellbeck H. New Approach To Turbochargers For Four-Cylinder Gasoline Engines. *MTZ worldwide* 2010; 71(12):46-53.

[4] Gabriel H, Jacob S, Münkel U, et al. The Turbocharger with Variable Turbine Geometry for Gasoline Engines. *MTZ worldwide* 2007; 68(2): 96-103.

[5] Bandivadekar A, Bodek K, Cheah L, et al. On the Road in 2035 - Reducing Transportation's Petroleum Consumption and GHG Emissions. Report, MIT Laboratory for Energy and the Environment, USA, July 2008.

[6] Crabb D, Fleiss M, Larsson J, et al. New Modular Engine platform from Volvo. *MTZ worldwide* 2013; 74(9): 4-11.

[7] Turner J, Popplewell A, Patel R, et al. Ultra Boost for Economy: Extending the Limits of Extreme Engine Downsizing. *SAE Int. J. Engines* 2014; 7(1):387-417.

[8] Schorn NA. The Radial Turbine for Small Turbocharger Applications: Evolution and Analytical Methods for Twin-Entry Turbine Turbochargers. *SAE Int. J. Engines* 2014; 7(3):1422-1442.

[9] Szengel R, Middendorf H, Pott E et al. The TSI with 88 kW - the expansion of the Volkswagen family of fuel-efficient gasoline engines. In: *28th International Vienna Motor Symposium*, Vienna, Austria, 26-27 April 2007, Vienna: Austrian Society of Automotive Engineers.

[10] Brandt M, Rauscher M, Lejsek D et al. Scavenging to improve Low-End Torque of a Direct Injected Turbocharged SI Engine. *Online Referencing*, https://www.gtisoft.com/wp-content/uploads/publication/Bosch_Scavenging.pdf. (2005, accessed 10 August 2015).

[11] Tang H, Pennycott A, Akehurst S et al. A review of the application of variable geometry turbines to the downsized gasoline engine. *Int J Engine Res* 2014; 16(6): 810-825.

[12] Kerkau M, Knirsch S and Neußer HJ. The New Six-Cylinder Bi-Turbo Engine with Variable Turbine Geometry for the Porsche 911 Turbo. In: *27th International Vienna Motor Symposium*, Vienna, Austria, 27-28 April 2006, Vienna: Austrian Society of Automotive Engineers.

[13] Hu B, Akehurst S, Brace C et al. Optimization of Divided Exhaust Period for a Highly Downsized Turbocharged SI Engine – Scavenge Valve Optimization. *SAE Int. J. Engines* 2014; 7(3):1443-1452.

[14] Hu B, Akehurst S, Brace C et al. Fuel efficiency optimization for a divided exhaust period regulated two-stage downsized SI engine. *ASME J Gas Turb Pwr*. In press.

[15] Hu B, Brace C, Akehurst S et al. The effect of divided exhaust period for improved performance in a highly downsized turbocharged engine. In: *Institution of Mechanical Engineers 11th International Conference on Turbochargers and Turbocharging*, London, UK, 13-14 May 2014, London: Institution of Mechanical Engineers.

[16] Hu B, Brace C, Akehurst S et al. Simulation Study of Divided Exhaust Period for a Regulated Two-stage Downsized SI Engine. SAE paper 2014-01-2550, 2014.

[17] Hu B, Brace C, Akehurst S, et al. Divided Exhaust Period System for Downsized SI Engine. In: *SIA International Conference and Exhibition - the Spark Ignition Engine of the Future,* Strasbourg, France, 04 December-05 December 2013. Société des Ingénieurs de l'Automobile.

[18] Roth D, Keller P and Sisson J. Valve-Event Modulated Boost System. SAE paper 2010-01-1222, 2010.

[19] Roth D and Becker M. Valve-Event Modulated Boost System: Fuel Consumption and Performance with Scavenge-Sourced EGR. *SAE Int. J. Engines* 2012; 5(2):538-546.

[20] Roth D and Becker M. Valve-Event Modulated Boost System: Fuel Consumption and Performance Potential. In: *21st Aachen Colloquium Automobile and Engine technology,* Beijing, China, 07 October-10 October 2012.

[21] Möller C, Johansson P, Grandin B, et al. Divided Exhaust Period - A Gas Exchange System for Turbocharged SI Engines. SAE paper 2005-01-1150, 2005.

[22] Gundmalm S, Cronhjort A and Angstrom HE. Divided Exhaust Period on Heavy-Duty Diesel Engines. In: *THIESEL 2012 Conference on Thermo- and Fluid Dynamic Processes in Direct Injection Engines,* Valencia, Spain, 11 September-14 September 2012.

[23] Gundmalm S, Cronhjort A and Angstrom H. Divided Exhaust Period: Effects of Changing the Relation between Intake, Blow-Down and Scavenging Valve Area. *SAE Int. J. Engines* 2013; 6(2):739-750.

[24] Gundmalm S. Divided Exhaust Period on Heavy-Duty Diesel Engines. PhD Thesis, Royal Institute of Technology, Sweden, 2013.

[25] Williams A, Baker A and Garner C. Turbo-Discharging: Predicted Improvements in Engine Fuel Economy and Performance. SAE paper 2011-01-0371, 2011.

[26] Williams AM, Baker AT and Garner CP. Turbo-Discharging for improved engine torque and fuel economy. In: *Institution of Mechanical Engineers 10th International Conference on Turbochargers and Turbocharging,* London, UK, 15 May–16 May 2012, London: Institution of Mechanical Engineers.

[27] Williams AM, Baker AT and Garner CP. Turbo-discharging turbocharged internal combustion engines. *Proc Institution of Mechanical Engineers Part D: J Automobile Engineering* 2013*;* 227: 52-65.

[28] Gunston B. *World Encyclopaedia of Aero Engines*. 3rd ed. Sparkford: Patrick Stephens Limited, 2005.

[29] Hooker S, Reed H and Yarker A. *Performance of a Supercharged Aero Engine*, Derby: Rolls-Royce Heritage Trust, 1941.

[30] Robson G. *Rallying - The Four-Wheel Drive Revolution*. Yeoville: Haynes Publishing, 1986, p. 109-130.

[31] Krebs R, Szengel R, Middendorf H et al. The New Dual-Charged FSI Petrol Engine by Volkswagen Part 1: Design. *MTZ worldwide* 2005; 66(11):2-7.

[32] Krebs R, Szengel R, Middendorf H et al. The New Dual-Charged FSI Petrol Engine by Volkswagen Part 2: Thermodynamics. *MTZ worldwide* 2005; 66(12):23-26.

[33] Doble IM. Supercharging with an Axial Compressor SAE paper 870722, 1987.

[34] McAllister MJ and Buckley DJ. Future gasoline engine downsizing technologies - CO2 improvements and engine design considerations. In: *Institution of Mechanical Engineers Internal Combustion Engines Conference*, London, UK, 8-9 December 2009, paper no. C684/018, pp. 19-26. London: Institution of Mechanical Engineers.

[35] Jian C. Downsizing Turbo-charged Gasoline Engine with Small Displacement, Volkswagen 1.4 TSi 96 kW (China). *Internal Combustion Engines* 2010; 4: 5-12.

[36] Curtis E, Kunde O, McCarthy T, et al. EcoBoost: Downsized Gasoline DI Turbo Engines as the Backbone of Ford's CO2 and Fuel Economy Product Strategy. In: *FISITA Congress*, Budapest, Hungary, 30 May – 4 June 2010, paper no. F2010A130. UK: FISITA.

[37] Gouzonnat F, Merckx P, Cazenave R, et al. New challenges encountered when designing highly downsized gasoline engines (through new PSA Peugeot Citroen powertrain examples). In: *SIA International Conference and Exhibition - the Spark Ignition Engine of the Future,* Strasbourg, France, 4 -5 December 2013. Société des Ingénieurs de l'Automobile.

[38] Lumsden G, OudeNijeweme D, Fraser N, et al. Development of a Turbocharged Direct Injection Downsizing Demonstrator Engine. *SAE Int. J. Engines* 2009; 2(1):1420-1432.

[39] Sauer C, Kulzer A, Rauscher M, et al. Analysis of Different Gasoline Combustion Concepts with Focus on Gas Exchange. *SAE Int. J. Engines* 2009; 1(1): 336-345.

[40] Heywood JB, *Internal Combustion Engine Fundamentals*. New York: McGraw-Hill. 1988.

[41] Copeland C, Gao X, Freeland P, et al. Simulation of Exhaust Gas Residuals in a Turbocharged, Spark Ignition Engine. SAE paper 2013-01-2705, 2013.

[42] Fraser N, Blaxill H, Lumsden G, et al. Challenges for Increased Efficiency through Gasoline Engine Downsizing. *SAE Int. J. Engines* 2009; 2(1):991-1008.

[43] Chadwell C, Alger T, Zuehl J, et al. A Demonstration of Dedicated EGR on a 2.0 L GDI Engine. *SAE Int. J. Engines* 2014; 7(1):434-447.

[44] Watson N and Janota MS. *Turbocharging the Internal Combustion Engine*. London: MacMillan, 1982, p.264.

[45] Prevedel K, Pinter A, Wolkerstorf J, et al. Fahrspab trotz Hubraumverkleinerung: eine lo¨sbare Herausforderung durch Aufladung? In: *8th supercharging conference*, Dresden, Germany, 2002

[46] G.C., Capon, *Turbocharging the Automotive Diesel Engine*, Forthcoming

[47] Autozine Technical School. Intake and Exhaust. http://www.autozine.org/technical_school/engine/Intake_exhaust.html#VIM. (accessed 2 December 2012).

[48] CHRYSLER 300 CLUB INTERNATIONAL, INC. Ram Theory. http://www.chrysler300club.com/uniq/allaboutrams/ramtheory.htm. (accessed 3 December 2012).

[49] R Fong. Honda's VTEC Technology: Past, Present and Future. *Online Referencing*, http://www.importtuner.com/features/0511it_honda_vtec_information/viewall.html. (2005, accessed 4 December 2012).

[50] Eichhorn R, Boot M and Luijten C. Waste Energy Driven Air Conditioning System (WEDACS). *SAE Int. J. Engines* 2010; 2(2):477-492.

[51] Eichhorn R, Boot M, and Luijten C. Throttle Loss Recovery using a Variable Geometry Turbine. SAE paper 2010-01-1441, 2010.

[52] Turner J, Pearson R, Bassett M, et al. Performance and Fuel Economy Enhancement of Pressure Charged SI Engines through Turboexpansion – An Initial Study. SAE paper 2003-01-0401, 2003.

[53] Turner JWG and Pearson RJ. High Output Supercharging without Intercooling: Theory and Results. In: *ATA High Performance Engines Seminar*, 2001.

[54] Hooker S, Reed H and Yarker A. *The Performance of a Supercharged Aero Engine*. Rolls-Royce Heritage Trust, 1941.

[55] Whelans CD and Richards RA. Turbo-cooling applied to light duty vehicle engines. In: *Institution of Mechanical Engineers 8th International Conference on Turbochargers and Turbocharging*, London, UK, 2008, London: Institution of Mechanical Engineers.

[56] Whelans CD, Richards RA, Spence SWT, et al. Design and Development of a Turbo-expander for Charge Air Cooling. In: *Institution of Mechanical Engineers 9th International Conference on Turbochargers and Turbocharging*, London, UK, 2010, London: Institution of Mechanical Engineers.

[57] Turner J, Pearson R, Bassett M, et al. The Turboexpansion Concept - Initial Dynamometer Results. SAE paper 2005-01-1853, 2005.

[58] Taitt DW, Garner CP, Swain E, et al. An Automotive Engine Charge-Air Intake Conditioner System: Thermodynamic Analysis of Performance Characteristics. *Proc Institution of Mechanical Engineers Part D: J Automobile Engineering* 2005; 219: 389-404.

[59]Romagnoli A, Wan-Salim WS-I, Gurunathan BA, et.al. Assessment of supercharger boosting component for heavily downsized gasoline engines. In: *Institution of Mechanical Engineers 11th International Conference on Turbochargers and Turbocharging*, London, UK, 13-14 May 2014, London: Institution of Mechanical Engineers.

[60] Hu B, Copeland C, Brace C, et al. A New Turboexpansion Concept in a Twin-Charged Engine System. SAE 2014-01-2596, 2014.

[61] Hu B, Copeland C, Brace C, et al. A New De-throttling Concept in a Twin-charged Gasoline Engine System. *SAE Int. J. Engines* 2015; Epub ahead of print 4 April 2015. DOI: 10.4271/2015-01-1258.

[62] Alger T, Hall M and Matthews R. Fuel Spray Dynamics and Fuel Vapor Concentration Near the Spark Plug in a Direct-Injected 4-Valve SI Engine. SAE paper 1999-01-0497, 1999.

[63] Brehob D, Fleming J, Haghgooie M, et al. Stratified-Charge Engine Fuel Economy and Emission Characteristics. SAE paper 982704, 1998.

[64] Kano M, Saito K, Basaki M, et al. Analysis of Mixture Formation of Direct Injection Gasoline Engine. SAE paper 980157, 1998.

[65] Iwamoto Y, Noma K, Nakayama O, et al. Development of the Gasoline Direct Injection Engine. SAE paper 970541, 1997.

[66] Buckland J, Cook J, Kolmanovsky I, et al. Technology Assessment of Boosted Directed Injection Stratified Charge Gasoline Engines. SAE paper 2000-01-0249, 2000.

[67] Kirwan J, Shost M, Roth G, et al. 3-Cylinder Turbocharged Gasoline Direct Injection: A High Value Solution for Low CO2 and NOx Emissions. *SAE Int. J. Engines* 2010; 3(1): 355-371.

[68] Cairns A, Blaxill H and Irlam G. Exhaust Gas Recirculation for Improved Part and Full Load Fuel Economy in a Turbocharged Gasoline Engine. SAE paper 2006-01-0047, 2006.

[69] Brustle C and Hemmerlein N. Exhaust gas turbocharged SI engines and their ability of meeting future demands. In: *Institution of Mechanical Engineers International Conference on Turbochargers and Turbocharging,* London, UK, 1994, London: Institution of Mechanical Engineers.

[70] Alger T, Hanhe S, Roberts C, et al. The Heavy Duty Gasoline Engine - A Multi-Cylinder Study of a High Efficiency, Low Emission Technology. SAE paper 2005-01-1135, 2005.

[71] Grandin B and Angstrom HE. Replacing Fuel Enrichment in a Turbo Charged SI Engine: Lean Burn or Cooled EGR. SAE paper 1999-01-3505, 1999.

[72] Duchaussoy Y, Lefebvre A and Bonetto R. Dilution Interest on Turbocharged SI Engine Combustion. SAE paper 2003-01-0629, 2003.

[73] Potteau S, Lutz P, Leroux S, et al. Cooled EGR for a Turbo SI Engine to Reduce Knocking and Fuel Consumption. SAE paper 2007-01-3978, 2007.

[74] Alger T, Chauvet T and Dimitrova Z. Synergies between High EGR Operation and GDI Systems. *SAE Int. J. Engines* 2009; 1(1):101-114.

[75] Jerald AC. A thermodynamic comparison of external and internal exhaust gas dilution for high-efficiency internal combustion engines. *Int J Engine Res* 2015; Epub ahead of print 7 January 2015. DOI: 10.1177/1468087414560593.

[76] Roth D, Zhang R, Sauerstein R, et al. New Aspects of Application of Hybrid EGR Systems to Turbocharged GDI Engines. In: *18th Aachen Colloquium Automobile and Engine Technology*, Germany, 05 October-07 October 2009.

[77] Takaki D, Tsuchida H, Kobara T, et al. Study of an EGR System for Downsizing Turbocharged Gasoline Engine to Improve Fuel Economy. SAE paper 2014-01-1199, 2014.

[78] Alger T and Mangold B. Dedicated EGR: A New Concept in High Efficiency Engines. *SAE Int. J. Engines 2009;* 2(1):620-631.

[79] Roth D, Keller P and Becker M. Requirements of External EGR Systems for Dual Cam Phaser Turbo GDI Engines. SAE paper 2010-01-0588, 2010.

[80] Kwon H and Min K. Laminar Flame Speed Characteristics and Combustion Simulation of Synthetic Gas Fueled SI Engine. SAE paper 2008-01-0965, 2008.

[81] Hoffmeyer H, Montefrancesco E, Beck L, et al. CARE - CAtalytic Reformated Exhaust Gases in Turbocharged DISI-Engines. *SAE Int. J. Fuels Lubr* 2009*;* 2(1): 139-148.

[82] Rebbert M, Kreusen G and Lauer S. A New Cylinder Deactivation by FEV and Mahle. SAE paper 2008-01-1354, 2008.

[83] Das Auto. Active Cylinder Technology (ACT) – Fuel saving cylinder deactivation technology, http://www.volkswagen.co.uk/technology/petrol/active-cylinder-technology-act (accessed 28 May 2014).

[84] Osborne R, Li G, Sapsford S, et al. Evaluation of HCCI for Future Gasoline Powertrains. SAE paper 2003-01-0750, 2003.

[85] Milovanovic N, Blundell D, Gedge S, et al. SI-HCCI-SI Mode Transition at Different Engine Operating Conditions. SAE paper 2005-01-0156, 2005.

[86] Wu H, Collings N, Regitz S, et al. Experimental Investigation of a Control Method for SI-HCCI-SI Transition in a Multi-Cylinder Gasoline Engine. SAE paper 2010-01-1245, 2010.

[87] Zhang Y, Xie H, Zhou N, et al. Study of SI-HCCI-SI Transition on a Port Fuel Injection Engine Equipped with 4VVAS. SAE paper 2007-01-0199, 2007.

[88] Shingne P, Assanis D, Babajimopoulos A, et al. Turbocharger Matching for a 4-cylinder Gasoline HCCI Engine Using a 1D Engine Simulation. SAE paper 2010-01-2143, 2010.

[89] Martins, M. and Zhao, H. 4-Stroke Multi-Cylinder Gasoline Engine with Controlled Auto-Ignition (CAI) Combustion: a comparison between Naturally Aspirated and Turbocharged Operation. SAE paper 2008-36-0305, 2008.

[90] Dec, J. and Yang, Y. Boosted HCCI for High Power without Engine Knock and with Ultra-Low NOx Emissions - using Conventional Gasoline. *SAE Int. J. Engines* 2010; 3(1):750-767.

[91] Hong H, Parvate-Patil GB and Gordon B. Review and analysis of variable valve timing strategies – Eight ways to approach. *Proc Institution of Mechanical Engineers Part D: J Automobile Engineering 2004;* 218 (10): 1179-1200.

[92] Dresner T and Barkan P. A Review of Variable Valve Timing Benefits and Modes of Operation SAE paper 891676, 1989.

[93] Asmus TW. Effects of valve events on engine operation. In: Hilliard JC and Springer GS(eds) *Fuel economy in Road Vehicles Powered by Spark Ignition Engines.* New York: Plenum, 1984.

[94] Siewert RM. How individual valve timing events affect exhaust emissions. SAE paper, 710609, 1971.

[95] Taylor J, Fraser N, Dingelstadt R, et al. Benefits of Late Inlet Valve Timing Strategies Afforded Through the Use of Intake Cam In Cam Applied to a Gasoline Turbocharged Downsized Engine. SAE paper 2011-01-0360, 2011.

[96] Miller, RH. Supercharging and the Internal Cooling Cycle for High Output. *Trans. ASME* 1947; 69.

[97] Wang Y, Lin L, Roskilly AP, et al. An analytic study of applying Miller cycle to reduce NOx emission. *Appl. Therm. Eng.* 2007; 27: 1779-1789.

[98] Wang Y, Lin L, Zeng S, et al. Application of the Miller cycle to reduce NOx emissions from petrol engines. *Appl. Energy* 2008; 85: 463-474.

[99] Bozza F, De Bellis V, Gimelli A, et al. Strategies for Improving Fuel Consumption at Part-Load in a Downsized Turbocharged SI Engine: a Comparative Study. *SAE Int. J. Engines* 2014; 7(1):60-71.

[100] Martins JJG, Uzuneanu K, Ribeiro BS, et al. Thermodynamic Analysis of an Over-Expanded Engine. SAE paper 2004-01-0617, 2004.

[101] Akihisa D and Sawada D. Research on Improving Thermal Efficiency through Variable Super-High Expansion Ratio Cycle. SAE paper 2010-01-0174, 2010.

[102] Li T, Gao Y, Wang J, et al. The Miller cycle effects on improvement of fuel economy in a highly boosted, high compression ratio, direct-injection gasoline engine: EIVC vs. LIVC. *Energ Convers Manage* 2014; 79:59-65.

[103] Hitomi M, Sasaki J, Hatamura K, et al. Mechanism of Improving Fuel Efficiency by Miller Cycle and Its Future Prospect. SAE paper 950974, 1995.

[104] Goto T, Hatamura K, Takizawa S, et al. Development of V6 Miller Cycle Gasoline Engine. SAE paper 940198, 1994.

[105] Luttermann C, Schünemann E and Klauer N Enhanced VALVETRONIC Technology for Meeting SULEV Emission Requirements. SAE paper 2006-01-0849, 2006.

[106] Hara S, Nakajima Y and Naguma S. Effects of intake-valve closing timing on spark-ignition engine combustion. SAE paper 850074, 1985.

[107] Petitjean D, Bernardini L, Middlemass C, et al. Advanced Gasoline Engine Turbocharging Technology for Fuel Economy Improvements. SAE paper 2004-01-0988, 2004.

[108] Lundstrom RR and Gall J. A Comparison of Transient Vehicle performance Using a Fixed Geometry, Wastegated Turbocharger and a Variable Geometry Turbocharger. SAE paper 860104, 1986.

[109] Singer DA. Comparison of a Supercharger vs. a Turbocharger in a Small Displacement Gasoline Engine Application. SAE paper 850244, 1985.

[110] Capobianco M and Gambarotta A. Variable Geometry and Waste-Gated Automotive Turbochargers: Measurements and Comparison of Turbine Performance. *J. Eng. Gas Turbines Power* 1992; 114(3): 553-540.

[111] Lezhnev L, Kolmanovsky I and Buckland J. Boosted Gasoline Direct Injection Engines: Comparison of Throttle and VGT Controllers for Homogeneous Charge Operation. SAE paper 2009-32-0169, 2009.

[112] Ito N, Ohta T, Kono R, et al. Development of a 4-Cylinder Gasoline Engine with a Variable Flow Turbo-charger. SAE paper 2007-01-0263, 2007.

[113] Andersen J, Karlsson E and Gawell A. Variable Turbine Geometry on SI Engines. SAE paper 2006-01-0020, 2006.

[114] Taylor J, Fraser N and Wieske P. Water Cooled Exhaust Manifold and Full Load EGR Technology Applied to a Downsized Direct Injection Spark Ignition Engine. *SAE Int. J. Engines* 2010; 3(1):225-240.

[115] Société R. *Improvements in or relating to Internal Combustion engines*. Patent 179,926, UK, 1924.

[116] Deutz AG. *Turbocharged four stroke cycle fuel injection engine*. Patent 2,979,887, USA, 1961.

[117] Fleming Thermodynamics Ltd. I.C. engine with an exhaust driven turbine or positive displacement expander. Patent 2,185,286, UK, 1987.

[118] SAAB Automobile AB. Patents SE507030C2, SE521615C2, SE521174C2, SE514806C2, SE514969C2, SE512943C2, SE518687C2. Patent, Sweden, 1998-2003.

[119] Roth D. Controlling Exhaust gas flow divided between turbocharging and exhaust gas recirculating. Patent, 20110000470, USA, 2011.

[120] Ross T. Mehrzylinder-Ottomotor mit Abgasturboaufladung und Verfahren zu dessen Betrieb. Patent DE102008036308A, German, 2010.

[121] Fujii S, Kaneko K and Tsujikawa T. Mirror Gas Turbines: A Newly Proposed Method of Exhaust Heat Recovery. *ASME J Gas Turb Pwr* 2001; 123(3): 481-486.

[122] Chen Z and Copeland C. Inverted Brayton Cycle Employment for a Highly Downsized Turbocharged Gasoline Engine. SAE paper 2015-01-1973, 2015.

[123] Rose ATJM, Akehurst S and Brace CJ. Modelling the performance of a continuously variable supercharger drive system. *Proc Institution of Mechanical Engineers Part D: J Automobile Engineering* 2011*;* 225: 1399-1414.

[124] Turner JWG and Pearson RJ. The turbocharged direct-injection spark-ignition engine. In: Zhao H (eds) *Advanced Direct Injection Combustion Engine Technologies and Development: Volume 1: Gasoline and Gas Engines: Science and Technology.* 1st ed. Cambridge: Woodhead Publishing Limited, 2009.

[125] Lysholm AJR. A New Rotary Compressor. *Proc. Instn Mech. Engrs* 1942; 148.

[126] Volvo Car Group. Volvo Car's new Drive-E Powertrains – efficient driving pleasure with world-first technologies, https://www.media.volvocars.com/global/en-gb/media/pressreleases/124738/volvo-cars-new-drive-e-powertrains-efficient-driving-pleasure-with-world-first-technologies. (2013, accessed 24 August, 2015).

[127] Turner JWG, Pearson RJ and Parrott A. The Performance of a High Compression Ratio, High Speed Supercharged Engine. In: *Global Powertrain Congress*, Detroit, USA, 2004, Global Automotive Management Council.

[128] Fitzen M, Hatz W, Eiser A et al. The Audi 3.0l TFSI - the new top-of-the-range V6 engine. In: *29th International Vienna Motor Symposium*, Vienna, Austria, 24-25 April 2008, Vienna: Austrian Society of Automotive Engineers.

[129] Sandford M, Page G and Crawford P. The All New AJV8. SAE paper 2009-01-1060, 2009.

[130] Froehlich M and Stewart N. TVS® V-Series Supercharger Development for Single and Compound Boosted Engines. SAE paper 2013-01-0919, 2013.

[131] Lysholm. Lysholm screw rotors. (https://commons.wikimedia.org/wiki/File:Lysholm_screw_rotors.jpg) (2006, accessed 17 August 2015).

[132] Hu B, Tang H, Akehurst S et al. Modelling the Performance of the Torotrak V-Charge Variable Drive Supercharger System on a 1.0L GTDI – Preliminary Simulation Results. SAE paper 2015-01-1971, 2015.

[133] Pomeroy L. The Background, Layout and Performance of the B.R.M. Engine. *The Motor Magazine*.

[134] Hooker S. *Not much of an Engineer*, Ramsbury: The Crowood Press Ltd, 1991.

[135] Turner JWG, Popplewell A, Marshall DJ et al. SuperGen on Ultraboost: Variable-Speed Centrifugal Supercharging as an Enabling Technology for Extreme Engine Downsizing. *SAE Int. J. Engines* 2015; 8(4).

[136] Phillips F, Gilbert I, Pirault J-P et al. Scuderi Split Cycle Reserch Engine: Overview, Architecture and Operation. *SAE Int. J. Engines* 2011; 4(1): 450-466.

[137] Meldolesi R, Bailey G, Lacy C et al. Scuderi Split Cycle Fast Acting Valvetrain: Architecture and Development. *SAE Int. J. Engines* 2011; 4(1): 467-481.

[138] Meldolesi R and Badain N. Scuderi Split Cycle Engine: Air Hybrid Vehicle Powertrain Simulation Study. SAE paper 2012-01-1013, 2012.

[139] Schechter MM. New Cycles for Automobile Engines. SAE paper 1999-01-0623, 1999.

[140] Branyon D and Simpson D. Miller Cycle Application to the Scuderi Split Cycle Engine (by Downsizing the Compressor Cylinder). SAE paper 2012-01-0419, 2012.

[141] Jackson N, Atkins A, Eatwell J et al. An Alternative Thermodynamic Cycle for Reciprocating Piston Engines. In: *36th International Vienna Motor Symposium*, Vienna, Austria, 7-8 May 2015, Vienna: Austrian Society of Automotive Engineers.

[142] Aoki H. Pressure wave supercharger. (https://commons.wikimedia.org/wiki/File:US4563997_Fig1_Pressure_wave_supercharger.png) (2014, accessed 19 August 2015).

[143] Flückiger L, Tafel S and Spring P. Pressure-wave supercharged spark-ignition engines. *MTZ worldwide* 2006; 67(12): 6-9.

[144] Wenger U. Spark ignition engine with pressure-wave supercharger. Patent application US 6089211 A, USA, 2000.

[145] Spring P. *Modeling and Control of Pressure-Wave Supercharged Engine Systems.* PhD Thesis, Swiss Federal Institute of Technology ETH Zurich, Swiss, 2006.

[146] Oguri Y, Suzuki T, Yoshida M et al. Research on Adaptation of Pressure Wave Supercharger (PWS) to Gasoline Engine. SAE 2001-01-0368, 2001.

[147] Pullen KR, Etemad S, Thornton W et al. Electrically driven supercharger using the TurboClaw compressor for engine downsizing. In: *Institution of Mechanical Engineers 10th International Conference on Turbochargers and Turbocharging*, London, UK, 15 May-16 May 2012, London: Institution of Mechanical Engineers.

[148] Pullen KR, Etemad S and Cattell R. Experimental Investigation of the Turboclaw Low Specific Speed Turbocompressor. In: *ASME Turbo Expo 2012,* Copenhagen, Denmark, 11-15 June 2012, paper no. GT2012-69074. New York: ASME.

[149] Martinez-Botas R, Pesiridis A and Yang M. Overview of boosting options for future downsized engines. *Sci China Tech Sci* 2011; 54(2): 318-331.

[150] Copeland C, Martinez-Botas F, Turner J et al. Boost system selection for a heavily downsized spark ignition prototype engine. In: *Institution of Mechanical Engineers 10th International Conference on Turbochargers and Turbocharging*, London, UK, 15 May-16 May 2012, London: Institution of Mechanical Engineers.

[151] Lewis A. *Data from Ultraboost engine*. Bath: University of Bath, 2013.

[152] Wicke V, Brace CJ and Vaughan ND. The Potential for Simulation of Driveability of CVT Vehicles. SAE paper 2000-01-0830, 2000.

[153] Wetzel P. Downspeeding a Light Duty Diesel Passenger Car with a Combined Supercharger and Turbocharger Boosting System to Improve Vehicle Drive Cycle Fuel Economy. SAE paper 2013-01-0932, 2013.

[154] Stoffels H, Quiring S and Pingen B. Analysis of Transient Operation of Turbo Charged Engines. *SAE Int. J. Engines* 2010; 3(2):438-447.

[155] Birckett A, Engineer N, Arlauskas P et al. Mechanically Supercharged 2.4L GDI Engine for Improved Fuel Economy and Low Speed Torque Improvement. SAE paper 2014-01-1186, 2014.

[156] Ostrowski G, Neely GD, Chadwell CJ et al. Downspeeding and Supercharging a Diesel Passenger Car for Increased Fuel Economy. SAE paper 2012-01-0704, 2012.

[157] King J, Heaney M, Bower E et al. HyBoost – An intelligently electrified optimised downsized gasoline engine concept. London, UK, 15 May-16 May 2012, London: Institution of Mechanical Engineers.

[158] Vasilash GS. Volvo's Drive-E: Environmentally Efficient & Clever – Powertrains. *Automotive Design and Production*, March 2014, p.24.

[159] Meghani A, Allen J, Turner JWG et al. Effects of Charging System Variability on the Performance and Fuel Economy of a Supercharged Spark-Ignition Engine. SAE paper 2015-01-1286, 2015.

[160] Wikipedia. Mercedes-AMG, https://en.wikipedia.org/wiki/Mercedes-AMG#.2232.22_3.2.C2.A0L_V6_KOMPRESSOR (accessed 11 Sep 2015)

[161] Choshi M, Asanomi K, Abe H et al. Development of V6 Miller cycle engine. *JSAE review* 1994; 15: 195-200.

[162] Kobayashi A, Satou T, Isaji H et al. Development of New I3 1.2L Supercharged Gasoline Engine. SAE paper 2012-01-0415, 2012.

[163] Rose ATJM, Akehurst S and Brace CJ. Investigation into the trade-off between the part-load fuel efficiency and the transient response for a highly boosted downsized gasoline engine with a supercharger driven through a continuously variable transmission. *Proc Institution of Mechanical Engineers Part D: J Automobile Engineering* 2013*;* 227: 1674-1686.

[164] Volvo. VEP HP Super-Turbo. Supercharger Pre-spin.

[165] McBroom S, Smithson RA, Urista R et al. Effects of Variable Speed Supercharging Using a Continuously Variable Planetary on Fuel Economy and Low Speed Torque. *SAE Int. J. Engines* 2012; 5(4):1717-1728.

[166] Romagnoli A, Wan-Salim WS-I, Gurunathan BA et al. Assessment of supercharger boosting component for heavily downsized gasoline engines. In: *Institution of Mechanical Engineers 11th International Conference on Turbochargers and Turbocharging*, London, UK, 13-14 May 2014, London: Institution of Mechanical Engineers.

[167] Lontra. Blade Compressor Video, http://lontra.co.uk/technology/blade-compressor/blade-compressor-video/ (accessed 11 Sep 2015).

[168] VanDyne SuperTurbo. Technology, http://www.vandynesuperturbo.com/technology.html (accessed 11 Sep 2015).

[169] The slides from MSc course internal combustion engine technology at University of Bath

[170] Aymanns R, Uhlmann T, Nebbia C et al. Electric supercharging - New opportunities with higher system voltage. *MTZ worldwide* 2014; 75(7):4-11.

[171] Hu B, Akehurst S and Brace C. Novel approaches to improve the gas exchange process of downsized turbocharged spark-ignition engines – A review. *Int J Engine Res* 2015; in press.

[172] Wu C, Puzinauskas PV and Tsai JS. Performance analysis and optimization of a supercharged Miller cycle Otto engine. *Appl Therm Eng* 2013; 23(5):511-521.

[173] Li T, Zheng B and Yin T. Fuel conversion efficiency improvements in a highly boosted spark-ignition engine with ultra-expansion cycle. *Energ Convers Manage* 2015; 103:448-458.

[174] Schmitz G. Five-stroke internal combustion engine. Patent 6553977, United States, 2003.

[175] Schmitz G. Five stroke internal combustion engine. (http://www.5-stroke-engine.com/Dateien/5T%20Beschreibung%20%26%20Studie.pdf) (2011, accessed 10 August 2015).

[176] Aillod C, Delaporte B, Schmitz G et al. Development and Validation of a Five Stroke Engine. SAE paper 2013-24-0095, 2013.

[177] Noga M and Sendyka B. New design of the five-stroke SI engine. *J KONES Powertrain Transp* 2013; 20(1): 239-246;

[178] Noga M and Sendyka B. Increase of efficiency of SI engine through the implementation of thermodynamic cycle with addition expansion. *Bull Polish Acad Sci* 2014; 62(2):349–55.

[179] Lu Y and Pei P. Performance evaluation of 4-cylinder 5-stroke internal combustion engine. *Chin Int Combust Engine Eng* 2015; 36(2):18–24.

[180] Brace C. Prediction of Diesel Engine Exhaust Emissions using Artificial Neural Networks. In: *Neural Networks in Systems Design*, Solihull, UK, 10 June 1998, London: Institution of Mechanical Engineers.

[181] Gamma Technologies. GT-Suite Flow Theory Manual, 2013

[182] Gamma Technologies. GT-Suite Engine Performance Application Manual, 2013

[183] Capon G. Some practical considerations of automotive turbocharging. Lecture notes, University of Bath, 2015.

[184] Pesiridis A, Salim WSIW and Martinez-Botas RF. Turbocharger matching methodology for improved exhaust energy recovery. In: *Institution of Mechanical Engineers 10th International Conference on Turbochargers and Turbocharging*, London, UK, 15 May-16 May 2012, London: Institution of Mechanical Engineers.

[185] Burke R. Powertrain Control Systems, Lecture notes, University of Bath, 2015.

[186] Carey C, McAllister M, Sandford M et al. Extreme engine downsizing. In: *Institution of Mechanical Engineers – Innovations in Fuel Economy and Sustainable Road Transport.* Institution of Mechanical Engineers, Pune, India, 8 November – 9 November 2011, London: Institution of Mechanical Engineers.

[187] Birckett A, Tomazic D, Bowyer S et al. Transient Drive Cycle Modeling of Supercharged Powertrains for Medium and Heavy Duty On-Highway Diesel Applications. SAE paper 2012-01-1962, 2012.

[188] Biller BD, Wetzel P, Chandras P et al. Vehicle Level Parameter Sensitivity Studies for a 1.5L Diesel Engine Powered Passenger Car with Various Boosting Systems. SAE *Int. J. Fuels Lubr.* 2015; 8(2).

[189] Ernst R, Friedfeldt R, Lamb S., et al. The New 3 Cylinder 1.0L Gasoline Direct Injection Turbo Engine from Ford. In: *20st Aachen Colloquium Automobile and Engine Technology*, Aachen, Germany, 11-12rd October 2011.

[190] Westin F, Grandin B and Angstrom H. The Influence of Residual Gases on Knock in Turbocharged SI-Engines, SAE paper 2000-01-2840, 2000.

[191] Douaud A and Eyzat P. Four-Octane-Number Method for Predicting the Anti-Knock Behavior of Fuels and Engines. SAE paper 780080, 1978.

[192] Agarwal A, Jung H, Byrd K, et al. Blowdown Interference on a V8 Twin-Turbocharged Engine. SAE *Int. J. Eng*. 2011; 4(1): 202–218.

[193] Turner J, Pearson R and Milovanovic N. 12 Reducing the Octane Appetite of Pressure-Charged Gasoline Engines using Charge Air Conditioning Systems," In: *JSAE Annual Congress*, Japan, May, 2006.

[194] Cieslar D. *Control for Transient Response of Turbocharged Engines.* PhD Thesis. University of Cambridge, UK, 2013.

[195] Friedfeldt R, Zenner T, Ernst R, et al. Three-cylinder Gasoline Engine with Direct Injection. *MTZ worldwide* 2013; 2(2): 32-37.

[196] Hu B, Turner JWG, Akehurst S, et al. Observations on and potential trends for mechanically supercharging a downsized passenger car engine: a review. *Proc Institution of Mechanical Engineers Part D: J Automobile Engineering* 2016, in press.